ANGLED CURTAIN COATING: AN EXPERIMENTAL STUDY

An experimental investigation into the effect of die angle on air entrainment velocity in curtain coating under a range of operating conditions.

Mansour Masoud Elgadafi

Submitted for the degree
of Doctor of Philosophy

School of Engineering, Design & Technology

University of Bradford

JUNE, 2010

ANGLED CURTAIN COATING: AN EXPERIMENTAL STUDY

Abstract:

In all coating applications, a liquid film displaces air in contact with a dry solid substrate. At a low substrate speed a thin uniform wetting line is formed on the substrates surface, but at a high speed the wetting line becomes segmented and unsteady as air becomes entrained between the substrate and the liquid. These air bubbles affect the quality of the coated product and any means to postpone this at higher speeds without changing the specifications of the coating liquid is desirable. This research assesses the validity of a theoretically based concept developed by Blake and Rushack [1] and exploited by Cohu and Benkreira [2] for dip coating. The concept suggests that angling the wetting line by an angle β would increase the speed at which air is entrained by a factor 1/cos β. In practice, if achieved this is a significant increase that would result in more economical operation. This concept was tested in a fast coating operation that of curtain coating which is already enhanced by what is known as hydrodynamic assistance [2]. Here we are effectively checking an additional assistance to wetting. The work, performed on a purposed built curtain coater and a rotating die, with a range of fluids showed the concept to hold but provided the data are processed in a way that separate the effect of curtain impingement from the slanting of the wetting line.

Key words: curtain coating, die angle, air entrainment, hydrodynamic assist, dynamic wetting.

TABLE OF CONTENTS

ACKNOWLEDGEMENTS

Firstly, I would like to thank Professor Benkreira for giving me the opportunity to become part of his research group and carrying out this valuable research and for his supervision and guidance throughout my research. I would also like to thank Dr Patel for his assistance during my study on the practical aspects of the project. Secondly, I would also like to thank my wife *Ebtisam Elmsalaty* and my children and the rest of my family for their constant courage and support throughout my academic career. Thirdly, I would like to thank all the academic, administrative and technical support staff (Mr David Steele and Mr Ian Mackay) in the School of Engineering, Design and Technology for their assistance and support during the period of my research. Many thanks are also due to my friends and colleagues in the Coating Laboratory of Bradford University. Finally, I must thank Dr Raj Patel for his invaluable help.

Nomenclature

q_{die}	Actual flow rate from the die	l/m
q_{sub}	Actual flow rate on the substrate	cm^2/s
q`	relative wetting line position at V_{aemax}	
Ca	Capillary number = $\mu U/\sigma$	
V_{ae}	Air entrainment velocity	m/s
$V_{ae,max}$	Maximum air entrainment speed over flow rate	m/s
V_{ae0}	Air entrainment of plunging tape flows	m/s
G	Gravitational acceleration	m/s^2
H	Curtain coating height	mm
L	Characteristic capillary length = square root of $2\sigma/\rho g$.	
A	Die area	m^2
Θ	Curtain coating die angle	degree
Q	Flow rate of the film flowing through the nip	m^3/s
R	Refers to reverse roll coating	
r_c	Radius of curvature	
T	Temperature	°C
t	Time	s
U	Velocity	(m/s)
V_C	Critical velocity	(m/s)
V_{ae} %	Speed set on the inverter	
η	Viscosity	mPa.s
γ_{lv}	Surface tension of the liquid vapour interface	mN/m

γ_{LS}	Surface tension across solid-liquid interface.	mN/m
γ_{SV}	Surface tension across the solid-vapour interface.	mN/m
β	Die angle	degree
λ	Distance between two adsorption or desorption sites.	
τ	Relaxation time of the surface properties in equation 2.15	
K	Boltzman constant	
σ	Surface tension	mN/m
ρ	Density	kg/m^3
A	Substrate angle	degree
θ_A	Advancing contact angle	degree
θ_d	Dynamic contact angle	degree
W	width of the curtain above the impingement point	mm

LIST OF FIGURES

CHAPTER 1: INTRODUCTION

1.1 INTRODUCTION

Curtain coating, the subject of this research, is an operation, which has been widely used in the photographic paper industry because it is fast (10 m/s) and can achieve very thin films (10 microns) in a single or multilayer form (see Figure 1.1). In recent years, this fast coating technique has been gradually incorporated in to other industries, particularly the paper industry where it is often desired to coat in a non-contact method such as in the traditional blade coating technique (see Figure 1.2). With the advent of plastic electronics and other sensitive coating applications such as pharmaceutical and photovoltaic thin films, where a non-contact fast and thin coating method is required, curtain coating becomes the technique of choice. Any research that can enhance curtain coating to operate at even higher speed is clearly highly desirable. This is precisely the aim of this research, which uses a simple mechanical manipulation - *angling of the curtain die* (see Figure 1.3) - to achieve a step increase in coating speed. This "trick", which appears to be a technological artefact, is in fact solidly rooted in the fundamental understanding of dynamic wetting, as we shall discuss later. However, until it was discovered in Bradford (Cohu and Benkreira [2]) and tested in a limited way, this technique has been surprisingly ignored by industry. The purpose of this research is to re-examine this "discovery" and furnish it with solid experimental data to ensure it is indeed valid and worthy of industrial exploitation.

Before expanding on this aim and the objectives of the research, it is important to provide some background on coating technology in general, details of coating methods and associated flows and the problems and challenges faced to operate these flows in a *stable* manner. Stability here is the key word as coating flows by their very nature are prone to both surface instabilities (ribbing) and air entrainment (see Figure 1.4) and

operate in what is termed as a “coating window”, or within a range of operating conditions in which the films are stable.

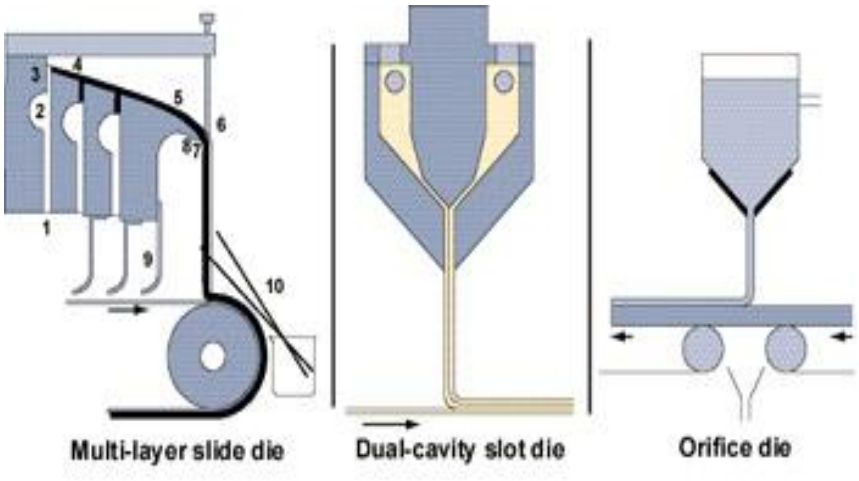

Figure 1.1: Single & Multiple Layers Curtain Coating, Wheeler [2].

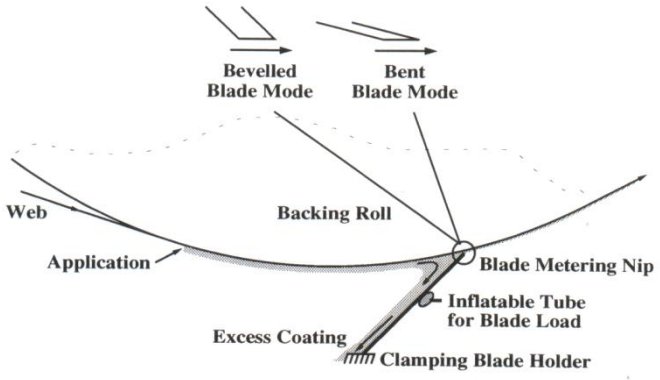

Figure 1.2: Typical blade coater design, Aidun [3].

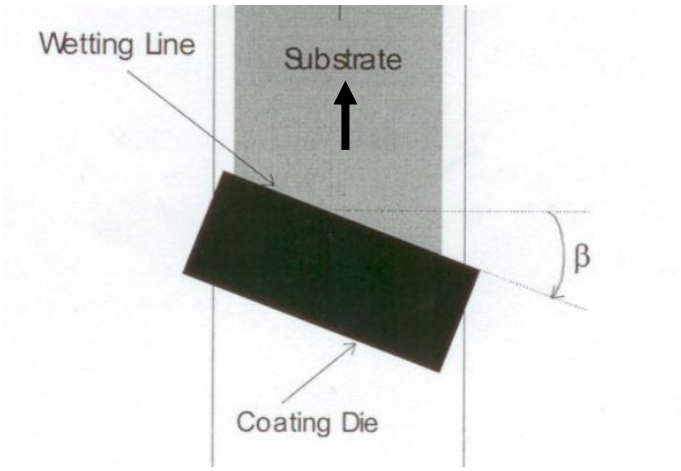

Figure 1.3: Angled curtain coating, Benkreira and Cohu [9].

Figure 1.4: Ribbing & Air Entrainment Coating Flow Instabilities Kistler [4]

1.2 COATING TECHNOLOGY

1.2.1. GENERALITIES

Coating has been *around* since the first humans living in caves started using paintings to communicate their life habits and decorate or protect their bodies against the environment. Since those early times, coating as a technology has evolved from an art or decorative form (paint and wall paper are prime examples) into a truly functional form (the photographic paper is an excellent example) with a number of various new applications. For example, pharmaceutical drugs are now applied as thin film coating on a patch (the nicotine patch is one such example) but more complex functions are now being achieved in electronics where the coating layer electrical activity is at the heart of the product function (plastic electronic). It is true to state that coating as an industrial activity is huge when one considers the consumption of paints, cosmetics, inks, paper, adhesives, etc. It is also not difficult to notice that almost everything we use is coated, so clearly coating as an industry is big and its growth has been fuelled by our ability to impart specific functions to coated layers. Table 1.1 below gives an overview of the coating sector, by activities and by markets and highlight the value of this industry.

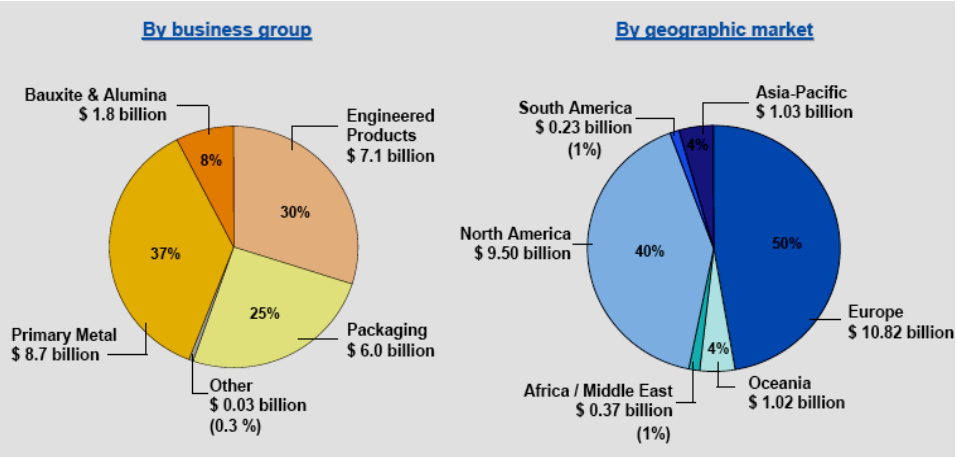

Table 1.1: Coating activity by sectors and geographical markets.

1.2.2 COATING FLOWS: DEFINITION

A coating flow may be defined as a fluid flow in which a layer or a film of a liquid or a "paste" is applied onto a surface at speed (Figure 1.5). The surface may be a solid but in multilayer coating (Figure 1.1 above), the coated surface may itself be a liquid and this explains why the physicists define coating as a process, which replaces gas on a surface by a liquid layer.

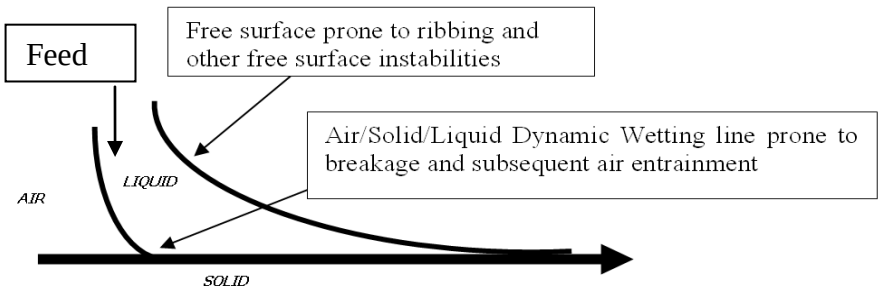

Figure 1.5: Boundaries defining a coating flow.

The key observation, however is that the liquid or paste is in general a complex formulation (a liquid + a functional solid or polymer + a binder + other additives), if it is to provide the particular function required. Necessarily, this "liquid" or "paste" will generally have a complex rheology, i.e. it will not be Newtonian in its flow character.

Figure1.6. this flow characteristic makes the study of coating particularly challenging, as we will describe later.

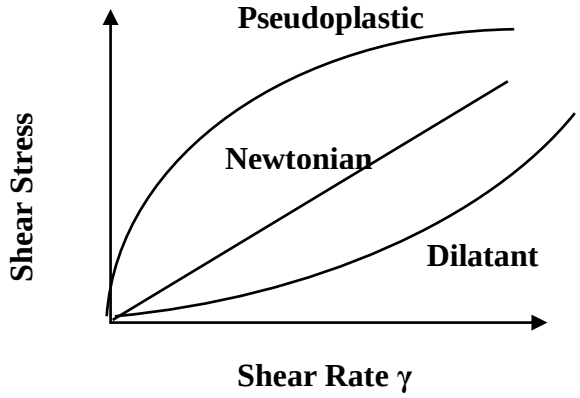

Figure 1.6: Non-Newtonian flow character of coating liquids.

Having defined coating as a process of film formation at speed, we now introduce the concept of *a free surface*. Because, the final film must have a finite constant thickness for it to be practically useable as delivering constant performance, the film formation must be developed via free surface as illustrated in Figure 1.5. By definition, because this surface is free, it will be prone to instabilities. These instabilities may be the result of the flow delivery which produces the free surface. The analogy with the wave on seas is a good one, albeit extreme. On a calm day, the flows current when very weak do not disturb the surface. When these currents are disturbed, waves will appear causing the free surface of the sea to become unstable. During coating, if the substrate speed is increased beyond a critical threshold, the free surface of the flow will becoming wavy (see Figure 1.4 above) with the net result that the final film will have thickness that oscillate thus not constant.

Another source of instabilities is associated with the *dynamic wetting line* which is the line that separates the liquid being deposited on the solid substrate from the gas phase as shown in Figure 1.5. At low coating speed, this line is straight but as the speed increases, a threshold is reached when this line adopts a saw teeth shape. With

further increase in the speed, the saw teeth shaped wetting line breaks further allowing air to be "gulped" into the flow with catastrophic effects on the quality of the final film formed (see Figure 1.7 below illustrating this behaviour). Clearly, postponing this occurrence to larger speed is very desirable and this research deals with this aspect of instabilities, central in practice to efficient economical operations.

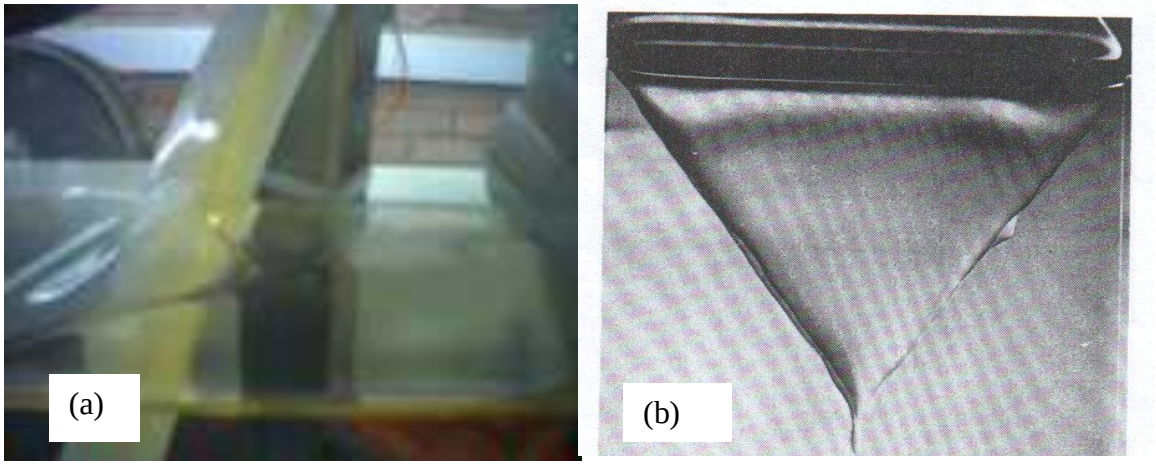

Figure 1.7: Air Entrainment & Dynamic Wetting Failure (a) from our work and (b) (Blake and Ruschak [5]).

1.2.3 COATING FLOWS AND METHODS: CLASSIFICATION

The above section defined a coating flow but did not explain how such a flow may be created or engineered. Clearly, if one were asked to develop a coating method several propositions would be made. Indeed if one reviews coating technology in this aspect, hundreds of coating methods will appear and all as if unrelated. Further scrutiny of these many methods and techniques would reveal that coating flows such as those used on flat surfaces can be classified into four categories (Benkreira et al.[6])

- free coating flows;
- metered coating flows;
- exact or pre-metered coating flows;
- print or gravure coating flows.

1.2.3.1 FREE COATING FLOWS

This is the most basic category in which a film is formed when a substrate exits from a large pool of liquid (Figure 1.8). The term "free" is used here to denote that the film is free to form and that the only controlling variables are fluid properties, the speed of withdrawal of the substrate and the angle the substrate forms with the surface of the fluid in the pool, normally 90^0.

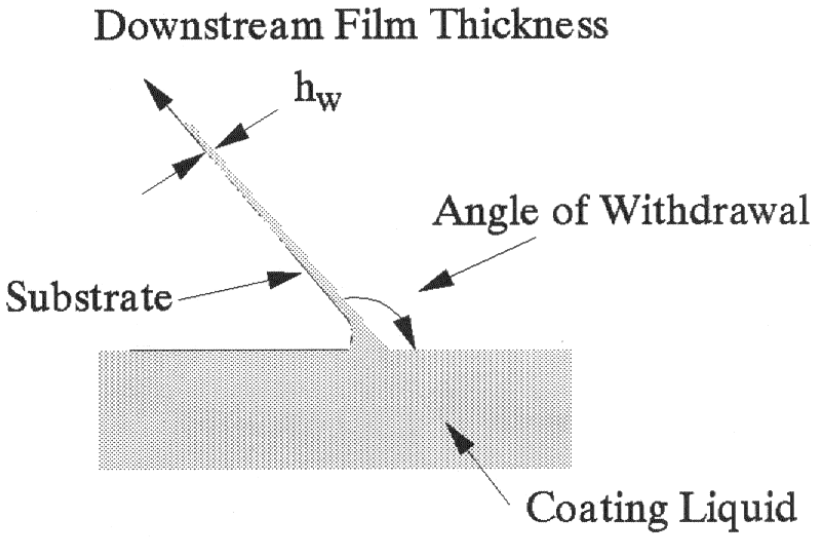

Figure 1.8: Free Withdrawal Coating.

Practically, free coating cannot coat one side only of the substrate and as a result is not much used. It is however attractive academically as it is the simplest coating flow and a basis to rank other coating flows against, in terms of film thickness that may be formed. Also, the plunging situation where the substrate enters a pool of liquid at speed depicts very well dynamic wetting (Figure 1.9) and enables it and subsequent air entrainment to be studied relatively easily compared to other coating flows as it will become clear later. A variation of this simple technique is when a roller rather that a "straight line" substrate is used (Figure 1.10). This situation is practical in that one side of a substrate can be coated when the roller is in kiss contact with the substrate (Figure 1.11). This combined situation is however not a free coating flow *per se* but a

combination of coating flows as it will become apparent later once all the four coating flows have been introduced.

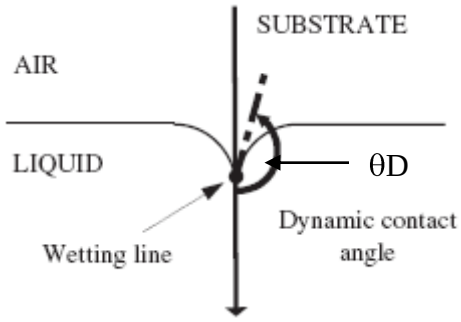

Figure 1.9: Dip Coating for the Study of Dynamic Wetting, Cohu and Benkreira, [7].

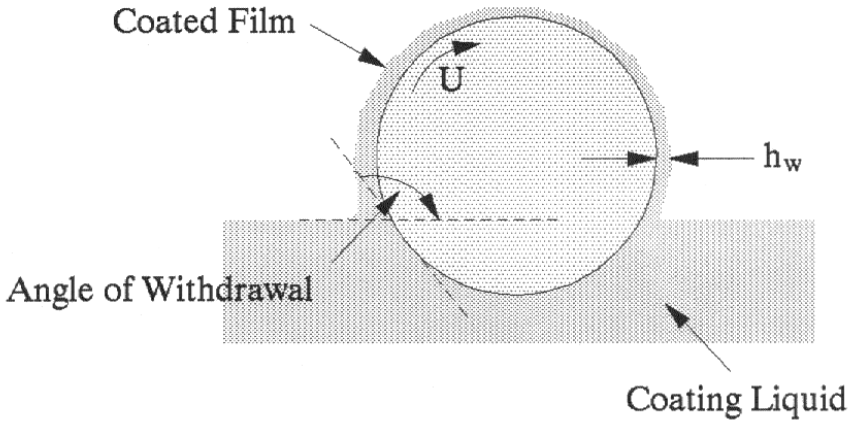

Figure 1.10: Free Withdrawal Roll Coating, Benkreira [5].

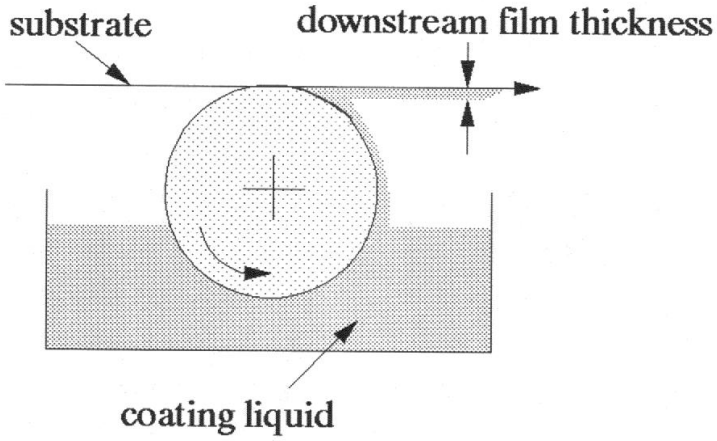

Figure 1.11: Variation of Free Withdrawal Coating, Benkreira [5].

1.2.3.2 METERING COATING FLOWS

This is a natural progression from free coating if one considers the coating flow situation when the side of the trough containing the pool of liquid in free coating moves closer to the substrate thus metering the otherwise "free" flow (Figure 1.12). If this side is slanted, it is easy to see it acting as a blade, hence the denomination "blade coating" used in practice (Figure 1.13). Effectively, with metering coating, a coating gap or nip is being introduced and it is this nip, which constrains and meters the flow further in comparison with the free coating situation. Now, it is easy to see several variants of this situation, particularly when a curved blade or a roller is introduced, hence the denomination roll coating (Figure 1.14). Also the constraint does not have to be a solid restriction, it can be a jet of gas, hence the denomination jet knife coating (Figure 1.15) much used for example in galvanising-coating of steel where it is more practical to use a non contact solid nip. Having introduced a coating gap as a constraint, why not allow the solid boundaries to be moving rollers? We have now reached a large category of coating methods known collectively as "roll coating" with one, two, three or more rollers rotating in the same or opposite direction at the coating nip (Figure 1.16). In these, we have effectively introduced several coating flow constraints: a gap, a moving surface and a direction of movement splitting (forward roll coating) or returning fluid (reverse roll coating). What makes these coating methods very attractive practically is the use of rollers, which are ideally suited to drive substrates, which are wrapped around them. Roll coating is the method of choice of most coating industry because two rollers can easily be used to create an accurate gap between them, draw fluids from a trough, whilst also driving a substrate (Figure 1.14a) to complete the operation. There is however one practical limit with operating a gap in that when a very thin film is required, a very small gap is required. In practice

the best rollers cannot be machined and polished to produce a gap between two rotating rollers accurate to +/- 5 microns. Roll coating thus appears to be not practical for thin film coating until we realise that we can operate the rollers at a negative gap if a rubber and a steel roller are used side by side (Figure 1.16c). In such situation, the coating gap is formed as a result of the high viscous forces generated and deflecting the rubber, which is in elasto-hydrodynamic rolling contact. We shall review the flow aspects later in the literature survey.

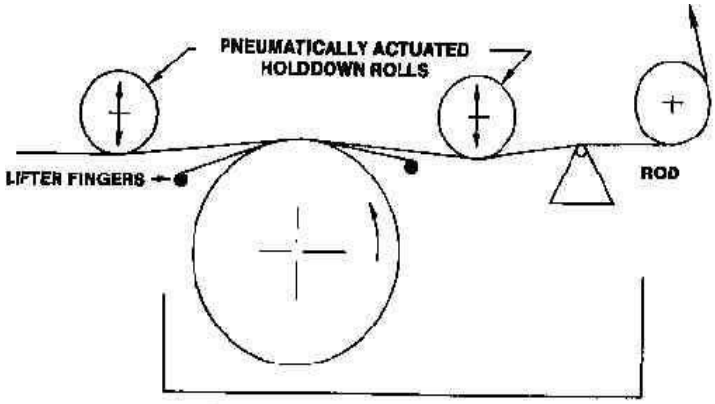

Figure 1.12: Mayer Rod coating
Mayerhttp://www.webcoatingblog.com/blog/2005/07/mayer_rod_coate.html

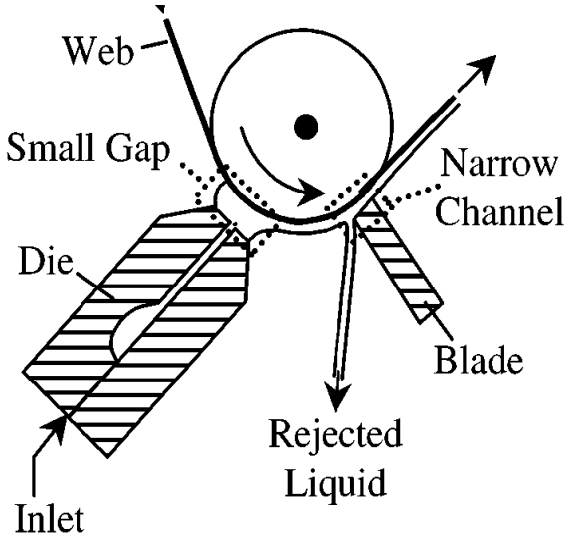

Figure 1.13: Blade coating.

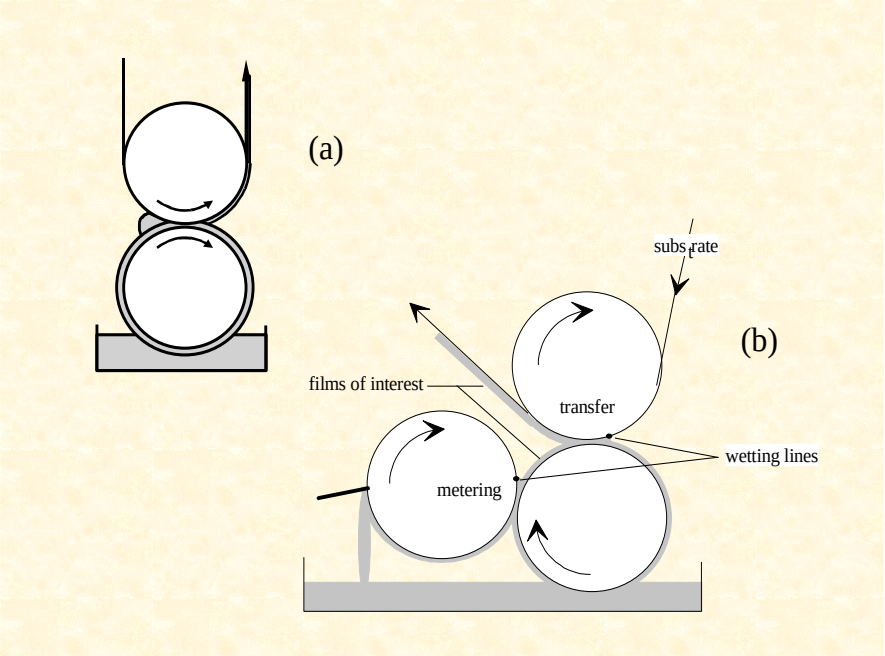

Figure 1.14: Rigid metering rolls coating Benkreira [5].

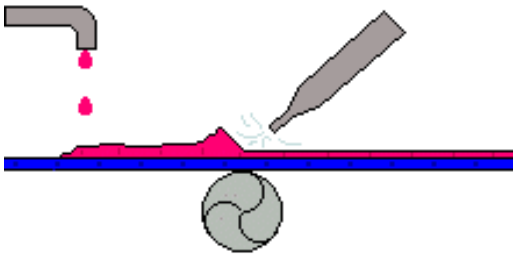

Figure 1.15: Air Knife- coating process.

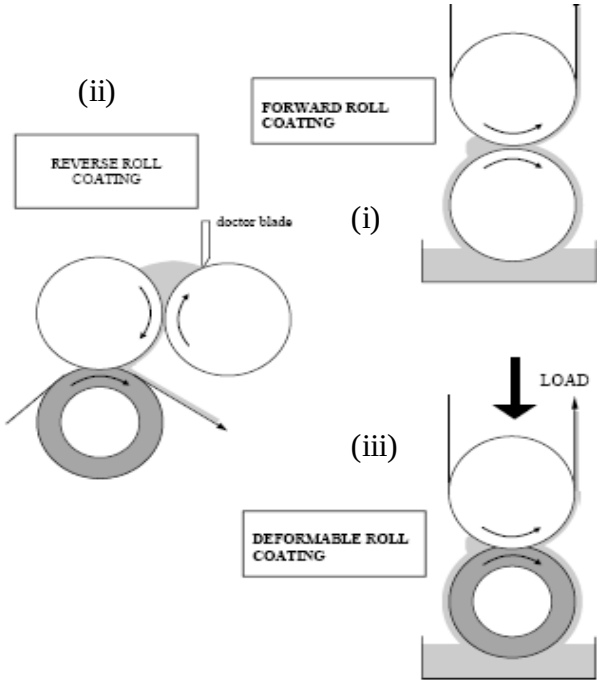

Figure 1.16: A selections of metering flows, (i) 2-rolls forward roll coating, (ii) 3-rolls reverse roll coating, (iii) 2-rolls deformable roll coating, [6].

1.2.3.3 METERED COATING FLOWS

This is a radically different category a coating flows, in a way simpler in outcome that both free coating and metering coating. Metered coating flows are flows in which an exact amount of fluid is transferred to a substrate, from a pump usually and via a die (Figure 1.17). The die does not meter the flow but delivers it to the required width hence the denomination curtain coating, slot coating and slot die coating (Figure 1.18). The main difference between curtain, slot and slot die is the distance the liquid sheet has to travel before it is deposited onto the substrate. Whereas in curtain coating the curtain height can be 10cm and larger, in slot and slot die it is only a few mm long. The difference between slot and slot die in terminology, slot being a die with no land and slot die being a die with an upstream and downstream lands (see Figure 1.18). In all cases, the die can be shimmed to allow flexibility in width applications. Clearly, this is a simple yet ingenious method but one, which is expensive as the die, must deliver equal flow at each point along its width (Figure

1.19). The pump also has to be pulse free to ensure no variation of flow in time. In such a flow, the film thickness on the substrate is fixed by "mass balance" (Figure 1.20) and the faster the speed the lower the film thickness for a given die flow delivery. Alternatively, at fixed substrate speed, film thickness can only be reduced by reducing the die flow rate. This appears in principle simple but there is the problem of instabilities (air entrainment and ribbing), which limits the coating window (as in the other coating flows reviewed above). We will examine this later when we review the analysis of flow. It is important in the context of this research to point that it is this flow, which is the subject of this study, and how to enlarge the coating window is the central theme of the study. As explained earlier, enlarging the coating window means operating at the largest speed possible before air entrainment and/or ribbing occurs. One very important attractive feature of this type of flow is that more than one layer can be coated simultaneously (Figure 1.20) making the method of choice of the photographic industry (11 layers can be coated at once here!) and the new high tech industries (plastic electronics, photovoltaics, medical patches and other requiring multiple functional layers).

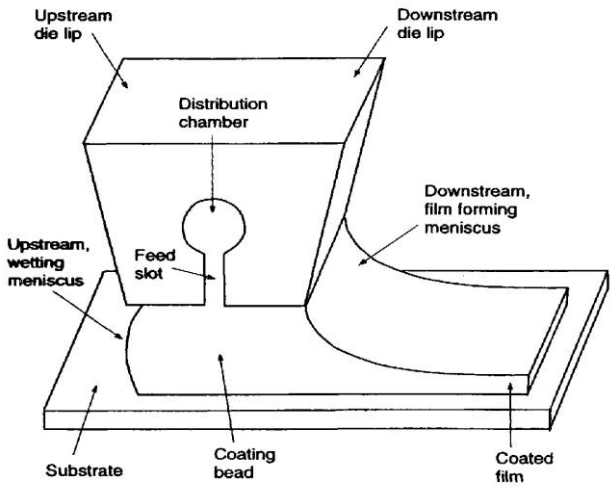

Figure 1.17: Slot Coater (Daniels and Savage [8]).

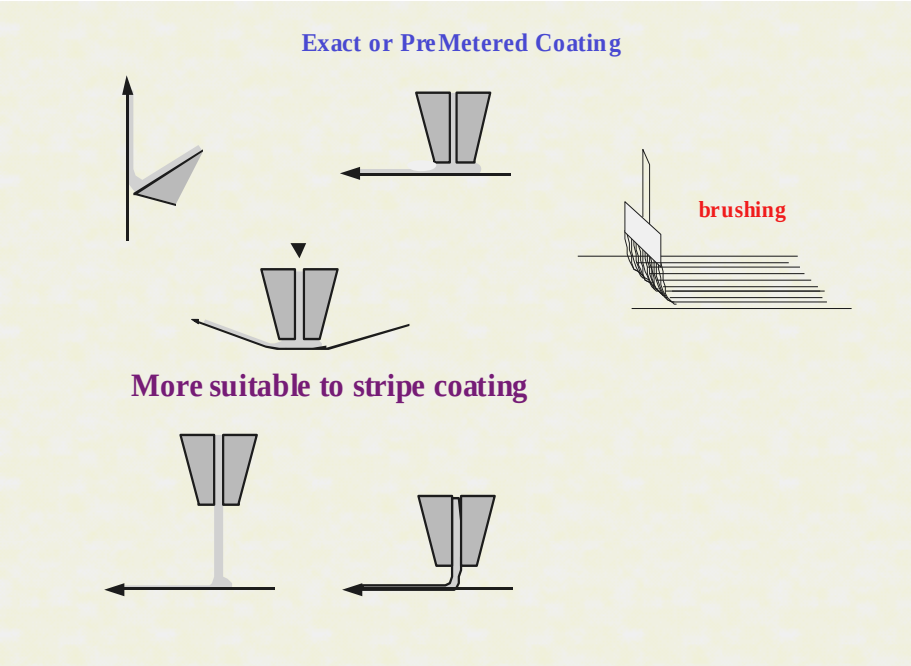

Figure 1.18: Exact or pre-metered coating

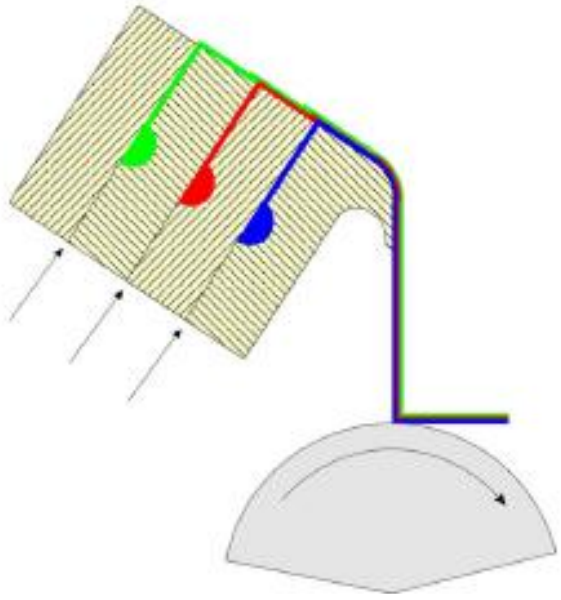

Figure 1.19: Multi- layers (3) curtain coating, PM Schweizer [9]

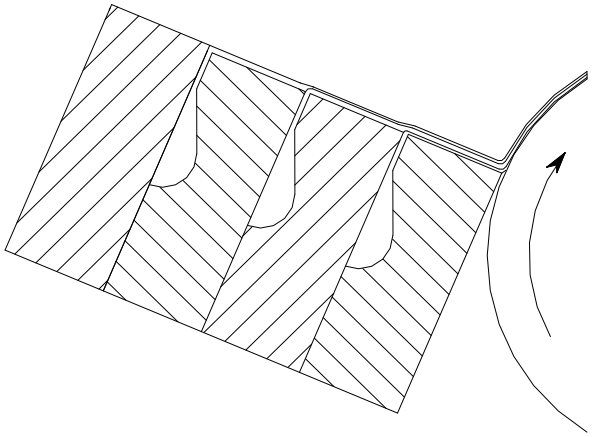

Figure 1.20: Multi-layer (3) slide bead coater**.**

1.2.3.3 PRINT OR GRAVURE COATING

This too is a radically different flow category and is reminiscent of printing hence its denomination. Gravure coating uses rollers that have been carefully chemically or mechanically engraved with tiny identical cells to hold fluid. Some typical patterns are the quadrangular, tri-helical and pyramidal (see Figure 1.21). The prefixes 220, 85, 60 refer to the number of cells or 'lines per inch' on the surface of the roller. The substrate is then brought into kiss contact with these cells causing the fluid trapped in the cell to be partly transferred. As the cells are closed together and sometimes linked together, a uniform film results on the substrate. In practice, gravure coating is achieved by applying an excess of coating solution to the gravure roll then wiping away surplus liquid using a flexible doctor blade pressed against the rotating roller. As the roller rotates the cells pass through the coating nip where a fraction of the fluid in the cells is transferred either to the substrate in direct gravure coating, (see Figure 1.22a) or to the offset roll in offset gravure coating, (see Figure 1.22b). Such a simple coating method is capable of producing very thin films (5 microns) at very high speeds (10m/s) but is practical only when the fluid is of low viscosity (water like) to enable it to flow out of the cells easily. Also, if a film of different thickness is required, the cell geometry has

to be changed. Wear and tear on the gravure roller may also become a problem if abrasive coating solutions are used.

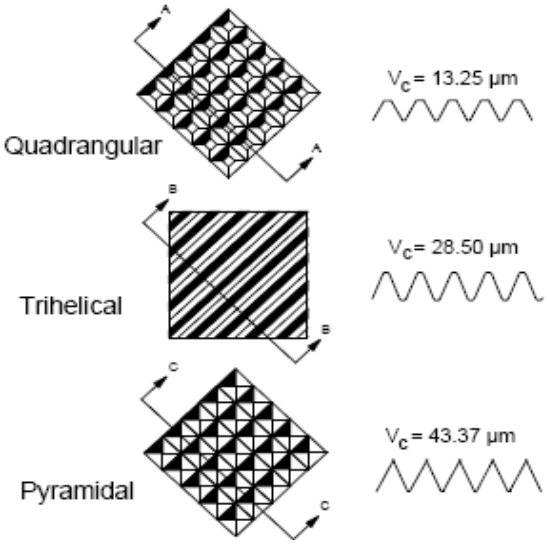

Figure 1.21: Typical gravure or cells geometry (Patel 1989).

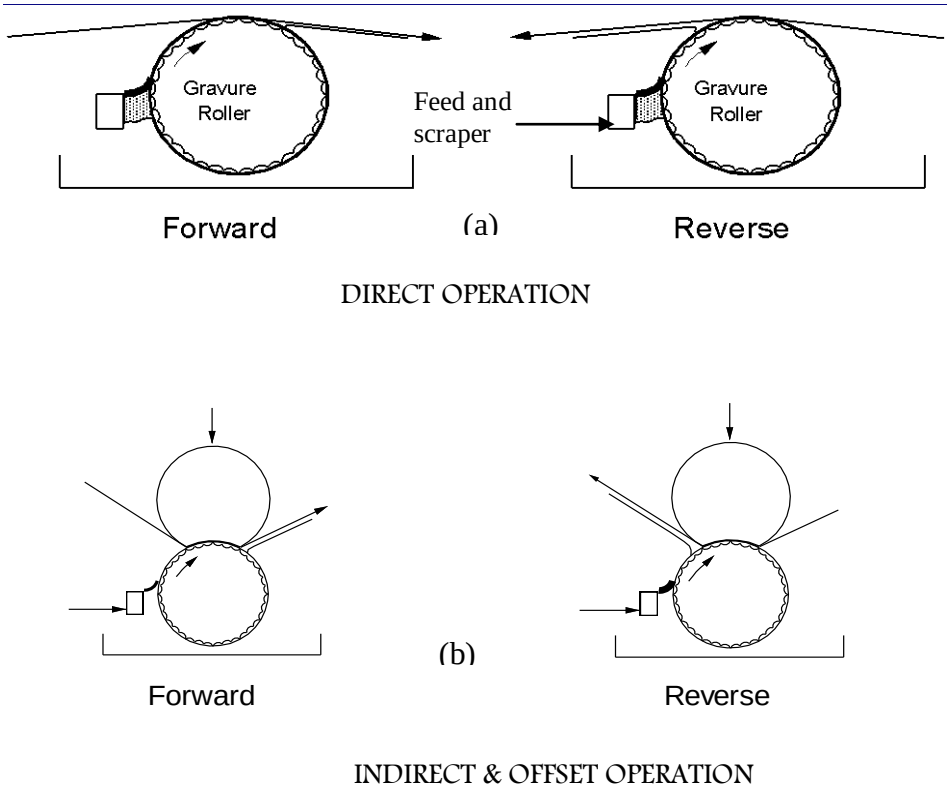

Figure 1.22, a & b: Direct and indirect gravure coating (Cohu and Benkreira[10]).

1.3 CURTAIN COATING AND WHY IT IS A FAST FLOW

As explained above, curtain coating is a metered coating flow delivered from a die *from a height* onto a moving web. This delivery from a height is the key to why this method is fast. It imparts the curtain with "strength"that by impinging onto the substrate is able to prevent air from being entrained at low speed. In the scientific literature this is referred as "hydrodynamic assistance" (further discussion in the Literature Review chapter). The curtain flow however has to be appropriate and the position of the curtain in relation to the dynamic wetting line is the key: the curtain must be in line with the dynamic wetting line for hydrodynamic assistance to be fully effective (see Figure 1.23 depicting the various flow zones of a curtain coating flow). This can be likened to a pressure effect being the largest in this arrangement, pinning the dynamic wetting line forcefully thus preventing air to be entrained. In the photographic industry, operations with curtain coating are normally carried out in the range of speeds of 5-15 m/s which are much greater than any other coating methods which are of order 1-3m/s.

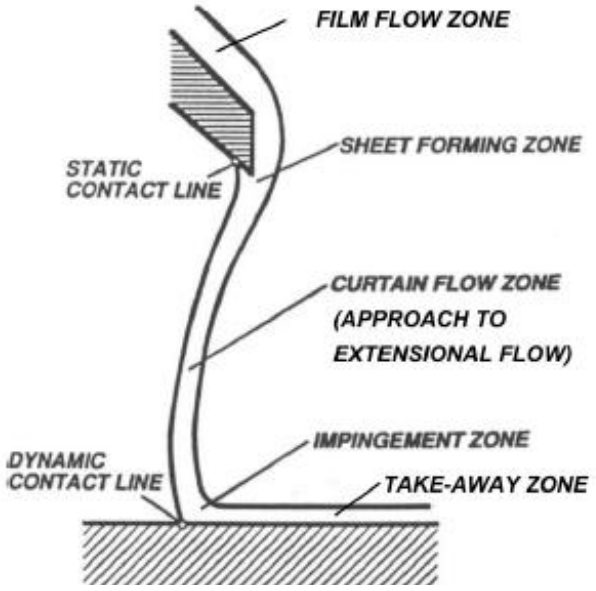

Figure 1.23: Flow zones in curtain coating, Hyun Wook Jung, J.S.L et.el [11]

1.4 EVEN FASTER CURTAIN COATING: RESEARCH HYPOTHESIS

As explained above the key aspect that permits curtain coating to be a fast coating flow is the delivery of the fluid from a height directly onto the dynamic wetting line. Dynamic wetting is thus still the *controlling factor*. As explained earlier, dynamic wetting failure in all coating flow is manifested by the wetting line changing at a critical speed from a straight line into a saw-teeth shaped line (further details in the Literature Review Chapter). Research by Blake and Ruschak [5] has shown that for dip coating this "vee" line is in fact the dynamic wetting line adopting the largest wetting interface between the liquid and the substrate. When measured carefully, the angle of the vees formed (see Figure 1.24 defining the relevant angle, ϕ) defines what Blake and Ruschak called the maximum speed of wetting, V_{max}. This V_{max} is found to relate with the substrate speed of air entrainment V_{ae} simply as:

$$V_{max}=V_{ae}\cos\phi \tag{1.1}$$

Cohu and Benkreira (1998), twelve years after Blake and Ruschak reported this observation and equation argued that a corollary to these is that slanting the dynamic wetting line at an angle β (see Figure 1.25 defining the appropriate angle, β) would increase V_{ae} by a factor $1/\cos\beta$. Cohu and Benkreira (1998) verified this comprehensively in their angled dip coating experiments. They also produced preliminary data on angled die coating (see Figure 1.26 showing their original data). No work was pursued to test experimentally if the corollary hold true in curtain coating. This is precisely the main aim of this research and has the potential to step change curtain coating speed by a factor of $1/\cos\beta$ if the die angle is increased.

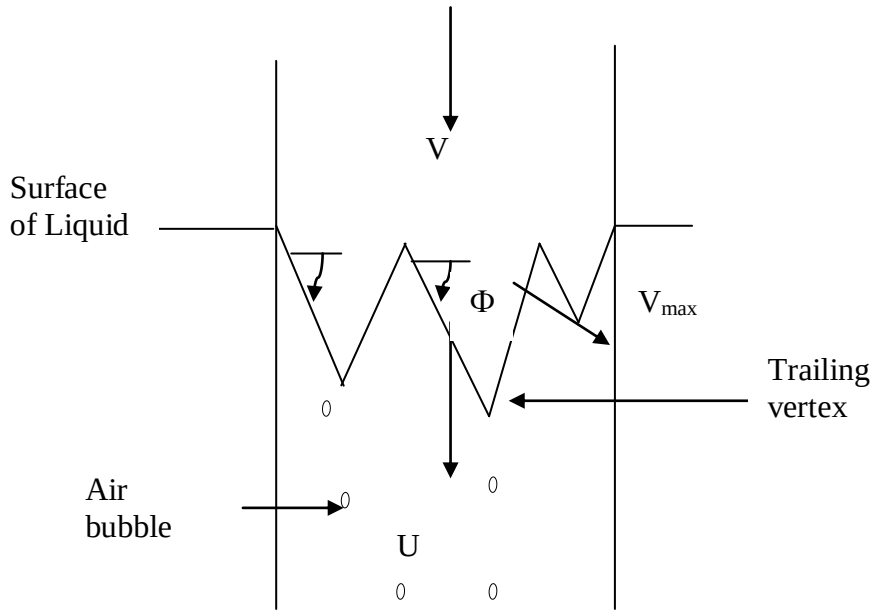

Figure 1.24: Schematic representation of the saw-teeth wetting line and corresponding angle ϕ obtained when a tape plunges vertically into a pool of liquid at a speed, V, greater than maximum speed of wetting, U. The wetting line shows both leading and trailing vertices with air bubbles entrained.

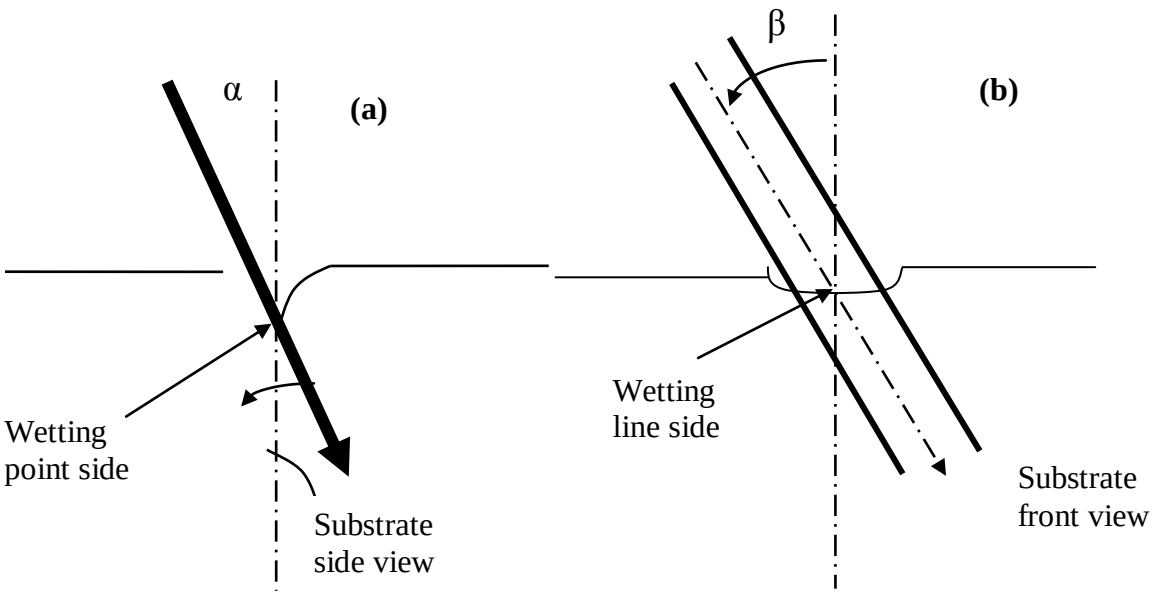

Figure 1.25: Inclined dip coating (a) vs. Angled dip coating (b): note that only in angled curtain coating is the dynamic wetting line at an angle β with the direction of motion of the subs

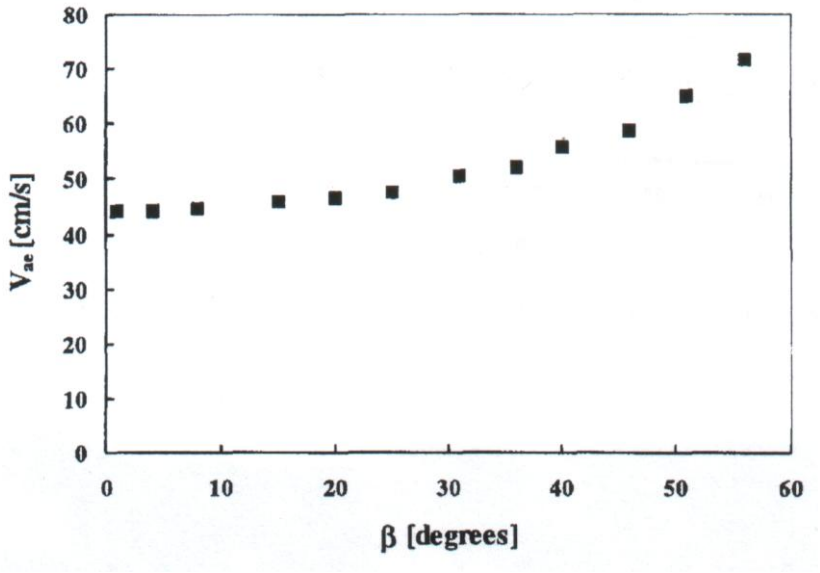

Figure 1.26: Effect of the substrate inclination angle β on the measured air entrainment velocity for a glycerine solution in dip coating, Cohu and Benkreira [7].

1.5 AIM AND OBJECTIVES OF THIS RESEARCH

Having introduced the main hypothesis of the research and the corresponding aim, we defined here the objectives or the lines of research to be followed in order to test the hypothesis. The aim is thus:

- To test experimentally that angled curtain coating follows Cohu and Benkreira [7] observation that V_{ae} should increase with the inclination angle β by a factor of $1/\cos\beta$.

The objectives of this research are:

- To review critically research in dynamic wetting in relation to this aspect.
- To build an experimental set-up to test this hypothesis. The set-up should include the provision for a rotating die and coating on a substrate at high speeds. This is a *major challenge* as no research in academia has been reported on curtain coating with substrate. Rather work has been carried out without substrate (further details in literature review).

- To develop a technique that can measure accurately the air entrainment V_{ae}. This is a serious challenge since visualisation of the dynamic wetting line underneath the curtain is problematic particularly when the substrate is travelling at high speed.
- To carry out experiments in a range of conditions to assess the extent and limit of the fit with the hypothesis. This includes varying fluid properties (viscosity and surface tension) as well as flow rates delivered by the die.

The thesis presenting this research is organized in the usual way:

- this Introduction chapter, setting the "scene" of the work,
- a Literature Review, reviewing coating flows essential scientific progress but concentrating particularly on dynamic wetting and curtain coating,
- an Experimental Methods chapter describing the equipments, the measuring technique and the characterization of the fluid and other materials used.
- a Results & Discussion chapter, bringing the data together and discussing them in relation to principles covered in the Literature review chapter
- a Conclusions & Recommendations chapter, pointing subsequent researchers in directions that can improve our understanding of curtain coating flow further.

CHAPTER 2: LITERATURE SURVEY

2.1 INTRODUCTION

Coating flows as explained in the introductory chapter have complex features that make their theoretical analysis particularly difficult. These features are a free surface prone to waving instabilities and a dynamic wetting line prone to breaking and subsequent air entrainment. This research is concerned with the latter feature and thus the literature review will concentrate on this critical aspect. Of course there are other aspects of coating flows that present challenges but the "issue" of the dynamic wetting line is crucial and difficult because at this line three phases are in contact, air-solid-liquid, and also although the substrate is moving this line appear to be stationary and hence the singularity in the flow which is at the heart of the problem. As explained also in the introductory chapter all coating flows exhibit a dynamic wetting line, so its study in any one flow give clues on the essential problem of how this line breaks and gives way to air to be entrained. Clearly dip coating, where a substrate plunges into a pool of liquid, is the simplest physical representation of this complex problem. Its study has thus attracted a lot of attention and the literature review will begin there. The review will show the "break-through" leading to the formulation of the research addressed in this thesis. This break-through follows directly from the important work of Blake and Ruschak [5] on the concept of the maximum speed of wetting which was "exploited" further by Cohu and Benkreira [7] into the idea of angling the wetting line to postpone air entrainment to higher speed compared with normal non angled wetting. Details are given in chapter (4) later. Following from this, we can then approach the problem at hand with respect to curtain coating, which has the additional feature of a curtain of liquid "dropping" onto a substrate. The analogy between dip coating is there but the fluid is not at rest, rather it impinges with force onto the substrate hence the

concept of “hydrodynamic assistance” which also needs to be reviewed in this research. Basically hydrodynamic assistance postpones air entrainment to larger speeds compared with dip coating and other coating flows where no pressure can be exerted at the dynamic wetting line. Angling the die, as it will be demonstrated by preliminary work reviewed here, should in principle enhance even further the performance of curtain coating. So in conclusion, this review will examine:

- Dynamic wetting and air entrainment in dip coating, particularly the important work of Blake and Ruschak [5]
- The follow-up “exploitative” work of Cohu and Benkreira on angled dip coating [12]and angled slide coating [12]
- Dynamic wetting and air entrainment in curtain coating and how angling the dynamic wetting line should in principle increase air entrainment speed.

2.2 DYNAMIC WETTING FAILURE IN DIP COATING

The study of dynamic wetting and its subsequent failure that allows air to be entrained can be divided into four tranches. The first tranche of research on this topic, undertaken by many investigators, Deryagin and Levi, [13] was essentially observing how the dynamic wetting line breaks and measuring the speed at which this happens when fluid properties and substrate characteristic were changed. The second set of work, a break-through due to Blake and Rushak [5] was in establishing the concept of the maximum wetting speed. The third research, directly exploiting the results of the maximum speed into angled coating is due to Cohu and Benkreira [10]. The new research on dynamic wetting in dip coating, outside the scope of the present study but very relevant to it is the manipulation of the gas phase, hitherto ignored by all previous workers. Details on these four tranches of research are now given.

2.2.1 Dynamic Wetting Failure in Dip Coating: the early work

Deryagin and Levi [13]were the first to reveal experimentally how dynamic failure in dip coating occurred. The dip-coater represents a typical solid/liquid/gas system, which meets at the three-phase contact line. At low magnification, the interface appears to intersect the solid as a line (known as the wetting line) and the angle measured at the solid / liquid interface is termed the macroscopic (or apparent) contact angle. (see Figure 2.1a)

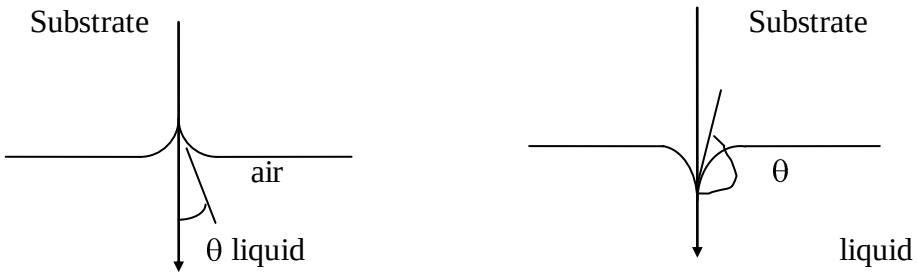

Figure 2.1a and b: Schematic diagram showing the average in contact angle with speed.

At the lowest speeds, the contact angle formed between the liquid and solid surface approaches the advancing static contact angle (Figure 2.1a). As speed is increased, the wetting line is pulled below the level of the free surface of the liquid (Figure 2.1b). The contact angle steadily increases, reaching 180° at some critical speed V*. At t substrate speeds exceeding V*, Deryagin and Levy [13] observed that the wetting line being originally straight, suddenly breaks up with the "appearance of dark triangles where the contact between the liquid and the support is broken" and the flow becomes unstable and three-dimensional. Air bubbles are entrained at the trailing vertices where two straight-line segments of the wetting line seem to intersect as shown in Figure 2.2.

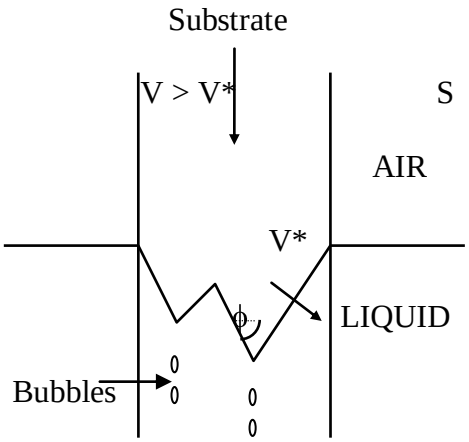

Figure 2.2: vvv-shaped wetting line

Since the original work of Deryagin and Levy [13], several studies have been carried out and they all confirm that indeed dynamic wetting failure and subsequent air entrainment occur at a critical speed, immediately or very shortly after the dynamic wetting line breaks up into a "vvvv" pattern. Such works have been reviewed by Blake *et al.* [14]and in addition to the key observation of how failure occurs, these works bring in quantitative measures of the air entrainment speed, V_{ae}, found to coincide with the speed, V^* at which the vvv pattern appears. For example, Burley and Kennedy [15] and Burley and Jolly [16], measured V_{ae} with various fluids and smooth plastic substrates and arrived at the following correlation:

$$V^* \approx 67.88\left(\mu\sqrt{\frac{g}{\rho\sigma}}\right)^{-0.672} . \qquad [2.1]$$

This correlation appears to indicate that viscosity, μ as well as density, ρ and surface tension, σ of the coating liquid are all important. Gutoff and Kendrick [17]however found that viscosity is the only important parameter. In disagreement with Burley [18], they showed that adding a surfactant to the solution did not affect contact angles or air entrainment velocities significantly. Their correlation is simply:

$$V^* \approx 5.11\mu^{-0.67} \qquad [2.2]$$

This correlation is in very good agreement with Burley and co-workers experimental results in terms of the dependence on viscosity. Burley and co-workers also found that above a coating liquid viscosity of 0.462 Pa.s, the critical velocity V* was a constant of about 7 to 10 cm/s. Such a result was confirmed by O'Connell [19] but not by Gutoff and Kendrick [17]

Although the observation on the importance of viscosity would suggest consideration of non-Newtonian effects, shear thinning in particular to increase air entrainment speed, surprisingly very little work has been done in this area. Gutoff and Kendrick [17]included some polymeric solutions to their study but did not analyse the data. The major difficulty is to calculate the proper viscosity for shear-thinning fluids and to account for the viscoelastic behaviour of polymeric solution correctly. Interesting empirical results have been reported by Bolton and Middleman [20], using viscoelastic polyacrylamide solutions having a nearly constant shear-viscosity but exhibiting an important elastic behaviour. They showed that elasticity has a significant stabilizing effect postponing the onset of air entrainment to higher speeds. Cohu and Benkreira [7] followed on these leads and measured V_{ae} for a range of viscoelastic polymer solutions (dilute PAA and CMC in glycerine/water mixture) as well as with Newtonian fluids. They found that Gutoff liquid elasticity gives rise to flow instabilities that might lead to air entrainment.

One important observation from all the work on the effect of viscosity is that low viscosity leads to high V_{ae} and large viscosity to low V_{ae}. This would suggest that prewetting a substrate with a low viscosity fluid prior to coating would result in V_{ae} higher than with a dry substrate. Also as air entrainment is strictly the inclusion of air between a dry substrate and a liquid, prewetting a substrate will make it more difficult

for air to be entrained as it would have to penetrate the liquid. Indeed when we compare, as in Figure 2.3, data of dry substrates, for example those of Burley and Jolly (1984) or Gutoff and Kendrick (1982) with those of prewetted substrates, for example those of Wilkinson [21], Bolton and Middleman [20], Ghannam and Esmail [1992] or Kistler and Shweizer [22], we find that prewetting delays the onset of air entrainment but the effect however is low and not comparable in terms of viscosity effect.

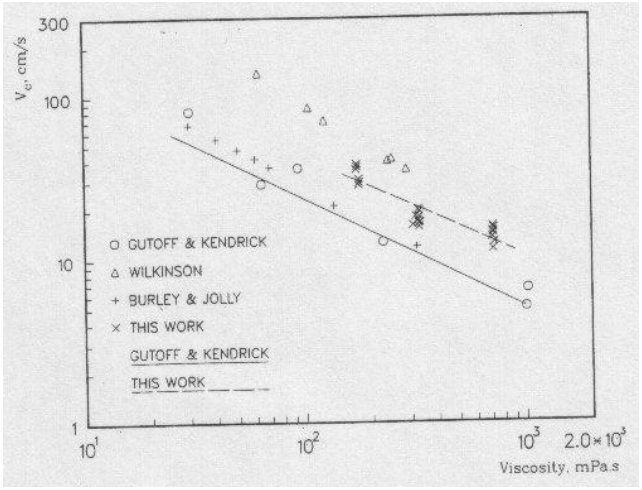

Figure 2.3: Critical velocity Vs Viscosity (Kistler [23])

All the work reviewed above made use of smooth substrates when in practise substrates display different roughness and wettability, paper is one example but others are steel and fabrics. The experimental data of Buonoplane *et al.* [24]showed clearly that air entrainment is postponed to much higher speeds with rough surfaces compared to smooth surfaces. This agrees with the suggestion of Scriven (1982) that near the wetting line with rough surfaces, air can escape through the valleys between peaks in the surface. Opposite conclusions, however, have been carried out by Burley [18], from the data of Kennedy (Burley and Kennedy, [15]) and Perry [25]. According to them, the rougher the surface the sooner the air entrainment occurs, whilst this parameter is believed to have only a secondary effect on air entrainment.

The data of Buonoplane *et al.* [24]also indicate that surface wettability has little or no effect on air entrainment velocities. This explains the relative agreement among most experimental works in which different tape materials were used. The reason is that hydrodynamic rather than surface forces control high-speed coating flows, and then surface wettability may only play an important role at very low speeds, where the dynamic contact angle is close to the static contact angle Inverarity, [26].

Wetting line instabilities due to surface electric charge have been observed by Burley and Jolly [16]. Surface charge was a result of tape high-speed winding. However, Burley and Jolly found that this did not alter the air entrainment velocity, and they could stabilise the interface by grounding their equipment.

2.2.2 Dynamic Wetting in Dip Coating: the work of Blake and Rushak [5].

Decades after the important marker work of Deryagin and Levy [13], Blake and Ruschak [5] repeated the classical dip coating experiments using a transparent and smooth polyester substrate and water-glycerine solutions which behave in a Newtonian manner. The data they obtained on the onset of air entrainment confirmed the observations of Deryagin and Levy [13] and those of Burley and co-workers and Gutoff and Kendrick [17]. They also introduced the term “saw teeth shape” to describe the broken dynamic wetting line and this term is now widely used to describe the dynamic wetting line at break. In addition to measuring the air entrainment speed and how it varied with fluid properties, Blake and Ruschak [5] measured the angle ϕ of these saw teeth formed (see Figure 2.2) at speeds V higher than the value for initial break-up. In performing these measurements, Blake and Ruschak were zooming into the mechanism of wetting and distinguishing between V*, the speed when the first vvv appear sawteeth and V_{ae} when air is actually entrained. By tracking the angle ϕ of these saw teeth, there data, reported in Nature, were effectively measuring the speed of

wetting and they made the remarkable observation that the product $V\cos\phi$ remained constant. Blake and Ruschak [5] termed this component of the speed normal to the straight-line segments of the wetting line, the "maximum speed of wetting" V^*, which they assumed is the maximum speed at which the wetting line can advance normal to itself. Expressed mathematically, at speeds V equal or higher than V^*, the wetting line segments adopt the minimum possible inclination ϕ such that:

$$V^* = V\cos\phi \qquad V \geq V^* \qquad [2.3]$$

In other words, at speeds above V^*, by adopting a saw teeth shape, the lengthened segmented wetting lines continue to wet the solid uniformly until ϕ approaches 90^0; wetting can no longer be sustained and gross air engulfment occurs. This explains why air is first observed to be entrained at the apices of these segments.

This important work seemed at the time to reveal all there is to know about dynamic wetting failure and air entrainment. First, under this scenario, air entrainment appears to be a *consequence* of the break-up of the wetting line, i.e. air through its properties *is not at the origin* of these instabilities. Second, as there was established a maximum wetting speed, no higher speed could be envisaged.

2.2.3 Dynamic Wetting in Dip Coating: the work of Cohu and Benkreira [7]

Cohu and Benkreira [7] revisited the work of Deryagin and Levy [13] and Blake and Ruschak [5] and again collected data that confirmed earlier correlations between fluid properties and air entrainment speed. Interestingly however, they argued that the findings of Blake and Ruschack [5] showing the existence of a maximum speed of wetting imply, through a simple physical argument, that the break-up of the wetting line should be postponed to tape speeds greater than V* provided that the angle β between the tape velocity and the (stable) wetting line is not 90^o. This case corresponds

clearly to the situation depicted in Figure 1.25b., and here the wetting line is expected to adopt a saw teeth shape once the tape speed exceeds V*/cosβ. Cohu and Benkreira [7] carried out experiments under this situation by angling the substrate in dip coating and observed from their data that indeed the expected gain in air entrainment speed, V*/cosβ was in fact realised. This simple but remarkable finding suggests that by angling the wetting line by an angle β, air entrainment speed will increase by a factor 1/ cosβ. This is precisely the lead followed in this thesis but in curtain coating where the die is rotated by an angle β so that to achieve the analogy with angle dip coating. Note that Benkreira and Cohu [12] performed preliminary experiments with a slide die, not in curtain coating mode, and achieved this gain in air entrainment speed. Were it to be achieved in curtain coating where the speeds are much, much larger because of hydrodynamic assistance, then this would make curtain coating indeed the fastest air free coating method, precisely the aim of the present research.

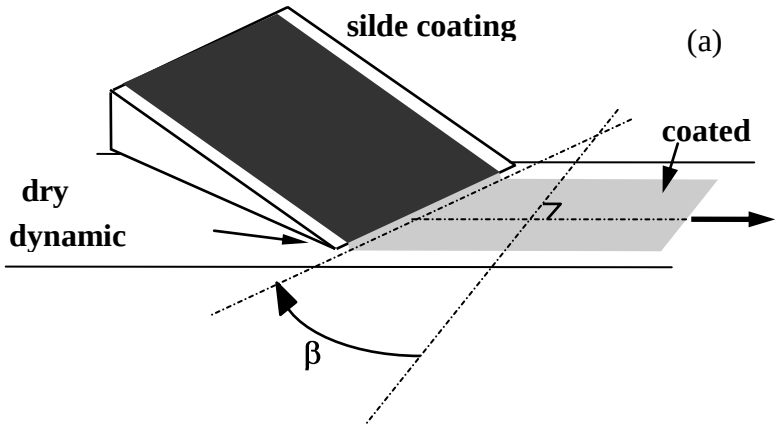

Figure 2.4a: Tilting the slid coating die, Benkreira and Cohu [12]

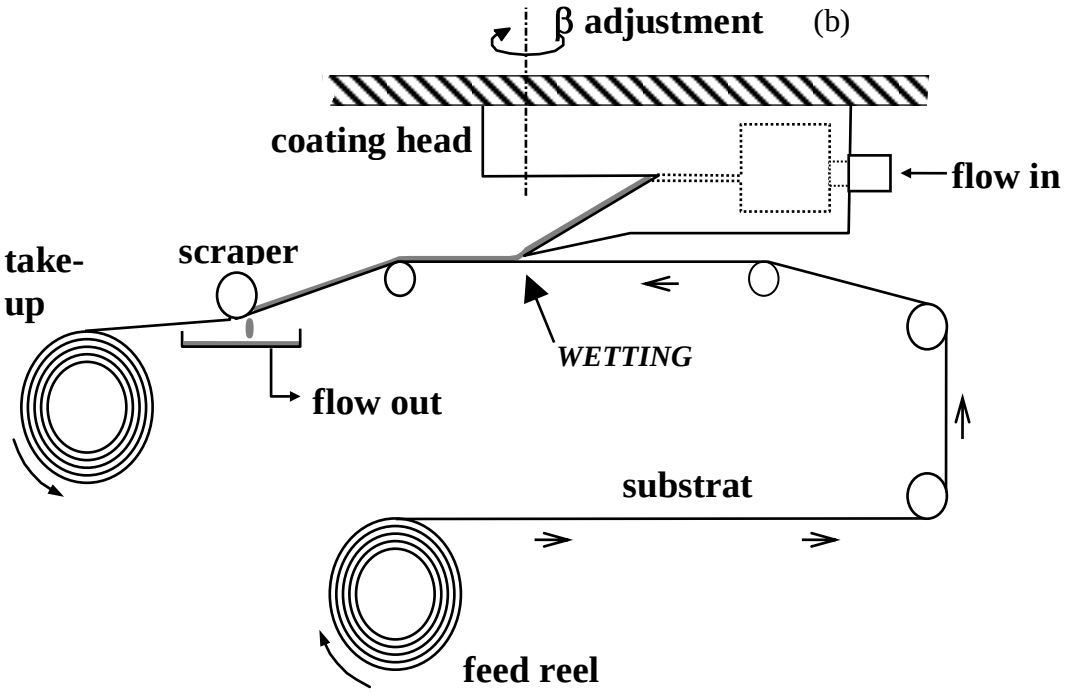

Figures 2.4b: Schematic diagramof slid coating rig Benkreira and Cohu [12].

2.2.4 Dynamic Wetting in Dip Coating: the effect of the gas phase

Until recently, all research in dip coating had ignored the presence of the gas phase when clearly it is at the origin of gas entrainment. If no gas was there in the first place how could it be entrained at any speed! So is it thus that the breaking of the dynamic wetting line is purely a wetting effect unaffected by the gas phase? The maximum wetting speed concept and data brought in by Blake and Ruschak [5] would suggest that it is the case and that *the properties* of the gas are irrelevant in terms of dictating the speed at which gas entrainment occurs. Benkreira and Khan [27] and Benkreira and Ikin [1]sought to investigate the effect of gas properties on air entrainment and dynamic wetting by performing dip coating experiments under various levels of vacuum and with different gases. Their innovative experimental set up which effectively encased a dip coater inside a gas chamber is shown in Figure 2.5.

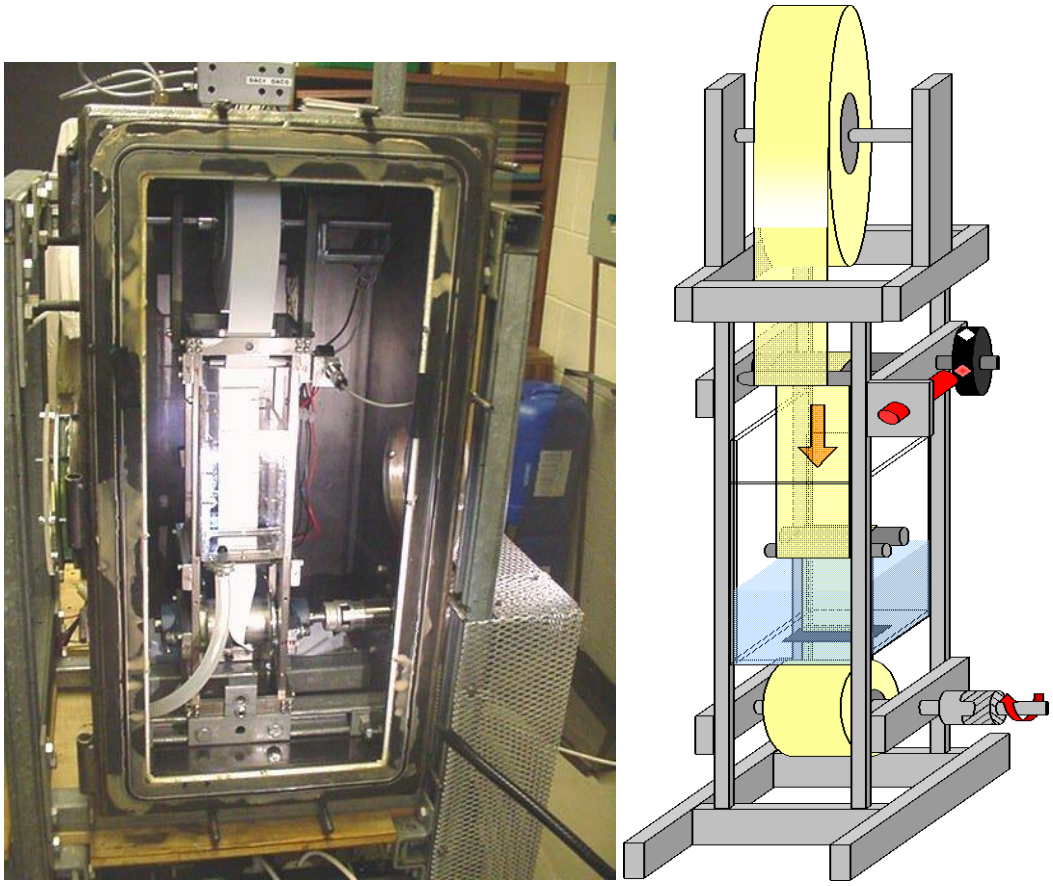

Figure 2.5: Photo & schematic diagram of the dip coating rig at Bradford University, Benkreira [28].

Using this set-up, Benkreira and Khan [27]and Benkreira and Ikin [1] demonstrated that the properties of the gas phase generally do matter and indeed can be manipulated to increase this maximum speed of wetting, V^* and consequently the bubble entrainment speed V_{ae} in the case of air or V_e for a gas. Their key finding is that the viscosity of the gas phase was the important variable that dictated the gas entrainment speed. This important finding and corresponding underpinning data are presented in Figure 2.6. It shows that V_{ae} can be more than doubled from 0.4 m/s to 0.83 m/s Benkreira and Khan [29], when the pressure is reduced from atmospheric to 50 mbar. As air viscosity reduces drastically with vacuum pressure, Benkreira and Khan [29] and Benkreira and Ikin [1] made the link with viscosity which is firmly rooted in

theories of dynamic wetting: see hydrodynamic theories of wetting (Hugh and Scriven, [30]; Voinov, [31]; Cox, [32]; Dussan, [33]) and the "fresh" interface formation theory of Shikhmurzaev, 1977. Except for the molecular kinetic theory of wetting, which considers air viscosity to be irrelevant, both the hydrodynamic and the "fresh" interface theories point to an infinite maximum speed of wetting when the gas phase is inviscid (zero viscosity). Shikhmurzaev for example showed that as the gas-to-liquid viscosity ratio (k_μ) decreases, the contact-line speed corresponding to the onset of gas entrainment increases rapidly when k_μ approaches zero. This research infers that gas viscosity is an important variable in dynamic wetting, particularly if in practice it can be reduced significantly.

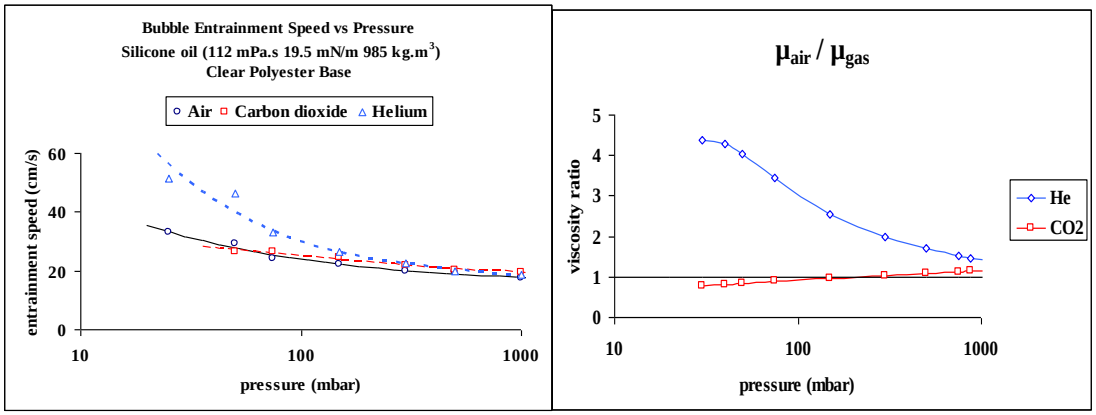

Figure 2.6: Example of saw-teeth wetting line.(Benkreira and Ikin [1])

There is clearly a practical benefit to manipulating the gas properties (viscosity via reduction of vacuum or using lower viscosity gases such as Helium) as this provides coating practitioners with an additional variable to manipulate in their quest to coat at higher speeds to increase productivity. There is also an academic benefit to this finding as it opens up new possibilities to improve or develop further models of dynamic wetting. The situation at present is that there is a huge disagreement between theoretical models of dynamic wetting and this is well reviewed by Blake et al., [14]. Also none of the models actually reproduce measured data; they merely give a trend (see for example,

Shikhmurzaev's predictions, though giving an important pointer to the role of gas viscosity, do not permit a quantification of this effect in the various coating flows available. This is because there are many effects contributing in different forms: coating fluid properties, substrate properties and now gas properties. Even experimentally, these effects can be very difficult to unravel because may be unexpected. Interestingly for example, Benkreira, [28]showed that depending on the viscosity of the coating fluid, V_{ae} measured in dip coating with a rough substrate could be higher or smaller compared to V_{ae} with a smooth substrate. All these observations (see also the work of Clarke [34] with curtain coating) point clearly that air entrainment is a complex phenomenon that involves the properties of all three phases, that is liquid, substrate and gas.

The other, very different, hypothesis on gas entrainment is the one made by Miyamoto and Scriven [35] and based on the experimental studies of Mues *et al.* [36]and Miyamoto [37]. It suggests that air entrainment is not sudden but always and continuously occurring. In the words of Miyamoto and Scriven [35], "a very thin air film is always entrained in low speed coating. It is unstable and then breaks into tiny bubbles that may dissolve and disappear quickly. As speed is increased, a thicker film is entrained that cannot be dissolved. Therefore, what matters is not *whether* air is entrained but *how much*." Miyamoto [37]published strong experimental evidence that when coating by curtain in air at atmospheric pressure, bubbles were temporarily entrained at speeds significantly less than that for visible defects.

The above depiction of the state of modelling of dynamic coating reinforces the importance of collecting accurate and new data in specific coating flows, a research necessity acknowledged by all recent reviews (see Blake and Ruschak [[5]]). This justifies the experimental approach adopted in this research with respect to the all-important curtain coating flow.

2.3 AIR ENTRAINMENT IN FLOWS OTHER THAN DIP COATING

Very few data for the onset of air entrainment in flows other than a solid plunging into a pool of liquid have been published, although the flow fields near the wetting line

may be quite different. This is particularly the case in curtain coating where the fluid impinges on the substrate and work in this configuration is reviewed separately below. In all other coating flows, the dynamic wetting region is very similar to that in dip coating with little "important" flow that is high pressures being developed and the expectation is that similar results will be found. Gutoff and Kendrick [38] considered the limits of coatability on a slide coater, and found that indeed the onset of air entrainment was the same as in dip-coating. Benkreira [39] measured air entrainment in metering roll coating (forward and reverse) and he too found similar air entrainment speed, except when he controlled the inlet flow coming to the nip so that the wetting region will experience strong flow. In such situations, the air entrainment speeds measured were larger, proving that hydrodynamic assistance could also be initiated in flows other than curtain coating. It is important to note however, the effects are not as important as it is very difficult if not impossible to generate strong flows in the dynamic wetting regions of metering coating flows.

One important work directly relevant to the present research is the study by Benkreira and Cohu [12] of angled slide coating which followed from their research of angled dip coating. The experimental set-up is illustrated in Figure 2.4a and b showing a slide die rotated at angle β with the "normal" direction. The results of the measured air entrainment speeds are shown in Figure 2.7 which highlight the influence of β. In this figure the component of the substrate speed normal to the wetting line, Vcosβ, is reported for various film thicknesses, $h = Q/VL$ at the onset of air entrainment. In spite of the scattering of the data, the curves obtained for a given liquid with various die angles β,do superimpose. This shows that the speed which is relevant to air entrainment in slide coating is not the velocity V of the substrate itself but its component normal to the wetting line, Vcosβ. Therefore, as in dip coating (Cohu and

Benkreira, [7]), angling the wetting line with respect to the substrate motion (*i.e.* increasing β) increases air entrainment velocities by a factor 1/cosβ regardless of any other parameter. These findings are the stimulus of the present research, which is to assess if the same concept applies in the complex curtain coating flow, which has hydrodynamic assistance.

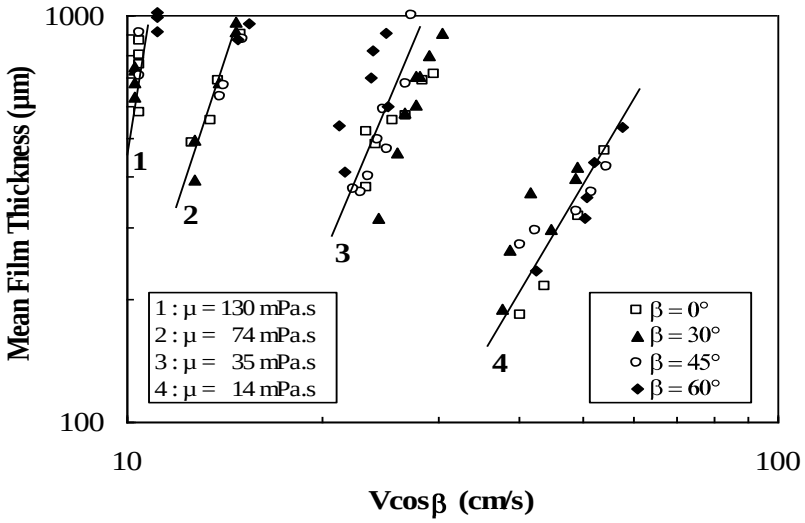

Figure 2.7: Air entrainment velocities with respect to the wetting line in Angled Slide Coating. The viscosities μ of the liquids used are indicated in the legend. Benkreira and Cohu [12]

2.4 AIR ENTRAINMENT IN CURTAIN COATING

2.4.1 The Broad Features and Design and Operation Challenges

This is the flow known amongst all coating flows to be able to coat air free at much higher speeds. For this reason and because it can be constructed to operate in multilayer form, it is the flow by excellence in the photographic industry. The photographic industry connection explains the eminence of scientists from this industry in dynamic wetting, Blake, Ruschak, Gutoff and Scriven's sponsored work. Blake *et al.* [14, 40, 41]at Kodak demonstrated the ability of curtain coating (fig.35) to

operate air free at speeds of up to 10 m/s when all other coating flows can barely reach the 1m/s mark. The reason for this higher performance as Blake et al [14] explained is due to the hydrodynamic assistance of the liquid curtain as it impinges onto the substrate (see Figure 2.8a and b). The curtain coating flow is complex and presents several zones as illustrated in (Figure 2.8b) interlinking to produce the final film on the moving substrate.

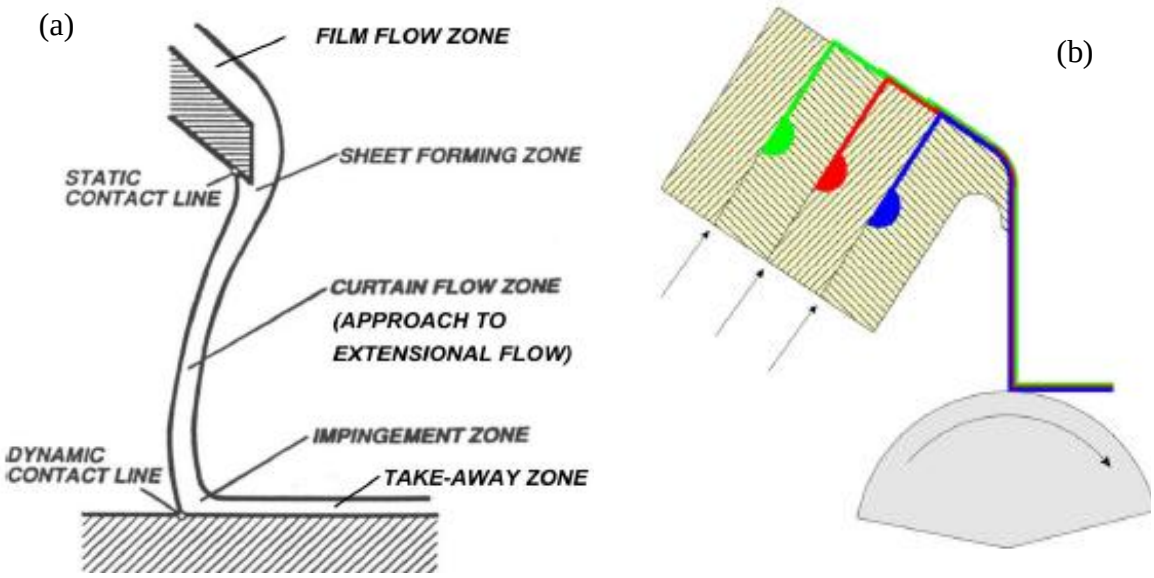

Figure 2.8a and b: Flow zone in curtain coatingHyun Wook Jung et al, [11] and

Schweizer [9] Clearly as can be observed from the above Figure 209a and b drawn in 2D, the flow uniformity in Practice is also required in 3D - that is a very good die is required to deliver a uniform film across the width of the substrate. Also this uniformity of flow must be maintained all down the curtain to create a uniform hydrodynamic assistance across the web. Large curtain heights are desirable for effective hydrodynamic assistance (we shall discuss this important feature later) and they are not in practiced easy to achieve as the curtain contracts because of surface tension acting on the edges causing the tendency to "neck in" and form a thread rather than a sheet. Technological solutions (tricks as known in the trade and carefully

patented, see example of a design in Figure x) are thus required to operate curtain coating so that hydrodynamic assistance is at play. One simple solution is to run a large surface tension stream of liquid (water) on the edge guides but even this which in principle would solve the problem requires the design of carefully positioned edge guides to trickle a minute flow of water at the edges and permit operation over a full range of flow rates and curtain heights to produce the required thickness of film at high speeds.

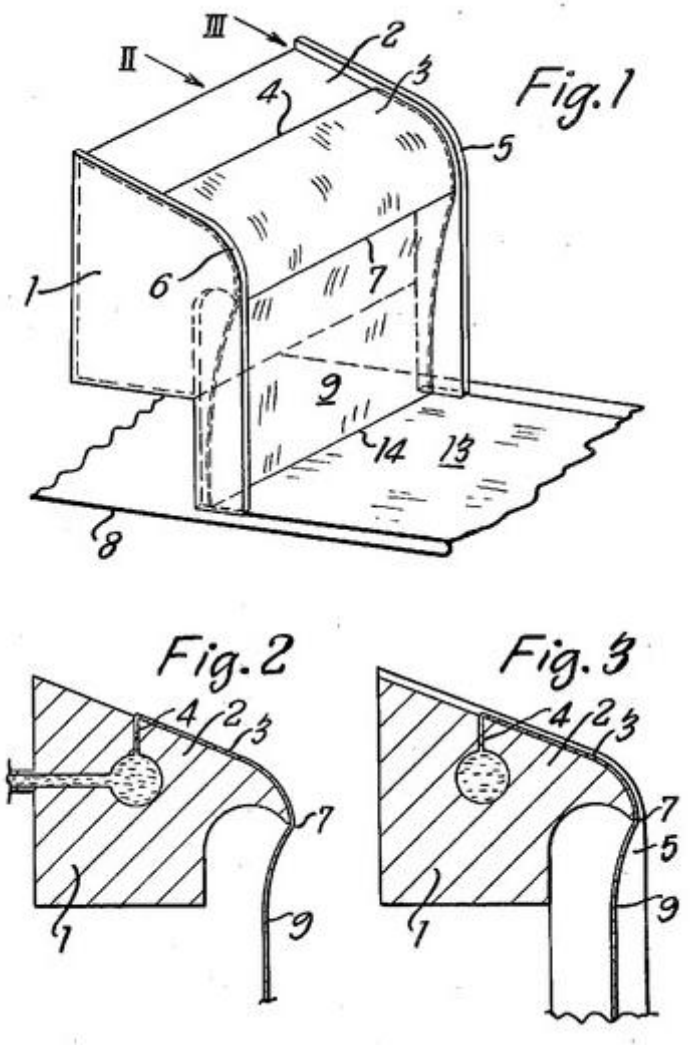

Figure 2.9: Curtain coating die and edge guide US4135477

These mechanical features are noted here to explain that the design and operation of a curtain coater in an academic laboratory is challenging. The set-up used by Blake et al

at Kodak (see Figure 2.9) demonstrates the challenges. The requirements are: a good die that delivers uniform flow across the web, a pumping system that does not pulsate so that the flow remains uniform in time and edge guides so that the curtain is maintained. This may be the reason why no experimental research work in "real" (i.e. with a fresh dry substrate) curtain coating has emanated from university academics. This justifies the research challenge taken by the present research: to build and operate a real prototype curtain coating rig that can produce hydrodynamic assistance over a wide range of die flow rates and curtain height. There have been alternative approaches, using for example a flow from an orifice die or a narrow die placed above a rotating cylinder to simulate dynamic wetting in curtain coating (further details later as illustrated in Figure 2.10). This clearly removes the important consideration that the substrate is always dry in curtain coating whereas with a rotating roller a thin wet layer will always persist even if the roller is scrapped cleaned.

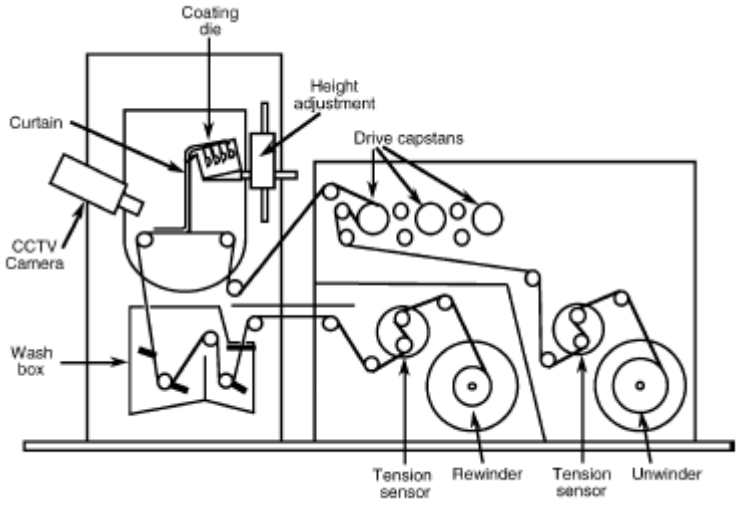

Figure 2.10: Schematic diagram of apparatus used for curtain coating experiment by Blake et al [40]

2.4.2 PRIOR EXPERIMENTAL RESEARCH FINDINGS

Having explained the important features of curtain coating, we now review work in relation to the evaluation and assessment of air entrainment velocity, which is the prime consideration of the present research and this is in order to develop a basis from which to make comparison with the findings of this research.

The first consideration relates to the range of flow rates that can be produce and the stability of the curtain as without it no uniform coating can proceed. One of the first papers on curtain coating is by Brown [42]who described with the aid of experimental observations the basic dynamics of a falling sheet. Essentially, he observed that the sheet is in free fall for the majority of the curtain and to remain stable to disturbances provided that the Weber number (which represents a balance between inertia and surface tension forces)should be greater than unity :

$$We = \rho q V / 2\sigma \geq 1 \qquad 2.4$$

In this equation, q is the volumetric liquid flux, V the local fluid velocity, ρ the density of the coating fluid and σ its surface tension. Conversely with this equation, if a free edge or hole occurs where *We* < 1, the curtain disintegrates into a series of vertical liquid threads as demonstrated by Pritchard (1986). Clearly according to this criterion, there will be a minimum q below which curtain coating cannot operate in a stable manner to lead uniform films. In practice, the minimum flow rate per unit width of substrate is about $1cm^2/s$. Therefore if the wet film thickness required is 10 microns, a web speed of 10 m/s or larger is required and this explains why curtain coating *must* be a high speed coating method. And the question how is it that it can driven at such high speed compared to dip coating which as we discussed earlier barely reach 1m/s?

The second consideration addresses precisely this question and centers around the concept of hydrodynamic assistance. Explained simply, the inertia of the falling curtain causes the wetting line to be stabilised and pinned thus not breaking and letting air to be entrained until at very high substrate speeds. Immediately, we observe that for this pinning to be at its most effective, the curtain impact on the moving substrate must be positioned appropriately. This is precisely the subject of many research studies all agreeing that this positioning is when a heel just begin to form at the foot of the curtain. The data in Figure 2.10, taken from the original work of Blake et al [40] demonstrate this very well. It shows how for a given flow rate (the y-coordinate in the Figure 2.11) the flow at the foot of the curtain changes as substrate speed (the x-coordinate) is varied. The curve in this graph delimits the condition for the onset of air entrainment and displays, a minimum flow rate below which the curtain is unstable and an optimum curtain flow rate that gives maximum air entrainment speed, U_{max}. We see from the illustrations in the figure that this corresponds to the situation where a heel is just about to form.

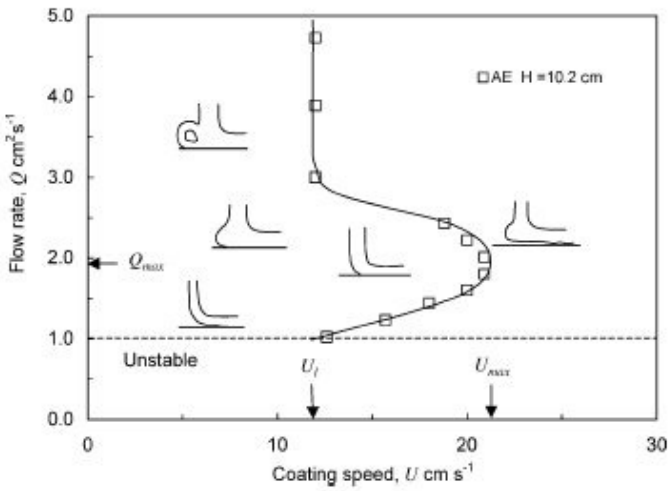

Figure 2.11: Map of coating speed U at the onset of air entrainment (AE) against linear flow rate Q for a curtain height H = 10.2 cm. Blake et al.,[40]

To reinforce and quantify the extent of hydrodynamic assistance on the air entrainment velocity it is helpful to compare the speed achieved in curtain coating with those in dip coating. Figure 2.12 taken from the review by Yamamura [43] explains this very well. It shows that by carefully operating curtain coating at optimum flow rate, the air entrainment speed is 5 times that which limits dip coating.

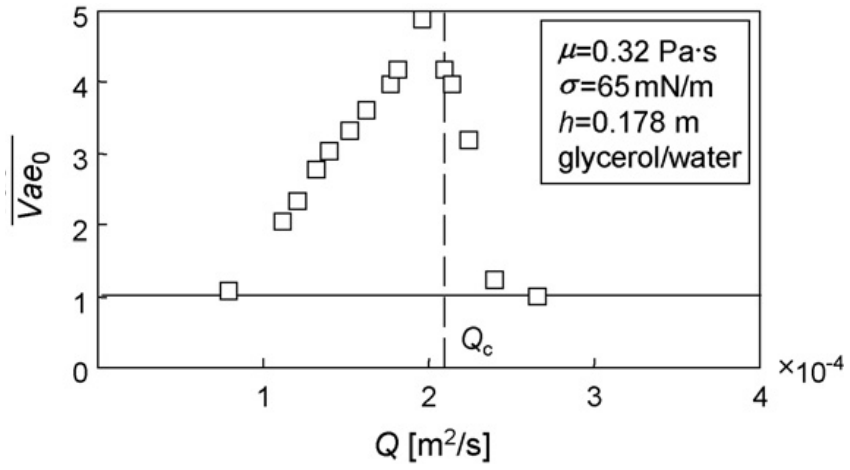

Figure 2.12: Onset velocities of air entrainmentin in curtain coating Yamamura [43]study the hydrodynamic forces acts on the contact line to delay the onset of air entrainment to highrerspeeds near the criticcal flow rate Qc.

As the figure on the various flow regimes just presented lacks clarity, we have reviewed the literature and summarised the important features of the curtain coating window in Figure 2.14. At low flow rates (below 10^{-4} m^2/s according to Blake *et al.*[40], the curtain is unstable and the liquid falls as spatially peridiodic streamers or even dribbles off on the substrate (region 1 denoted in Figure 2.14). At high flow rates and low speeds, a large heel containing regions of recirculation forms at the base of the curtain (region 2). Because in such cases the dynamic wetting line is isolated from the curtain, the air entrainment velocity is low and of same order as in dip-coating (i.e. here there is no hydrodynamic assistance). As the flow rate decreases, the dynamic wetting line moves towards the rear plane of the curtain and the air entrainment

velocity increases (region 3). At even lower flow rates, the wetting line is located downstream the plane of the curtain (region 4), which results in a decrease of the air entrainment velocity. Both Figures 2.11 and 2.12 show clearly that hydrodynamic assistance is not simply a matter of increasing flow rate. Rather it is that flow rate, Q_{opt} which results with the largest inertia being applied on the dynamic wetting line. Finding it experimentally requires careful manipulation of both coating speed and flow rate. In this regard Clarke [45] work of visualising the flow at the foot of the curtain using particle tracking velocimetry see Figure 2.13 is very insightful and underpinned the idea that for hydrodynamic assistance to be at its most effective, the impinging curtain flow must be in line with the dynamic wetting line.

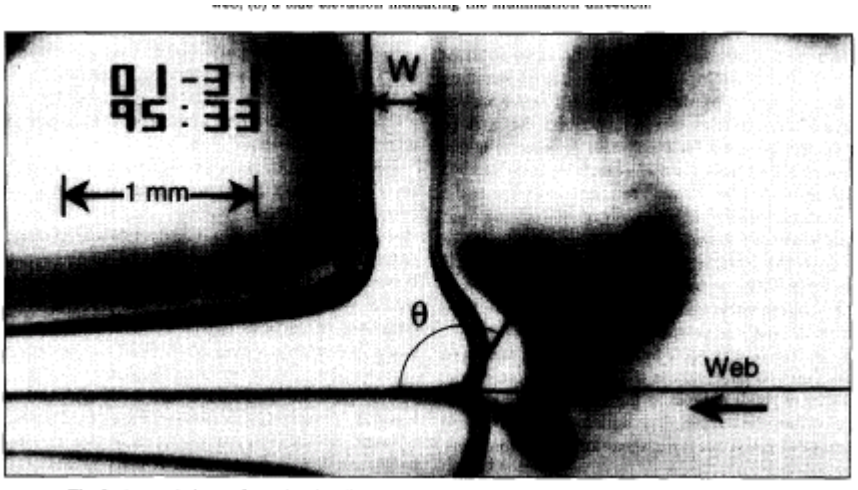

Figure 2.13 : A sample image from the visualisation experiment showing the key features of the flow field and the curtain is shown having a width W and dynamic contact angle is θ. Clarke [45]

Another feature of the coating window, later revealed (see the work of Marstonx) is the existence of a region of air entrainment hysteresis, which results from the interplay between hydrodynamics and wetting. When this occurs, the critical velocity of interest is that where air entrainment clears as the substrate speed is decreased (the bold line in figure 2.14). In that sense, the experimental way of

measuring the air entrainment velocity in curtain coating differs from that we used in dip- and slide coating, where the onset of air entrainment is determined by *increasing* the speed until the break-up of the wetting line could be observed.

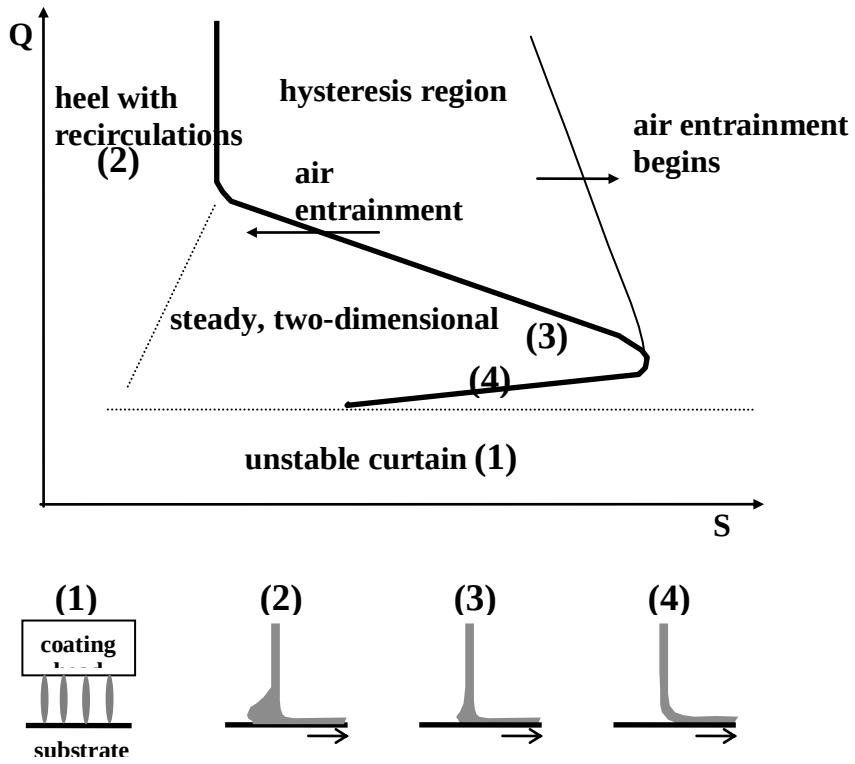

Figure 2.14: Schematic operating window and flow fields of the impinging curtain coating.

These observations regarding how the flow at the foot of the curtain affect air entrainment speed have been reproduced by Yamamura et al. [46] in the simple situation of a jet impinging onto a roller scrapped as clean as possible to mimick a dry substrate in actual curtain coating operation. The experimental set-up used and the flow observations made are shown in Figure 2.15.

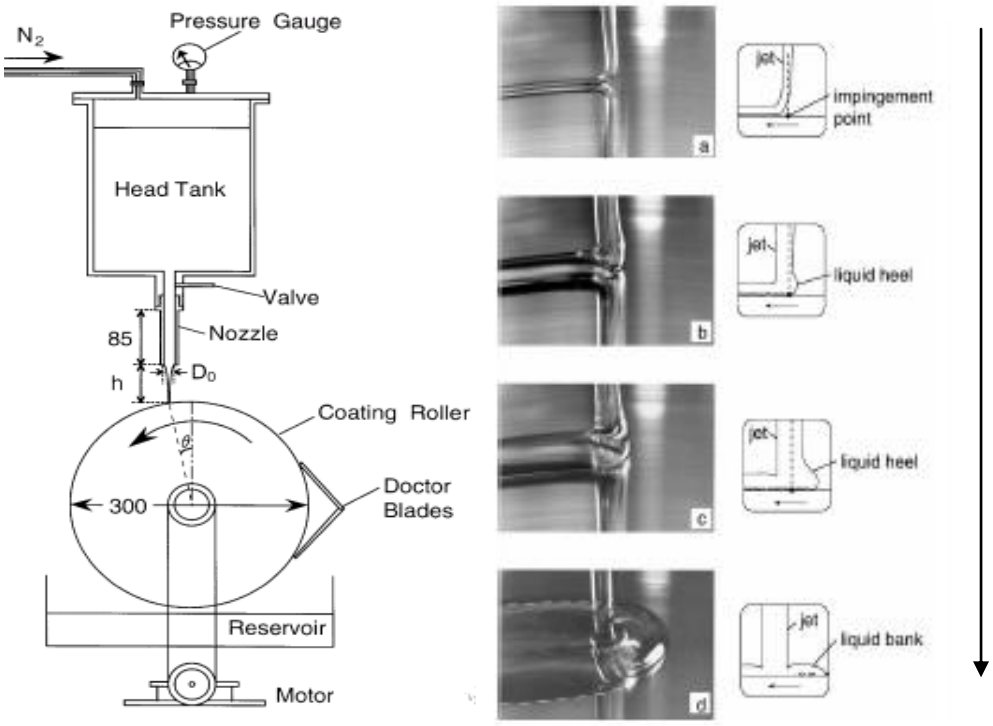

Figure 2.15: Shows the shape of the liquid film at point a-d. Yamamura et al [46].

The corresponding data on air entrainment collected by Yamamura et al [46] are now presented in Figure 2.16 (difficult to reproduce clearly). The important point to note is that the regime where a heel is just beginning to form (regime b in their figures) is the optimum curtain flow rate leading to maximum air entrainment speed

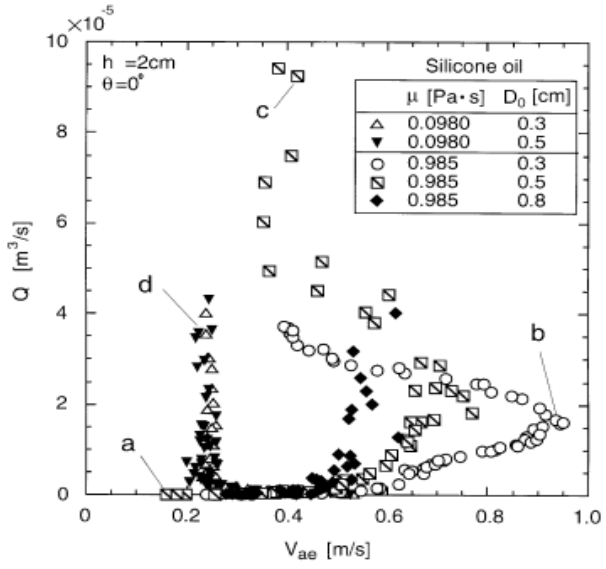

Figure 2.16: Data of air entrainment velocity for different nozzle diameters. Yamamura et al [42].

Having explained how hydrodynamic assistance best occurs in relation to positioning of the curtain and the dynamic wetting line, we know examine the design and operating parameters that can be manipulated to tune this assistance. Thinking of it in terms of inertia, the first parameter must be curtain height as the curtain is in free fall. Indeed all the work to date see original data of Blake et [40] and Yamamura et al [42] confirms this point. Figure 2.17 display the data of recent work by Marston et al [47] and illustrate this aspect very well.

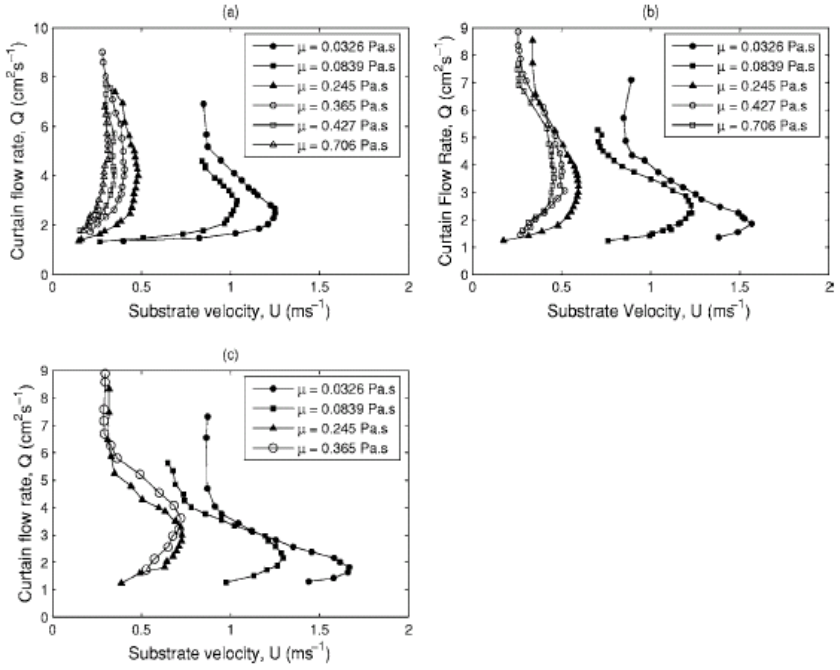

Figure 217: Air entrainment curves for three set height: (a) 35 mm, (b) 65 mm, and (c) 85 mm low viscosity, the viscosity in Pa.s. Marston et al. [47].

Turning our attention now on fluid properties, the work in dip coating reviewed above suggested that coating fluids glycerol solution viscosity is a limiting factor, that is decreasing viscosity is beneficial to operating at higher speeds before air entrainment occurs. Until recently, the research carried out in curtain coating has been undertaken with low viscosity fluids and the data obtained showed that indeed

reductions in viscosity are beneficial. This point is well made from the data in Figure 2.17 above just presented. However recent work by Blake [40] with a glycerol-water solution of 0.32 Pa.s (much higher viscosity than in any other prior work on curtain coating) that air free operation could maintained without limit in air entrainment speed. Blake et al data (Dobson and Ruschak,) [40] are shown in Figure 2.18 which show that with a curtain height of 25.2cm, the operating speed achieved is approximately 100 times that limiting dip coating! Blake et al [37] explain this unusual behaviour by suggesting that an intense hydrodynamic assistance regime could be found even with viscous fluids. Although further research is required to elucidate these recent data, hydrodynamic assistance has been shown to be induced by other mechanisms. In another research, Blake et al [48] showed that they could create intense hydrodynamic assistance by using electrostatic forces to pin down the wetting line. They explained that the electrostatic field at the dynamic wetting line generates a force, which acts normally to the lower free surface where the liquid is conductive. This pressure force enhances wetting by reducing the dynamic contact angle thus postponing air entrainment to higher speeds. Their data, presented in Figure 2.19, shows that by increasing the applied voltage they could double the air entrainment speed compared with that observed in dip coating. A similar electrostatic assistance in curtain coating as well as in slot coating has been demonstrated by Fermin et al. Another method of realising hydrodynamic assistance has been demonstrated by Benkreira in dip coating. Their data are displayed in Figure 2.20 and reinforces the many ways in which hydrodynamic assistance can be generated. This brings us to the present research which seeks to develop a new- equipment design method-to realise further hydrodynamic assistance in curtain coating.

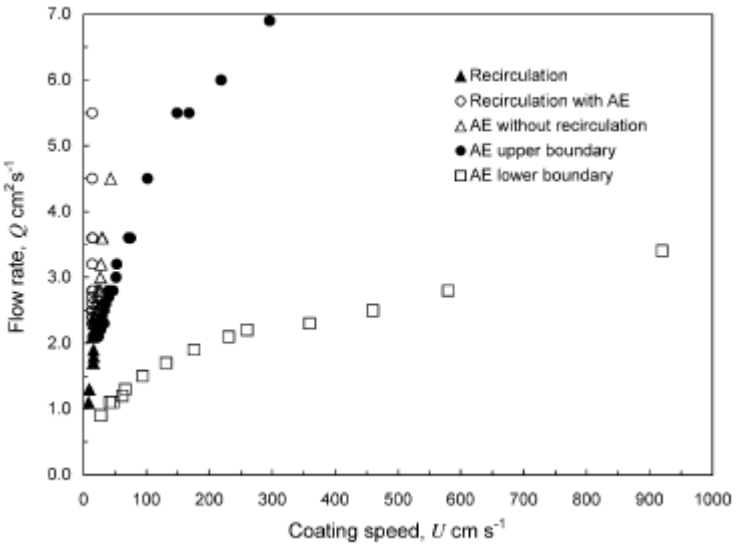

Figure 2.18: Map of coating speed U at the onset of air entrainment versus flow rate Q for a 25.2 cm curtain. Blake et al [37].

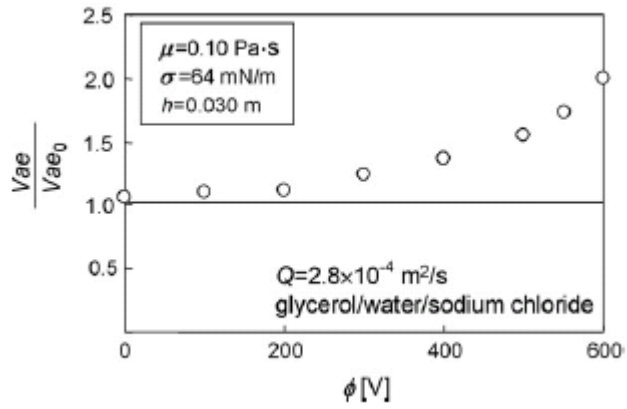

Figure 2.19: Onset velocities of air entrainment in curtain coating on charged surface. Blake et al [48].

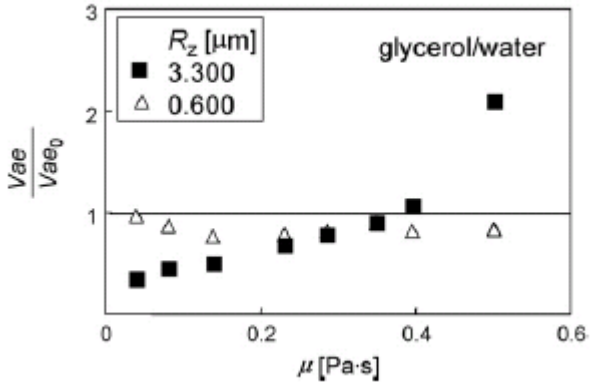

Figure 2.20: Onset velocity of air entrainment in plunging tape flow on a rough surface. Benkreira [28]

2.4.3 Previous Theoretical Research Findings

In the above review, the gain in air entrainment speed was attributed to hydrodynamic assistance causing the impinging flow at the foot of the curtain to be directly located on the dynamic wetting line. Thus, as a boundary layer must form on the moving substrate, the flow situation is as depicted in Figure 2.21.

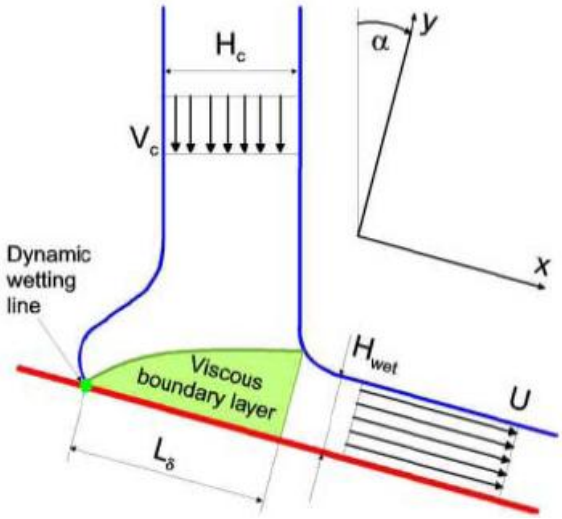

S

Figure 2.21: Schematic diagram of curtain coating impingement zone, Blake et al. [44] .

Where is :

- U = web speed
- V_c = curtain speed
- H_{wet} = wet film thickness
- H_c = curtain thickness
- L_δ = length of boundary layer
- Ά = impingement angle[1]

The area of interest is the boundary layer zone of length L_δ, starting from the dynamic wetting line where the curtain hits the substrate and is being entrained by it and finishing when the flow is fully developed and moving on the substrate as a film at uniform speed S. Now, as this boundary layer is in the wetting line zone, it, suggests that its length is central to the problem. Clearly the shorter it is, the quicker the flow will develop and the less likely it will give rise to air being entrained at that speed. This is precisely what Blake ([48]) argued proposingthat there must be an optimal boundary layer length that leads to the highest hydrodynamic assistance. Following this simple argument and using a semi-empirical approach, Blake computed L_δ following classical fluid mechanics approach and obtained the following expression for the boundary length:

$$L=3H_{wet}/20\ [\rho Q/\mu][(3+2\varphi)/(1+2\varphi)] \qquad \text{with} \qquad \varphi=\delta \sin\alpha$$

2.5

In this equation H_{wet} is the final film thickness formed on the substrate, and φ is the component of the curtain speed, S, on the direction of motion of the substrate. It is effectively dictated by the angle α at which the substrate is positioned with respect to

[1] The impingement angle in curtain coating is the angle that the substrate makes with the horizontal and must not be confused with the angle β, the angle by which the die is rotated.

the impinging curtain. When the curtain and the substrate are positioned at right angle, φ=0. L can be suitably non-dimensionalised as using the curtain thickness and the inclination angle or:

$$l=L/\cos\alpha\ /W \qquad 2.6$$

Having calculated *l*, Blake et al [14]proceeded to compared it with the optimum *l'*, which gives rise to the largest hydrodynamic assistance. At this is a difficult task to carry out mathematically, Blake used the data that gave the largest air entrainment speed, S' and obtained a series of *l'* for all his data. He now had all the information required to test if the data fitted in a master curve of S/S' against *l*/*l*'. As shown in Figure, the fit is excellent supporting the concept that the optimum positioning of the curtain flow on the substrate is central to hydrodynamic assistance.

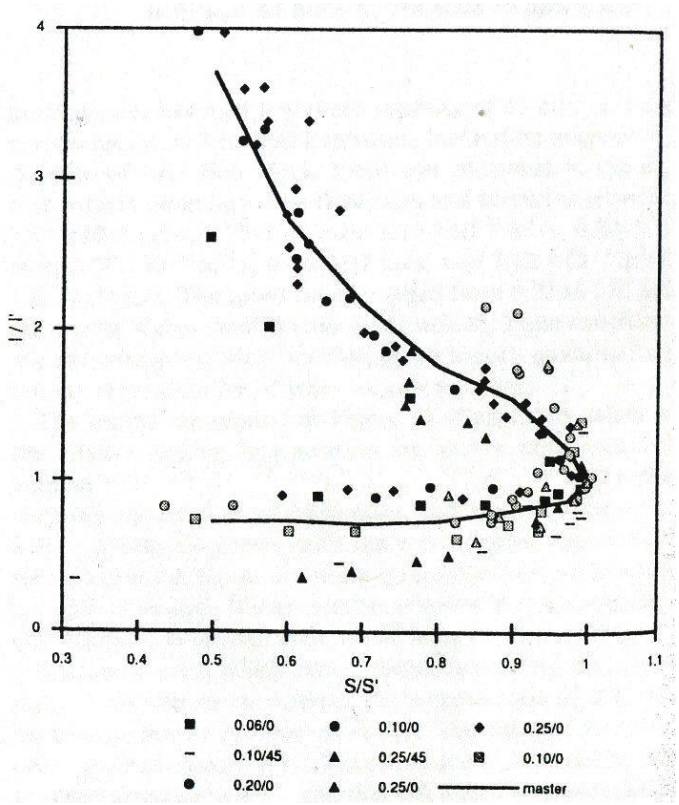

Figure 2.22: Data for the clearing of air entrainment plotted as normalized relative wetting line position vs. normalized speed. Blake and Clark [14].

Reviewing further this approach, Yamamura [42] used Blake's data and computed from the same boundary layer model the critical Reynolds number at which the contact line is directly located beneath the impinging liquid. As Re_c can be defined as $R_{ec}=(\rho Q/\mu)(S/S')$, by substituting the data and the measured air entrainment speed S', Yamamura could check if that led to the optimum flow rate used which he found to be true. Thus we can say clearly that the idea of hydrodynamic assistance being equivalent to the contact line being located beneath the impinging liquid is verified both theoretically and semi-empirically. We have yet to develop a full model, which can at the outset prescribe the optimum conditions from operating and design variables.

CHAPTER 3: EXPERIMENTAL METHOD

3.1 INTRODUCTION

As stated in the introductory chapter, this research seeks to assess the validity of the theoretical concept of angling the dynamic wetting line in curtain coating. This aspect of curtain coating has never been tested experimentally before and it required the development of appropriate equipment, essentially a curtain die that could be rotated to vary the angle of interest with the substrate. The literature review showed that mimicking a substrate with a rotating roller was perfectly legitimate as the roller system reproduced the essential features including the air entrainment limited coating window. However, with a roller system, situating the die so that it is angled with the roller (cross axes) would have "bended" the dynamic wetting line (see Figure 3.1) hence the need in our study to use a flat substrate. A curtain-coating rig with fresh substrate as operated with Blake and colleagues at Kodak would be an ideal system. This arrangement, for a comprehensive experimental programmer of the type required for a PhD study, however would result with thousand of meters of substrate and a hundred of liters of coating solution being wasted, hence here the choice of a looped substrate configuration, i.e. arrange the substrate to continuously go around and being scraped clean before re-entry in the coating flow to simulate an on-line operation. The arrangements here are a sort of middle ground between a fresh flat substrate and the roller experiments. As curtain coating is a fast coating technique, the substrate will be driven in excess of 1m/s and maintaining the substrate straight on the line could be problematic. At the outset attention to the design and operation of the substrate drives was very important. The other critical aspect is the die, which by necessity must deliver uniform flow and a curtain that does not break as explained earlier. Finally, there is the important aspect of developing a technique to view and detect air

entrainment consistently. This is difficult when the speeds are high and this will be a challenge of this research. There are other experimental aspects to consider: the pumping of the coating fluid to the die which must be carried out smoothly to ensure uniformity in time (no pulsing) of the flow and the practicality of handling, removing and disposing the thousands of meters of wetted substrate as a result of the experiments carried out. Finally and equally important is the preparation and characterisation of the coating fluids used. In this research, we have used simple Newtonian fluids of varying viscosity and surface tension but also industrial coatings, paper coating solutions which are non-Newtonian. The reason for using paper coating solutions was to assess the potential for coating these in curtain coating which is a non contact coating method compared to the classical method of coating paper via blade coating. It is important to state at the outset that the bulk of the experimental programme concentrate on the Newtonian fluids to take into consideration the important effect of varying viscosity.

In this chapter we will present and describe all these experimental aspects as well as the operational procedure including calibration methods. [Please note that we may refer to the substrate as a belt or a web to avoid repetition].

Legend for the plan of the curtain coating rig in Figure 3.1 shown below:

1- Bearing of the rollers	12- Outlet
2- Web guide system	13- Major scraper
3- Rollers	14- Catch tray
4- Drive roller	15- Stirrer
5- Rig	16- Coil
6- Halogen lamp	17- Pump
7- Curtain clot die	18- Temperature control
8- Die angled	19- Mixing tank
9- Camera	20- Tension control
10- Computer	21- Cooper rod
11- Idler roller	

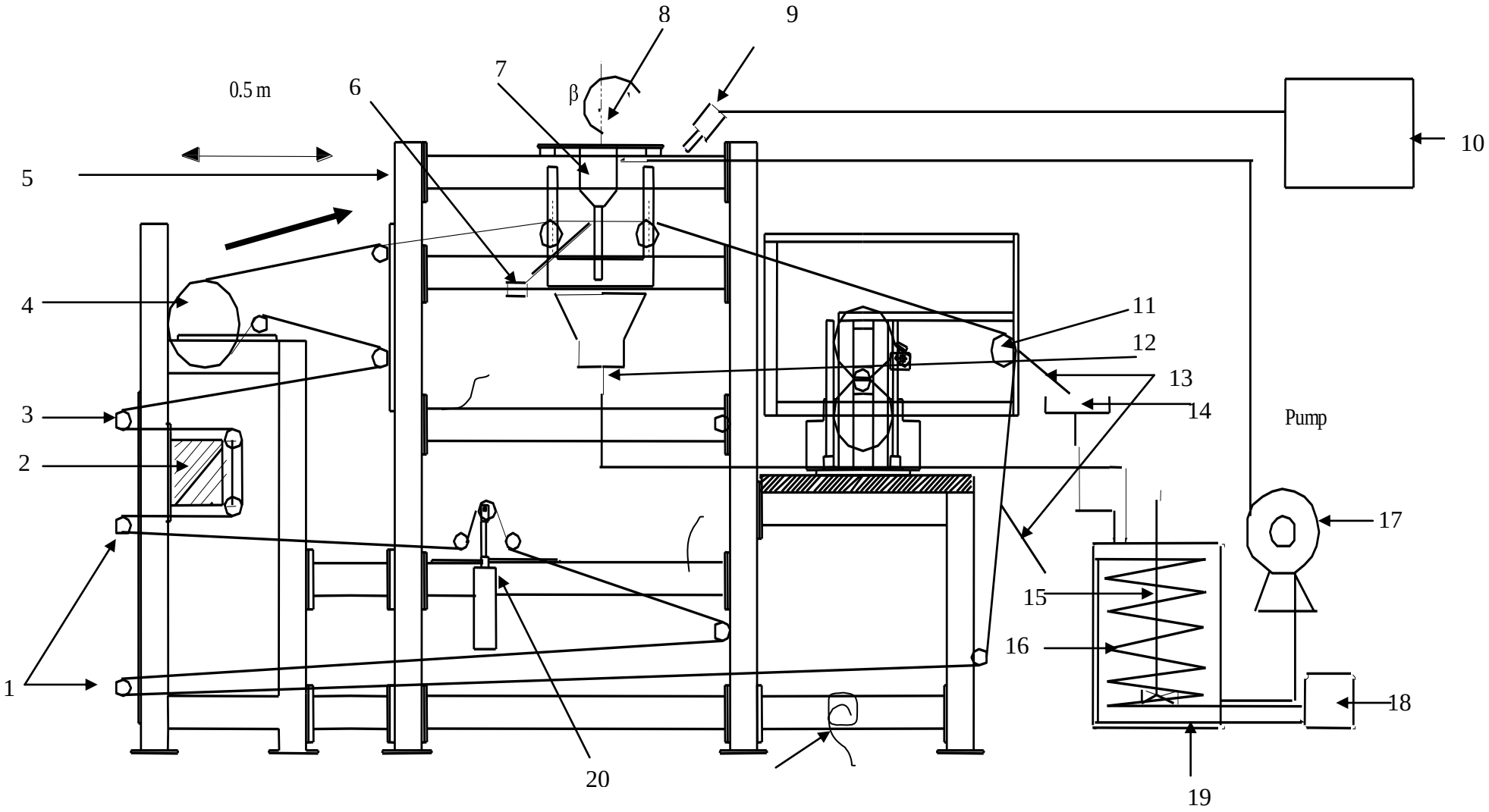

Figure 3.1: Plan of schematic representation of curtain coating rig (Bradford University, Rheology and coating Lab).

3.2 CURTAIN DIE AND FEED SYSTEM

Curtain die, as explained earlier, must be designed to deliver a stable and uniform sheet of fluid that can be deposited at speed onto a moving substrate situated 0-20cm below. The requirements of a uniformity across the width and stability down the length of the curtain made such that the design had to be carried out in collaboration with a curtain die provider, Troller & Co AG, Switzerland, renown in the field. The die, essentially a long cylinder-slot-cylinder-slot device (see Drawing of the die Figure 3.1), was constructed from stainless steel and has four parts, namely the lower die half, upper die half, side plate with feed slot and edge guides. The two cavities-slots designed ensured the uniformity of flow across the width and the edge guides the stability along the height of the curtain. The design and operation parameters of the die were:

Coating thickness: 10- 100 micron or 10-100 gr/m^2 mass flow rate

Coating width: 200 mm

Die gap: 250 μm

Heating and cooling rate: 1 °C/h

Figure 3.1 shows the die complete with all its parts and assembled and Figure 3.2 show design features, including the edge guides. With regard to feeding the die, this was arranged with a pump withdrawing the coating solution from a tank that had a temperature-controlled coil inside it (see Figure 3.1). In order to deliver flow within a wide range and at the accuracy required (± 1%), an inverter controlled gear motor hydraulic pump (model HCD Chementz Germany) was used together with an in-line filter to retain any solid contaminant in the pumping loop. Temperature control in curtain coating is very important to not only to control the operation of the die which has a 250 microns gap and where high pressures are developed but also maintain the

properties of the coating solution constant. Thus the coil which was inserted in the feed tank was connected to an open loop refrigerator temperature control system (HAAKE) able to maintain a constant temperature in the tank to an accuracy of ± 0.2°C. As the coil was sitting in the tank, an agitator (HYNAV) rotating at low speed continuously mixed the coating liquid to ensure uniformity of temperature throughout. Now, as the curtain coating experiments were to be operated at a wide range of flow rates, an accurate calibration of the flow rate delivered by the pump was necessary. Thus a calibration of the pump at different set points for each liquid at a set temperature was performed by collecting and weighing volume collected to establish the flow rate delivered to the die. The results are tabulated in Table 3.1-3 with further data shown in **Appendix 1.**

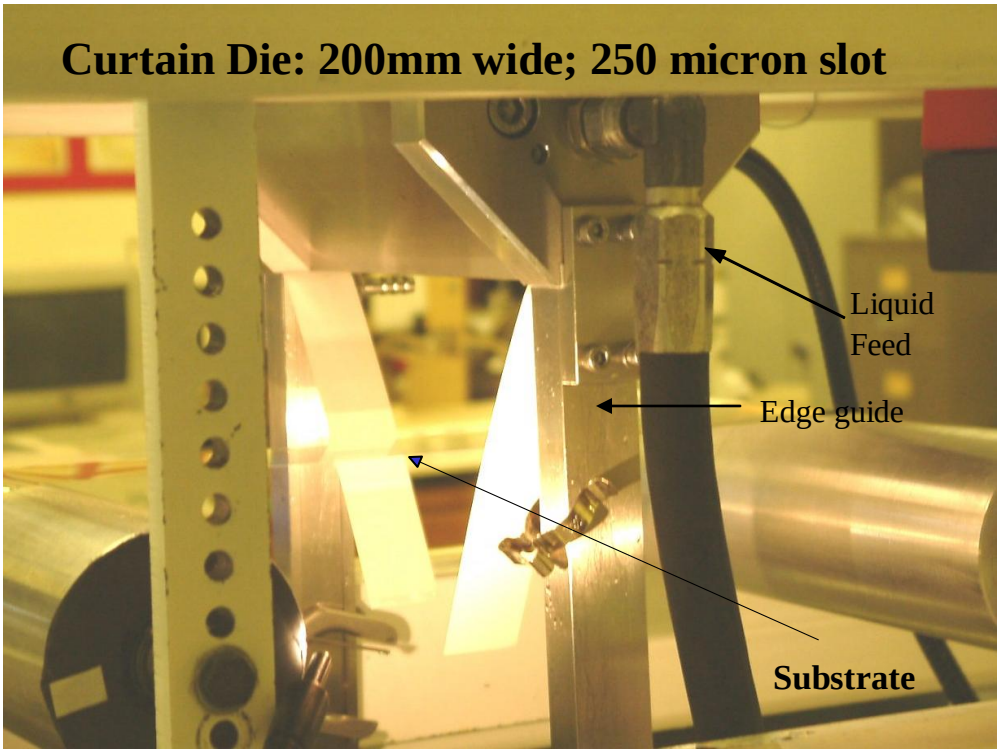

Figure 3.2: Main feature of curtain slot die**.**

3.3 THE CURTAIN COATING RIG AND SUBSTRATE DRIVE

Having described the curtain die and the feeding arrangements, we know describe the substrate handling aspects and then how the curtain die is positioned in the rig to give flexibility in the control of die angle and height. Figure 3.4 gives a schematic of the complete rig.

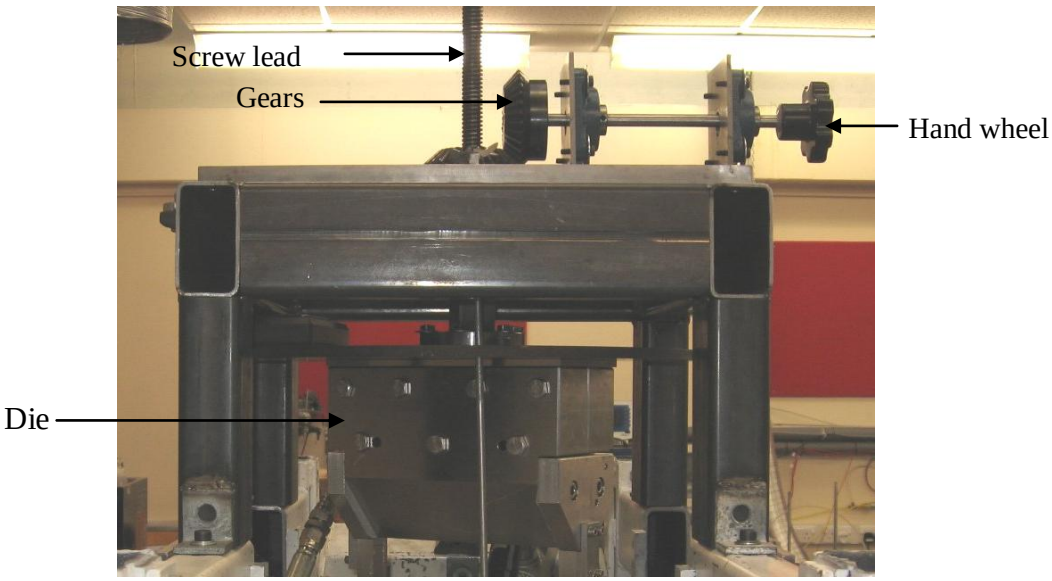

Figure 3.4: Improvement of curtain coating height adjustment.

3.3.1 SUBSTRATE HANDLINGS

One difficult design and operation feature of a curtain coating rig is handling the high speed which are inherent to this particular coating operation and which may reach speeds of 15m/s. Clearly maintaining the substrate loop moving in the system straight for sufficient time to perform the coating and visualization experiments is the challenge. As the speeds are large, if not operated and maintained long enough, this aspect can lead to loosing the substrate and having to loop it again and again and possibly not being able to perform any meaningful coating experiments.

Note that a tachometer (Compact Model CT2) with an accuracy of 0.05% was used to measure the roller speed and thus the substrate speed. Further details will be presented later.

Web Guiding System

Curtain coating is the fastest coating process and in order to keep the substrate loop in the centre of the rollers during the coating operation, it was necessary to use a web guiding system. The web guiding systems consisted here have a pivoting frame (ELGUIDER DRS 227), which was designed especially to drive and control a small width of web, typically less than 30cm. With the provision of an ultrasonic edge sensor (type FX45), the guiding system (see Figure 3.5) could change the guiding directions (in and out) and make correction to the web direction and thus avoid loss of path or creasing of the substrate loop.

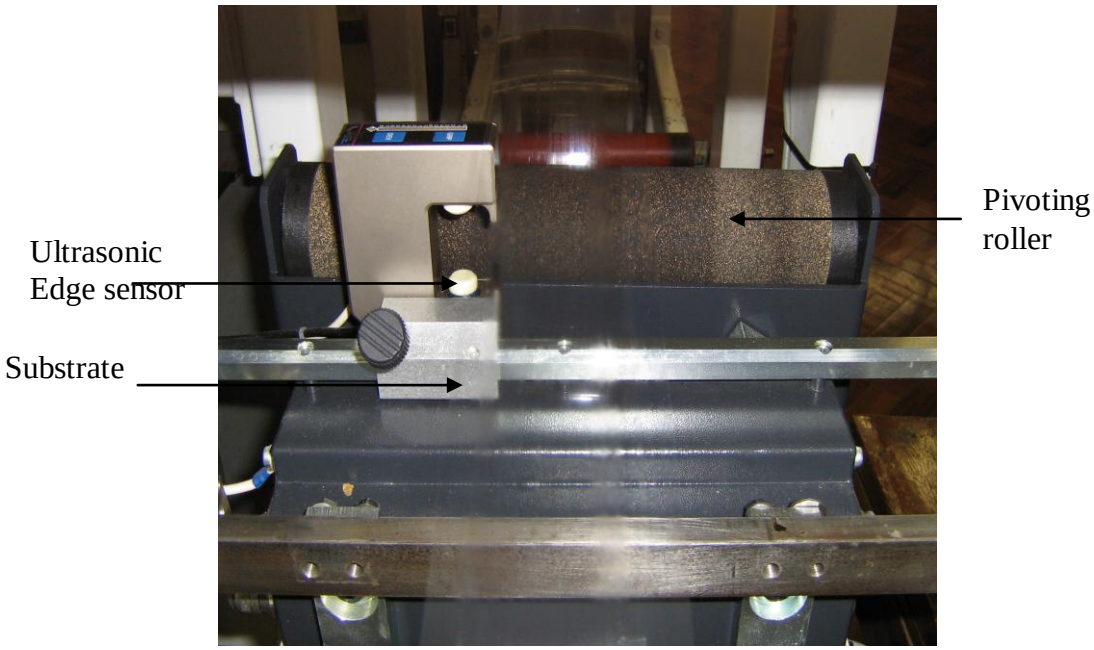

Figure 3. 5: Web guiding system.

Web Tension Control

A condition of keeping the substrate loop moving around in a straight line is the maintenance of a good tension and this was achieved with two pneumatic cylinders and a drive roller connected to a metal bar to push it up and down depending on the tension required (see Figure 3.6). In this context it is important to place the drive roller tensing the web at a lower position when the ends of the belt forming the substrate loop are joined together. The joining of the belt must be straight and strong enough to withstand the tension. To make sure it is straight, before joining two ends of substrate, they are made to overlap by about 0.5 m. Also to ensure a good strength of the joint, several layers (5) of adhesives are put around.

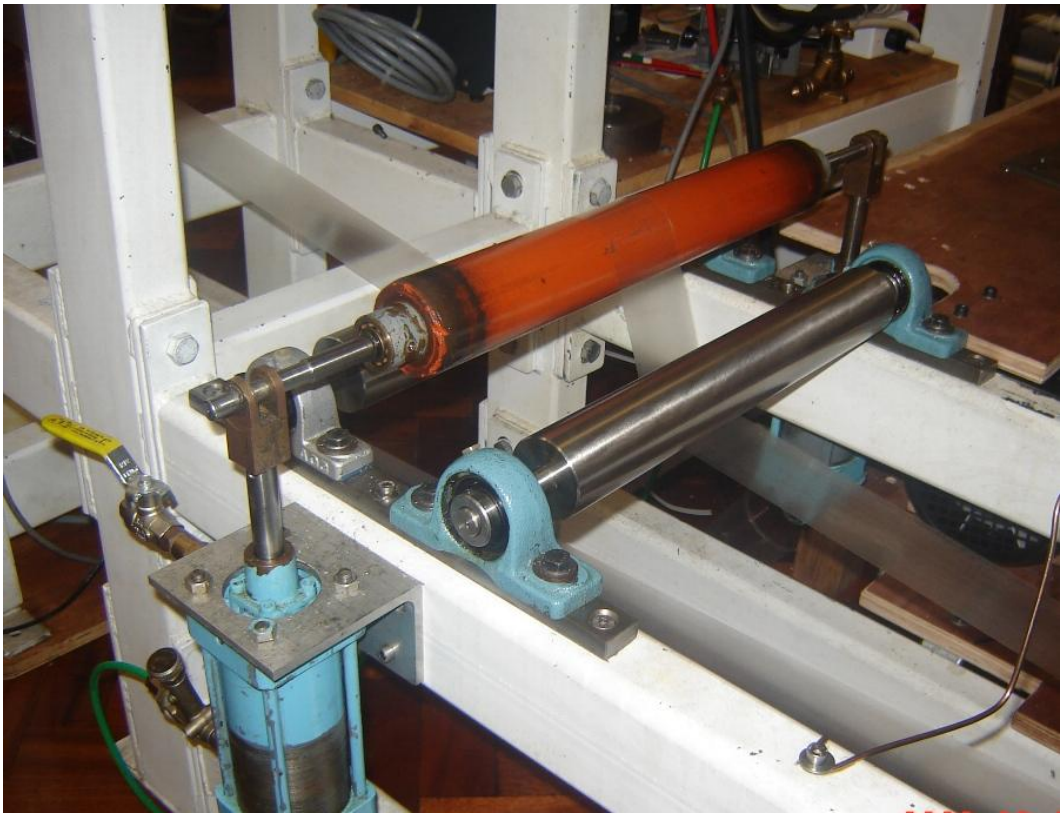

Figure 3.6: Web tension control.

Rollers System

In order to ensure an effective control of its motion, the substrate loop was threaded around a 16 rollers system to ensure that it was moving around the drive roller and the idler roller as long as possible and maintained centralized. The main drive roller is a rubber covered steel roller 76.35 cm in diameter and 28.00 cm long. A control drive mechanism was needed to control the drive roller speed. An inverter drive motor connected to a 3-phase gear motor with high power (4.0 kw) controlled the drive roller speed to give sufficient torque at low speeds with an accuracy of ± 1%. In addition, at some stage of the programme and in order to increase the speed, the gearbox was removed and the motor connected directly to the drive shaft. Also, when necessary, pullies of various sizes were fitted to drive to ensure correct range of speeds.

Scraping System

A prerequisite for the study of dynamic wetting is the provision-strictly-of a dry fresh substrate. The literature survey however revealed that provided the arriving surface was wiped cleaned the study of dynamic wetting failure could reproduce identical features to those obtained with a fresh substrate. Therefore, in this loop configuration, provisions were made to scrap the substrate of its coating fluid before it re-entered the coating flow. In order to ensure as clean a substrate as possible, five scrapers were used, place at various positions in the substrate loop system. The main scraper consisted of a plastic plate pressed against the rotating idler roller and this enabled the bulk of the coating film to be removed and funnelled back to a separate tank. Two additional scrapers, fitted after the main one also on the idle roller provided further and complete removal of the coating fluid, checked consistently at being less than 0.5 micron. Also and in order to avoid slippage of the substrate, as scraping causes the

liquid to flow also on the reverse side of the substrate, two further scrapers were placed beneath as shown in Figure 3.7.

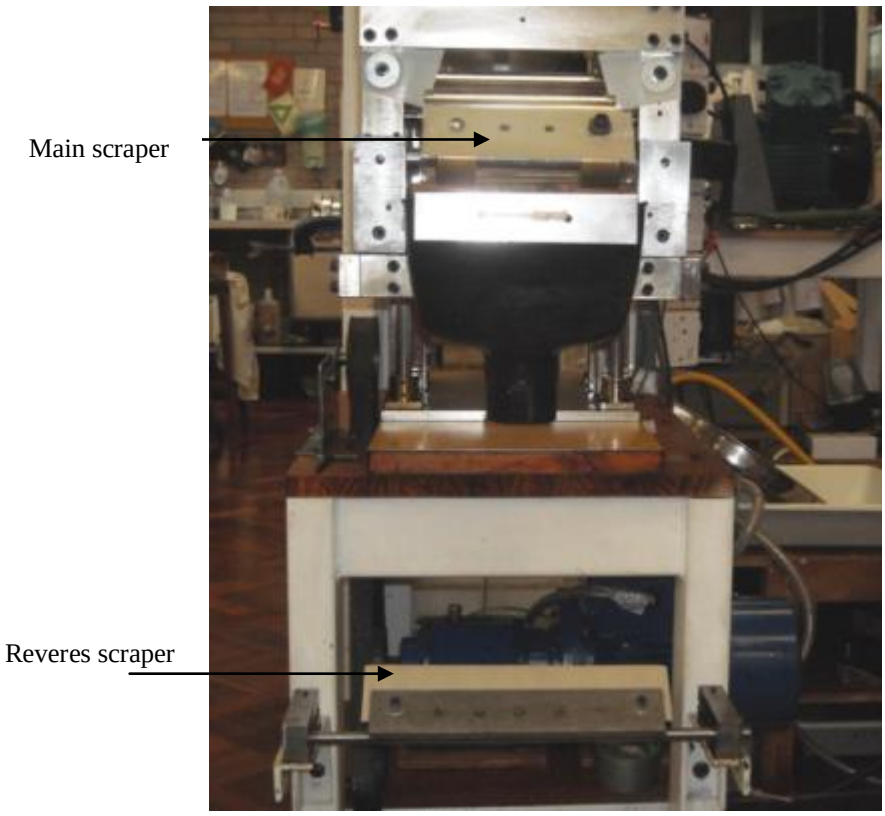

Figure 3.7: Shows the main and reverse scraper.

Note that in order to remove static charges, thin copper rods were used to earth the substrate to the metal frame of the rig.

3.3.2 Die Angle and Height Control

The die angle and its height are the primary operating variable and required accurate control. As the die was very heavy, the control was achieved by attaching it to a metal

plate that sat solidly on the frame of the rig with a screw lead and hand wheel connected to two gears allowing rotational and sliding down movements as shown in Figure 3.8.

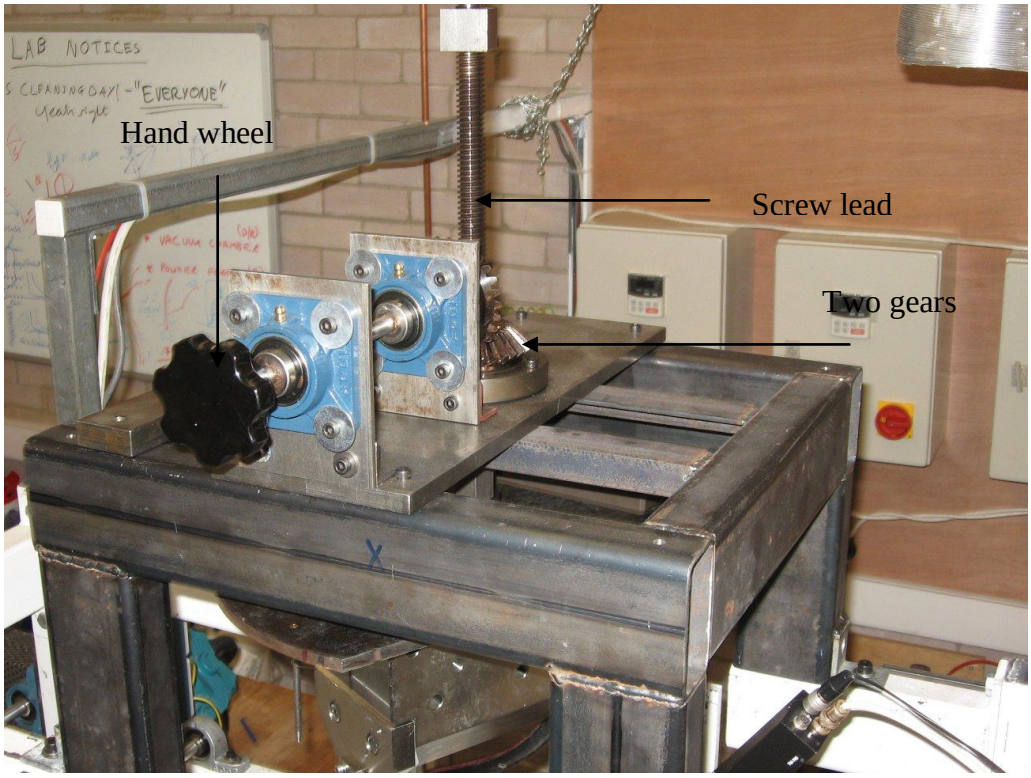

Figure 3. 8: Improvement of curtain coating height adjustment.

3.4 VISUALISATION AND IMAGING SYSTEM

The observation of dynamic wetting line failure or air entrainment in curtain coating experiments can be extremely difficult, because the substrate moves at high speeds. Although visual observations with the naked eye must never be discounted, they must be supplemented with a fast imaging system that can track and record the onset of air entrainment so that a systematic study with a consistent approach leading to reliable results can be obtained. For this reason, in this experimental investigation, 3 CCD cameras with different magnifications (Plunix TM-765E, TM-6CN and JVC TK-1270E) were used to zooming in the coating flow and view first the dynamic wetting

region, then the dynamic wetting line and finally how this line breaks into saw-teethteeth as explained in the literature review to let in streaks of very fine bubbles (microns in diameter).

Figure 3.9a and b: Camera set in the side.

Figure 3.9 shows how these cameras were mounted in different places in the coating rig. Two were fitted in the front of the curtain zone and the third fitted in front of the main scraper to track air bubble formation if these could not be seen in the impingement zone. The presence and the observation of the bubbles at the scraper with the coated layer viewed from above and illuminated from the underneath and the side with strong halogen lamps (SCHOTT KL 1500, GALLE LS 155 electronic) proved to be the most reliable proof on the repeatability of the data which had to be carried at least for 3 separate runs. In determining the substrate speed at which air entrainment occurred it was important to first increase the speed until air entrainment was observed then decrease the substrate speed back for air entrainment to disappear then increase the substrate back again until air entrainment is observed again. In doing so, a repeatable procedure was being used leading to accurate air entrainment speeds.

3.5 COATING FLUIDS: PREPARATION AND CHARACTERISATION

As explained earlier, this research programme was partly sponsored by the paper industry to test if curtain coating could reach the speed achieved by traditional blade

coating methods but with the benefit that curtain coating provides a non-contact method as blades often cause tearing of the paper. Thus in addition to "academic" coating liquids of the Newtonian type, industrial-coating solutions were also prepared and tested. Note that the literature survey gave guidance as to the importance of viscosity and the negligible effect of surface tension. Thus although measured, the variation of surface tension as a property was not a prime interest of the research. Rather testing the effect of angling the die with a range of viscosities of coating solutions was the important consideration. In this respect it is important to note that the bulk of the experimental programme was carried out with the "academic" fluids because they offered a perfect Newtonian behaviour whilst allowing a range of viscosities to be tested. Although the paper coating solutions were tested, their usage was only to assess if curtain coating was feasible with these solutions.

The errors involved in the collection of data are as flollws:

- Flow rate: the flow rate of the curtain is controlled by an inverter controlled, geared motor driven pump. There for the set flow rate error is expected to be less than 1 %.
- Human error: this as in most experimentals studies, is expected to about 5 %.
- Experimental error: Figure 3.10a and b, there is some of the experimental data with error bars set at 5 %.

It is clear from this Figure 3.10a and b that the data cpllected is well with the bonds of experimental error. There is, however greater error in the region when the curtain heel becomes to big making the observation of air entrainment very difficult.

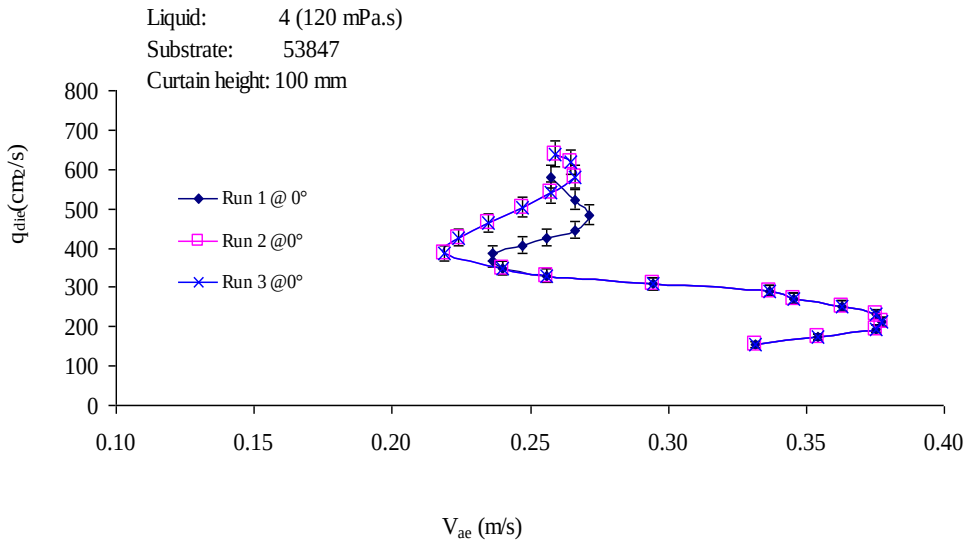

Figure 3.10a: shows the repeatability of liquid 4 (Millmax 46)

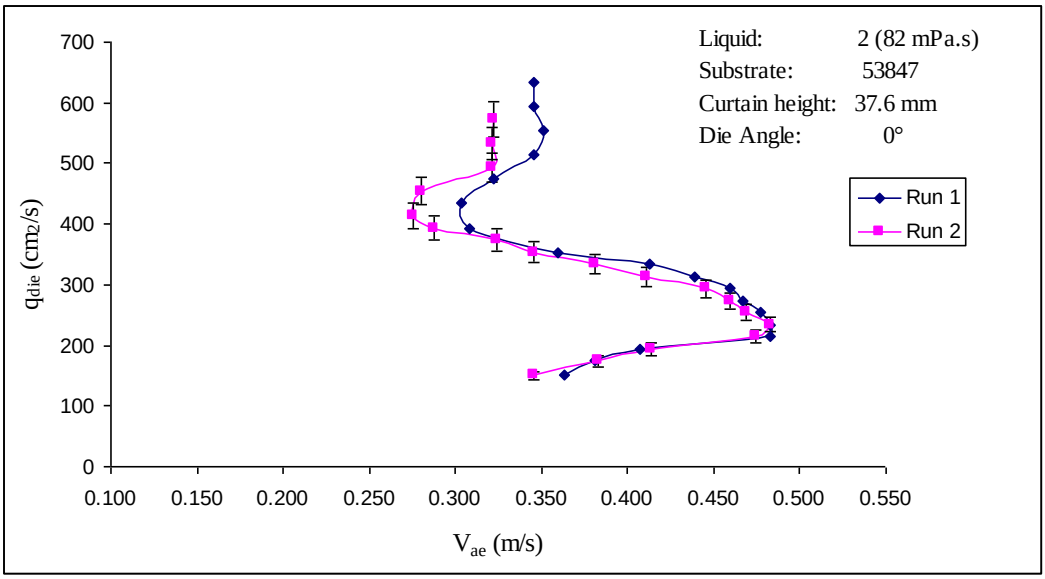

Figure 3.10b: shows the repeatability of liquid 2 (Milgear1)

3.5.1 Coating Solutions: Preparation

The "academic" coating fluids used in this programme were lubricating gear oils (see Table 3.1) of varying viscosities as purchased and characterised in our laboratories).

Table 3.1: Shows the physical properties of all the coating liquids at 19°C

No	Fluids names	Viscosity (mPa.s)	Density (kg/m^3)	Surface tension (mN/m)
1	Mix 1	89	882	0.031
2	Milgear 1	82	865	0.035
3	Millmax 37	97	882	0.032
4	Millmax 46	120	882	0.031
5	Millmax 68	185	885	0.034
6	Millube 68	200	849	0.033
7	Millmax 100	272.5	889	0.033
8	Millmax 150	456.89	894	0.035
9	Millmax 220	850	898	0.032
10	Millmax 320	1200	900	0.034
11	PVP	87	878	0.030
12	China clay	125	883	0.033

The paper coating solutions were more elaborate to prepare and required mixing China clay (kaolin) with water and a dispersant (sodium polyacrylate) according to an industrial formulation. In the context of this research, really the formulation effects did not matter; rather the interest was in the rheological properties, of course affected by the formulation. It is however important in the context of the research time to appreciate the relative effort spent on the preparation of the paper coating solution, preparation which consisted of the following steps:

- Powdering of the china clay using a pestle and a mortar.
- Weighing out the required amount of powdered clay to make the desired solids concentrations in the clay slurry (10, 20, 30, 40, 50, 60% by weight).

- Weighing out the corresponding amount of water to make the required suspension concentration, allowing for the moisture content of the raw clay.
- Dosing with sodium hydroxide at 0.1wt% to keep a natural pH. [The sodium polyacrylate dispersant is acidic and it will cause the solution pH to drop.]
- Adding an amount of sodium polyacrylate (CED) dispersant solution from a stock at 40% wt concentration CED to each of the solution to give a concentration of 0.05 wt% CED on a dry clay basis. All the calculations for the solutions prepared are presented in Appendix 1.
- Adding the powdered clay slowly to the water and dispersant with stirring until a smooth slurry is obtained and allowing enough time for mixing (up to one hour).
- Screening the slurries through a sieve (300# or 53μm) before viscosity measurements to remove the coarse grits that can cause damage to the viscometer and the coating die.

Note in the formulation, the important role of the dispersant sodium polyacrylate (CED), a high molecular weight water soluble additive, designed to be adsorbed onto the surface particle and produce a barrier that prevents agglomeration Zaman and Mathur [49].

3.5.2 Coating Solutions: Characterisation

Rheological Measurements

Solutions made out of clay, water and dispersant are renown in rheological research because such solutions are used in many industries (paints, ceramics, paper, etc.) and exhibit non-Newtonian behaviour sometimes very complex particularly at large clay concentrations. This is because clay can swell up and take up with water trapped in the

micro-pores of the clay causing in some instances for it display shear thickening (see Figure 3.11).

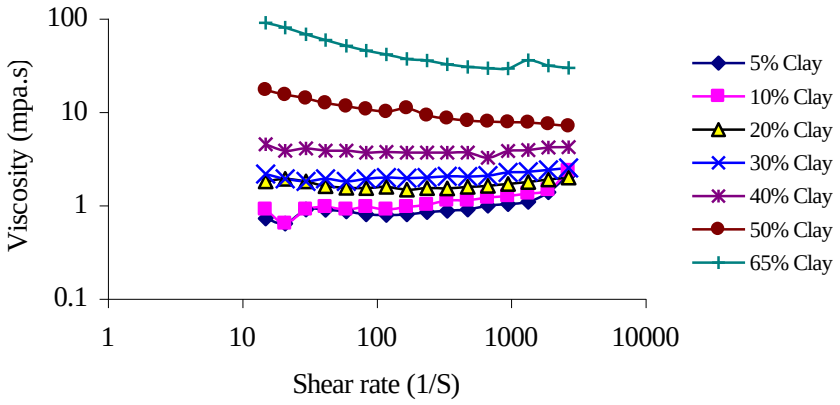

Figure 3.11: China clay behaviour with 0.6 wt% CED at 40°C with different concentration.

Such behaviour, which is an increase in viscosity at large shear rates is not desirable. Remember from the literature review that dynamic wetting failure is normally not helped with high viscosity. Thus a systematic measurement programme of all the coating solutions prepared was required to help with the assessment of the air entrainment speeds data. The measurements were carried out using a Brabender Rheotron viscometer shown in Figure 3.12. The instrument geometry is a concentric cylinder viscometer that can be made to rotate in a range of speeds and torques to produce a range of shear stresses ($1x10^3$ to $3x10^6$ dynes/cm^2) and rates ($5x10^2$ to $2x10^4$ s^{-1}) and apparent viscosities in the range 0.005-10^7 Poise.

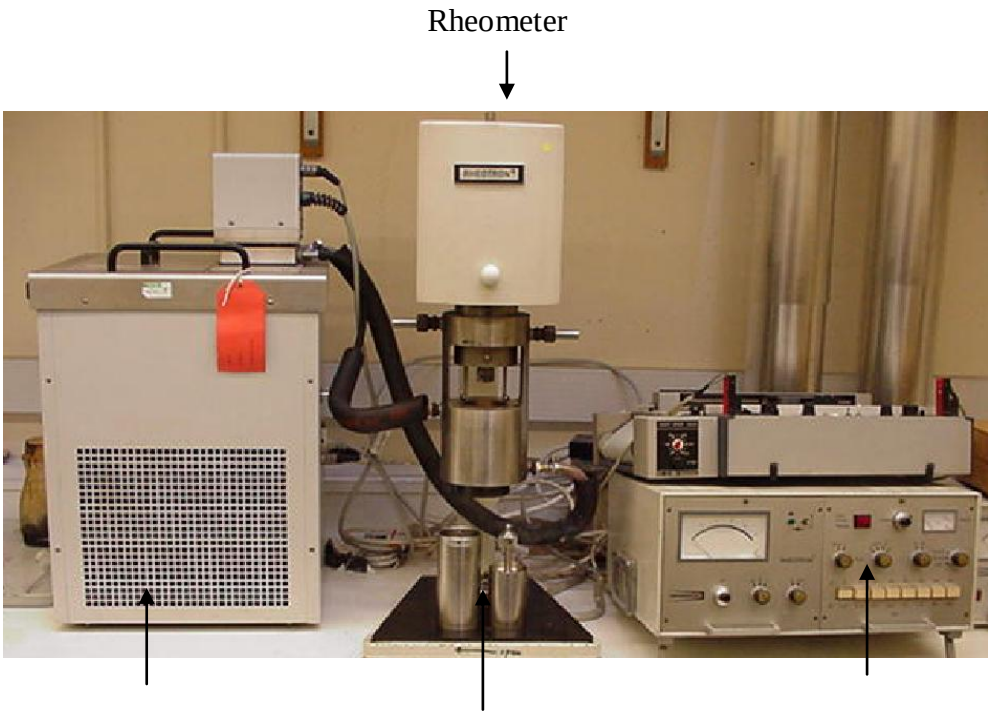

Figure 3.12: Brabender Rheotron Viscometer

The data on the viscosities measured with the various clay solutions are shown in Figure 3.13-3.16 for a range of temperatures, up to 60^{o}C. The important observations are:

1. At low clay concentrations, up to 10% wt, the solutions behave essentially in a Newtonian manner until a slight shear thicknening effect is observed at shear rate 1000 s^{1}and larger. This is shown clearly in Figure 3.13.
2. At concentration larger than 10% wt, shear thinning is observed from the very low shear rates all the way up to larger shear rates (see Figure 3.13). No shear thickening was detected, probably because higher shear rates were required before the effect could be detected.
3. The solutions those were prepared without dispersant exhibit relatively stronger shear thinning behaviour even at lower clay concentrations (see Figure 3.13).

This is because without dispersant, the solutions will have a tendency to agglomerate thus being more prone to shear thinning. The addition of dispersant remove the tendency to form agglomerate thus reducing the extent of shear thinning but not removing it completely.

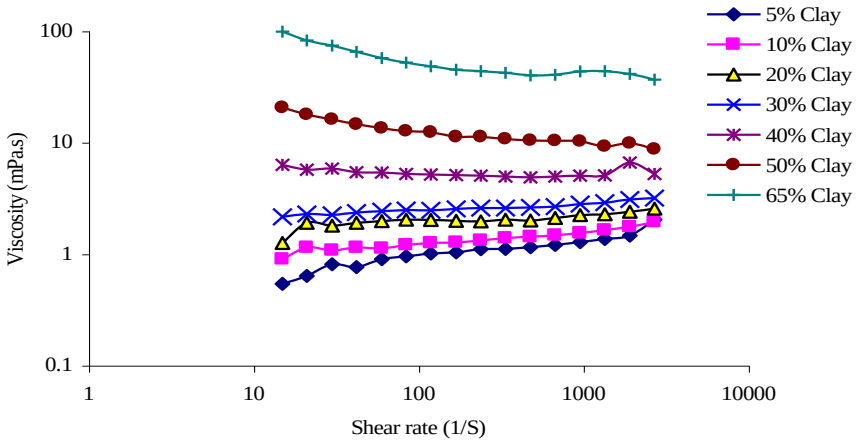

Figure 3.13: Change viscosity with varying concentration at 0.6 wt% CED and 25°.

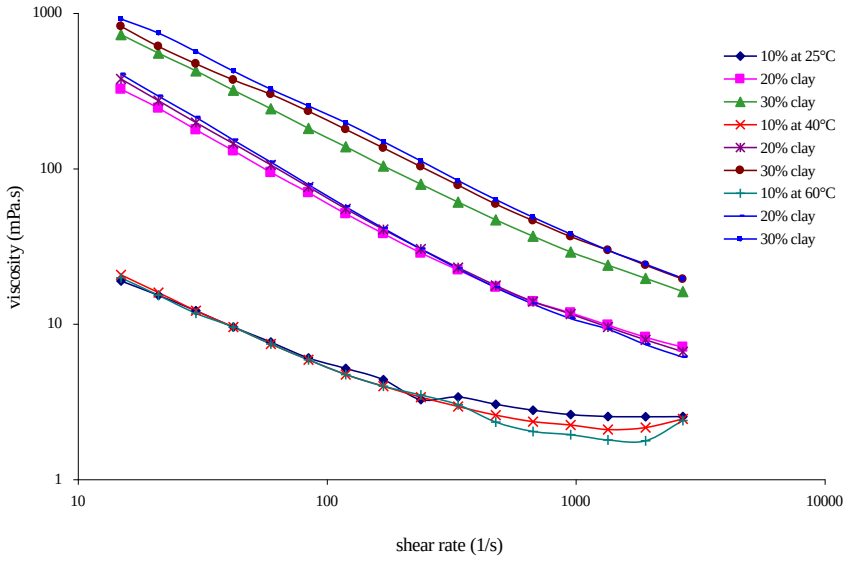

Figure 3.14: Change viscosity without CED for different clay concentration at 40°C

As for the lubricating oils, which formed the bulk of the experimental programme, as expected they exhibited a purely Newtonian behaviour with viscosity depending only on temperature. Figure 3.15 shows a typical flow curve and Table 3.1 list the values of the measured viscosities of the various oils used.

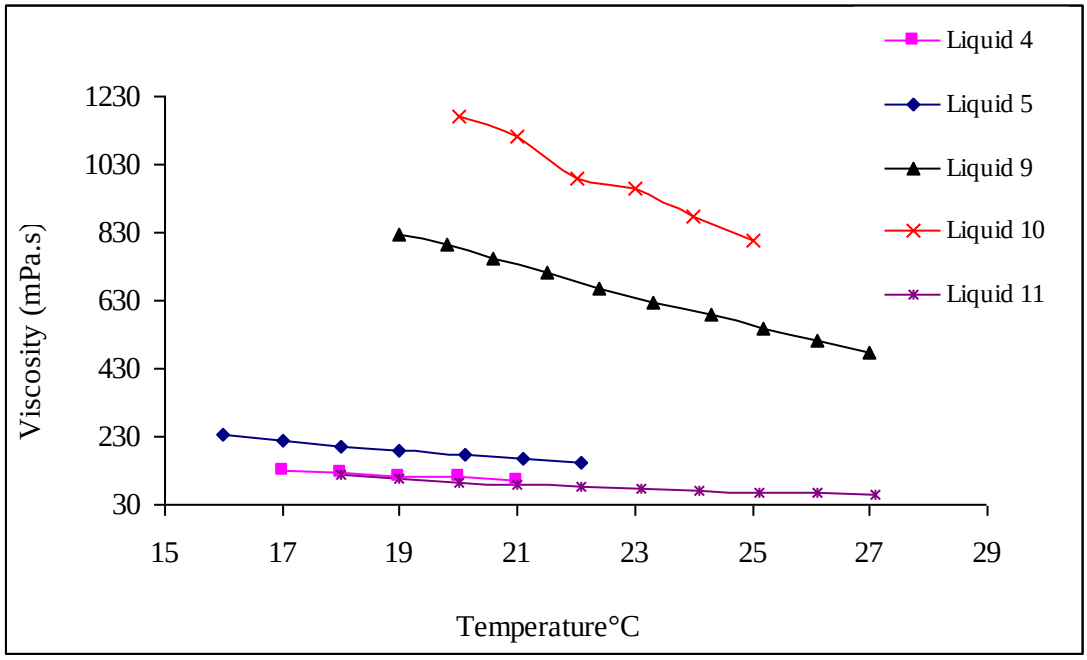

Figure 3.15: showing the effect of temperatures against the viscosity

Density and Surface Tension Measurements

As noted earlier, previous work reviewed indicated that these properties do not play a major part in dynamic wetting. Nevertheless, it is important that these properties are fully determined and in a precise manner to add accuracy to the experimental programme.

The densities of all coating liquids were measured using the standard density bottle technique with the volume of the bottle determined using doubly distilled water and weighing all the quantities used with a precision balance to +/- 0.01 g. The density data

of all the fluids used are listed in Table 3.1 for surface tension measurements, we used a modern FTA 188 video tensiometer as shown in Figure 3.16.

Figure 3. 16: FTA 188 video tensiometer

In this device, a drop is created by a needle fed at controlled rate by a precision syringe. Using the integrated video camera, a series of images of the pendant drop from the syringe were captured. These images were then fed to a pc with a purpose software that calculated the diameter and volume of the drop assumed to be spherical from which the surface tension could be calculated. The corresponding equation is simply a force balance between the weight of the drop and the surface tension holding it to the needle:

Contact Angle Measurement

As presented in the literature review, the contact angle is 'the measurement' of dynamic wetting as it defines how the liquid attached itself to the substrate. Clearly, the surface topography will play a major role in the contact angle thus to define a substrate require that the contact angle be measured with the fluid to be coated.

The FTA 188 instrument discussed above has also the ability to measure the contact angle that the drop formed with a substrate from time=0 when the drop first hits the substrate to time t as the drop spreads in time on the substrate. This angle was obtained from the fast capture of a series of images as the drop spreads on the substrate as shown in Figure 3.17a. The shape of the spreading drop is characteristically lenticular and the angle formed by the solid surface and the tangent line to the upper surface at the end point is the contact angle formed (see Figure 3.16b) as a result of the interface/surface tensions (surface free energies) between the liquid and solid substrate surrounded by the gas.

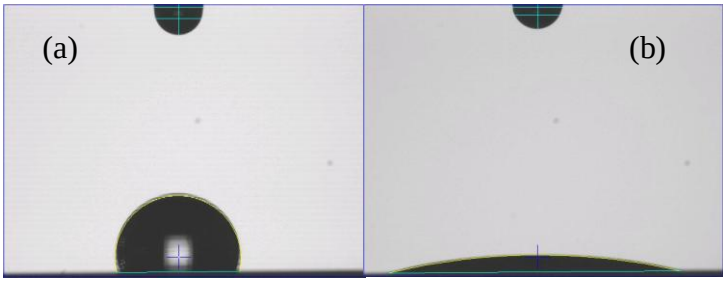

Figure 3.17a: shows the image as the drop spread on the substrate, for liquid 2 (Mix1 viscosity 82 mPa.s).

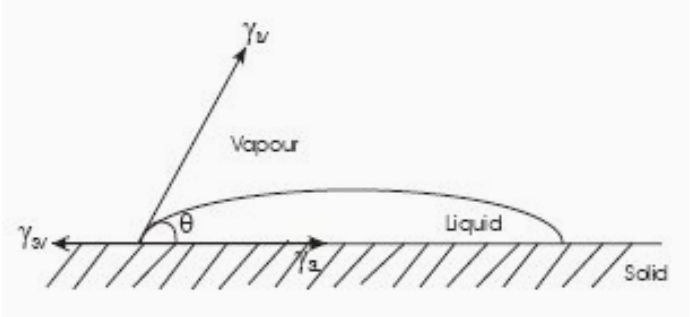

Figure 3. 17b: Schematic diagram of Static Contact Angle.

The angle is measured according to the Young equation given by

$$\gamma_{SV} - \gamma_{LS} = \gamma_{LV} \cos ine\theta_e \quad (3.1)$$

γ_{SV} = the interfacial tension across the solid substrate-gas interface.

γ_{LS} = the tension across the solid substrate-liquid interface.

γ_{LV} = the tension across the liquid-gas interface, known as the surface tension of the liquid.

θ_e = the equilibrium contact angle between the solid and liquid.

In this equation, the surface tension of the liquid, γ_{LV} and the equilibrium contact angle, θ_e are known, both measured by the FTA 188 device. The two unknowns are the solid/gas interface, γ_{SV} and the solid/liquid interface, γ_{LS}. Their difference (γ_{SV} - γ_{LS}) is a measure of the interaction between the substrate and the gas and liquid phases Gennes [50].

Figure 3.17 gives a plot of the contact angles measured with the substrate and coating fluids used in the curtain coating experiments. Further data are given in Appendix 1.

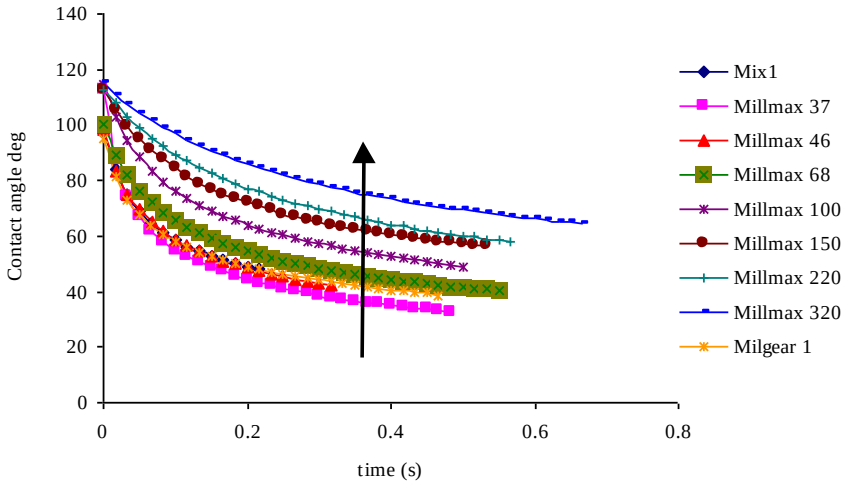

Figure 3. 18: Contact angle for different liquid with Substrate 53847[2]

[2] Please note that during reference will be made in this thesis to two substrates 5318 and 53847. These are strictly the same. The experiments started with 5318 substrate then the new supply was 53847.

3.6 CONCLUSIONS

This chapter has presented all the important design and operation details of the coating rig to be used in this programme of studies. A looped curtain coating was proposed to be suitable on account that previous studies in the field show that to be permissible. The curtain coating rig proposed was designed to the highest standard and capable of delivering a range of flow rate and coating speeds similar to those achieved in industrial lines. The purpose of the experimental programme is to collect the pertinent data on air entrainment speeds to test the hypothesis that angle curtain coating postpones air entrainment to speed higher by a factor $1/\cos\beta$. In order to test this hypothesis over a wide range of conditions, the prime operating parameter of viscosity was proposed to be tested in arrange of viscosity from 80 to 1200 mPa.s using Newtonian lubricating oils of similar surface tensions on a fully characterised substrate. The characterisation of the substrate is given uniquely by the dynamic contact angle measured, i.e. the measured contact angle of the substrate-liquid from time zero until the contact angle reaches its equilibrium value. How the contact angle varies in time gives a unique characteristic of the substrate.

CHAPTER 4: RESULTS AND DISCUSION

4.1 INTRODUCTION

Following the experimental method described in the previous chapter, we present in this chapter the pertinent data to test the validity of the hypothesis put which is that angling the die in curtain coating results in postponing the air entrainment at speeds higher than in normal non-angled operations, which are of the order $1/\cos\beta$ greater. The data are presented in the form of 4 sets:

1. Testing the hypothesis at a fixed curtain height of 60 mm, with 4 lubricating fluids of different viscosities at die angles 0, 10, 20 and 30^0
2. Testing the hypothesis with varying curtain heights between 22.6 and 67.6 mm with 4 lubricating fluids of different viscosities at die angles 0 and 30^0.
3. Testing the hypothesis with varying curtain heights but using comparatively viscous fluids and at die angles 0, 30, 45 and 55^0.
4. Testing the hypothesis using PVP, the coating fluid used in the original study of Blake et al [14], under similar curtain heights but using die angles of 0 and 30^0.

In addition to this proof of concept testing, observations of how the flow develops in the dynamic wetting region are also presented and discussed to assess if the alignment of the curtain with the dynamic wetting line provides the optimum condition for hydrodynamic assistance when the die is angled.

Finally an assessment of angled curtain coating of the coating of paper is made to test the feasibility of introduce it in industrial operations that currently use blade coating.

The chapter finishes with conclusions made from the data and the flow observations and their comparison with earlier work reported in the literature.

4.2 ANGLING DIE CONCEPT TESTING

To be valid, testing the hypothesis that angling the die increases the air entrainment speed by a factor of 1/cosβ, requires data for a wide range of conditions of the key parameters conditions of curtain coating which are curtain flow rates and curtain height with a range of coating fluid viscosities. Also as the literature review revealed an unexpected step change in hydrodynamic assistance when using viscous fluids, tests data are also reported for fluids of viscosity up to 1200 mPa.s, much larger than previously tested.

4.2.1 DATA AT FIXED CURTAIN HEIGHT

First let us present observations on the wetting line position and shape of the wetting region. The onset of air entrainment was measured by increasing the substrate speed at various flow rates. At low substrate speed and constant flow rate, the wetting line is straight across substrate. However, as the substrate speed increases, the curtain is pulled forward and air is entrained between the coating liquid and the solid substrate at the three-phase interface solid, liquid/ gas. The dynamic wetting contact angle approaches 180° at the point of air entrainment. At this stage the wetting line is pulled forward and at some critical substrate speed, V_{ae}, saw-teeth or V shapes appear at the wetting line as shown in Figure 4.1. Air starts being entrained across the wetting line and appears as air bubble on the moving substrate. At a high flow rate and low substrate speed, very large bead forms at the wetting point as shown in Figure 4.2a. As the substrate speed is increased the heel breaks up as show in Figure 4.2b. For each flow rate the substrate speed was increased steadily, until air entrainment was detected and the speed then reduced until air entrainment disappeared. This sequence was

repeated several times to ensure consistency and limit the experimental error in the measurement of the speed which was not greater than 5%.

Figure 4.1: Air entrainment started saw teethteeth or V shape at low flow rate 1.16l/m and Vae 0.219 m/s.

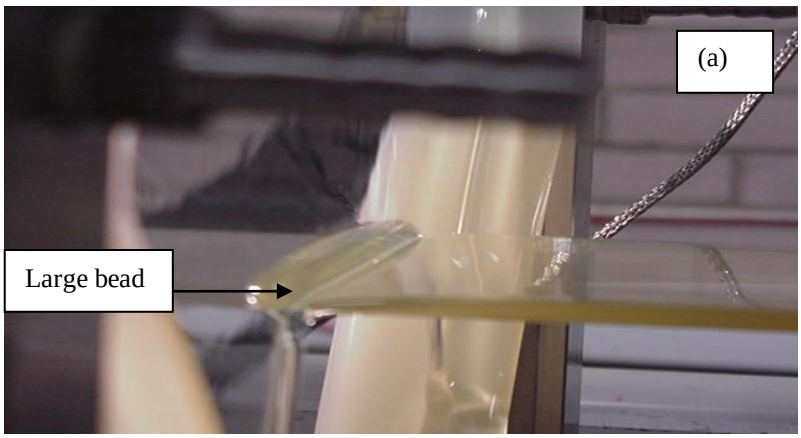

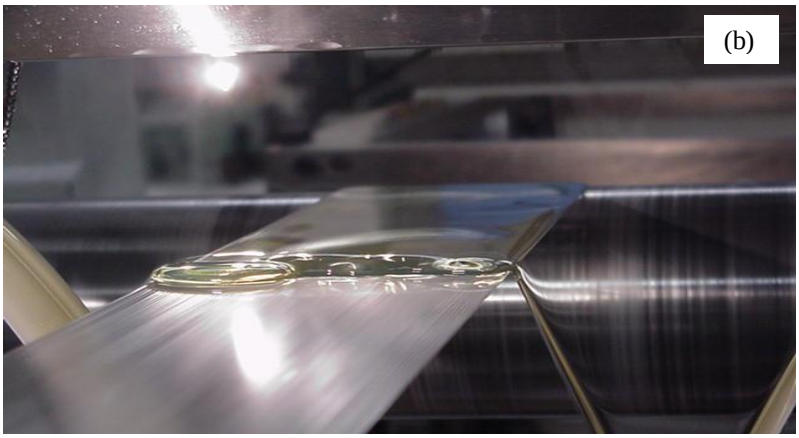

Figure 4.2a, and b: Large bead and heel formation at low speed (0.295) and height flow rate (8.37 l/m).

Now let us present the actual measuredl data at fixed curtain height plotted first as die flow rate q_{die} against air entrainment speed, V_{ae} and then as q_{die} against $V_{ae}\cos\beta$ to test if the data superimpose when the wetting line at an angle β. Figures 4.3-4.7 give the corresponding plots. Although the superimposition is not perfect, there is a clear shift in the data indicating that the strategy of angling the die works to a *certain* extent but not according to prediction. Although Figure 4.4 may suggest that the fit is better at low viscosities, Figures 4.5-4.7 do not support this lead.

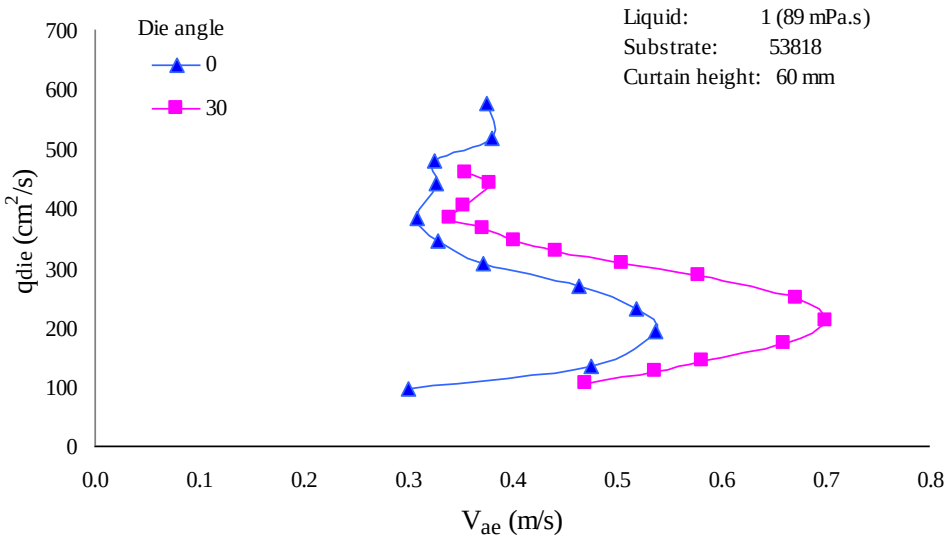

Figure 4.3a: Air entrainment V_{ae} verses flow rate (q_{die}) with liquid 1 (Mix 1).

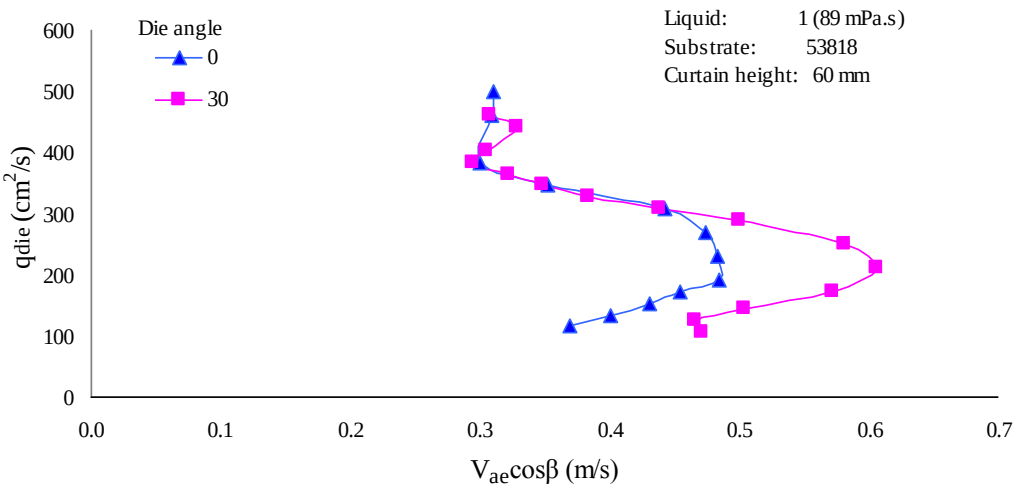

Figure 4.3b: $V_{ae}\cos\beta$ vs. flow rate (q_{die}) with liquid 1 (Mix 1).

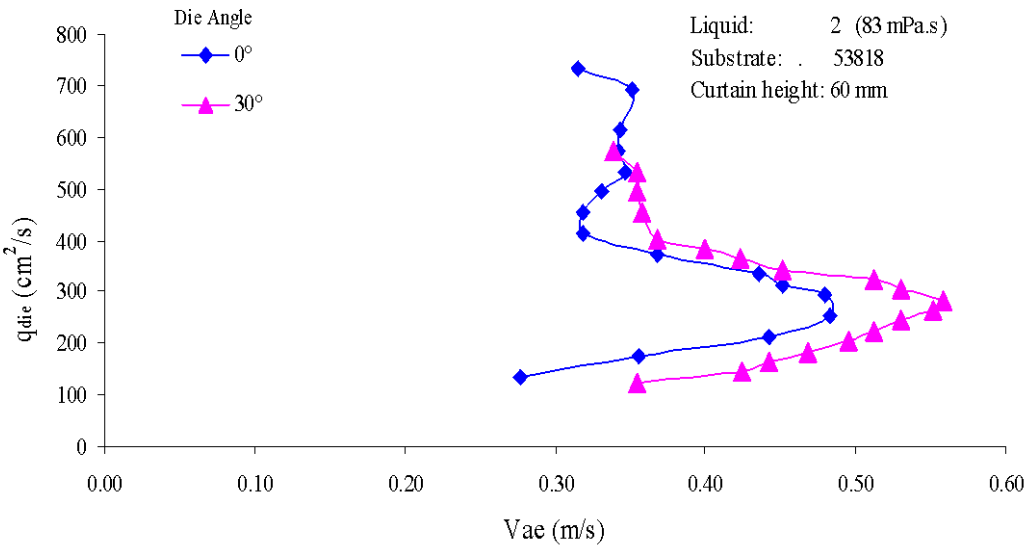

Figure 4.4a: V_{ae} vs. flow rate (q_{die}) with liquid 2 (Milgear 1)

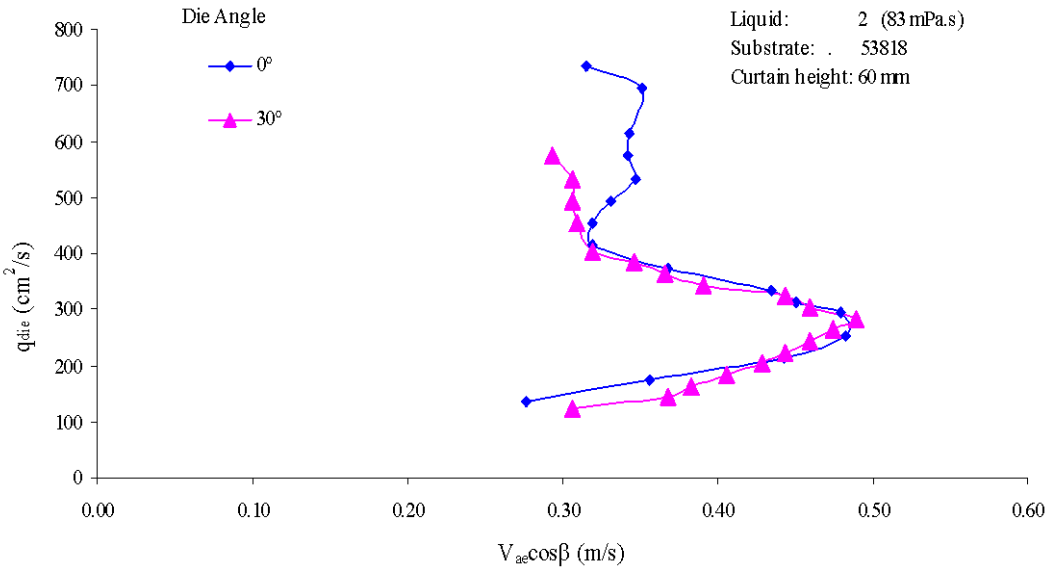

Figure 4.4a: V_{ae} cosβ vs. flow rate (q_{die}) with liquid 2 (Milgear 1)

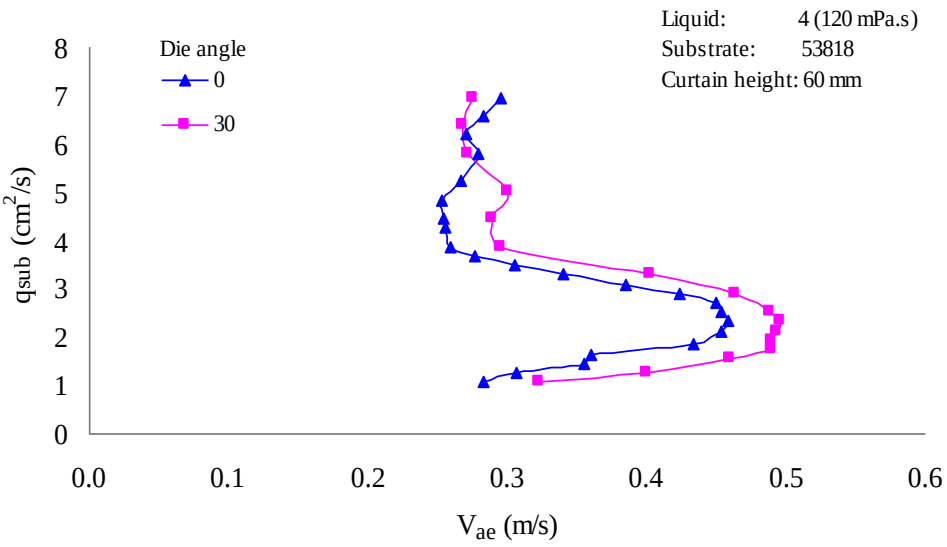

Figure 4.5a: Air entrainment V_{ae} vs. flow rate (q_{die}) with liquid 4 (Millmax 46).

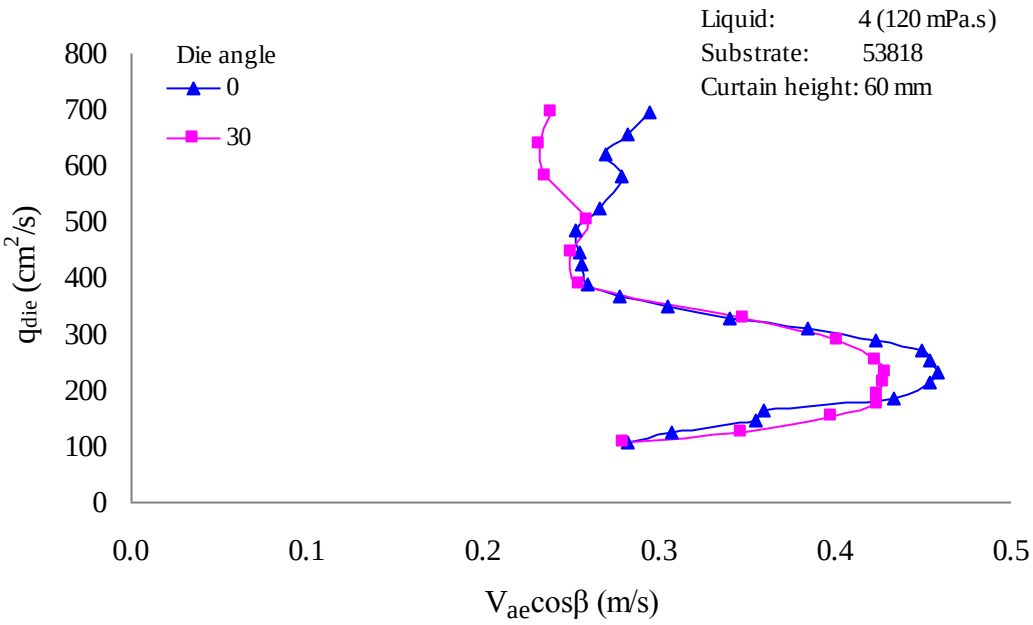

Figure 4.5b: $V_{ae}\cos\beta$ vs flow rate (q_{die}) with liquid 4 (Millmax 46).

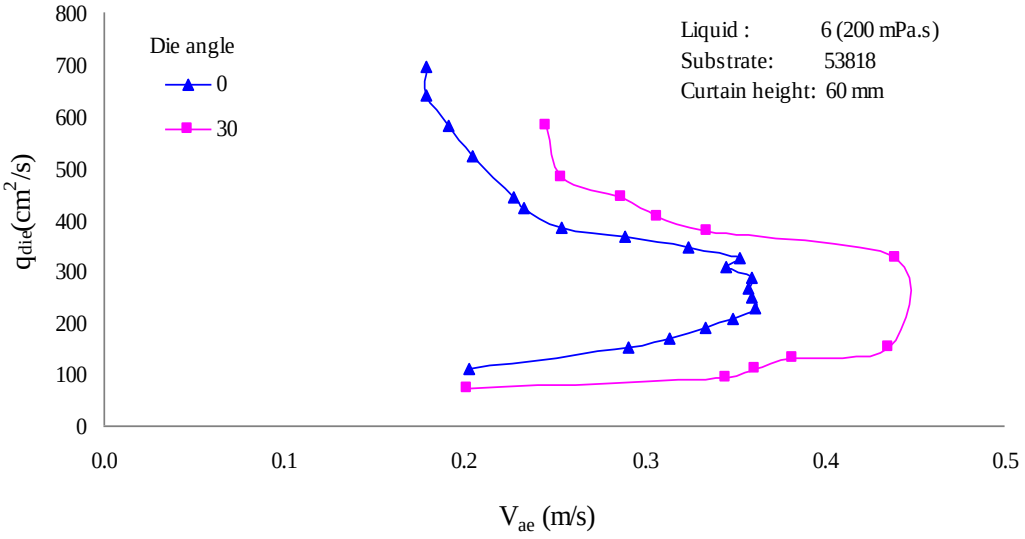

Figure 4.6a: Air entrainment V_{ae} vs flow rate (q_{die}) with liquid 5 (Millmax 68).

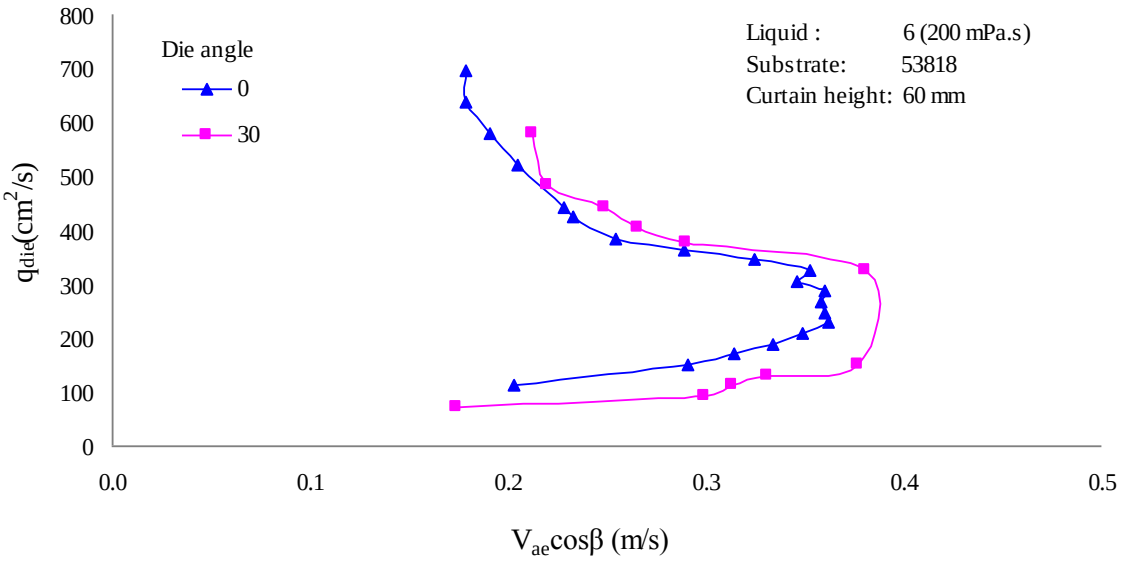

Figure 4.6b: $V_{ae}\cos\beta$ vs flow rate (q_{die}) with liquid 5 (Millmax 68).

Clearly the data so far presented do not fully confirm the hypothesis put forward regarding the effect of angling the die although a second plot at constant flow rate (Figure 4.7a) reveals a real gain practice as to the effect of angling on postponing the air entrainment velocity to high speeds. Figure 4.7b, shows the data for the 120 mPa.s liquid at 60 mm curtain height and die angle of 0°, 10°, 20° and 30°.

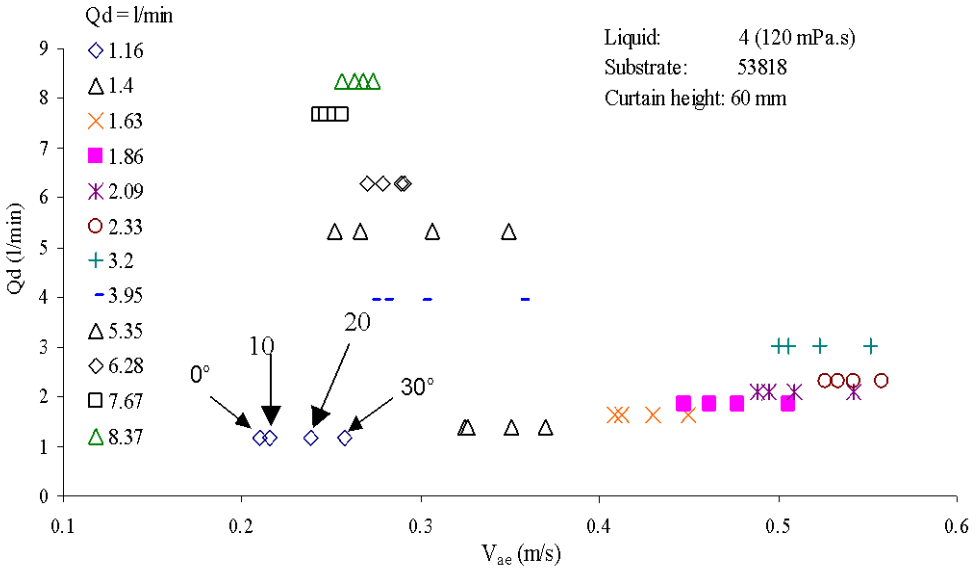

Figure 4.7a: Air entrainment vs fixed flow rate at different die angle liquid 4.

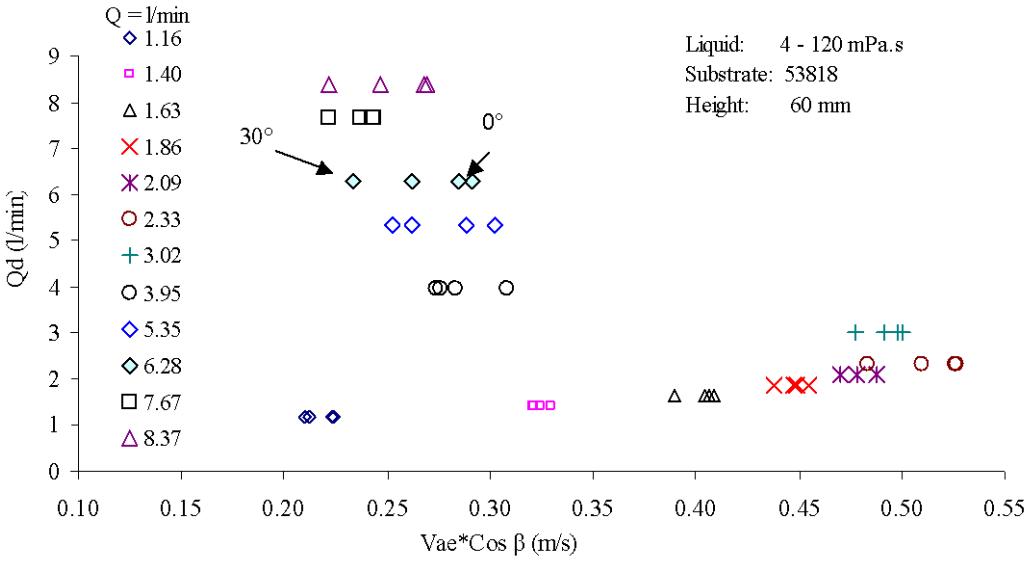

Figure 4.7b: $V_{ae}Cos\beta$ vs. fixed flow rate and different angle at 60 mm height.

The non total superimposition of the data suggests two non-linear effects are taking place. One is the *standard* hydrodynamic assistance inherent to curtain coating which is documented in the literature survey chapter section 2.4. The second is *the angling effect* hydrodynamic assistance which we are adding to the standard effect. Clearly by slanting the wetting line, the curtain flow cannot always impinge favourably on the wetting line as when the die is straight onto the substrate. Thus, what is required is linearising the standard effect analytically in the manner suggested by Blake et al [14] and reviewed earlier by plotting as in Figure 4.8, $V_{ae}/V_{ae,max}$ vs. q/q`, where is $V_{ae,max}$ is the maximum speed of air entrainment and at each curtain height and die angles and q` the liquid flow rate corresponding to the maximum air entrainment speed. Using this master curve, the data now superimpose quite well.

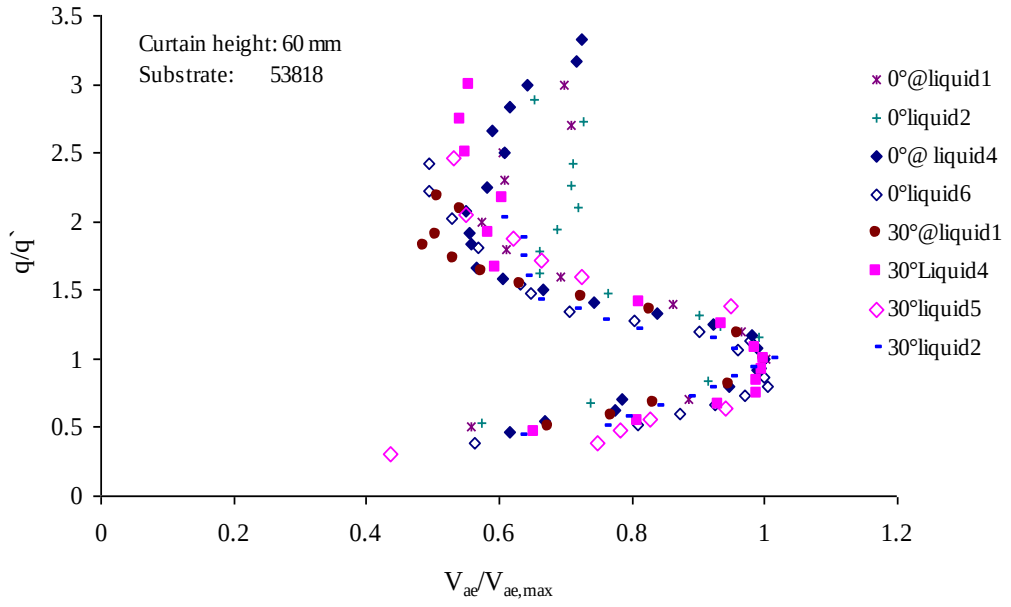

Figure 4.8: Data clearing of air entrainment plotted as normalized wetting line position vs. normalized speed for different liquids and die angle.

4.2.2 DATA AT VARYING CURTAIN HEIGHTS

Having established the validity of the angling hypothesis at one curtain height, we now present data for a series of heights, respectively from 22.6 to 37.6, 52.6, and 67.6 mm as shown in Figure 4.9-4.13 at die angle 0 and 30°, again plotting flow rate against V_{ae} and against V_{ae} cosβ to further underpin the hypothesis with a range of data. The data in Figure 4.9a and b presented below show clearly the benefit of increasing height and angling to increasing air entrainment speeds, nearly a doubling of the speed.

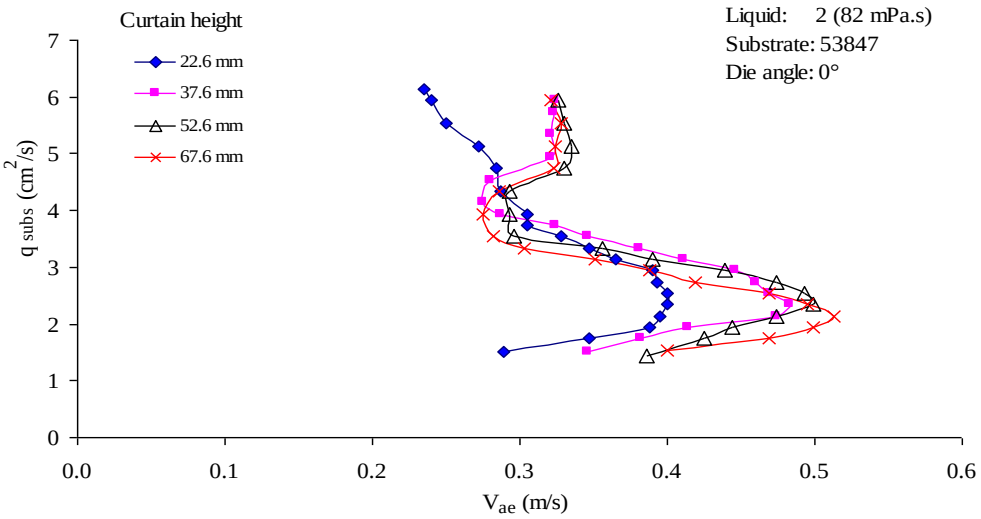

Figure 4.9a: V_{ae} vs. the flow rate (q_{die}) for liquid 2 with different height at 0°.

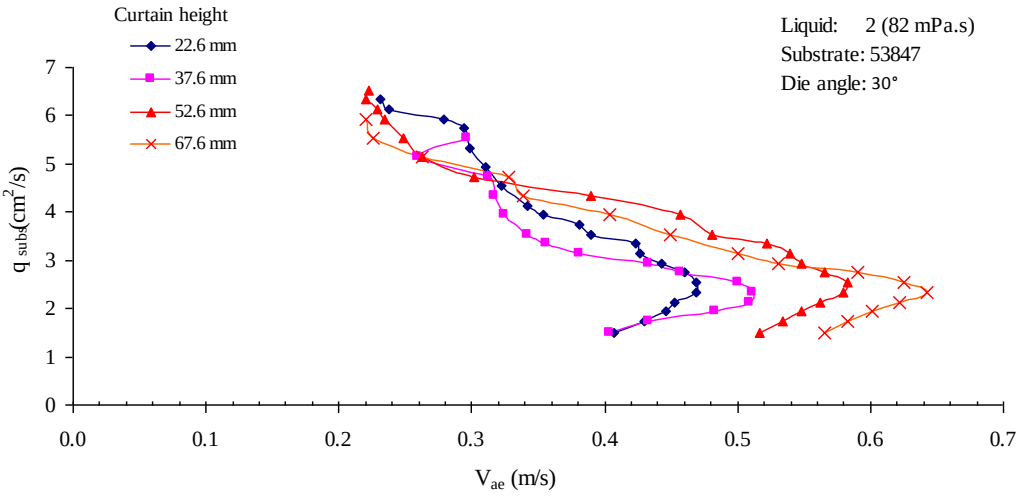

Figure 4.9b: V_{ae} vs. the flow rate (q_{die}) for liquid 2 with different height at 30°.

The individual plots are presented below comparing the effect of angling at fixed heights for a series of heights. Further plots can be found in Appendix 2 covering the complete range of conditions investigated.

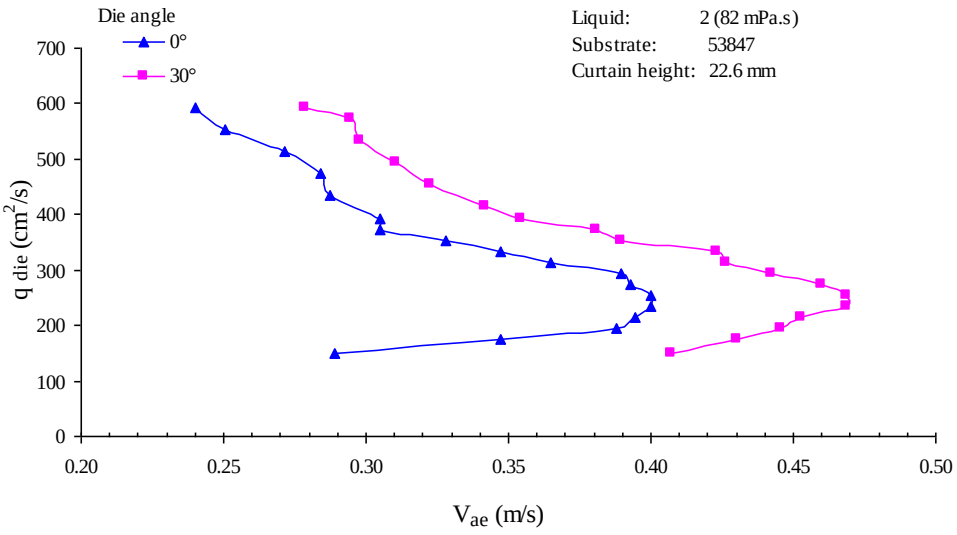

Figure 4.10a: V_{ae} vs. the flow rate (q_{die}) with liquid 2 for substrate 53847.

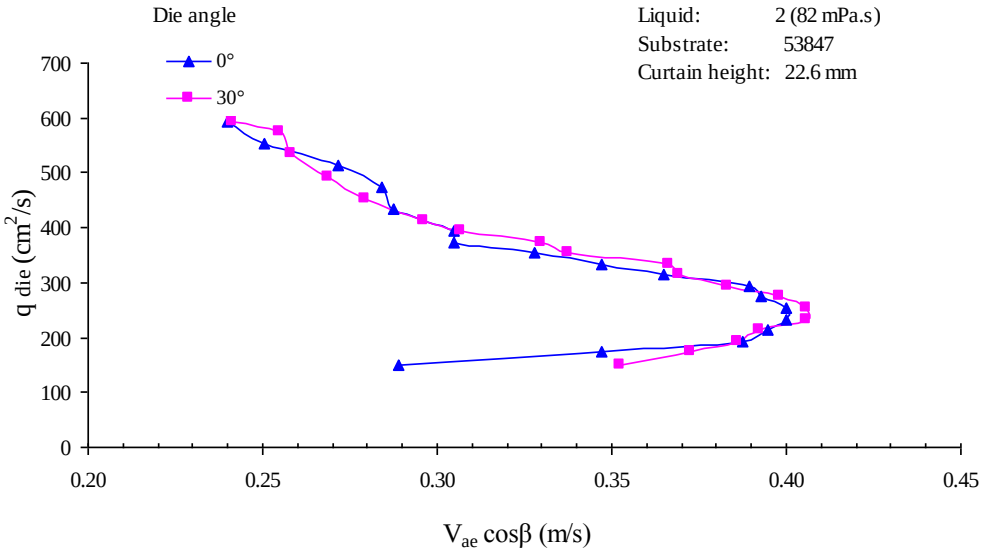

Figure 4.10b: $V_{ae}\cos\beta$ vs. the flow rate (q_{die}) with liquid 2 for substrate 53847.

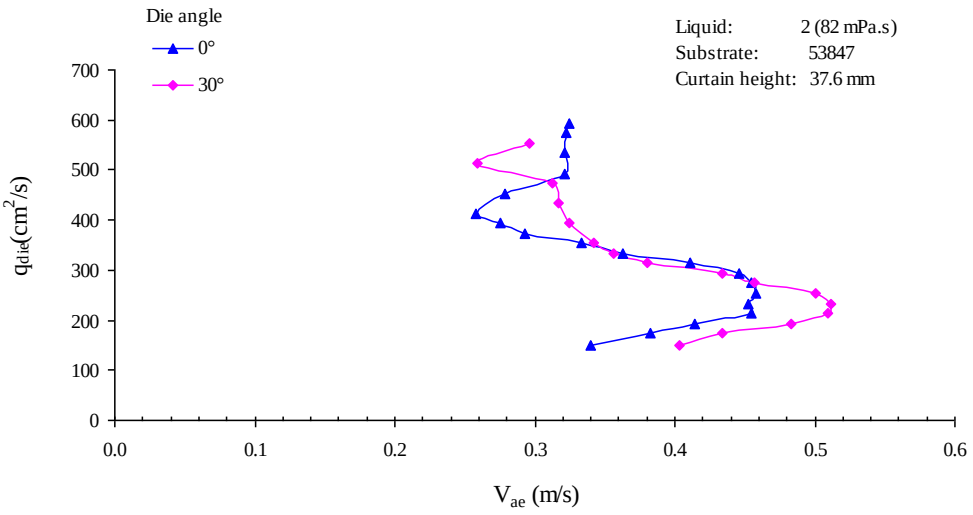

Figure 4.11a: V_{ae} vs. the flow rate (q_{die})with liquid 2 for substrate 53847.

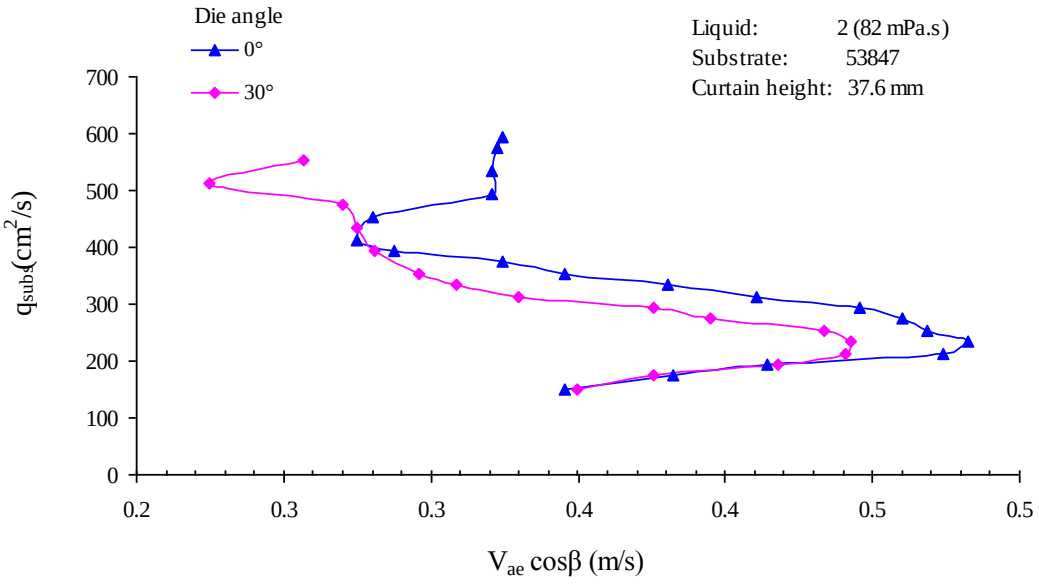

Figure 4.11b: $V_{ae}\cos\beta$ vs. the flow rate (q_{die}) with liquid 2 for substrate 53847.

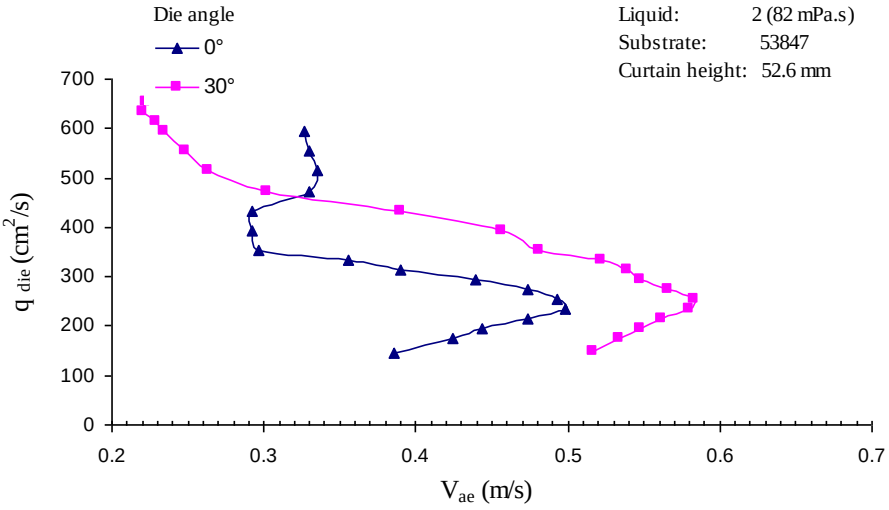

Figure 4.12a: V_{ae} vs. the flow rate (q_{die}) with liquid 2 for substrate 53847.

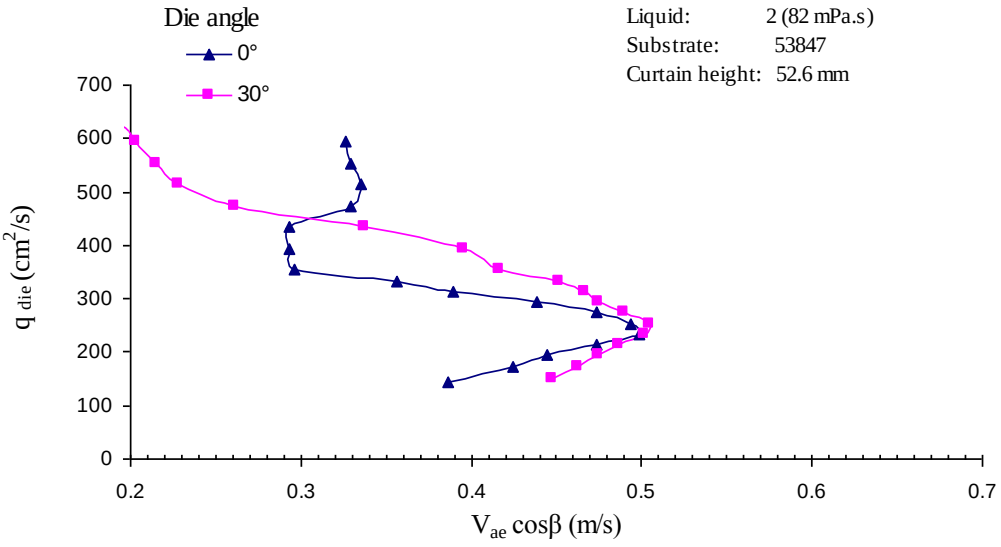

Figure 4.12b: $V_{ae}\cos\beta$ vs. the flow rate (q_{die}) with liquid 2 for substrate 53847.

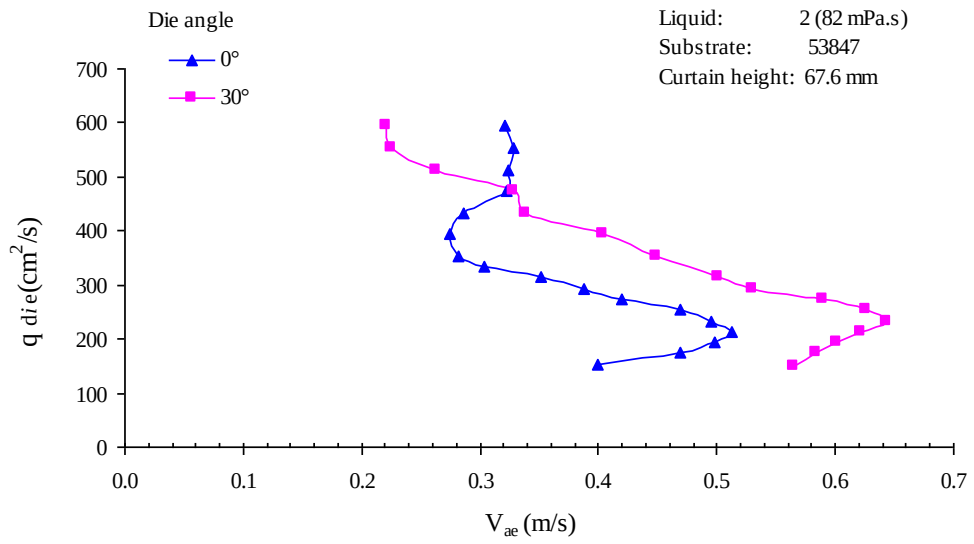

Figure 4.13a: V_{ae} vs. the flow rate (q_{die}) with liquid 2 for substrate 53847.

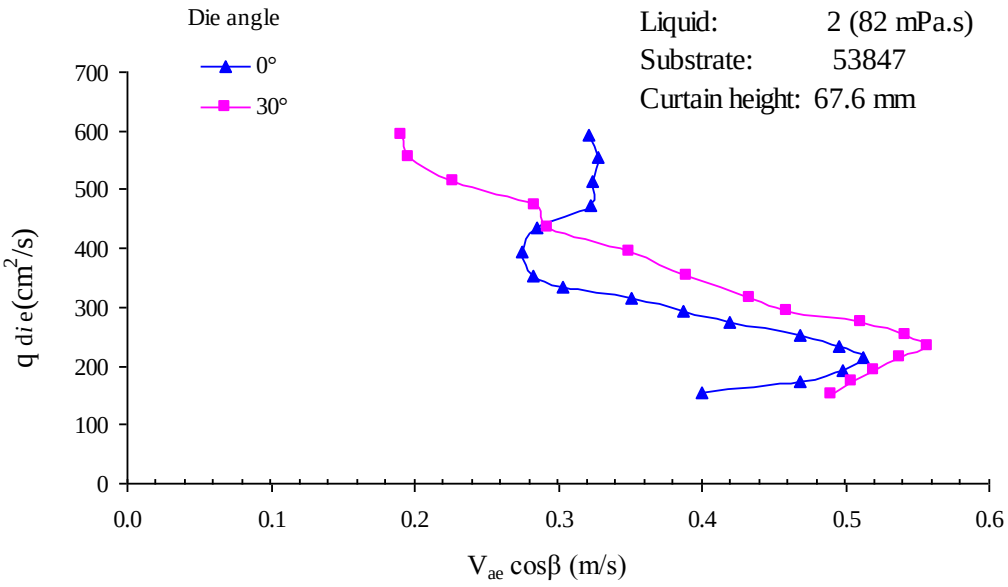

Figure 4.13b: $V_{ae}\cos\beta$ vs. the flow rate (q_{die}) with liquid 2 for substrate 53847.

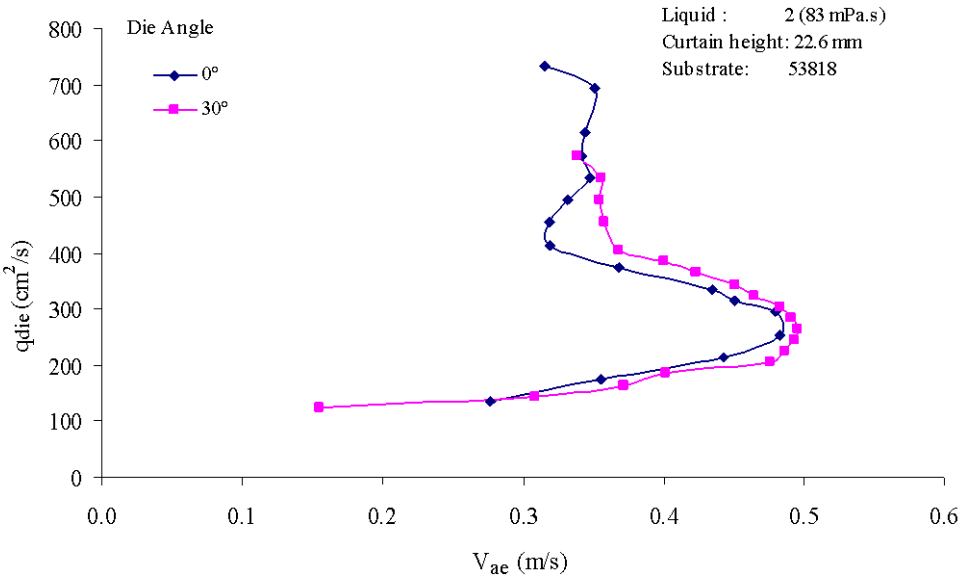

Figure 4.14a: V_{ae} vs. the flow rate (q_{die}) with liquid 2 for substrate 53818.

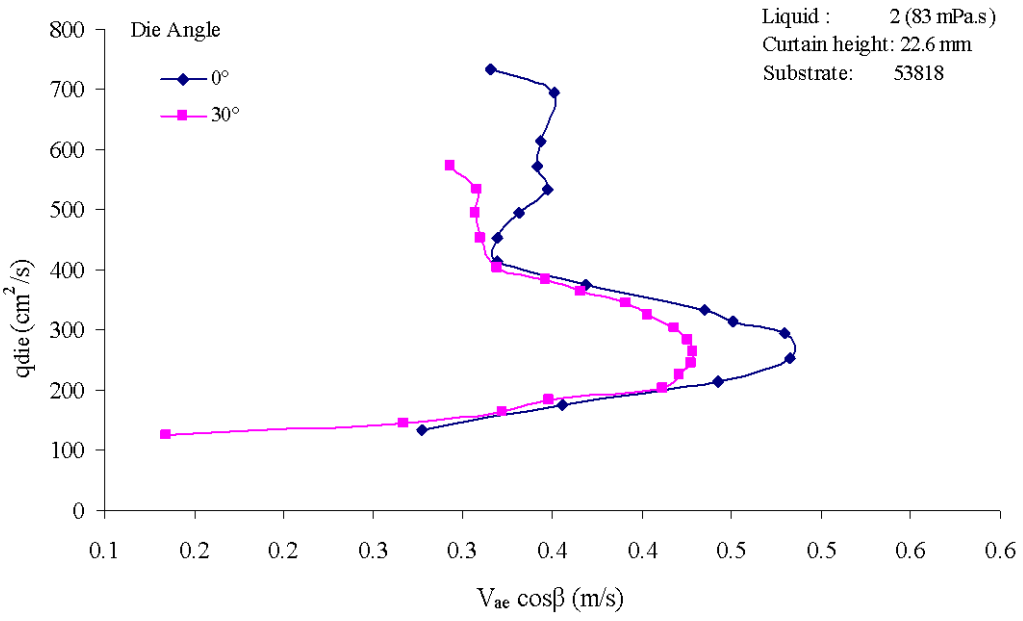

Figure 4.14b: $V_{ae}\cos\beta$ vs. the flow rate (q_{die}) with liquid 2 for substrate 53818.

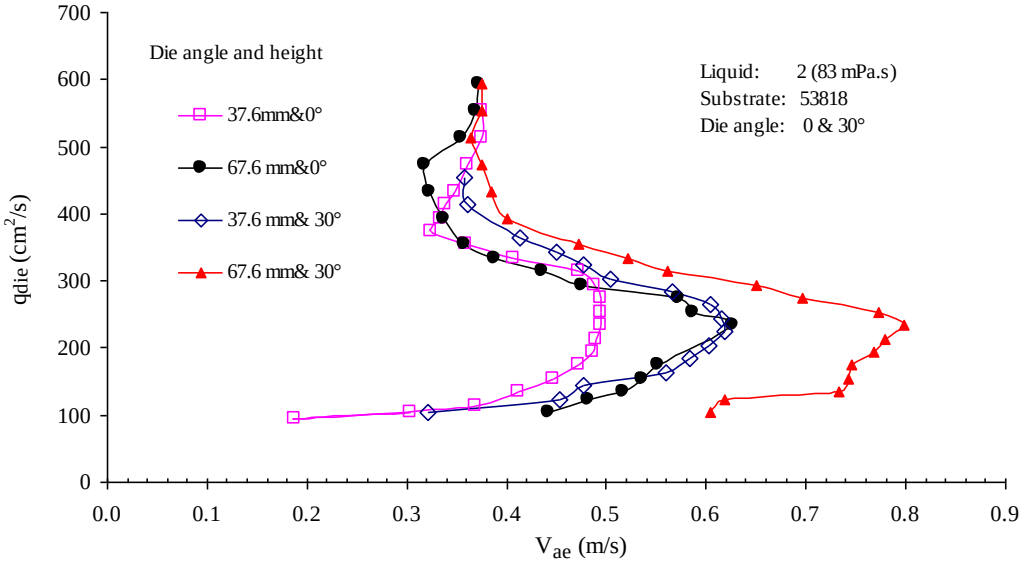

Figure 4.14c: V_{ae} vs. the flow rate (q_{die}) with liquid 2 for substrate 53818.

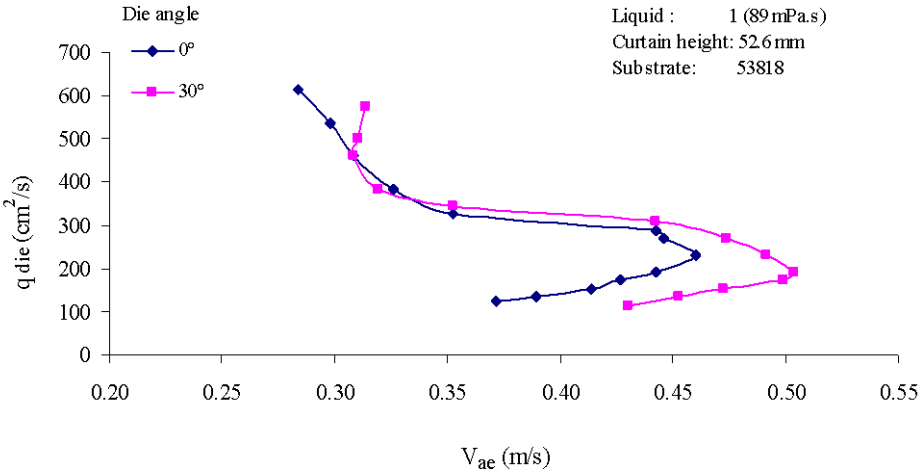

Figure 4.15a: V_{ae} vs. the flow rate (q_{die}) with liquid 1 for substrate 53818.

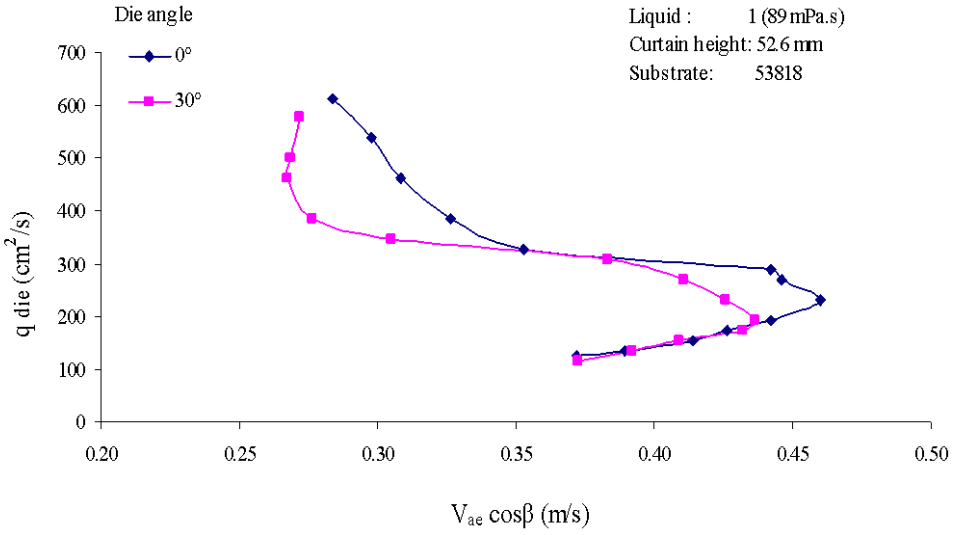

Figure 4.15b: $V_{ae}\cos\beta$ vs. the flow rate (q_{die}) with liquid 1 for substrate 53818.

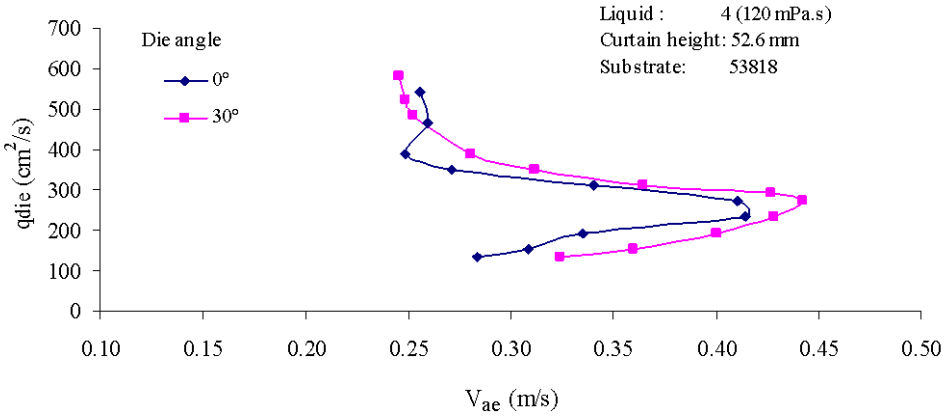

.

Figure 4.16a: V_{ae} vs. the flow rate (q_{die}) with liquid 4 for substrate 53818.

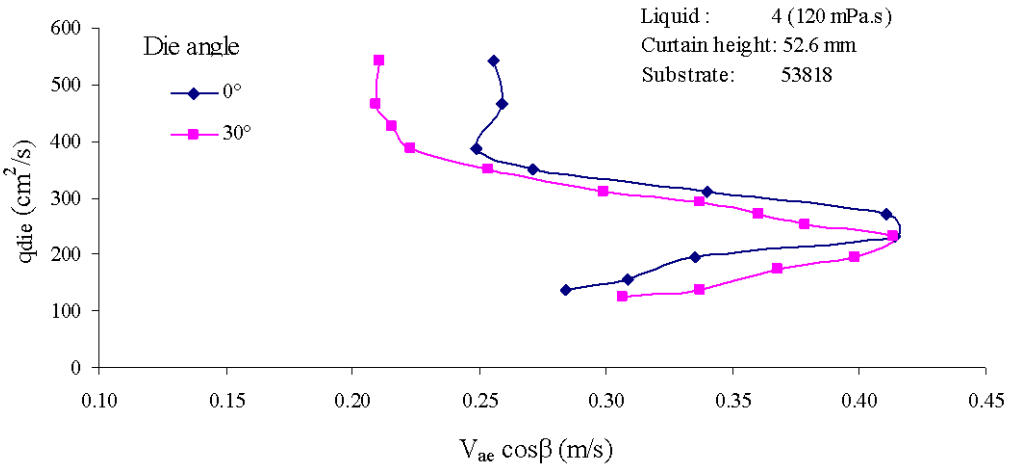

Figure 4.16b: $V_{ae}\cos\beta$ vs. the flow rate (q_{die}) with liquid for substrate 53818

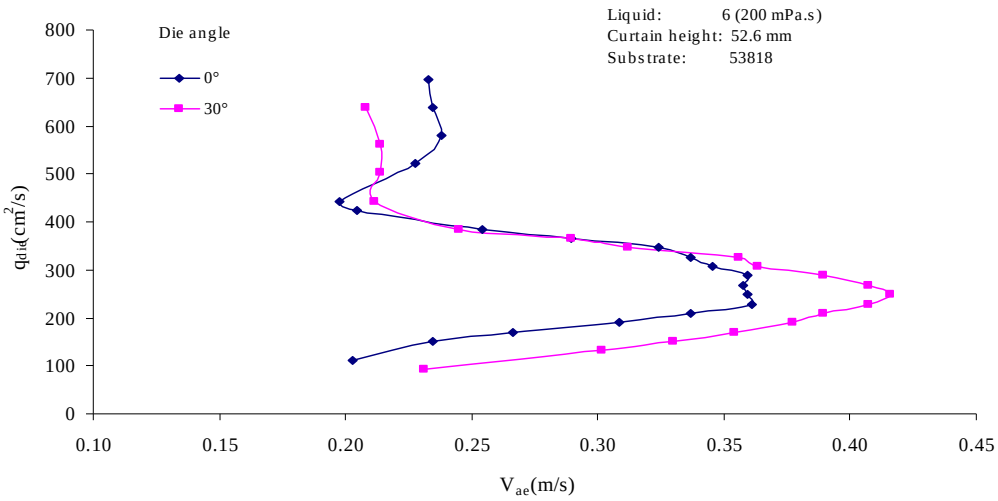

Figure 4.17a: V_{ae} vs. the flow rate (q_{die}) with liquid 6 for substrate 53818.

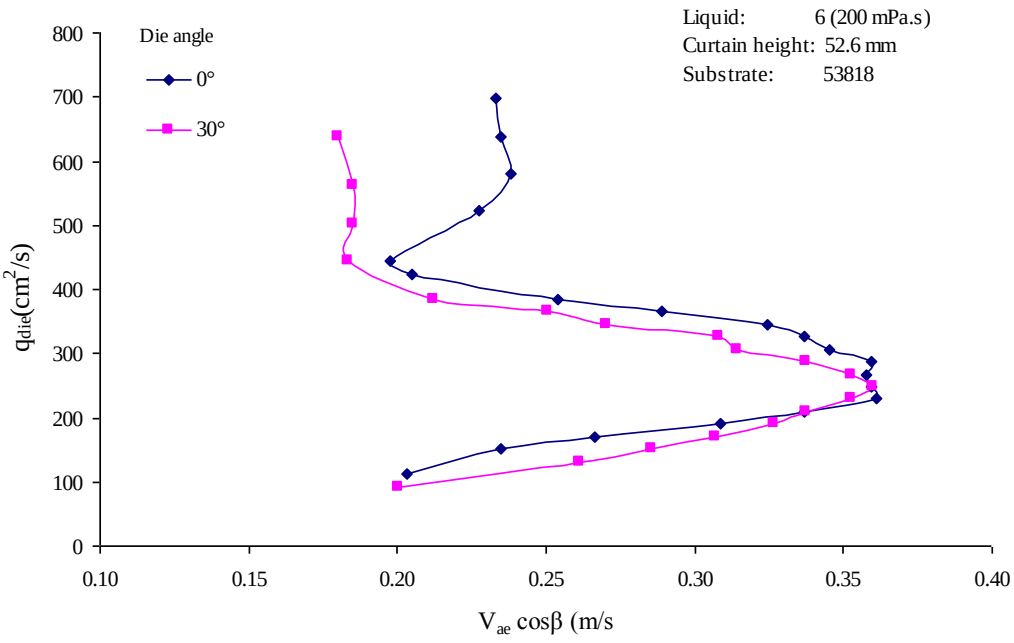

Figure 4.17b: $V_{ae}\cos\beta$ vs. the flow rate (q_{die}) with liquid 6 for substrate 53818.

4.2.3 DATA WITH VISCOUS FLUIDS

Spurred by previous work that showed that viscous fluids can, against *normal* expectations, yield very large hydrodynamic assistance, we performed experiments with viscous fluids and also increasing height and angling further to assess how much extra gain can be obtained when combining all potential aspects of hydrodynamic assistance effects. The data are presented below in Figure 4.17-4.20 for three Newtonian fluids of viscosity 457, 850 and 1200mPa.s (liquids 8, 9 and 10) at curtain heights of 100, 150 and 200 mm for angles 0 and 30° in the case of liquid 8 and up to an angle of 55^0 for the most viscous fluid tested in this and other research programmes (1200mPa.s). Again the plots are presents in terms of q_{die} vs V_{ae} and q_{die} vs. Vae cosβ to assess the validity of the angling hypothesis.

The data taken progressively, for liquids 8 (457mPa.s.), 9 (850mPa.s) and 10 (1200mPa.s) for detailed analysis are very revealing. They show that as the viscosity and heights are increased, the coating window expands greatly showing a maximum speed and no large upturn as with low viscosity. More interestingly, the air entrainment speed is seen to increase by a factor up to 10 suggesting real step changes in coating speeds are possible when combining all the elements of hydrodynamic assistance.

Figure 2.24 shows the comparison of air entrainment velocities between low viscosity liquid and high viscosity liquids. It is clear from this figure that at relative large curtain heights, the air entrainment velocity are greater for high viscosity liquid than for low viscosity liquids.

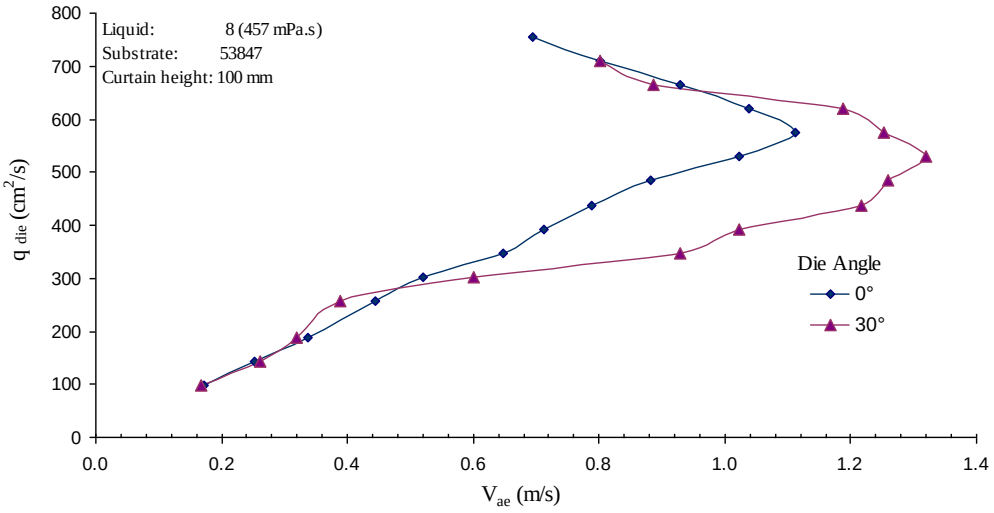

Figure 4.17a: V_{ae} vs. the flow rate (q_{die}) with liquid 8 for substrate 53847.

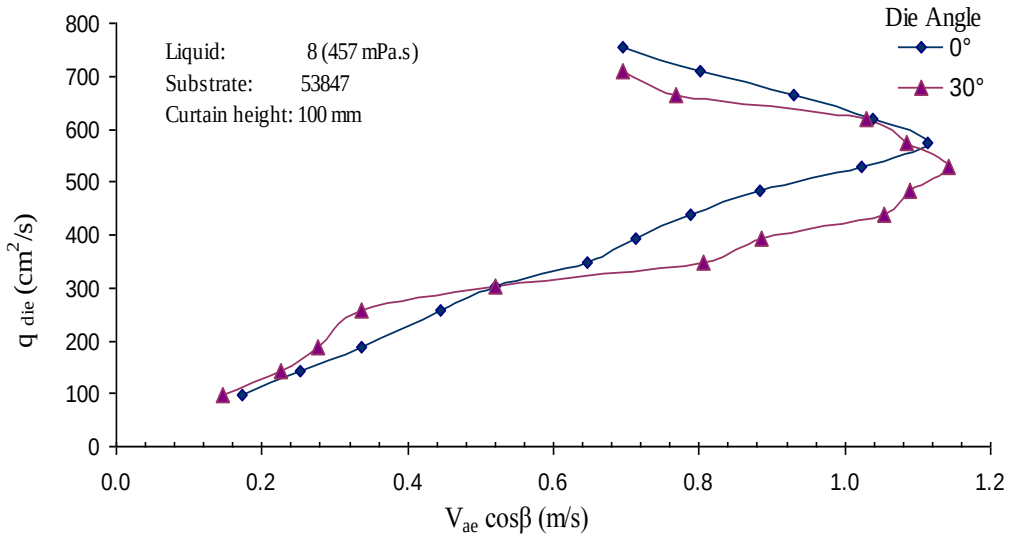

Figure 4.17b: $V_{ae}\cos\beta$ vs. the flow rate (q_{die}) with liquid 8 for substrate 53847.

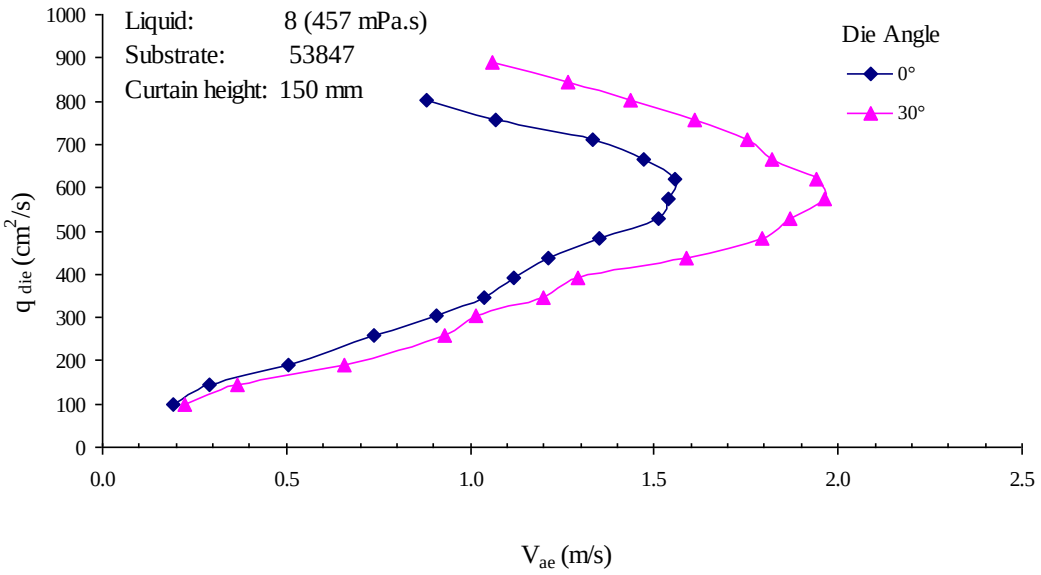

Figure 4.18a: V_{ae} vs. the flow rate (q_{die}) with liquid 8 for substrate 53847.

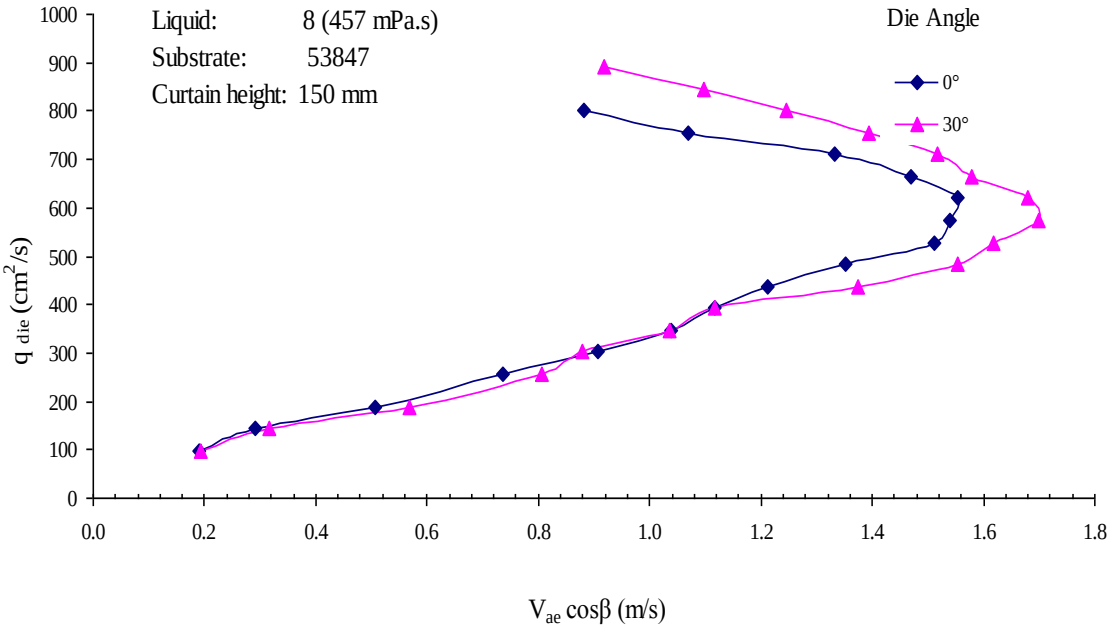

Figure 4.18b: $V_{ae}\cos\beta$ vs. the flow rate (q_{die}) with liquid 8 for substrate 53847

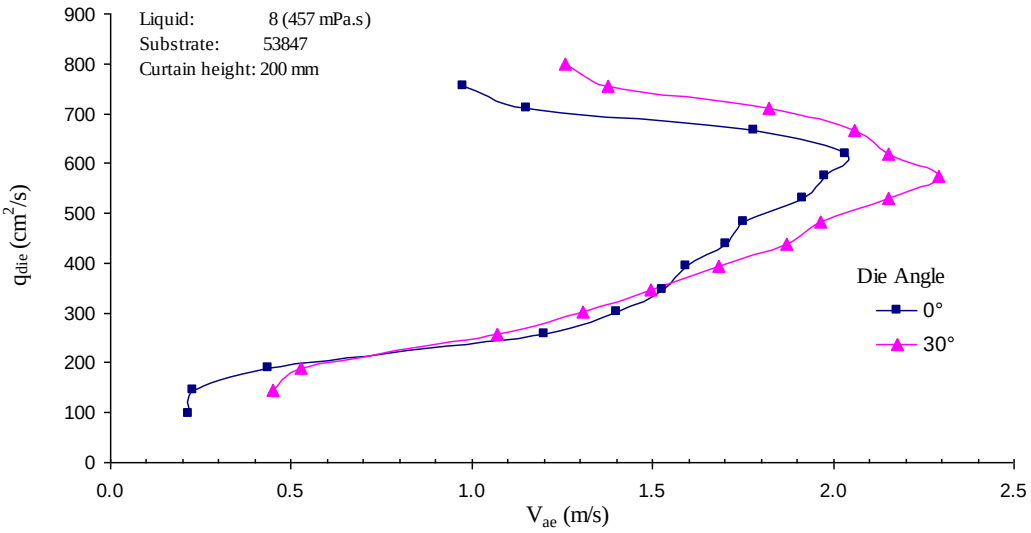

Figure 4.19a: V_{ae} vs. the flow rate (q_{die}) with liquid 8 for substrate 53847.

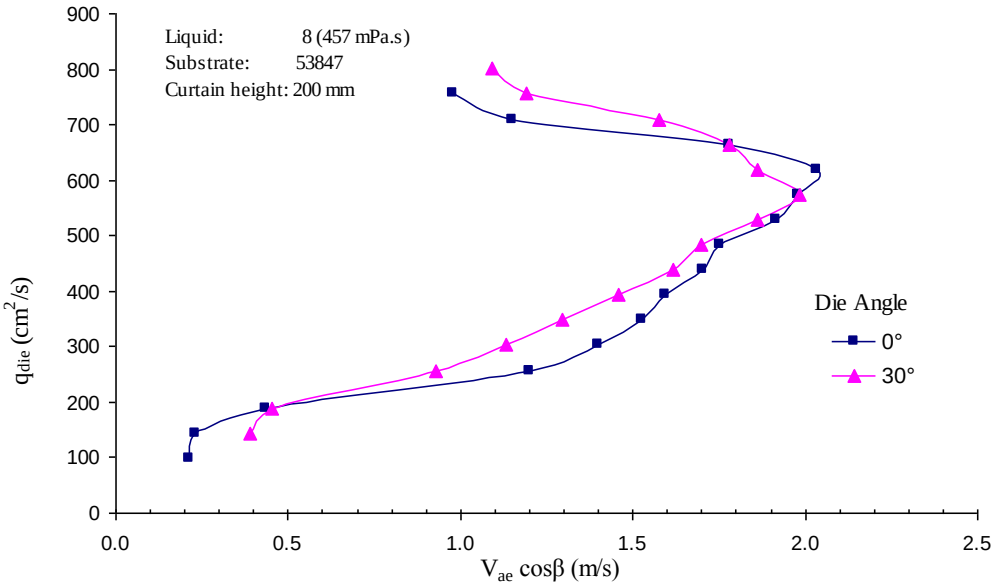

Figure 4.19b: V_{ae}cosβ vs. the flow rate (q_{die}) with liquid 8 for substrate 53847.

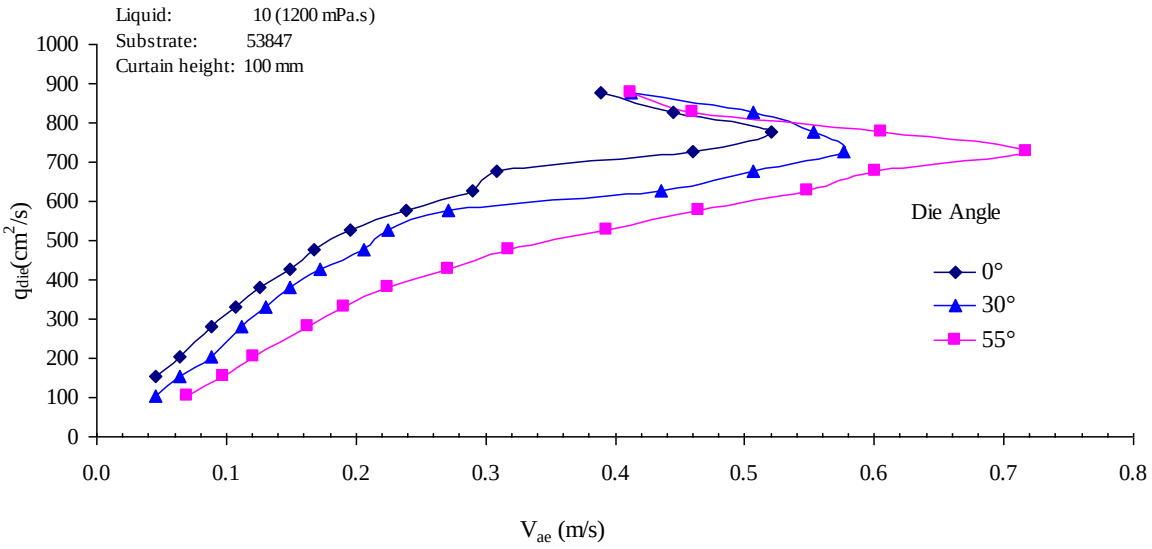

Figure 4.20a: V_{ae} vs. the flow rate (q_{die}) with liquid 10 for substrate 53847.

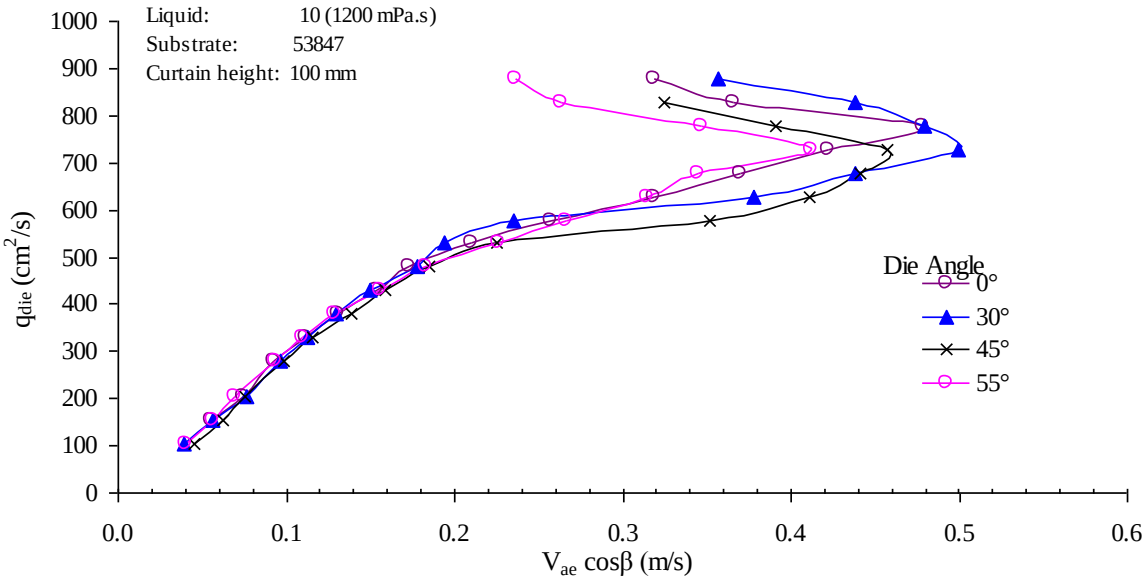

Figure 4.20b: V_{ae}cosβ vs. the flow rate (q_{die}) with liquid 10 for substrate 53847.

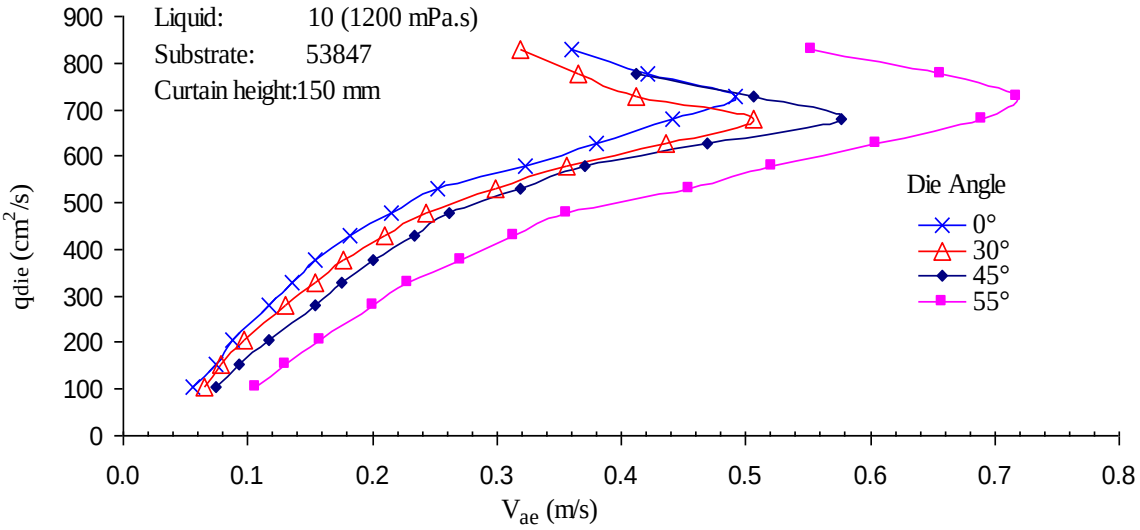

Figure 4.21a: V_{ae} vs. the flow rate (q_{die}) with liquid 10 for substrate 53847.

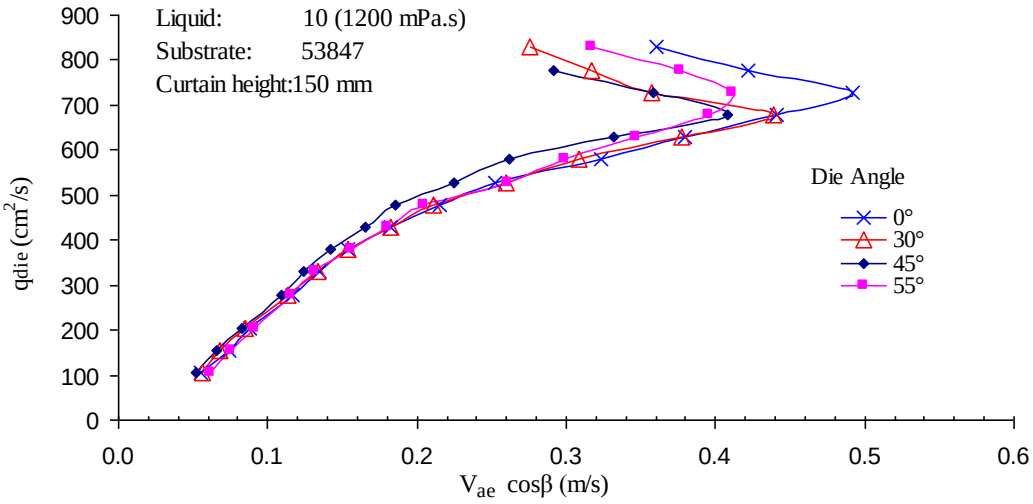

Figure 4.21b: $V_{ae}\cos\beta$ vs. the flow rate (q_{die}) with liquid 10 for substrate 53847

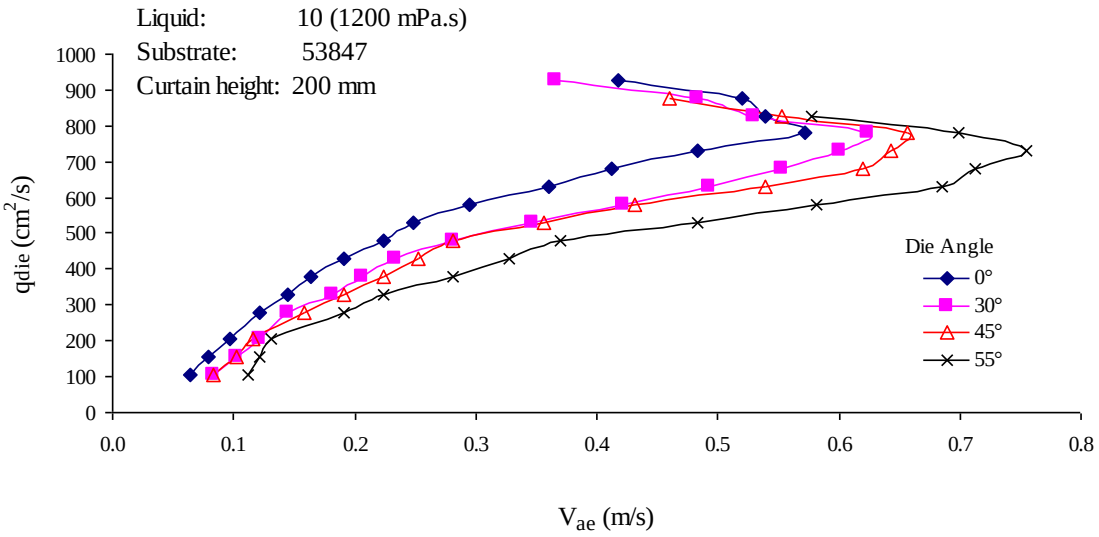

Figure 4.22a: V_{ae} vs. the flow rate (q_{die}) with liquid 10 for substrate 53847.

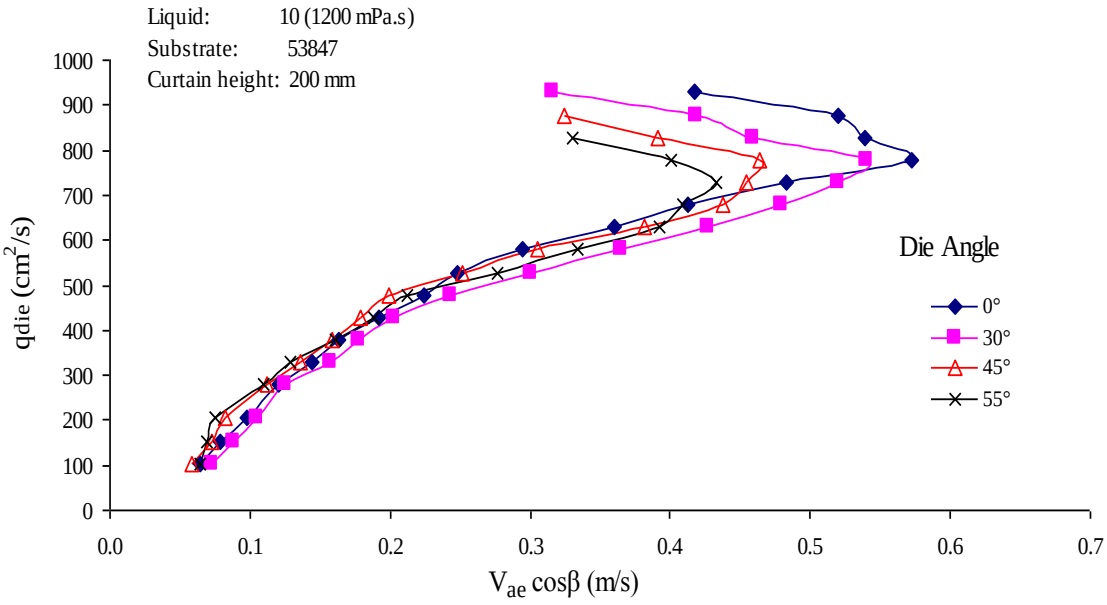

Figure 4.22b: $V_{ae}\cos\beta$ vs. the flow rate (q_{die}) with liquid 10 for substrate 53847.

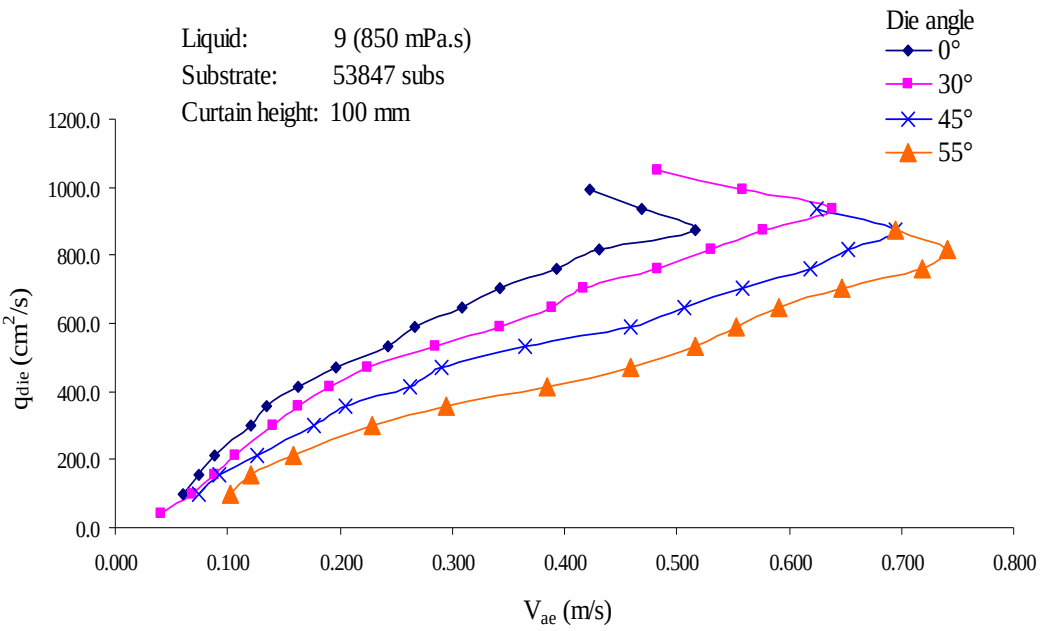

Figure 4.23a: V_{ae} vs. the flow rate (q_{die}) with liquid 9 for substrate 53847

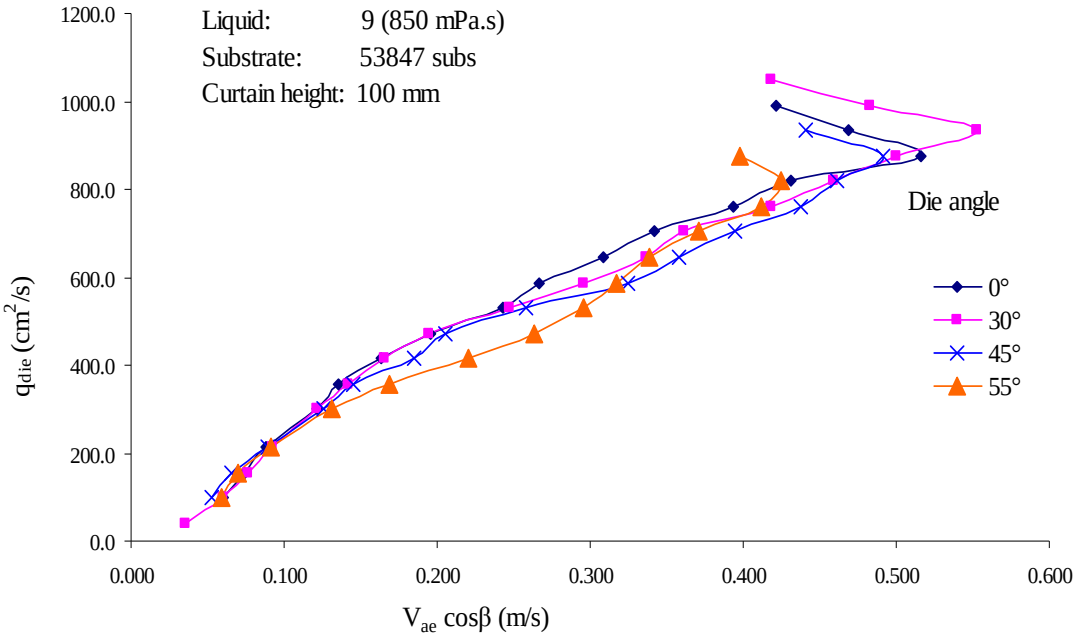

Figure 4.23b: $V_{ae}\cos\beta$ vs. the flow rate (q_{die}) with liquid 9 for substrate 53847.

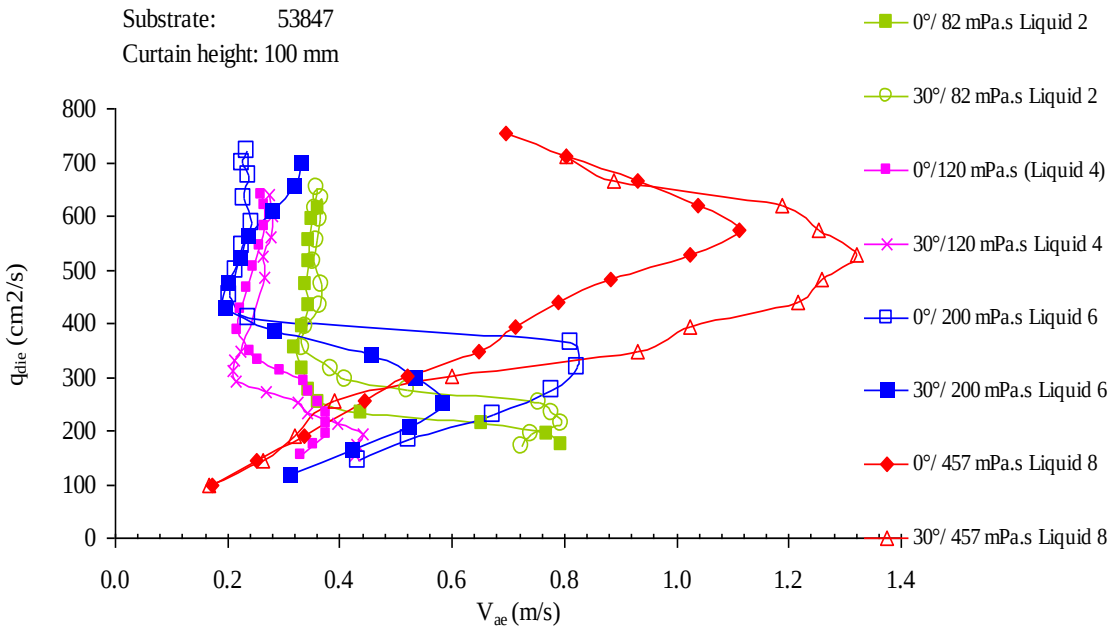

Figure 4.24: Shows the effect of Vae vs. flow rate for different liquid viscosity at 100 mm curtain height.

4.2.4 DATA WITH THE COATING FLUID PVP USED BY D Blake et al. [14]

Having underpinned extensively the angling hypothesis over a very wide range of conditions, here we present data in an attempt to compare performance of an angled die using the exact coating formulation (PVP solution or liquid 11 with viscosity 87 mpa.s) as described in the Experimental chapter reported by Blake et al [11], the pioneer of hydrodynamic assistance in curtain coating. The data are presented in Figure 4.25 for curtain height of 100, 150 and 200 mm and die angles of 0° and 30° for the 53847 substrate. The data are first expressed simply as q_{die} vs V_{ae} and then q_{die} vs. Vae cosβ and presented below.

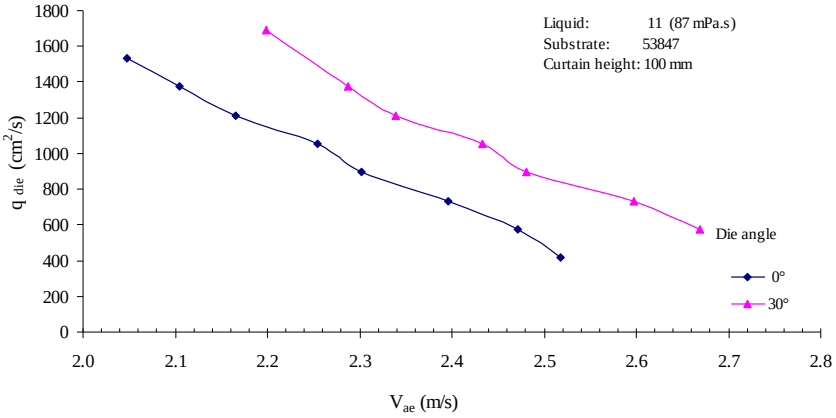

Figure 4.25a: V_{ae} vs. the flow rate (q_{die}) with liquid 11 for substrate 53847.

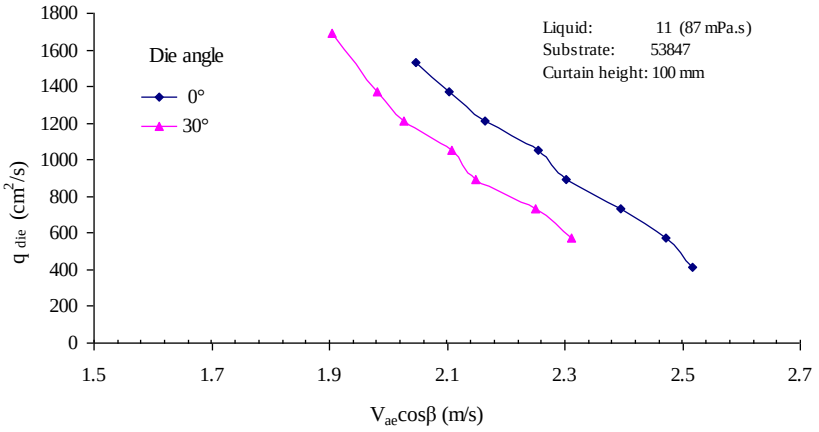

Figure 4.25b: $V_{ae}\cos\beta$ vs. the flow rate (q_{die}) with liquid 11 for substrate 53847

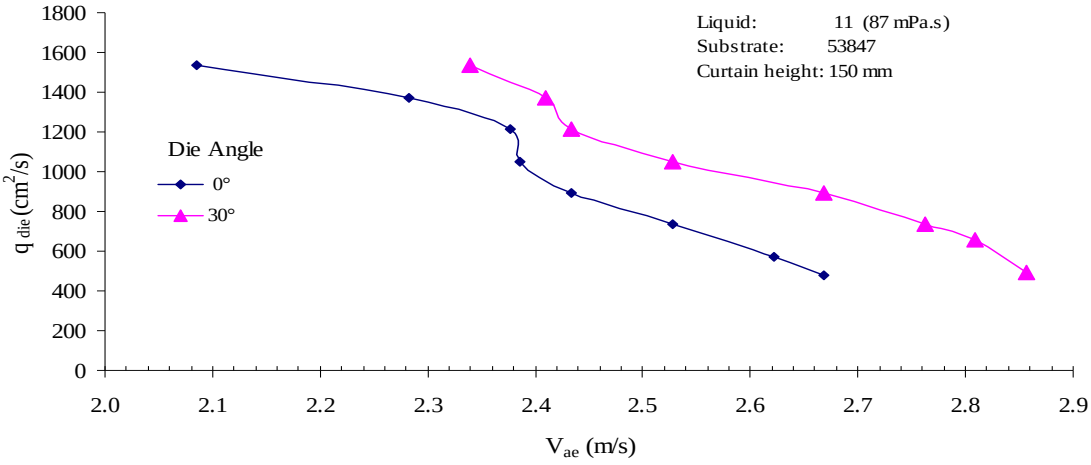

Figure 4.26a: V_{ae} vs. the flow rate (q_{die}) with liquid 11 for substrate 53847

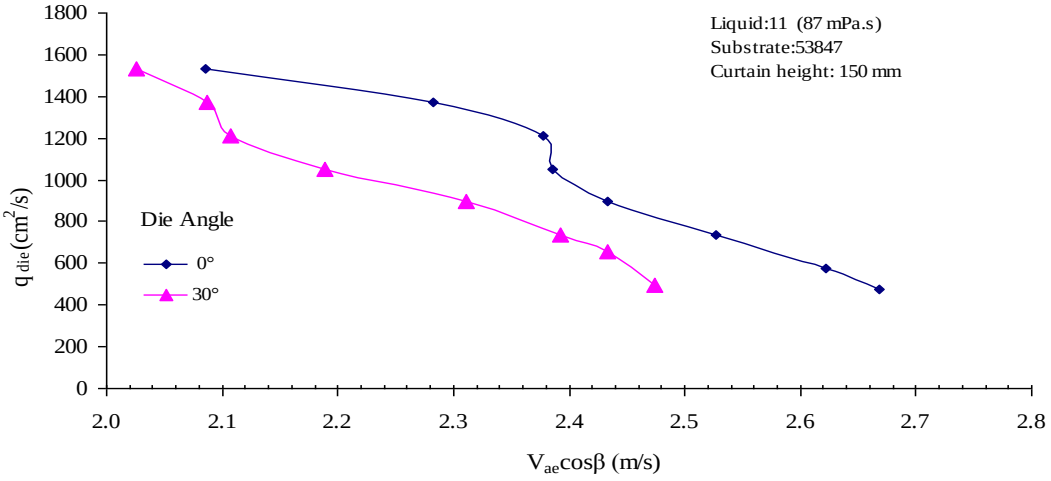

Figure 4.26b: $V_{ae}\cos\beta$ vs. the flow rate (q_{die}) with liquid 11 for substrate 53847

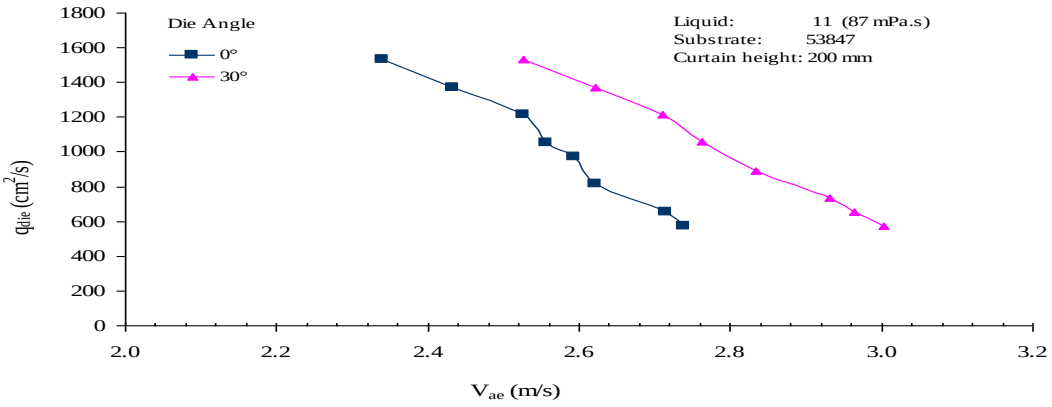

Figure 4.27a: V_{ae} vs. the flow rate (q_{die}) with liquid 11 for substrate 53847.

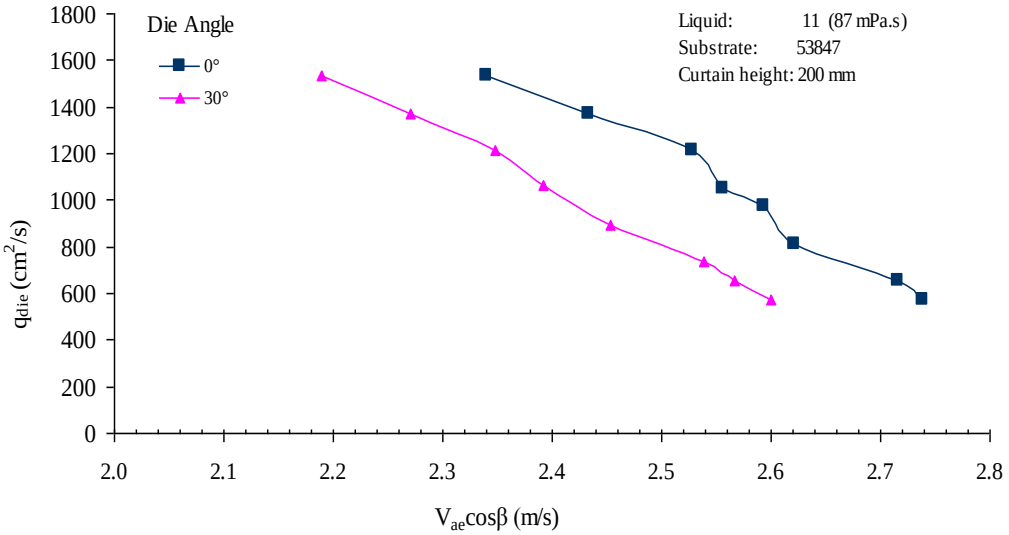

Figure 4.27b: $V_{ae}\cos\beta$ vs. the flow rate (q_{die}) with liquid 11 for substrate 53847.

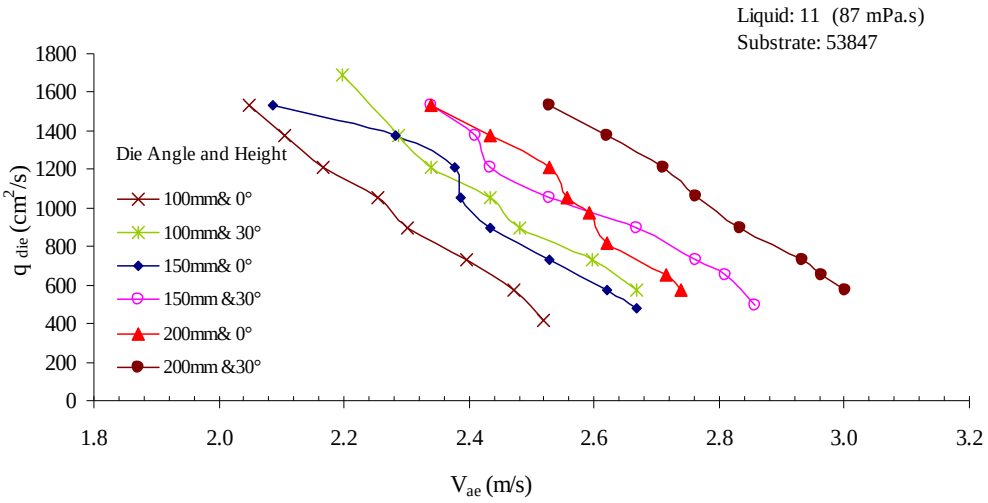

Figure 4.28a: V_{ae} vs. the flow rate (q_{die}) with liquid 11 for substrate 53847.

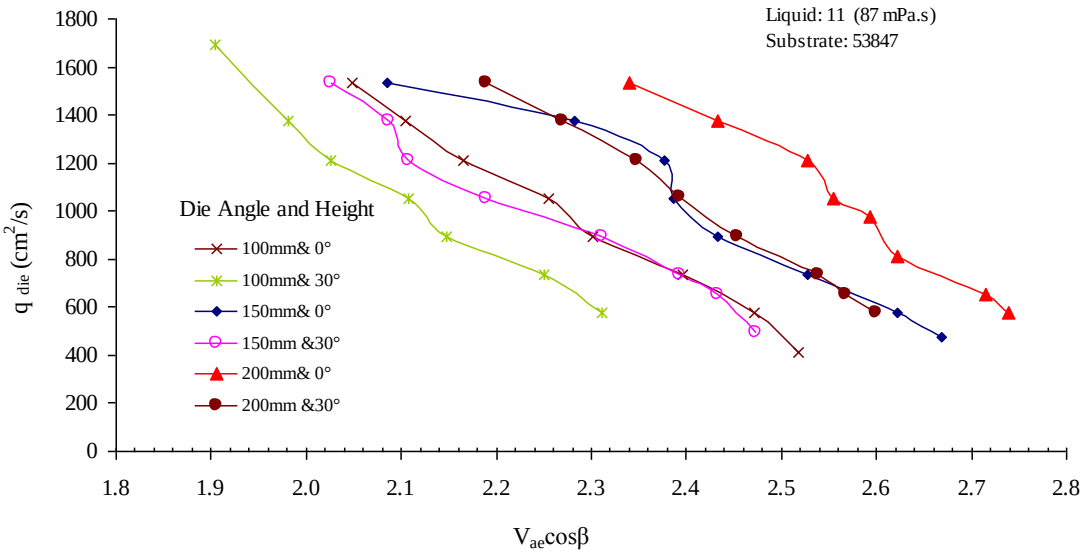

Figure 4.29b: $V_{ae}\cos\beta$ vs. the flow rate (q_{die}) with liquid 11 for substrate 53847.

As explained in Section 4.2.1 above, the non-superimposition suggests a flaw in the hypothesis of angling the curtain die effect on air entrainment speed. Data then process according to Blake et al. [11] analysis reviewed earlier. By plotting the data as in Figure 4.8, in Section 4.2.1, $V_{ae}/V_{ae,max}$ vs. q/q`, where S` is the maximum speed of

air entrainment at each curtain height and die angles and q` is relative to the maximum air entrainment speed. Using this master curve, again the superimposition of the data is observed (see Figure 4.30a below)

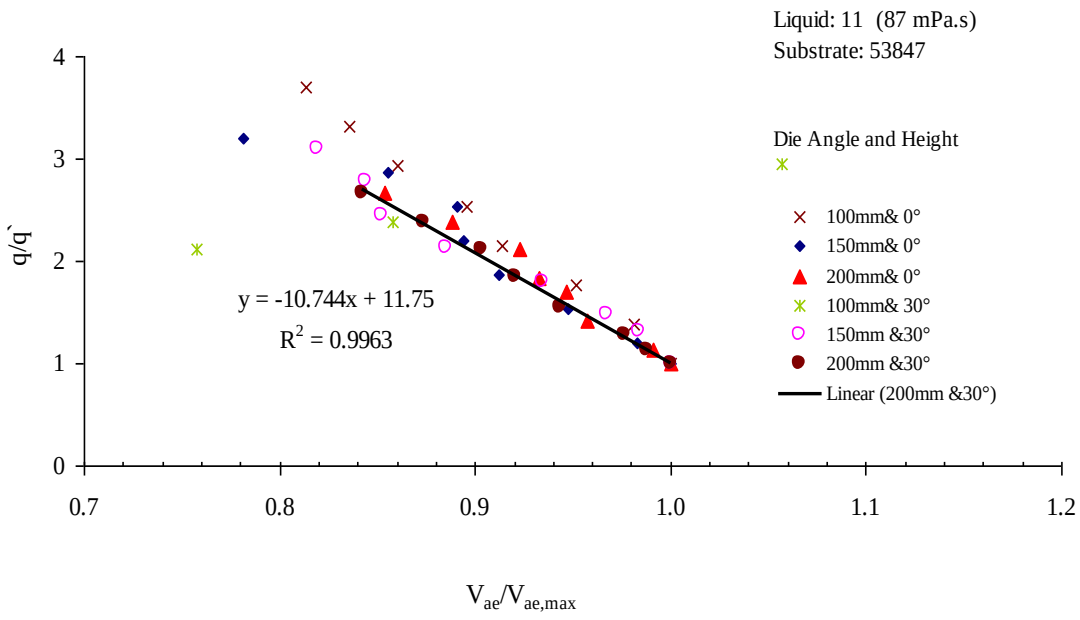

Figure 4.30a: Master curve with PVP fluid or normalized wetting line position vs. normalized speed for different liquid and die angle.

From the above data, a simple linear equation can be fitted:

$$V_{ae}/V_{ae,max}=-10.744(q/q`) + 11.75 \quad (4.1)$$

Comparison of this data and those of Blake et al [14] shown below in Figure 4.30b show a good agreement in the appropriate upper branch of the coating window.

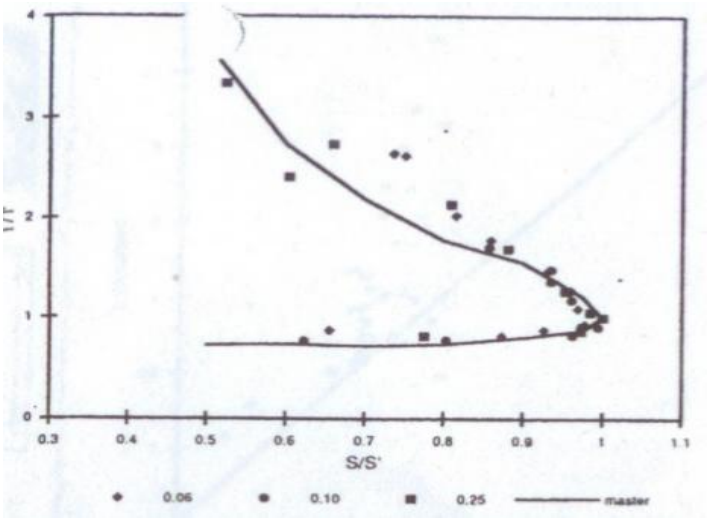

Figure 4.30b: Original data master curve of PVP 59 mPa.s at different height and substrate angle 0° of Blake et al [2].

4.3 CONCLUSIONS

In this chapter a comprehensive set of data has been presented to test the validity of the main argument put in this thesis. That is that angling a curtain die would increase the air entrainment speed by a factor 1/cosβ in conformity with Cohu and Benkreira [2] finding in dip coating. This finding results directly from Blake and Rushack [5]original concept of the maximum speed of wetting. We have shown however that a raw presentation of the data disguises this argument and that the data should be presented according to Blake et al [11] master curve approach in order to dissociate the angle effect from the main hydrodynamic effect of the curtain impingement.

The data here taken to high curtain heights and very viscous fluids, up to 1200 mPa.s show that curtain coating is a faster coating operation. As a measure of comparatively with dip and other coating operation,. As a measure of comparison, Table 4.1 shows some comparative speeds obtained in this study and the same measured in dip coating. As for the application of the concept to coating paper, the

data suggests that the concept is applicable to all curtain coating situations. In this programme the experiments with the coating of paper substrates with clay solutions were not successful, despite the time spent on the trials. The reasons were two-fold: (1) the clay nature of the coating solution made it such that the

particles broke the stability of the die and (2) even after filtering the solution and operating at low curtain flow rate, the paper substrate were too absorbing and resulted in poor web tension and an impossibility in getting reproducible data. Paper substrates require to be coated very fast so as not to give time for the coating solution to infiltrate quickly the substrate.

Table 4.1 Date obtained from this experimental work in curtain coating and dip coating from (I. K theses 2006).

Liquid	Viscosity (μ) mPa.s	V_{ae} Dip coating. IK (m/s)	$V_{ae,max}$ Curtain coating (0°) (m/s)	$V_{ae,max}$ Curtain coating (30°) (m/s)
Sample 1	9.39	0.541	-	-
Sample 2	17.74	0.369	-	-
Sample 3	52.52	0.20	-	-
Sample 4	63.	-	2.418	2.668
Sample 5	83	0.192	0.483	0.558
Sample 5	91.6	0.137		
Sample 6	120	-	0.458	0.553
Sample 7	123	-	0.432	0.446
Sample 8	151	0.113		
Sample 9	190	0.113	0.36	0.462
Sample 10	201	-	0.36	.462
Sample 11	577	-	0.431	0.577
Sample 12	779	-	0.135	0.163
Sample 13	1037	-	0.173	0.196

CHAPTER 5: CONCLUSIONS AND RECOMMENDATIONS FOR FUTURE WORK

This study tested experimentally the validity of an important concept in the physics of wetting of fluids. According to an original study of Blake and Ruschak [1] published in Nature, wetting of solids proceeds at speeds that are limited by a maximum limit above which air entrainment occurs. Cohu and Benkreira [2] observed from this concept the implication that slanting the wetting line at an angle should increase this maximum limit by a factor of 1/cos(angle). In this research, this concept was tested for curtain coating which is an important coating operation. Indeed curtain coating is known to operate at high speeds before air entrainment occurs. This is because of hydrodynamic assistance where the curtain impinges on the wetting line at pressure and delays the breaking of this line. In this study, a rig was built and data were obtained for a range of fluids, curtain heights and angles. It was found that the concept of angling the die holds but a proper presentation of the data was necessary (Blake et al [11]) in order to separate the effect of the curtain hydrodynamic assistance from the angling of the wetting line. More generally, the data from this study support previous work (Marton et al [47] and Blake et al [40]) that curtain coating offers the possibility of coating fast not only for very low viscosity fluids but probably fluids of all viscosities as here the data showed increase in air entrainment speeds for viscosity from 80mPa.s to 1200 mPa.s.

The work presented here although wholly experimental is based on sound theoretical principles and serve as a test case for further theoretical work such as

computer simulations to give further insight on the flow in the wetting region where the die is angled. The following are the recommendations for future work.

- Theoretical simulations of the flow in curtain coating with an angle die to assess the separate roles of angling and curtain impingements on hydrodynamic assistance
- Experiments with various substrates to assess these effects as in practice substrate may be very differents (steel, plastic, paper, smooth and rough substrates).
- Experiments with non-Newtonian fluids as these are the real solutions coated in practice, a mix of polymers, additives and binders to ensure good flow and adhesion of the coating to the substrate.
- Finally and importantly, experiments with real fresh substrate to assess further this important effect as coating really occur first time only when the substrate is presented perfectly dry.

There is also the need to develop further the visualisation techniques to speed up the experimental programme which is very difficult and time consuming otherwise.

REFERENCES

1. Benkreira, H. and J.B. Ikin, *Dynamic wetting and gas viscosity effects.* Chemical Engineering Science, 2010. **65**(5): p. 1790-1796.
2. Wheeler, J., *Curtain coating of adhesive.* June 2003 Converting Magazine, 2003.
3. Aidun, C.K. and N.G. Triantafillopoulos, *High Speed Blade Coating, in liquid Film Coating, S.F. Kistler and P. M. Schweizer, Editors,1997.* Chapman & Hall London, 1997.
4. Walter, P. and W. Strong, *solving common coating flows in reverse roll coating.* converting Magazine, 2003,.
5. Blake, T.D. and K.J. Ruschak, *A maximum speed of wetting.* Nature., 1979. **282:**: p. 489 - 491.
6. Benkreira, H., Patel, R., Edwards, M.F. and Wilkinson, W. L., *Classification and analyses of Coating Flows.* Fluid mechanic, 1994. **54**: p. 437, 447.
7. Cohu, O. and H. Benkreira, *Air entrainment in angled dip coating.* Chemical Engineering Science, 1998. **53**(3): p. 533-540.
8. Daniels, N., P.H. Gaskell, and M.D. Savage, *Slot coating: Aparametric study of the onset of ribbing.* in ECS. University of Erlangen-Nurnberg, 1999. **Shaker Verlag**.
9. SCHWEIZER, P.M., *Curtain coating: stability a critical operating parameter.* Paper technology, 2004. **45**: p. 28 - 35.
10. Cohu. O, a. and H. Benkreira., *Entrainment of air by a solid surface plunging into a non-Newtonian liquid.* AICheE,, 1998. **44**: p. p. 2360-2368.

11. Hyun Wook Jung, J.S.L., Jae Chun Hyun, See Jo Kim' and L. E. Seriven, *Simplified modeling of slide curtain coating flow.* Korea Australia Rheology Jurnal, 2004. **16,**(4): p. 227 - 233.

12. Benkreira and O. H. Cohu, *Angling the wetting line retrads air entrainment in premetered coating flows.* AIChE Journal, 1998. **44**: p. 1207- 1209.

13. Deryagin, B.M. and S.M. Levi, *Film Coating Theory* . Focal Press, London, UK., 1964: p. 137.

14. Terence D. Blake., A.C. and K. Ruschak, *Hydrodynamic Assist of Dynamic Wetting.* AIChE Journal, 1994. **40**(2): p. 229 - 241.

15. Burley, R. and B.S. Kennedy, *An experimental study of air entrainment at a solid/liquid/gas interface.* Chemical Engineering Science, 1976. **31**(10): p. 901-911.

16. Burley, R. and R.P.S. Jolly, *Entrainment of air into liquids by a high speed continuous solid surface.* Chemical Engineering Science, 1984. **39**(9): p. 1357-1372.

17. Gutoff, E.B. and C.E. Kendrick, *Dynamic Contact Angle.* AIChE Journal, 1982. **28**: p. 459- 466.

18. Burley, R., *Air entrainment and limits of coatability.* Journal of the oil and Colour Chemists Association., 1992. **75**(5): p. p. 192 - 202.

19. Connell, o., *Observation of air entrainment and the limit of coatability. In: PhD. Thesis,*. 1989, Heriot-Watt University: Edinburgh, Scotland.

20. Bolton, B. and S. Middleman, *Aire entrainment in a roll coatingsystem.* Chem eng. s, 1980. **35**(597).

21. Wilkinson, W.L., *Entrainmentof air by a solid surface entering a liquid/ air interfacec.* Chem. Eng. Sciences., 1975. **30**: p. p 1227-1230.

22. Kistler, S.F. and a.P.M. Shweizer, *Scientific principlees and their technological implications*, in *Liquid Film Coating*. 1997: London: Chapman and Hall. p. 1997.

23. Ghannam, M.T.a.M.N.E., *Effect of Substrate Entry angle on Air Entrainmentin Liquid Coating.* AIChE Journal, 1990. **36 (8)**: p. p. 1283 - 1286.

24. Buonopane, R.A., E. B. Guttoff, and M. M. Rimore,, *Effect of plunging Tape Surface properties on Air Entrainment Velocity.* AIChE Journal., 1986. **32**(4): p. p. 682 - 683.

25. Perry, R.T., *Fluid Mechanics of entrainment through liquid-liquid and liquid solid junctures in University of Minnesota.* 1967.

26. Inverarity, G., *Dynamic wetting of glass fiber and polymer fibre.* British Polymer Journal., 1969. **1**: p. 245- 251.

27. Benkreira, H. and M.I. Khan, *Air entrainment in dip coating under reduced air pressures.* Chemical Engineering Science, 2008. **63**(2): p. 448-459.

28. Benkreira, H., *The effect of substrate roughness on air entrainment in dip coating.* Chemical Engineering Science, 2004. **59**(13): p. 2745-2751.

29. Benkreira, H. and M.I. Khan, *Air entrainment in dip coating under reduced air pressures.* Chemical Engineering Science, 2007. **In Press, Accepted Manuscript**.

30. C.Huh, L.E. and J. Scriven, *Colloid Interface Sci.* 1971. **35**(1): p. 85.

31. Voinvo, O.V., *Fluid Dynamics.* 1976. **11**: p. 714.

32. Cox, R., *The Dynamic of the Sepreading of Liquids on a Soild Surface Part I.* Viscous Flow, " I. Fluid Mech., 1986: p. 168 - 169.

33. Dussan V., E.B., *On The Spreading of Liquids on Solid Surfaces Static and Dynamic Contact Angles,.* Ann. Rev. Fluid Mech., 1979. **11**: p. 371.

34. Clarke, A., *Coating on a Rough Surface.* AIChE Journal, 2002. **48**(10): p. P: 2149 - 2156.

35. Miyamoto, K. and L.E. Scriven, *Breakdown of air film entrained by liquid coated on web.* Paper read at AIChE Annual Meeting Los Angeles, CA., 1982.

36. Mues, W., J. Hens, and L. Boiy,, *Observation of a dynamic wetting process using laser-Doppler Velocity.* AIChE Journal, 1989. **35**: p. 1521 - 1526.

37. Miyamoto, K., *On the Mechanism of Air Entrainment.* Industrial Coating Research, 1991. **1**: p. 71- 88.

38. Gutoff, E.B. and a.C.E. Kendrick, *Low Flow Limits of Coatability on a Solide Coater.* AIChE Journal, 1987. **33**(1): p. p. 141-145.

39. Benkreira, H., *Dynamic wetting in metering and pre-metered forward roll coating.* Chemical Engineering Science, 2002. **57**(15): p. 3025-3032.

40. Blake, T.D.D., Rosemary A. and K.J. Ruschak, *Wetting at high capillary numbers.* Journal of Colloid and Interface Science, 2004. **279**(1): p. 198-205.

41. Terence D. Blake, C. and A. Clarke, *Hydrodynamic Assist of Dynamic Wetting.* AIChE Journal, 1994. **40**(2): p. 229 - 241.

42. Brown. D. R, *A study of the behaviour of a thin sheet of moving liquid.* J. Fluid Mech,, 1960. **10**: p. 297-305.

43. Yamamura, M., *Assisted dynamic wetting in liquid coatings.* Colloids and Surfaces A: Physicochemical and Engineering Aspects. Engineering Particle Technology, 2007. **311**(1-3): p. 55-60.

44. Terence D. Blake, R.A.D.a.K.J.R., *Wetting at high capillary numbers.* Colloid and Interface Science, 2004. **279**: p. 198 - 205.

45. Clarke, A., *The application of particle tracking velocimetry and flow visualisation to curtain coating.* Chemical Engineering Science, 1995. **50**(15): p. 2397-2407.

46. Yamamura, M., et al., *Experimental investigation of air entrainment in a vertical liquid jet flowing down onto a rotating roll.* Chemical Engineering Science, 1999. **55**(5): p. 931-942.

47. Marston J. O., Simmons M. J., and S.P. Decent, *Influence of viscosity and immpingement speed on intense hydrodynamics assist in curtain coating.* Experiment Fluids, 2007. **42,**: p. p 483-488.

48. T.D. Blake, A. Clarke, and E.H. Stattersfield, *An investigation of electrostatic assist in dynamic wetting.* Langmuir, 2000. **16**: p. 2928 - 2935.

49. Zaman, A.A. and S. Mathur, *Influence of dispersing agents and solution conditions on the solubility of crude kaolin.* Journal of Colloid and Interface Science, 2004. **271**(1): p. 124-130.

50. Gennes, P.G.D., *Wetting: statics and dynamics.* Reviews of Modern Physics., 1985. **57(3)**: p. p.827.

APPENDIX 1

1.1 PUMP CALIBRATION OF THE CURTAIN FLOW RATES

Curtain coating operates at various flow rate and different liquid viscosities, an accurate control of this flow rate was necessary. This was a achieved by calibrating the pump at set pointes that were used for each liquid tested. For each pumping speed set points the coating fluid was collected for known period of time and weighed. The mass flow rate (g/s) and volumetric flow rate (l/m). The results of all liquids used in this thesis are presented in Table 1.1 to 1.9.

Table 1.1: Calibration data for liquid 1 (Mix 1)

Liquid 3; Viscosity at 19°C = 89 mPa.s			
Coating fluid pumping speed set point (%)	Weight of oil collected (g)	Time of collection (sec)	Flow rate (l/m)
0	0	0	0
5	1774.2	103	1.18
10	2426.7	71	2.34
15	2604	52	3.43
20	2910	43	4.64
25	2998.6	35	5.87
30	3104.5	31	6.86

Table 1.2: Calibration data for liquid 2 (Milgear 1)

Liquid 3; Viscosity at 22°C = 82 mPa.s			
Coating fluid pumping speed set point (%)	Weight of oil collected (g)	Time of collection (sec)	Flow rate (l/m)
0	0	0	0
5	1890.6	117	1.11
10	2942.4	90	2.24
15	3453.4	67	3.53
20	3671.5	53	4.75
25	3597.7	42	5.87
30	3980.7	30	7.18

Table 1.3: Calibration data for liquid 3 (Millmax 37)

Liquid 3; Viscosity at 23°C = 97 mPa.s			
Coating fluid pumping speed set point (%)	Weight of oil collected (g)	Time of collection (sec)	Flow rate (l/m)
6	1947.1	76	1.25
8	2035.1	71	1.39
10	2115.7	67	1.54
12	2120.5	62	1.66
14	2292.7	59	1.89
16	2298.1	52	2.15
18	2278.8	49	2.26
20	2440.9	49	2.42
22	2503.4	44	2.77

Table 1.4: Calibration data for liquid 4 (Millmax 46)

Liquid 3; Viscosity at 24.8°C = 120 mPa.s			
Coating fluid pumping speed set point (%)	Weight of oil collected (g)	Time of collection (sec)	Flow rate (l/m)
0	0	0	0
5	1667	98	1.17
10	2335	69	2.32
15	2520.6	49	3.53
20	2702.4	40	4.63
25	2458.8	29	5.81

Table 1.5: Calibration data for liquid 5 (Millmax 68)

Liquid 3; Viscosity at 23°C = 120 mPa.s			
Coating fluid pumping speed set point (%)	Weight of oil collected (g)	Time of collection (sec)	Flow rate (l/m)
0	0	0	0
6	1568	75	1.43
8	1799.4	65	1.90
10	1980.9	58	2.34
12	1911	43	3.05
15	1875.9	35	3.67
18	1742.8	28	4.27
20	1753	23	5.22
25	1862.3	19	6.72
30	1811.3	15	8.28

35	1921.5	14	9.41
40	1923.5	13	10.14

Table 1.6: Calibration data for liquid 6 (Millube 68)

Liquid 3; Viscosity at 22°C = 200 mPa.s			
Coating fluid pumping speed set point (%)	Weight of oil collected (g)	Time of collection (sec)	Flow rate (l/m)
0	0	0	0
5	1910.4	116	1.13
10	2673.5	80	2.29
15	2563.6	51	3.45
20	2748.4	41	4.60
25	2605.4	31	5.76
30	2607.7	26	6.88
35	2823.4	25	7.74
40	3270.5	23	9.75

Table 1.7: Calibration data for liquid 8 (Millmax 150)

Liquid 3; Viscosity at 22°C = 450 mPa.s			
Coating fluid pumping speed set point (%)	Weight of oil collected (g)	Time of collection (sec)	Flow rate (l/m)
0	0	0	0
5	1568.6	94	1.14
10	1801.5	51	2.42
15	1686.7	32	3.61
20	1822.3	23	5.43
25	1892.3	19.38	6.69
30	1638	14	8.02
35	1758.7	12.27	9.83
40	1698.5	10.35	11.25

Table 1.8: Calibration data for liquid 9 (Millmax 220)

Liquid 3; Viscosity at 21°C = 850 mPa.s			
Coating fluid pumping speed set point (%)	Weight of oil collected (g)	Time of collection (sec)	Flow rate (l/m)
0	0	0	0
5	1822.3	98	1.27
10	1896.44	50	2.60
15	2171.9	40	3.72
20	2122.6	22	6.61
25	2064	18	7.86
30	2379	17	9.59
35	2304	13	12.15

Table 1.8: Calibration data for liquid 10 (Millmax 320)

Liquid 3; Viscosity at 23°C = 1200 mPa.s			
Coating fluid pumping speed set point (%)	Weight of oil collected (g)	Time of collection (sec)	Flow rate (l/m)
0	0	0	0
5	1687.6	94	1.23
7	1811.3	66	1.88
9	1872.3	53	2.42
12	2006.8	43	3.20
14	1971	37	3.65
18	2073.8	28	5.08
24	1890	20	6.48
28	1853	14.7	8.64

Table 1.9: Calibration data for liquid 11 (PVP)

Liquid 3; Viscosity at 23°C = 87 mPa.s			
Coating fluid pumping speed set point (%)	Weight of oil collected (g)	Time of collection (sec)	Flow rate (l/m)
0	0	0	0
43	2222.1	38	4.01
45	2415.8	40	4.14
47	2357.6	38	4.25
48	2355.3	36	4.48
50	2397	34	4.83

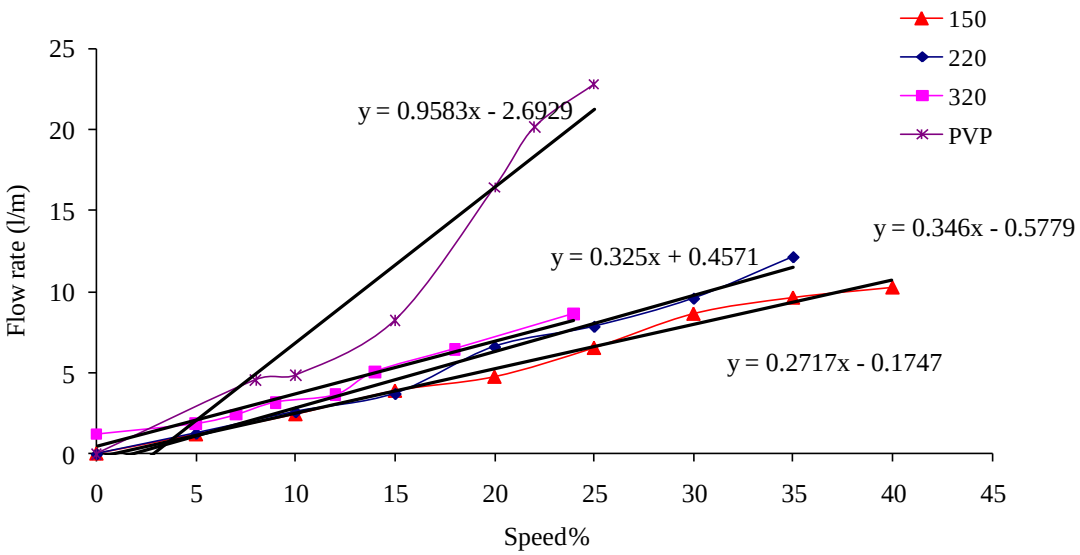

Figure 1.1: Pump calibration of different liquid at various flow rates

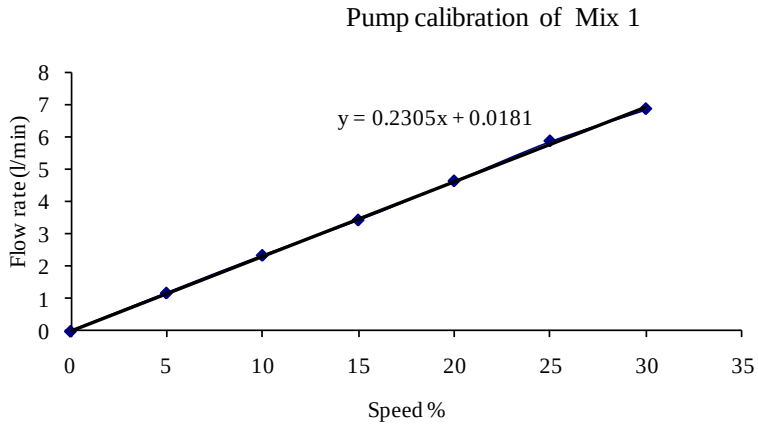

Figure 1.2: Pump calibration of liquid 1

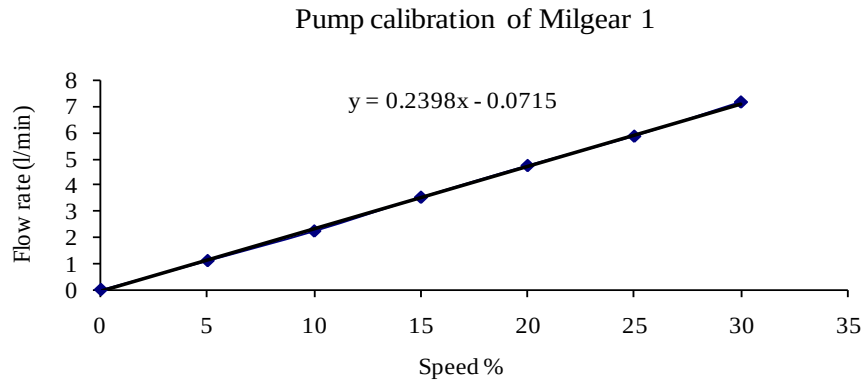

Figure 1.3: Pump calibration of liquid 2

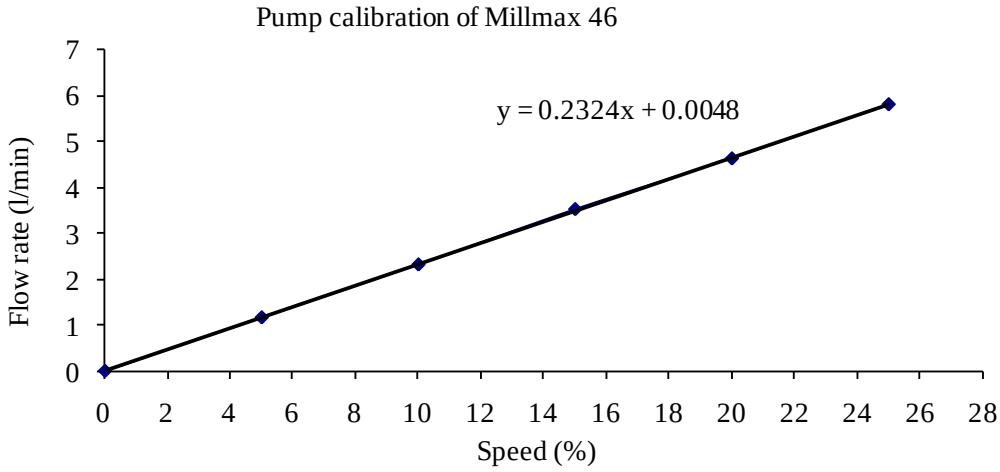

Figure 1.4: Pump calibration of liquid 4

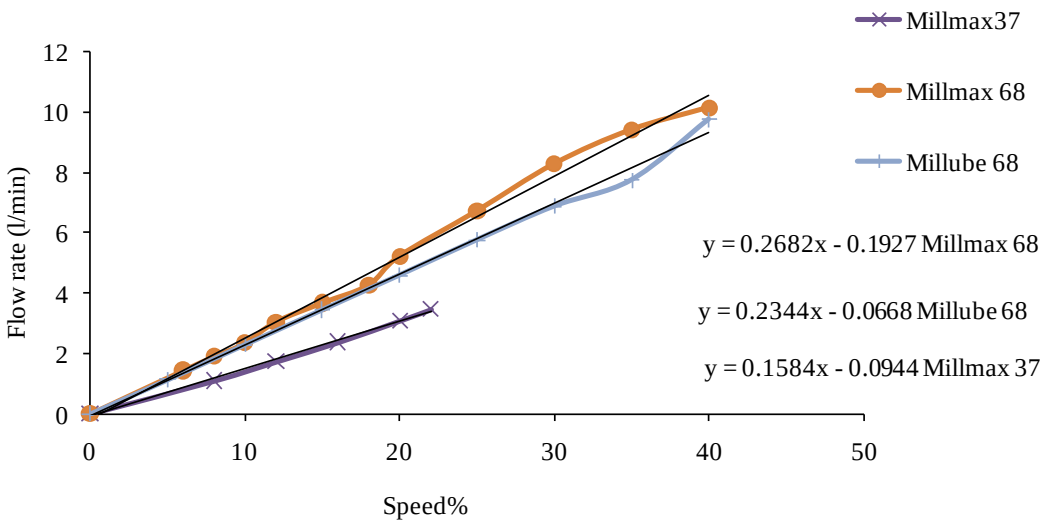

Figure 1.2: Pump calibration of liquid 3, 5 and 6

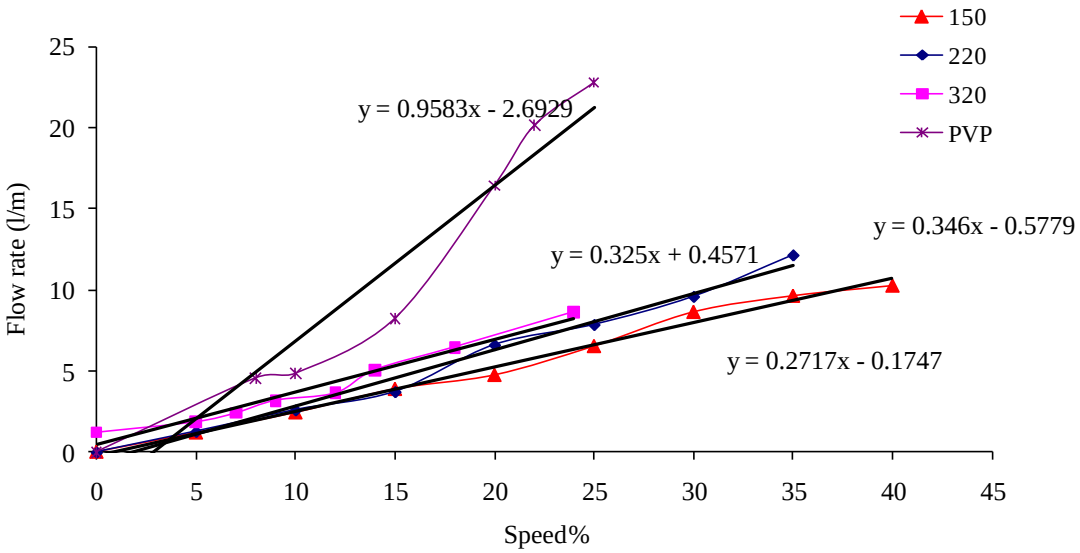

Figure 1.2: Pump calibration of liquid 8, 9, 10 and 11

1.2 CONTACT ANGLE

Table 1.1: Contact angle of Millgear 1 with substrate 53818 and polyester

.

First run		Second run		Third run		Contact angle average	
Graph Sec	Y-axis Angle	Graph Sec	Y-axis Angle	Graph Sec	Y-axis Angle	Graph Sec	Y-axis Angle
0	115.55	0	129.42	0	103.79	0.000	116.253
0.0167	92.13	0.0167	97.61	0.0167	88.22	0.017	92.653
0.0334	81.04	0.0667	70.12	0.0334	78.19	0.045	76.450
0.05	73.63	0.0834	66.88	0.05	72.45	0.061	70.987
0.0667	69.3	0.1	63.78	0.0667	68.02	0.078	67.033
0.0834	65.51	0.1167	61.77	0.0834	65.4	0.095	64.227
0.1	63.09	0.1334	59.58	0.1	62.72	0.111	61.797
0.1167	60.62	0.15	58.18	0.1167	61.1	0.128	59.967
0.1334	59.13	0.1667	56.45	0.1334	59.11	0.145	58.230
0.15	57.17	0.1834	55.36	0.15	58.07	0.161	56.867
0.1667	56.1	0.2	53.93	0.1667	56.53	0.178	55.520
0.1834	54.55	0.2167	53.05	0.1834	55.77	0.195	54.457
0.2	53.79	0.2334	51.83	0.2	54.49	0.211	53.370
0.2167	52.38	0.25	51.22	0.2167	53.83	0.228	52.477
0.2334	51.79	0.2667	50.04	0.2334	52.8	0.245	51.543
0.25	50.65	0.2834	49.57	0.25	52.32	0.261	50.847
0.2667	50.15	0.3	48.52	0.2667	51.32	0.278	49.997
0.2834	49.05	0.3167	48.14	0.2834	51	0.295	49.397
0.3	48.65	0.3334	47.2	0.3	50.08	0.311	48.643
0.3167	47.76	0.35	46.92	0.3167	49.87	0.328	48.183

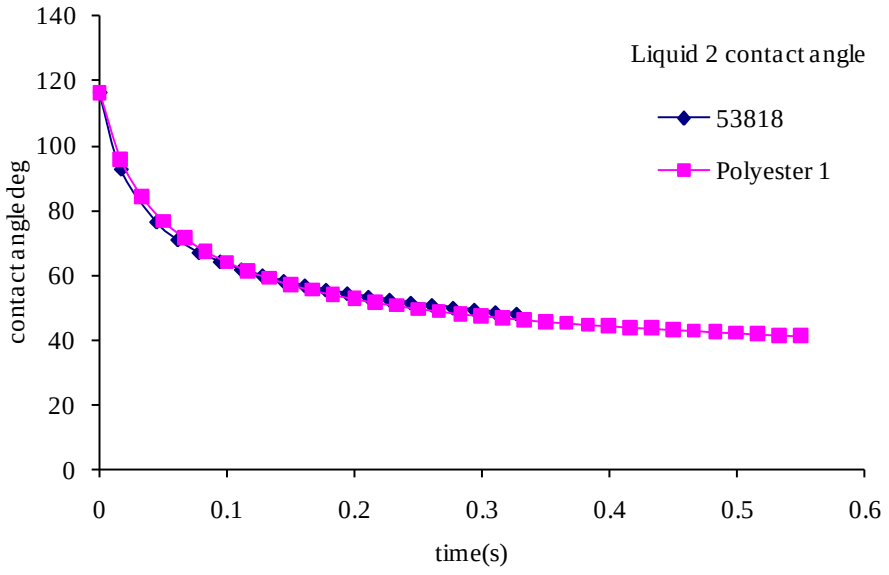

Figure 1.2: Liquid 2 (milgear1, 82 mPa.s) contact angle with different substrate

Table 1.2: contact angle of liquid 2 with 53818, polyester 1 and Hifi 400

First run		Second run		Third run		Contact angle average	
Graph Sec	Y-axis Angle	Graph Sec	Y-axis Angle	Graph Sec	Y-axis Angle	Graph Sec	Y-axis Angle
0	111.47	0	120.41	0	117.21	0.000	116.363
0.0166	92.6	0.0167	95.18	0.0166	99.23	0.017	95.670
0.0333	81.38	0.0333	83.13	0.0333	88.08	0.033	84.197
0.05	73.29	0.05	74.84	0.05	81.83	0.050	76.653
0.0666	68.09	0.0667	69.97	0.0666	76.41	0.067	71.490
0.0833	63.77	0.0833	65.46	0.0833	72.59	0.083	67.273
0.1	60.7	0.1	62.79	0.1	68.81	0.100	64.100
0.1166	57.69	0.1167	59.83	0.1166	66.09	0.117	61.203
0.1333	56.08	0.1333	58.09	0.1333	63.21	0.133	59.127
0.15	53.83	0.15	55.98	0.15	61.24	0.150	57.017
0.1666	52.67	0.1667	54.83	0.1666	58.86	0.167	55.453
0.1833	51.23	0.1833	52.98	0.1833	57.56	0.183	53.923
0.2	50.32	0.2	52.22	0.2	55.73	0.200	52.757
0.2166	49.14	0.2167	50.68	0.2166	54.71	0.217	51.510
0.2333	48.66	0.2333	50.23	0.2333	53.09	0.233	50.660
0.25	47.46	0.25	49.08	0.25	52.27	0.250	49.603
0.2666	47.23	0.2667	48.58	0.2666	51.12	0.267	48.977
0.2833	45.91	0.2833	47.59	0.2833	50.48	0.283	47.993
0.3	45.88	0.3	47.36	0.3	49.43	0.300	47.557
0.3166	44.99	0.3167	46.5	0.3166	48.96	0.317	46.817
0.3333	44.72	0.3333	46.39	0.3333	47.9	0.333	46.337
0.35	43.7	0.35	45.64	0.35	47.57	0.350	45.637
0.3666	43.67	0.3667	45.36	0.3666	46.81	0.367	45.280
0.3833	42.95	0.3833	44.64	0.3833	46.48	0.383	44.690
0.4	42.99	0.4	44.64	0.4	45.58	0.400	44.403
0.4166	42.02	0.4167	44.2	0.4166	45.48	0.417	43.900
0.4333	42.14	0.4333	43.93	0.4333	44.78	0.433	43.617
0.45	41.33	0.45	43.48	0.45	44.69	0.450	43.167
0.4666	41.59	0.4667	43.28	0.4666	43.96	0.467	42.943
0.4833	40.72	0.4833	42.89	0.4833	43.77	0.483	42.460
0.5	40.72	0.5	42.74	0.5	43.17	0.500	42.210
0.5166	39.89	0.5167	42.42	0.5166	43.06	0.517	41.790
0.5333	39.85	0.5333	42.29	0.5333	42.47	0.533	41.537
0.55	39.36	0.55	41.96	0.55	42.42	0.550	41.247

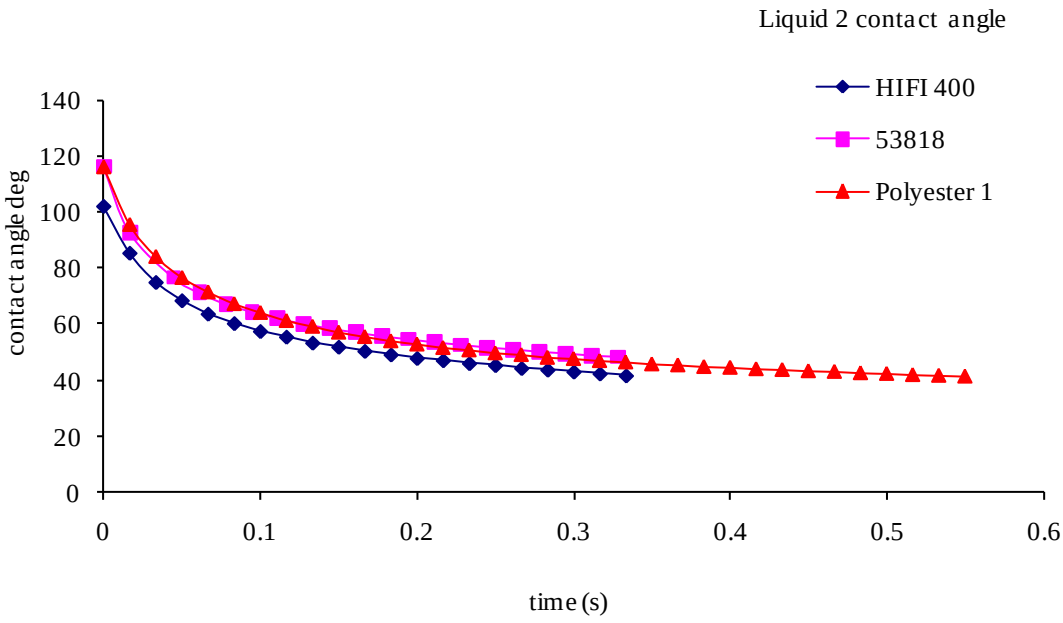

Figure 1.2: Liquid 2 (milgear 1, 82 mPa.s) contact angle with different substrate.

Table 1.3: Contact angle of liquid 1 with substrate 53847

First run		Second run		Third run		Contact angle average	
Graph Sec	Y-axis Angle	Graph Sec	Y-axis Angle	Graph Sec	Y-axis Angle	Graph Sec	Y-axis Angle
0	102.74	0	98.06	0	90.79	0.0000	97.197
0.0166	88.59	0.0166	84.44	0.0167	78.63	0.0166	83.887
0.0333	78.55	0.0333	75.43	0.0334	71.46	0.0333	75.147
0.05	72.17	0.05	68.76	0.05	65.8	0.0500	68.910
0.0666	67.43	0.0666	64.51	0.0667	62.21	0.0666	64.717
0.0833	64.14	0.0833	60.74	0.0834	58.74	0.0833	61.207
0.1	60.94	0.1	58.3	0.1	56.51	0.1000	58.583
0.1166	59.14	0.1166	55.71	0.1167	54.08	0.1166	56.310
0.1333	56.77	0.1333	54.08	0.1334	52.48	0.1333	54.443
0.15	55.29	0.15	52.1	0.15	50.71	0.1500	52.700
0.1666	53.63	0.1666	50.91	0.1667	49.56	0.1666	51.367
0.1833	52.5	0.1833	49.35	0.1834	48.17	0.1833	50.007
0.2	51.18	0.2	48.34	0.2	47.39	0.2000	48.970
0.2166	50.36	0.2166	47.11	0.2167	46.16	0.2166	47.877
		0.2333	46.36	0.2334	45.48		30.613
		0.25	45.23	0.25	44.45		29.893
		0.2666	44.61	0.2667	43.9		29.503
		0.2833	43.56	0.2834	42.95		28.837
		0.3	43.1	0.3	42.52		28.540
		0.3166	42.17	0.3167	41.71		27.960
		0.3333	41.75	0.3334	41.38		27.710
		0.35	40.92	0.35	40.55		27.157
		0.3666	40.57	0.3667	40.24		26.937
		0.3833	39.74	0.3834	39.56		26.433
		0.4	39.45	0.4	39.38		26.277
		0.4166	38.77	0.4167	38.75		25.840
		0.4333	38.55	0.4334	38.52		25.690

Table 1.4: Contact angle of liquid 3 with substrate 53847

First run		Second run		Third run		Contact angle average	
Graph Sec	Y-axis Angle	Graph Sec	Y-axis Angle	Graph Sec	Y-axis Angle	Graph Sec	Y-axis Angle
0	117.51	0	112.21	0	90. 108.5	0. 0.000	112.740
0.0167	87.63	0.0166	88.66	0.0166	84.52	0.017	86.937
0.0333	72.35	0.0333	76.31	0.0333	74.36	0.033	74.340
0.05	64.03	0.05	69.57	0.05	67.45	0.050	67.017
0.0667	58.55	0.0666	64.12	0.0666	62.88	0.067	61.850
0.0833	54.59	0.0833	60.47	0.0833	58.71	0.083	57.923
0.1	51.74	0.1	56.9	0.1	56.08	0.100	54.907
0.1167	49.98	0.1166	54.6	0.1166	53.26	0.117	52.613
0.1333	47.98	0.1333	52.04	0.1333	51.43	0.133	50.483
0.15	47.14	0.15	50.38	0.15	49.22	0.150	48.913
0.1667	45.21	0.1666	48.48	0.1666	47.96	0.167	47.217
0.1833	43.62	0.1833	47.3	0.1833	46.21	0.183	45.710
0.2	42.13	0.2	45.74	0.2	45.32	0.200	44.397
0.2167	41.18	0.2166	44.76	0.2166	43.9	0.217	43.280
0.2333	39.86	0.2333	43.46	0.2333	43.11	0.233	42.143
0.25	39.08	0.25	42.73	0.25	41.83	0.250	41.213
0.2667	37.83	0.2666	41.57	0.2666	41.23	0.267	40.210
0.2833	37.4	0.2833	40.99	0.2833	40.12	0.283	39.503
0.3	36.36	0.3	39.86	0.3	39.61	0.300	38.610
0.3167	35.88	0.3166	39.45	0.3166	38.66	0.317	37.997
0.3333	34.89	0.3333	38.46	0.3333	38.24	0.333	37.197
0.35	34.59	0.35	38.11	0.35	37.35	0.350	36.683
0.3667	33.71	0.3666	37.26	0.3666	37.07	0.367	36.013
0.3833	33.39	0.3833	36.96	0.3833	36.25	0.383	35.533
0.4	32.61	0.4	36.16	0.4	35.99	0.400	34.920
0.4167	32.41	0.4166	35.96	0.4166	35.29	0.417	34.553
0.4333	31.62	0.4333	35.19	0.4333	35.01	0.433	33.940
0.45	31.4	0.45	35	0.45	34.31	0.450	33.570
0.4667	30.76	0.4666	34.31	0.4666	34.18	0.467	33.083
0.4833	30.6	0.4833	34.16	0.4833	33.49	0.483	32.750
0.5	29.91	0.5	33.48	0.5	33.42	0.500	32.270
0.5167	29.82	0.5166	33.36	0.5166	32.73	0.517	31.970
0.5333	29.14	0.5333	32.77	0.5333	32.62	0.533	31.510
0.55	29.19	0.55	32.69	0.55	32.06	0.550	31.313
0.5667	28.48	0.5666	32.1	0.5666	32.02	0.567	30.867
0.5833	28.51	0.5833	32	0.5833	31.4	0.583	30.637
0.6	27.81	0.6	31.47	0.6	31.35	0.600	30.210
0.6167	27.9	0.6166	31.43	0.6166	30.85	0.617	30.060
0.6333	27.33	0.6333	30.85	0.6333	30.72	0.633	29.633
0.65	27.7	0.65	30.81	0.65	30.27	0.650	29.593
0.6667	27.15	0.6666	30.66	0.6666	30.28	0.667	29.363
0.6833	27.18	0.6833	30.35	0.6833	29.83	0.683	29.120
0.7	26.37	0.7	29.75	0.7	29.77	0.700	28.630
0.7167	26.39	0.7166	29.82	0.7166	29.32	0.717	28.510
0.7333	25.66	0.7333	29.34	0.7333	29.32	0.733	28.107
0.75	25.88	0.75	29.36	0.75	28.84	0.750	28.027
0.7667	25.47	0.7666	28.8655	0.7666	28.86	0.76766	27.730

Table 1.5: Contact angle of liquid 4 with substrate 53847

First run		Second run		Third run		Contact angle average	
Graph Sec	Y-axis Angle	Graph Sec	Y-axis Angle	Graph Sec	Y-axis Angle	Graph Sec	Y-axis Angle
0	103.93	0	97.14	0	93.17	0.000	98.080
0.0167	87.14	0.0167	82.3	0.0166	81.08	0.017	83.507
0.0334	77.59	0.0333	74.58	0.0333	73.16	0.033	75.110
0.05	71.86	0.05	68.58	0.05	68.25	0.050	69.563
0.0667	66.9	0.0667	64.62	0.0666	63.82	0.067	65.113
0.0834	63.62	0.0833	60.85	0.0833	60.92	0.083	61.797
0.1	60.41	0.1	58.3	0.1	57.86	0.100	58.857
0.1167	58.27	0.1167	55.55	0.1166	55.96	0.117	56.593
0.1334	55.84	0.1333	53.84	0.1333	53.67	0.133	54.450
0.15	54.31	0.15	51.82	0.15	52.28	0.150	52.803
0.1667	52.39	0.1667	50.44	0.1666	50.45	0.167	51.093
0.1834	51.29	0.1833	48.86	0.1833	49.41	0.183	49.853
0.2	49.78	0.2	47.88	0.2	47.9	0.200	48.520
0.2167	48.87	0.2167	46.51	0.2166	47.14	0.217	47.507
0.2334	47.7	0.2333	45.69	0.2333	45.86	0.233	46.417
0.25	47.07	0.25	44.56	0.25	45.23	0.250	45.620
0.2667	45.75	0.2667	43.95	0.2666	44.1	0.267	44.600
0.2834	45.28	0.2833	42.83	0.2833	43.5	0.283	43.870
0.3	44.21	0.3	42.29	0.3	42.53	0.300	43.010
0.3167	43.84	0.3167	41.43	0.3166	42.09	0.317	42.453

Table 1.6: Contact angle of liquid 5 with substrate 53847

First run		Second run		Third run		Contact angle average	
Graph Sec	Y-axis Angle	Graph Sec	Y-axis Angle	Graph Sec	Y-axis Angle	Graph Sec	Y-axis Angle
0	98.55	0	98.69	0	103.1	0.0000	100.1133
0.0167	88.87	0.0166	87.56	0.0167	91.76	0.0167	89.3967
0.0334	81.48	0.0333	80.71	0.0333	84.14	0.0333	82.1100
0.05	76.64	0.05	75.04	0.05	77.69	0.0500	76.4567
0.0667	72.03	0.0666	71.26	0.0667	73.16	0.0667	72.1500
0.0834	68.92	0.0833	67.59	0.0833	68.92	0.0833	68.4767
0.1	65.69	0.1	65.13	0.1	66.17	0.1000	65.6633
0.1167	63.57	0.1166	62.34	0.1167	63.33	0.1167	63.0800
0.1334	61.12	0.1333	60.6	0.1333	61.24	0.1333	60.9867
0.15	59.53	0.15	58.4	0.15	59.05	0.1500	58.9933
0.1667	57.45	0.1666	57.07	0.1667	57.57	0.1667	57.3633
0.1834	56.28	0.1833	55.22	0.1833	55.78	0.1833	55.7600
0.2	54.6	0.2	54.21	0.2	54.63	0.2000	54.4800
0.2167	53.64	0.2166	52.72	0.2167	52.99	0.2167	53.1167
0.2334	52.32	0.2333	51.93	0.2333	52.26	0.2333	52.1700
0.25	51.54	0.25	50.67	0.25	50.92	0.2500	51.0433
0.2667	50.28	0.2666	49.97	0.2667	50.3	0.2667	50.1833
0.2834	49.68	0.2833	48.85	0.2833	49.03	0.2833	49.1867
0.3	48.63	0.3	48.34	0.3	48.55	0.3000	48.5067
0.3167	48.08	0.3166	47.29	0.3167	47.54	0.3167	47.6367
0.3334	47.07	0.3333	46.84	0.3333	47	0.3333	46.9700
0.35	46.65	0.35	45.89	0.35	46.02	0.3500	46.1867
0.3667	45.81	0.3666	45.62	0.3667	45.55	0.3667	45.6600
0.3834	45.46	0.3833	44.79	0.3833	44.73	0.3833	44.9933
0.4	44.62	0.4	44.48	0.4	44.16	0.4000	44.4200
0.4167	44.41	0.4166	43.66	0.4167	43.41	0.4167	43.8267
0.4334	43.6	0.4333	43.45	0.4333	43.13	0.4333	43.3933
0.45	43.29	0.45	42.7	0.45	42.37	0.4500	42.7867
0.4667	42.64	0.4666	42.49	0.4667	42.12	0.4667	42.4167
0.4834	42.45	0.4833	41.77	0.4833	41.37	0.4833	41.8633
0.5	41.79	0.5	41.62	0.5	41.31	0.5000	41.5733
0.5167	41.68	0.5166	40.99	0.5167	40.66	0.5167	41.1100
0.5334	40.95	0.5333	40.87	0.5333	40.49	0.5333	40.7700
0.55	40.88	0.55	40.21	0.55	39.83	0.5500	40.3067

Table 1.7: Contact angle of liquid 7 with substrate 53847

First run		Second run		Third run		Contact angle average	
Graph Sec	Y-axis Angle	Graph Sec	Y-axis Angle	Graph Sec	Y-axis Angle	Graph Sec	Y-axis Angle
0	111.99	0	113.01	0	119.72	0.0000	114.9067
0.0166	101.76	0.0167	102.39	0.0167	105.34	0.0167	103.1633
0.0333	93.52	0.0333	93.83	0.0333	96.42	0.0333	94.5900
0.05	88.06	0.05	88.12	0.05	89.2	0.0500	88.4600
0.0666	83	0.0667	83	0.0667	84.5	0.0667	83.5000
0.0833	79.63	0.0833	79.55	0.0833	80.01	0.0833	79.7300
0.1	76.16	0.1	76.08	0.1	76.89	0.1000	76.3767
0.1166	73.82	0.1167	73.7	0.1167	73.54	0.1167	73.6867
0.1333	71.14	0.1333	71	0.1333	71.33	0.1333	71.1567
0.15	69.46	0.15	69.29	0.15	68.8	0.1500	69.1833
0.1666	67.3	0.1667	67.09	0.1667	67.21	0.1667	67.2000
0.1833	65.96	0.1833	65.77	0.1833	65.2	0.1833	65.6433
0.2	64.11	0.2	63.91	0.2	63.98	0.2000	64.0000
0.2166	63.12	0.2167	62.89	0.2167	62.3	0.2167	62.7700
0.2333	61.53	0.2333	61.27	0.2333	61.33	0.2333	61.3767
0.25	60.65	0.25	60.39	0.25	59.83	0.2500	60.2900
0.2666	59.27	0.2667	59.05	0.2667	59.04	0.2667	59.1200
0.2833	58.6	0.2833	58.29	0.2833	57.69	0.2833	58.1933
0.3	57.3	0.3	56.98	0.3	57.07	0.3000	57.1167
0.3166	56.7	0.3167	56.42	0.3167	55.88	0.3167	56.3333
0.3333	55.57	0.3333	55.24	0.3333	55.36	0.3333	55.3900
0.35	55.02	0.35	54.71	0.35	54.28	0.3500	54.6700
0.3666	54.06	0.3667	53.65	0.3667	53.84	0.3667	53.8500
0.3833	53.61	0.3833	53.23	0.3833	52.8	0.3833	53.2133
0.4	52.65	0.4	52.26	0.4	52.43	0.4000	52.4467
0.4166	52.31	0.4167	51.93	0.4167	51.53	0.4167	51.9233
0.4333	51.34	0.4333	51	0.4333	51.23	0.4333	51.1900
0.45	51.05	0.45	50.71	0.45	50.45	0.4500	50.7367
0.4666	50.31	0.4667	49.75	0.4667	50.15	0.4667	50.0700
0.4833	49.94	0.4833	49.59	0.4833	49.34	0.4833	49.6233
0.5	49.24	0.5	48.66	0.5	49.12	0.5000	49.0067

Table 1.8: Contact angle of liquid 8 with substrate 53847

First run		Second run		Contact angle average	
Graph Sec	Y-axis Angle	Graph Sec	Y-axis Angle	Graph Sec	Y-axis Angle
0	114.79	0	110.38	0.0000	112.5850
0.0166	107.23	0.0166	103.87	0.0166	105.5500
0.0333	101.5	0.0333	97.82	0.0333	99.6600
0.05	97.05	0.05	93.64	0.0500	95.3450
0.0666	93.44	0.0666	89.33	0.0666	91.3850
0.0833	89.59	0.0833	85.9	0.0833	87.7450
0.1	86.96	0.1	81.96	0.1000	84.4600
0.1166	83.95	0.1166	79.17	0.1166	81.5600
0.1333	82.01	0.1333	76.22	0.1333	79.1150
0.15	79.76	0.15	74.34	0.1500	77.0500
0.1666	78.32	0.1666	72.09	0.1666	75.2050
0.1833	76.42	0.1833	70.54	0.1833	73.4800
0.2	76.42	0.2	68.56	0.2000	72.4900
0.2166	74.59	0.2166	67.59	0.2166	71.0900
0.2333	73.53	0.2333	65.84	0.2333	69.6850
0.25	70.94	0.25	64.93	0.2500	67.9350
0.2666	70.2	0.2666	63.61	0.2666	66.9050
0.2833	68.93	0.2833	62.91	0.2833	65.9200
0.3	68.27	0.3	61.76	0.3000	65.0150
0.3166	66.96	0.3166	61.17	0.3166	64.0650
0.3333	66.42	0.3333	60.18	0.3333	63.3000
0.35	65.25	0.35	59.63	0.3500	62.4400
0.3666	64.74	0.3666	58.81	0.3666	61.7750
0.3833	63.69	0.3833	58.52	0.3833	61.1050
0.4	63.28	0.4	57.67	0.4000	60.4750
0.4166	62.34	0.4166	57.39	0.4166	59.8650
0.4333	61.83	0.4333	56.71	0.4333	59.2700
0.45	60.99	0.45	56.61	0.4500	58.8000
0.4666	60.66	0.4666	55.82	0.4666	58.2400
0.4833	59.83	0.4833	55.72	0.4833	57.7750
0.5	59.52	0.5	54.98	0.5000	57.2500
0.5166	58.81	0.5166	54.83	0.5166	56.8200
0.5333	58.49	0.5333	54.21	0.5333	56.3500

Table 1.9: Contact angle of liquid 9 with substrate 53847

First run		Second run		Third run		Contact angle average	
Graph Sec	Y-axis Angle	Graph Sec	Y-axis Angle	Graph Sec	Y-axis Angle	Graph Sec	Y-axis Angle
0	119.38	0	101.4	0	118.15	0.0000	112.9767
0.0167	113.78	0.0166	98.04	0.0167	112.16	0.0167	107.9933
0.0334	108.17	0.0333	94.18	0.0333	105.88	0.0333	102.7433
0.05	104.2	0.05	91.59	0.05	102.08	0.0500	99.2900
0.0667	99.85	0.0666	88.44	0.0667	97.63	0.0667	95.3067
0.0834	96.87	0.0833	86.39	0.0833	94.62	0.0833	92.6267
0.1	93.32	0.1	83.79	0.1	91.14	0.1000	89.4167
0.1167	90.87	0.1166	82.08	0.1167	88.73	0.1167	87.2267
0.1334	88.05	0.1333	79.87	0.1333	85.76	0.1333	84.5600
0.15	86.1	0.15	78.5	0.15	83.88	0.1500	82.8267
0.1667	83.56	0.1666	76.58	0.1667	81.32	0.1667	80.4867
0.1834	82.02	0.1833	75.45	0.1833	79.8	0.1833	79.0900
0.2	79.95	0.2	73.78	0.2	77.62	0.2000	77.1167
0.2167	78.66	0.2166	72.8	0.2167	76.37	0.2167	75.9433
0.2334	76.83	0.2333	71.29	0.2333	74.48	0.2333	74.2000
0.25	75.77	0.25	70.53	0.25	73.33	0.2500	73.2100
0.2667	74.12	0.2666	69.21	0.2667	71.57	0.2667	71.6333
0.2834	73.23	0.2833	68.5	0.2833	70.73	0.2833	70.8200
0.3	71.75	0.3	67.26	0.3	69.19	0.3000	69.4000
0.3167	71.01	0.3166	66.67	0.3167	68.42	0.3167	68.7000
0.3334	69.63	0.3333	65.52	0.3333	67.04	0.3333	67.3967
0.35	68.99	0.35	65.05	0.35	66.37	0.3500	66.8033
0.3667	67.75	0.3666	63.96	0.3667	65.11	0.3667	65.6067
0.3834	67.15	0.3833	63.57	0.3833	64.58	0.3833	65.1000
0.4	65.96	0.4	62.57	0.4	63.43	0.4000	63.9867
0.4167	65.49	0.4166	62.23	0.4167	62.92	0.4167	63.5467
0.4334	64.4	0.4333	61.29	0.4333	61.86	0.4333	62.5167
0.45	64	0.45	61	0.45	61.49	0.4500	62.1633
0.4667	62.95	0.4666	60.09	0.4667	60.45	0.4667	61.1633
0.4834	62.61	0.4833	59.85	0.4833	60.12	0.4833	60.8600
0.5	61.63	0.5	59.05	0.5	59.2	0.5000	59.9600
0.5167	61.29	0.5166	58.86	0.5167	58.93	0.5167	59.6933
0.5334	60.42	0.5333	58.08	0.5333	58.08	0.5333	58.8600
0.55	60.13	0.55	57.93	0.55	57.82	0.5500	58.6267
0.5667	59.29	0.5666	57.15	0.5667	56.99	0.5667	57.8100

Table 1.10: Contact angle of liquid 10 with substrate 53847

First run		Second run		Third run		Contact angle average	
Graph Sec	Y-axis Angle	Graph Sec	Y-axis Angle	Graph Sec	Y-axis Angle	Graph Sec	Y-axis Angle
0	111.8	0	118.76	0	115.62	0.0000	115.3933
0.0167	107.97	0.0167	113.92	0.0167	111.15	0.0167	111.0133
0.0333	103.8	0.0334	110.73	0.0334	108.2	0.0334	107.5767
0.05	100.91	0.05	107.07	0.05	104.72	0.0500	104.2333
0.0667	97.6	0.0667	104.71	0.0667	102.37	0.0667	101.5600
0.0833	95.37	0.0834	101.83	0.0834	99.48	0.0834	98.8933
0.1	92.57	0.1	99.95	0.1	97.59	0.1000	96.7033
0.1167	90.86	0.1167	97.33	0.1167	95.16	0.1167	94.4500
0.1333	88.49	0.1334	95.71	0.1334	93.63	0.1334	92.6100
0.15	87.06	0.15	93.35	0.15	91.38	0.1500	90.5967
0.1667	84.97	0.1667	91.99	0.1667	90.13	0.1667	89.0300
0.1833	83.85	0.1834	89.94	0.1834	88.22	0.1834	87.3367
0.2	82	0.2	88.65	0.2	87.07	0.2000	85.9067
0.2167	81.03	0.2167	86.68	0.2167	85.37	0.2167	84.3600
0.2333	79.38	0.2334	85.66	0.2334	84.39	0.2334	83.1433
0.25	78.53	0.25	83.93	0.25	82.89	0.2500	81.7833
0.2667	77.09	0.2667	83.02	0.2667	82.12	0.2667	80.7433
0.2833	76.46	0.2834	81.42	0.2834	80.61	0.2834	79.4967
0.3	75.15	0.3	80.57	0.3	79.92	0.3000	78.5467
0.3167	74.58	0.3167	79.12	0.3167	78.56	0.3167	77.4200
0.3333	73.44	0.3334	78.48	0.3334	78.01	0.3334	76.6433
0.35	73.01	0.35	77.12	0.35	76.72	0.3500	75.6167
0.3667	71.97	0.3667	76.48	0.3667	76.26	0.3667	74.9033
0.3833	71.6	0.3834	75.25	0.3834	75.07	0.3834	73.9733
0.4	70.64	0.4	74.69	0.4	74.6	0.4000	73.3100
0.4167	70.35	0.4167	73.53	0.4167	73.51	0.4167	72.4633
0.4333	69.38	0.4334	73.06	0.4334	73.16	0.4334	71.8667
0.45	69.12	0.45	71.96	0.45	72.19	0.4500	71.0900
0.4667	68.23	0.4667	71.57	0.4667	71.87	0.4667	70.5567
0.4833	68.04	0.4834	70.53	0.4834	70.97	0.4834	69.8467
0.5	67.19	0.5	70.13	0.5	70.73	0.5000	69.3500
0.5167	67.01	0.5167	69.2	0.5167	69.93	0.5167	68.7133
0.5333	66.2	0.5334	68.88	0.5334	69.74	0.5334	68.2733
0.55	66.04	0.55	68	0.55	68.97	0.5500	67.6700
0.5667	65.27	0.5667	67.7	0.5667	68.75	0.5667	67.2400
0.5833	65.19	0.5834	66.83	0.5834	67.97	0.5834	66.6633
0.6	64.42	0.6	66.57	0.6	67.9	0.6000	66.2967
0.6167	64.27	0.6167	65.76	0.6167	67.13	0.6167	65.7200
0.6333	63.58	0.6334	65.54	0.6334	67.05	0.6334	65.3900
0.65	63.55	0.65	64.8	0.65	66.27	0.6500	64.8733
0.6667	62.83	0.6667	64.6	0.6667	66.22	0.6667	64.5500

1.2 EXPERIMENTAL CALCULATION OF CHINA CLAY

To make 5% clay suspension, let us start with 10 g of clay .as we know from the supplier (Imerys) that the clay is not dry; it is contains 6.5wt% moisture.

Desired suspension concentration = 5 wt% clay water suspension

Dispersant concentration = 0.05 wt% to the clay

Concentration = 0.1 wt% to the clay.

Weigh of dry clay $= 10 - \left(10 \times \frac{6.5}{100}\right)$ = 9.35 g

Water in the clay = 10 – 9.35 = 0.65 g water

Amount of water required to make 5 wt% suspension =x

$\frac{5}{100} = \frac{9.35}{x + 9.35}$ X= 177.65 g water or ml of water.

The amount of CED to make 0.05 wt% to the clay = Y

$\frac{0.05}{100} = \frac{y}{y + 9.35}$ Y = 0.004677 g CED

We know from the supplier that the CED is 40 % by wt solution.

The total amount of CED $= \frac{y}{100 - 40} = \frac{0.004677}{100 - 40} = 0.007796$ ml

Amount of NaOH to prepare 0.1 wt% to the clay = Z

$\frac{0.1}{100} = \frac{z}{z + 9.35},$ Z= 0.00935 g of NaOH

China Clay Experimental Calculations

clay weight (starting weight) = **20** g

moisture content = 6.5 % water

weight of dry clay= **18.7** g remaining moisture= **1.3** g

concentration of desired clay suspension = 10 wt% and the total sample weight **187** **g**

water to be added to prepare the desired concentration= **168.3** **g water**

quantity of NaOH to be added to make= 0.1 wt% NaOH on clay= **0.0187** g NaOH

Quantity of CED in order to make **0.6** wt% on clay = **0.112877** **g**

noting that that it is 40 % solution density of CED = **1.346** g/ml
so total amount of CED = **0.188129** water density = **1** g/ml

summarizing the sample contents as follows

	wt(g)	Percent				
dray clay	**18.7**	**9.988952**	**%**			
water	**168.3**	**89.90057**	**%**	**water ml=**	**168.3**	**ml**
NaOH	**0.0187**	**0.009989**	**%**			
CED (g)	**0.188129**	**0.100492**	**%**	**CED(ml) =**	**0.139769**	**ml**
sum	**187.2068**	**100**	**%**			

Instrument: Brabender Rheotron

GEOMETRY	A1			A2		
SPRING	A	B	C	A	B	C
D1	0.268	1.338	13.38	0.3	1.426	14.26
D2	2.985	2.985	2.985	1.033	1.033	1.033

Test Conditions

Geometry: A1
Spring: A
Temperature: 25 °C

Table 1.2.1: Viscosity measurement of 10% clay at different temperature

N	S	X	Shear	Shear	Viscosity	Viscosity
		range x	Stress	Rate		
(rpm)			(dynes/cm^2)	(s^{-1})	(poise)	(mPa.s)
5	10.5	1	2.81	15	0.189	18.8543
7.07	12.0	1	3.22	21	0.152	15.2389
10	13.5	1	3.62	30	0.121	12.1206
14.14	15.0	1	4.02	42	0.095	9.52428
20	17.0	1	4.56	60	0.076	7.63149
28.3	19.0	1	5.09	84	0.060	6.02778
40	23.0	1	6.16	119	0.052	5.16248
56.6	27.5	1	7.37	169	0.044	4.36221
80	29.0	1	7.77	239	0.033	3.25461
113	42.5	1	11.39	337	0.034	3.37677
160	54	1	14.47	478	0.030	3.03015
226	70	1	18.76	675	0.028	2.78087
320	31	3	24.92	955	0.026	2.6093
452	42.5	3	34.17	1349	0.025	2.53257
640	60	3	48.24	1910	0.025	2.52513
904	85.0	3	68.34	2698	0.025	2.53257
				Average	0.063	6.3477

Geometry: A1
Spring: A
Temperature: 40 °C
spring A

N	S	X	Shear	Shear	Viscosity	Viscosity
		range x	Stress	Rate		
(rpm)			(dynes/cm^2)	(s^{-1})	(poise)	(mPa.s)
5	11.5	1	3.08	15	0.206	20.6499
7.07	12.5	1	3.35	21	0.159	15.8738
10	13.5	1	3.62	30	0.121	12.1206
14.14	15.0	1	4.02	42	0.095	9.52428
20	16.5	1	4.42	60	0.074	7.40704
28.3	18.5	1	4.96	84	0.059	5.86916
40	21.0	1	5.63	119	0.047	4.71357
56.6	25.0	1	6.70	169	0.040	3.96565
80	30.0	1	8.04	239	0.034	3.36683
113	37	1	9.92	337	0.029	2.93977
160	46	1	12.33	478	0.026	2.58124
226	59	1	15.81	675	0.023	2.34387
320	26.5	3	21.31	955	0.022	2.23053
452	35	3	28.14	1349	0.021	2.08565
640	51	3	41.00	1910	0.021	2.14636
904	82.0	3	65.93	2698	0.024	2.44319

Average	0.063	6.2663

Geometry: A1
Spring: C
Temperature: 60 °C

N	S	X	Shear	Shear	Viscosity	Viscosity
		range x	Stress	Rate		
(rpm)			(dynes/cm^2)	(s^{-1})	(poise)	(mPa.s)
5	11.0	1	2.95	15	0.198	19.7521
7.07	12.0	1	3.22	21	0.152	15.2389
10	13.0	1	3.48	30	0.117	11.6717
14.14	15.0	1	4.02	42	0.095	9.52428
20	16.5	1	4.42	60	0.074	7.40704
28.3	18.5	1	4.96	84	0.059	5.86916
40	21.0	1	5.63	119	0.047	4.71357
56.6	25.0	1	6.70	169	0.040	3.96565
80	31.0	1	8.31	239	0.035	3.47906
113	38	1	10.18	337	0.030	3.01923
160	41.5	1	11.12	478	0.023	2.32873
226	51	1	13.67	675	0.020	2.02606
320	23	3	18.49	955	0.019	1.93593
452	30	3	24.12	1349	0.018	1.7877
640	42	3	33.77	1910	0.018	1.76759
904	80.0	3	64.32	2698	0.024	2.3836

Average	0.061	6.0544

Table 1.2.2: Viscosity measurement of 20% clay at different temperature.

Test Conditions

Geometry: A1
Spring: B
Temperature: 25 °C

N	S	X	Shear	Shear	Viscosity	Viscosity
		range x	Stress	Rate		
(rpm)			(dynes/cm^2)	(s^{-1})	(poise)	(mPa.s)
5	36.0	1	48.17	15	3.227	322.734
7.07	38.5	1	51.51	21	2.441	244.092
10	39.5	1	52.85	30	1.771	177.055
14.14	41.0	1	54.86	42	1.300	129.971
20	42.0	1	56.20	60	0.941	94.1307
28.3	44.0	1	58.87	84	0.697	69.6912
40	45.5	1	60.88	119	0.510	50.9874
56.6	48.0	1	64.22	169	0.380	38.0134
80	51.0	1	68.24	239	0.286	28.5754
113	56	1	74.93	337	0.222	22.2137
160	61.5	1	82.29	478	0.172	17.2293
226	70	1	93.66	675	0.139	13.8836
320	28	3	112.39	955	0.118	11.7663
452	33	3	132.46	1349	0.098	9.81767
640	39	3	156.55	1910	0.082	8.19441
904	47.5	3	190.67	2698	0.071	7.06575
				Average	**0.778**	**77.839**

Geometry: A1
Spring: B
Temperature: 40 °C

N	S	X	Shear	Shear	Viscosity	Viscosity
		range x	Stress	Rate		
(rpm)			(dynes/cm^2)	(s^{-1})	(poise)	(mPa.s)
5	42.0	1	56.20	15	3.765	376.523
7.07	43.0	1	57.53	21	2.726	272.622
10	44.0	1	58.87	30	1.972	197.226
14.14	45.5	1	60.88	42	1.442	144.236
20	47.0	1	62.89	60	1.053	105.337
28.3	48.0	1	64.22	84	0.760	76.0268
40	49.0	1	65.56	119	0.549	54.9095
56.6	51.0	1	68.24	169	0.404	40.3892
80	54.0	1	72.25	239	0.303	30.2563
113	58	1	77.60	337	0.230	23.0071
160	63	1	84.29	478	0.176	17.6495
226	70	1	93.66	675	0.139	13.8836
320	82.5	1	110.39	955	0.116	11.5562
452	32	3	128.45	1349	0.095	9.52017
640	37.5	3	150.53	1910	0.079	7.87924
904	44.5	3	178.62	2698	0.066	6.61949
				Average	**0.867**	**86.728**

Geometry: A1
Spring: C
Temperature: 60 °C

N	S	X	Shear	Shear	Viscosity	Viscosity
		range x	Stress	Rate		
(rpm)			(dynes/cm^2)	(s^{-1})	(poise)	(mPa.s)
5	45.0	1	60.21	15	4.034	403.417
7.07	46.0	1	61.55	21	2.916	291.642
10	47.5	1	63.56	30	2.129	212.915
14.14	48.0	1	64.22	42	1.522	152.161
20	49.0	1	65.56	60	1.098	109.819
28.3	49.5	1	66.23	84	0.784	78.4026
40	50.5	1	67.57	119	0.566	56.5905
56.6	52.0	1	69.58	169	0.412	41.1812
80	54.0	1	72.25	239	0.303	30.2563
113	57	1	76.27	337	0.226	22.6104
160	61	1	81.62	478	0.171	17.0892
226	67.5	1	90.32	675	0.134	13.3877
320	77	1	103.03	955	0.108	10.7858
452	31	3	124.43	1349	0.092	9.22266
640	35	3	140.49	1910	0.074	7.35396
904	41.0	3	164.57	2698	0.061	6.09886
				Average	**0.914**	**91.433**

Table 1.2.2: Viscosity measurement of 30% clay at different temperature.

Geometry: A1
Spring: B
Temperature: 25 °C

N	S	X	Shear	Shear	Viscosity	Viscosity
		range x	Stress	Rate		
(rpm)			(dynes/cm^2)	(s^{-1})	(poise)	(mPa.s)
5	27.0	3	108.38	15	7.262	726.151
7.07	29.0	3	116.41	21	5.516	551.584
10	31.5	3	126.44	30	4.236	423.588
14.14	33.5	3	134.47	42	3.186	318.587
20	36.0	3	144.50	60	2.421	242.05
28.3	38.0	3	152.53	84	1.806	180.564
40	41.0	3	164.57	119	1.378	137.834
56.6	43.5	3	174.61	169	1.033	103.349
80	47.0	3	188.66	239	0.790	79.0025
113	51	3	204.71	337	0.607	60.6911
160	55.5	3	222.78	478	0.466	46.6451
226	61.5	3	246.86	675	0.366	36.5931
320	69	3	276.97	955	0.290	28.9956
452	80	3	321.12	1349	0.238	23.8004
640	28	10	374.64	1910	0.196	19.6106
904	32.5	10	434.85	2698	0.161	16.1149
				Average	**1.872**	**187.2**

Geometry: A1
Spring: B
Temperature: 40 °C

N	S	X	Shear	Shear	Viscosity	Viscosity
		range x	Stress	Rate		
(rpm)			(dynes/cm^2)	(s^{-1})	(poise)	(mPa.s)
5	30.5	3	122.43	15	8.203	820.281
7.07	32.0	3	128.45	21	6.086	608.644
10	35.0	3	140.49	30	4.707	470.653
14.14	39.0	3	156.55	42	3.709	370.893
20	44.5	3	178.62	60	2.992	299.201
28.3	49.0	3	196.69	84	2.328	232.832
40	53.0	3	212.74	119	1.782	178.176
56.6	57.0	3	228.80	169	1.354	135.423
80	61.0	3	244.85	239	1.025	102.535
113	65.5	3	262.92	337	0.779	77.9464
160	70	3	280.98	478	0.588	58.8317
226	77.5	3	311.09	675	0.461	46.1133
320	26	10	347.88	955	0.364	36.4196
452	30	10	401.40	1349	0.298	29.7505
640	34	10	454.92	1910	0.238	23.8128
904	39.0	10	521.82	2698	0.193	19.3378
				Average	**2.194**	**219.43**

Geometry: A1
Spring: B
Temperature: 60 °C

N	S	X	Shear	Shear	Viscosity	Viscosity
		range x	Stress	Rate		
(rpm)			(dynes/cm^2)	(s^{-1})	(poise)	(mPa.s)
5	34.0	3	136.48	15	9.144	914.412
7.07	39.0	3	156.55	21	7.418	741.785
10	42.0	3	168.59	30	5.648	564.784
14.14	44.5	3	178.62	42	4.232	423.198
20	48.0	3	192.67	60	3.227	322.734
28.3	53.0	3	212.74	84	2.518	251.839
40	58.5	3	234.82	119	1.967	196.666
56.6	62.5	3	250.88	169	1.485	148.49
80	66.5	3	266.93	239	1.118	111.78
113	70	3	280.98	337	0.833	83.3015
160	75	3	301.05	478	0.630	63.0339
226	81.5	3	327.14	675	0.485	48.4934
320	27	10	361.26	955	0.378	37.8204
452	30	10	401.40	1349	0.298	29.7505
640	34.5	10	461.61	1910	0.242	24.163
904	39.5	10	528.51	2698	0.196	19.5858
				Average	**2.489**	**248.86**

APPENDIX 2

2.1 Coating with 53818 polyester substrate at different height, angles and liquids viscosity.

Table 2.1.1to 2.1.12: show the air entrainment velocity at fixed flow rate and different angles.

Table 2.1.1: Liquid. 4, viscosity 120 mPa.s (Millmax 46).

Curtain height: 60 mm Date: 16/05/2005
Substrate: 53818 Room temperature: 23°C

Die angle β	Liquid Temperature, °C	Viscosity μ (mPa.s)	Flow rate l/min	Vae%	Air entrainment V_{ae} (m/s)	V_{ae} Cos β
0	18.8	117	1.16	11.8	0.210	0.210
10	18.8	117	1.16	12.1	0.215	0.212
20	18.8	117	1.16	13.4	0.238	0.224
30	18.8	117	1.16	14.5	0.258	0.223

Table 2.1.2: Liquid. 4, viscosity 120 mPa.s (Millmax 46). 6
Curtain height: 60 mm Date: 16/05/2005
Substrate: 53818 Room temperature: 23°C

Die angle β	Liquid Temperature, °C	Viscosity μ (mPa.s)	Flow rate l/min	Vae%	Air entrainment V_{ae} (m/s)	V_{ae} Cos β
0	18.7	118	1.40	18.3	0.324	0.210
10	18.6	118	1.40	18.4	0.326	0.212
20	18.6	118	1.40	19.8	0.351	0.224
30	18.5	119	1.40	20.9	0.370	0.223

Table 2.1.3: Liquid. 4, viscosity 120 mPa.s (Millmax 46). 7
Curtain height: 60 mm Date: 13/06/2005
Substrate: 53818 Room temperature: 23°C

Die angle β	Liquid Temperature, °C	Viscosity μ (mPa.s)	Flow rate l/min	Vae%	Air entrainment V_{ae} (m/s)	V_{ae} Cos β
0	18.1	122	1.63	23.1	0.409	0.409
10	18.1	122	1.63	23.3	0.412	0.406
20	18.2	121	1.63	24.3	0.430	0.404
30	18.4	120	1.63	25.4	0.449	0.389

Table: 2.1.4: Liquid. 4, viscosity 120 mPa.s (Millmax 46). 8
Curtain height: 60 mm Date: 09/05/2005
Substrate: 53818 Room temperature: 23°C

Die angle β	Liquid Temperature, °C	Viscosity μ (mPa.s)	Flow rate l/min	Vae%	Air entrainment V_{ae} (m/s)	V_{ae} Cos β
0	18.2	121	1.86	25.3	0.448	0.448
10	18.2	121	1.86	26.1	0.462	0.455
20	18.1	122	1.86	27	0.478	0.449
30	18.3	120	1.86	28.6	0.506	0.438

Table 2.1.5: Liquid. 4, viscosity 120 mPa.s (Millmax 46). 9

Curtain height: 60 mm Date: 09/05/2005
Substrate: 53818 Room temperature: 23°C

Die angle β	Liquid Temperature, °C	Viscosity μ (mPa.s)	Flow rate l/min	Vae%	Air entrainment V_{ae} (m/s)	V_{ae} Cos β
0	18.1	122	2.10	27.6	0.488	0.488
10	18.1	122	2.10	28	0.495	0.488
20	18.1	122	2.10	28.8	0.509	0.478
30	18.1	122	2.10	30.7	0.543	0.470

Table 2.1.6: Liquid. 4, viscosity 120 mPa.s (Millmax 46).
Curtain height: 60 mm Date: 09/05/2005
Substrate: 53818 Room temperature: 23°C

Die angle β	Liquid Temperature, °C	Viscosity μ (mPa.s)	Flow rate l/min	Vae%	Air entrainment V_{ae} (m/s)	V_{ae} Cos β
0	18.1	122	2.33	29.8	0.527	0.527
10	18.1	122	2.33	30.2	0.534	0.526
20	18	122	2.33	30.7	0.543	0.510
30	18.1	122	2.33	31.6	0.558	0.484

Table 2.1.7: Liquid. 4, viscosity 120 mPa.s (Millmax 46).
Curtain height: 60 mm Date: 09/05/2005
Substrate: 53818 Room temperature: 23°C

Die angle β	Liquid Temperature, °C	Viscosity μ (mPa.s)	Flow rate l/min	Vae%	Air entrainment V_{ae} (m/s)	V_{ae} Cos β
0	18.2	121	3.03	28.3	0.500	0.500
10	18.2	121	3.03	28.6	0.506	0.498
20	18.2	121	3.03	29.6	0.523	0.492
30	18.2	121	3.03	31.2	0.551	0.478

Table: 2.1.8: Liquid. 4, viscosity 120 mPa.s (Millmax 46).
Curtain height: 60 mm Date: 09/05/2005
Substrate: 53818 Room temperature: 23°C

Die angle β	Liquid Temperature, °C	Viscosity μ (mPa.s)	Flow rate l/min	Vae%	Air entrainment V_{ae} (m/s)	V_{ae} Cos β)
0	18.4	120	3.96	15.4	0.273	0.273
10	18.3	120	3.96	15.8	0.280	0.276
20	18.5	119	3.96	17	0.302	0.283
30	18.5	119	3.96	20.1	0.356	0.308

Table 2.1.9: Liquid. 4, viscosity 120 mPa.s (Millmax 46).

Curtain height: 60 mm Date: 09/05/2005
Substrate: 53818 Room temperature: 23°C

Die angle β	Liquid Temperature, °C	Viscosity μ (mPa.s)	Flow rate l/min	Vae%	Air entrainment V_{ae} (m/s)	V_{ae} Cos β
0	18.4	120	5.35	14.2	0.252	0.252
10	18.4	120	5.35	15	0.266	0.262
20	18.5	119	5.35	17.3	0.307	0.288
30	18.6	118	5.35	19.7	0.349	0.302

Table 2.1.10: Liquid. 4, viscosity 120 mPa.s (Millmax 46).

Curtain height: 60 mm Date: 09/05/2005
Substrate: 53818 Room temperature: 23°C

Die angle β	Liquid Temperature, °C	Viscosity μ (mPa.s)	Flow rate l/min	Vae%	Air entrainment V_{ae} (m/s)	V_{ae} Cos β
0	18.8	117	6.28	16.4	0.291	0.291
10	18.7	118	6.28	16.3	0.289	0.285
20	19.2	114	6.28	15.7	0.279	0.262
30	19.2	114	6.28	15.2	0.270	0.234

Table 2.1.11: Liquid. 4, viscosity 120 mPa.s (Millmax 46).

Curtain height: 60 mm Date: 09/05/2005
Substrate: 53818 Room temperature: 23°C

Die angle β	Liquid Temperature, °C	Viscosity μ (mPa.s)	Flow rate l/min	Vae%	Air entrainment V_{ae} (m/s)	V_{ae} Cos β
0	18.3	120	7.67	13.7	0.243	0.243
10	18.2	121	7.67	13.9	0.247	0.243
20	18.7	118	7.67	14.2	0.252	0.237
30	18.7	118	7.67	14.4	0.256	0.221

Table 2.1.12: Liquid. 4, viscosity 120 mPa.s (Millmax 46).

Curtain height: 60 mm Date: 09/05/2005
Substrate: 53818 Room temperature: 23°C

Die angle β	Liquid Temperature, °C	Viscosity μ (mPa.s)	Flow rate l/min	Vae%	Air entrainment V_{ae} (m/s)	V_{ae} Cos β
0	18.4	0.120	8.37	15.1	0.268	0.268
10	18.6	0.118	8.37	15.4	0.273	0.269
20	19	0.116	8.37	14.8	0.263	0.247
30	19	0.116	8.37	14.4	0.256	0.221

Table 2.2.1: Liquid. 1, viscosity 94 mPa.s (Mix 1).

Curtain height: 60 mm Date: 09/05/2005
Substrate: 53818 Room temperature: 23°C

Die angle β	Liquid Temperature, °C	Viscosity μ (mPa.s)	Flow rate l/min	Vae%	Air entrainment V_{ae} (m/s)	V_{ae} Cos β
0	18.5	94	1.15	16.9	0.300	0.260
0	18.2	96	1.61	26.9	0.476	0.412
0	18	97	2.31	30.4	0.537	0.465
0	18.1	96	2.77	29.3	0.518	0.449
0	18.2	96	3.23	26.2	0.463	0.401
0	18.3	95	3.69	21	0.372	0.322
0	18.5	94	4.15	18.5	0.328	0.284
0	18.5	94	4.61	17.4	0.309	0.267
0	18.6	94	5.30	18.4	0.326	0.282
0	18.7	93	5.76	18.3	0.324	0.281
0	18.8	93	6.22	21.5	0.381	0.330
0	18.9	92	6.92	21.2	0.375	0.325

Table 2.2.2: Curtain height: 60 mm Date: 05/04/2005
Substrate: 53818 Room temperature: 21°C

Die angle β	Liquid Temperature, °C	Viscosity μ (mPa.s)	Flow rate l/min	V_{ae} %	Air entrainment V_{ae} (m/s)	V_{ae} Cos β
30	17.9	97	1.27	26.6	0.470	0.470
30	17.8	98	1.50	30.4	0.537	0.465
30	17.8	98	1.73	32.9	0.581	0.503
30	17.9	97	2.07	37.4	0.661	0.572
30	18	97	2.54	39.6	0.699	0.606
30	18	97	3.00	38	0.671	0.581
30	18.3	95	3.46	32.7	0.578	0.500
30	18.4	95	3.69	28.6	0.506	0.438
30	18.5	94	3.92	25	0.442	0.383
30	18.7	93	4.15	22.7	0.402	0.348
30	18.7	93	4.38	21	0.372	0.322
30	18.8	93	4.61	19.2	0.340	0.295
30	18.7	93	4.84	19.9	0.353	0.305
30	18.9	92	5.30	21.4	0.379	0.328
30	18.7	93	5.53	23	0.407	0.307

Table 2.3.1: Liquid. 6, viscosity 200 mPa.s (Millube 68).

Curtain height: 60 mm Date: 21/04/2005
Substrate: 53818 Room temperature: 24°C

Die angle β	Liquid Temperature, °C	Viscosity μ (mPa.s)	Flow rate l/min	V_{ae} %	Air entrainment V_{ae} (m/s)	V_{ae} Cos β
0	19.6	192	1.16	19.9	0.174	0.174
0	19.1	198	1.86	34.7	0.303	0.303
0	18.7	202	2.33	37.5	0.327	0.327
0	18.6	203	2.80	42	0.367	0.367
0	19	199	3.27	44.4	0.387	0.387
0	19.2	197	3.73	43	0.375	0.375
0	19.3	195	4.20	37	0.323	0.323
0	19.4	194	4.67	25.1	0.219	0.219
0	19.5	193	5.14	21.4	0.187	0.187
0	19.5	193	5.61	21.5	0.188	0.188
0	19.6	192	6.08	22	0.193	0.193

Table 2.3.2: Liquid. 6, viscosity 200 mPa.s (Millube 68).

Curtain height: 60 mm Date: 05/05/2005
Substrate: 53818 Room temperature: 24°C

Die angle β	Liquid Temperature, °C	Viscosity μ (mPa.s)	Flow rate l/min	V_{ae} %	Air entrainment V_{ae} (m/s)	V_{ae} Cos β
30	18.8	201	0.92	11.3	0.09941	0.153
30	18.9	200	1.16	19.5	0.17075	0.231
30	19.2	197	1.39	28.8	0.25166	0.241
30	18.8	201	1.63	36	0.3143	0.261
30	19.3	195	1.86	38	0.3317	0.278
30	19.5	193	3.97	50	0.4361	0.287
30	19.6	192	4.58	45	0.3926	0.289
30	19	199	4.91	40	0.3491	0.293
30	18.5	204	5.38	30	0.2621	0.301
30	19.1	198	5.84	25	0.2186	0.304
30	19.7	191	7.02	26.8	0.23426	0.314

Table 2.4.1: Liquid. 4, viscosity 120 mPa.s (Millmax 46).

Curtain height: 60 mm Date: 02/08/2005

Substrate: 53818 Room temperature: 23°C

Die angle β	Liquid Temperature, °C	Viscosity μ (mPa.s)	Flow rate l/min	V_{ae} %	Air entrainment V_{ae} (m/s)	V_{ae} Cos β
0	18.4	120	1.28	15.9	0.282	0.282
0	18.2	121	1.52	17.3	0.307	0.307
0	18	122	1.75	20	0.354	0.354
0	18	122	1.98	20.3	0.360	0.360
0	18	122	2.21	24.5	0.434	0.434
0	17.8	124	2.56	25.6	0.453	0.453
0	17.8	124	2.79	25.9	0.458	0.458
0	17.9	123	3.03	25.6	0.453	0.453
0	17.9	123	3.26	25.4	0.449	0.449
0	17.9	123	3.49	23.9	0.423	0.423
0	18.1	122	3.72	21.7	0.384	0.384
0	18.3	120	3.96	19.2	0.340	0.340
0	18.4	120	4.19	17.2	0.305	0.305
0	18.7	118	4.42	15.6	0.277	0.277
0	18.3	120	4.65	14.6	0.259	0.259
0	18.4	120	5.12	14.4	0.256	0.256
0	18.6	118	5.35	14.3	0.254	0.254
0	18.8	117	5.81	14.2	0.252	0.252
0	19	116	6.28	15	0.266	0.266
0	19	116	6.98	15.7	0.279	0.279
0	18.8	117	7.44	15.2	0.270	0.270
0	19	116	7.91	15.9	0.282	0.282
0	19.3	114	8.37	16.6	0.294	0.294
0	19.3	114	8.84	18.5	0.328	0.328
0	19.5	112	9.30	18.7	0.331	0.331

Table 2.4.2: Liquid. 4, viscosity 120 mPa.s (Millmax 4 6).

Curtain height: 60 mm Date: 02/08/2005
Substrate: 53818 Room temperature: 24°C

Die angle β	Liquid Temperature, °C	Viscosity μ (mPa.s)	Flow rate l/min	V_{ae} %	Air entrainment V_{ae} (m/s)	V_{ae} Cos β
30	18.3	120	1.28	18.2	0.323	0.279
30	18	122	1.52	22.6	0.400	0.346
30	17.9	123	1.86	26	0.460	0.398
30	17.9	123	2.10	27.7	0.490	0.424
30	17.9	123	2.33	27.7	0.490	0.424
30	18.1	122	2.56	27.9	0.493	0.427
30	18.1	122	2.79	28	0.495	0.429
30	18.2	121	3.03	27.6	0.488	0.423
30	18.2	121	3.49	26.2	0.463	0.401
30	18.2	121	3.96	22.7	0.402	0.348
30	18.3	120	4.65	16.6	0.294	0.255
30	18.4	120	5.35	16.3	0.289	0.250
30	18.3	120	6.05	16.9	0.300	0.260
30	18.7	118	6.98	15.3	0.272	0.235
30	18.8	117	7.67	15.1	0.268	0.232
30	19	116	8.37	15.5	0.275	0.238

Table: 2.5.1: Liquid. 6, viscosity 200 mPa.s (Millube 68).

Curtain height: 60 mm Date: 05/05/2005
Substrate: 53818 Room temperature: 24°C

Die angle β	Liquid Temperature, °C	Viscosity μ (mPa.s)	Flow rate l/min	V_{ae} %	Air entrainment V_{ae} (m/s)	V_{ae} Cos β
0	19.6	192	1.34	11.4	0.203	0.203
0	19.6	192	1.81	16.4	0.291	0.291
0	19.5	193	2.04	17.7	0.314	0.314
0	19.4	194	2.28	18.8	0.333	0.333
0	19.5	193	2.51	19.7	0.349	0.349
0	19.5	193	2.75	20.4	0.361	0.361
0	19.5	193	2.98	20.3	0.360	0.360
0	19.6	192	3.21	20.2	0.358	0.358
0	19.7	191	3.45	20.3	0.360	0.360
0	19.7	191	3.68	19.5	0.346	0.346
0	19.8	190	3.92	19.9	0.353	0.353
0	19.9	189	4.15	18.3	0.324	0.324
0	19.9	189	4.39	16.3	0.289	0.289
0	19.9	189	4.62	14.3	0.254	0.254
0	20	188	5.09	11.5	0.205	0.233
0	20	188	5.32	11.1	0.198	0.228

Table 2.5.2: Liquid. 6, viscosity 200 mPa.s (Millube 68).

Curtain height: 60 mm Date: 05/05/2005
Substrate: 53818 Room temperature: 24°C

Die angle β	Liquid Temperature, °C	Viscosity μ (mPa.s)	Flow rate l/min	V_{ae} %	Air entrainment V_{ae} (m/s)	V_{ae} Cos β
30	18.8	201	0.87	11.3	0.201	0.174
30	18.9	200	1.11	19.5	0.346	0.299
30	19.2	197	1.34	28.8	0.509	0.313
30	18.8	201	1.57	31.5	0.557	0.331
30	19.3	195	1.81	38.6	0.682	0.377
30	19.5	193	3.92	37	0.654	0.380
30	19.6	192	4.53	31.5	0.557	0.290
30	19	199	4.86	23.5	0.416	0.266
30	18.5	204	5.32	24	0.425	0.249
30	19.1	198	5.79	24.6	0.435	0.220
30	19.7	191	6.97	26.8	0.474	0.212

Table 2.6.1: Liquid. 4, viscosity 120 mPa.s (Millmax 4 6).

Curtain height: 52.6 mm Date: 19/10/2005
Substrate: 53818 Room temperature: 23°C

Die angle β	Liquid Temperature, °C	Viscosity μ (mPa.s)	Flow rate l/min	V_{ae} %	Air entrainment V_{ae} (m/s)	V_{ae} Cos β
0	19.3	114	1.31	14	0.249	0.249
0	19.3	114	1.52	15	0.266	0.266
0	19.3	114	1.75	16.8	0.298	0.298
0	19.2	114	2.10	18	0.319	0.319
0	19.1	115	2.33	20	0.354	0.354
0	19.1	115	2.56	22.3	0.395	0.395
0	19.1	115	2.79	23	0.407	0.407
0	19.1	115	3.14	22.9	0.405	0.405
0	19.1	115	3.49	22.3	0.395	0.395
0	19.4	113	3.96	18.4	0.326	0.326
0	19.3	114	4.42	14.5	0.258	0.258
0	19.3	114	4.89	13.2	0.235	0.235
0	19.3	114	5.35	13.6	0.242	0.242
0	19.3	114	5.81	14.2	0.252	0.252
0	19.5	112	6.28	14.2	0.252	0.252
0	19.5	112	6.74	14.3	0.254	0.254
0	19.8	110	8.14	14	0.249	0.249

Table 2.6.2: Liquid. 4, viscosity 120 mPa.s (Millmax 4 6).

Curtain height: 52.6 mm Date: 25/10/2005
Substrate: 53818 Room temperature: 23°C

Die angle β	Liquid Temperature, °C	Viscosity μ (mPa.s)	Flow rate l/min	V_{ae} %	Air entrainment V_{ae} (m/s)	V_{ae} Cos β
30	19.2	114	1.50	20	0.354	0.307
30	19.5	112	1.62	22	0.390	0.337
30	19.1	115	1.85	24	0.425	0.368
30	21.5	99	2.08	26	0.460	0.398
30	21	102	2.31	27	0.478	0.414
30	19.3	114	2.77	24.7	0.437	0.378
30	19.3	114	3.23	23.5	0.416	0.360
30	19.3	114	3.46	22	0.390	0.337
30	19.3	114	3.92	19.5	0.346	0.299
30	19.3	114	4.61	16.5	0.293	0.253
30	19.3	114	5.53	14.5	0.258	0.223
30	19.4	113	6.46	14	0.249	0.215
30	19.5	112	7.38	13.6	0.242	0.209
30	19.7	111	1.50	13.7	0.243	0.211

Table 2.7.1: Liquid. 6, viscosity 200 mPa.s (Millube 68).

Curtain height: 52.6 mm Date: 26/10/2005
Substrate: 53818 Room temperature: 23°C

Die angle β	Liquid Temperature, °C	Viscosity μ (mPa.s)	Flow rate l/min	V_{ae} %	Air entrainment V_{ae} (m/s)	V_{ae} Cos β
0	19.6	192	1.34	11.4	0.203	0.203
0	19.6	192	1.81	13.2	0.235	0.235
0	19.5	193	2.04	15	0.266	0.266
0	19.4	194	2.28	17.4	0.309	0.309
0	19.5	193	2.51	19	0.337	0.337
0	19.5	193	2.75	20.4	0.361	0.361
0	19.5	193	2.98	20.3	0.360	0.360
0	19.6	192	3.21	20.2	0.358	0.358
0	19.7	191	3.45	20.3	0.360	0.360
0	19.7	191	3.68	19.5	0.346	0.346
0	19.8	190	3.92	19	0.337	0.337
0	19.9	189	4.15	18.3	0.324	0.324
0	19.9	189	4.39	16.3	0.289	0.289
0	19.9	189	4.62	14.3	0.254	0.254
0	20	188	5.09	11.5	0.205	0.205
0	20	188	5.32	11.1	0.198	0.198
0	20	188	6.26	12.8	0.228	0.228
0	20	188	6.97	13.4	0.238	0.238
0	20	188	7.67	13.2	0.235	0.235
0	20	188	8.37	13.1	0.233	0.233

Table 2.7.2: Liquid. 6, viscosity 200 mPa.s (Millube 68).

Curtain height: 52.6 mm Date: 25/10/2005
Substrate: 53818 Room temperature: 23°C

Die angle β	Liquid Temperature, °C	Viscosity μ (mPa.s)	Flow rate l/min	V_{ae} %	Air entrainment V_{ae} (m/s)	V_{ae} Cos β
30	19.9	189	1.11	13	0.231	0.200
30	19.8	190	1.57	17	0.302	0.261
30	19.8	190	1.81	18.6	0.330	0.285
30	19.8	190	2.04	20	0.354	0.307
30	19.8	190	2.28	21.3	0.377	0.327
30	19.9	189	2.51	22	0.390	0.337
30	20	188	2.75	23	0.407	0.353
30	19.6	192	2.98	23.5	0.416	0.360
30	19.6	192	3.21	23	0.407	0.353
30	19.8	190	3.45	22	0.390	0.337
30	20.1	187	3.68	20.5	0.363	0.314
30	20.6	182	3.92	20.1	0.356	0.308
30	20.6	182	4.15	17.6	0.312	0.270
30	20.6	182	4.39	16.3	0.289	0.250
30	20.7	180	4.62	13.8	0.245	0.212
30	21	177	5.32	11.9	0.212	0.183
30	21.3	174	6.03	12	0.214	0.185

Table 2.8.1: Liquid. 1, viscosity 94 mPa.s (Mix 1).

Curtain height: 52.6 mm Date: 16/11/2005
Substrate: 53818 Room temperature: 21°C

Die angle β	Liquid Temperature, °C	Viscosity μ (mPa.s)	Flow rate l/min	V_{ae} %	Air entrainment V_{ae} (m/s)	V_{ae} Cos β
0	17.7	0.098	1.50	21	0.372	0.372
0	17.7	0.098	1.62	22	0.390	0.390
0	18	0.097	1.85	23.4	0.414	0.414
0	18	0.097	2.08	24.1	0.426	0.426
0	18	0.097	2.31	25	0.442	0.442
0	18.9	0.092	2.77	26	0.460	0.460
0	18.2	0.096	3.23	25.2	0.446	0.446
0	18.2	0.096	3.46	25	0.442	0.442
0	18.2	0.096	3.92	19.9	0.353	0.353
0	18.2	0.096	4.61	18.4	0.326	0.326
0	18.2	0.096	5.53	17.4	0.309	0.309
0	18.2	0.096	6.46	16.8	0.298	0.298
0	18.3	0.095	7.38	16	0.284	0.284

Table 2.8.2: Liquid. 1, viscosity 94 mPa.s (Mix 1).

Curtain height: 52.6 mm Date: 17/11/2005
Substrate: 53818 Room temperature: 21°C

Die angle β	Liquid Temperature, °C	Viscosity μ (mPa.s)	Flow rate l/min	V_{ae} %	Air entrainment V_{ae} (m/s)	V_{ae} Cos β
30	18.5	0.094	1.38	24.3	0.430	0.372
30	18.3	0.095	1.62	25.6	0.453	0.392
30	18.5	0.094	1.85	26.7	0.472	0.409
30	18.5	0.094	2.08	28.2	0.499	0.432
30	18.5	0.094	2.31	28.5	0.504	0.436
30	18	0.097	2.77	27.8	0.492	0.426
30	18	0.097	3.23	26.8	0.474	0.410
30	18.2	0.096	3.69	25	0.442	0.383
30	18.3	0.095	4.15	19.9	0.353	0.305
30	18.3	0.095	4.61	18	0.319	0.276
30	18.3	0.095	5.53	17.4	0.309	0.267
30	18.3	0.095	5.99	17.5	0.310	0.269
30	18.4	0.095	6.92	17.7	0.314	0.272

Tables' 2.8.3, 2.8.4 and 2.8.5 show the air entrainment velocity at different height and 30° angle.

Table 2.8.3: Liquid. 2, viscosity 89 mPa.s (Mix 1).

Curtain height: 67mm Date: 19/10/2006
Substrate: 53818 Room temperature: 23°C

Die angle β	Liquid Temperature, °C	Viscosity μ (mPa.s)	Flow rate l/min	V_{ae} %	Air entrainment V_{ae} (m/s)	V_{ae} Cos β
30	19.5	89	1.62	29.3	0.518	0.449
30	19.5	89	1.85	31.7	0.560	0.485
30	19.4	90	2.08	32.5	0.574	0.497
30	19.4	90	2.31	33	0.583	0.505
30	19.4	90	2.54	32	0.566	0.490
30	19.4	90	2.77	31	0.548	0.474
30	19.5	89	3.00	29	0.513	0.444
30	19.5	89	3.23	25	0.442	0.383
30	19.4	90	3.46	22.7	0.402	0.348
30	19.4	90	3.69	21	0.372	0.322
30	19.4	90	4.15	19.4	0.344	0.298
30	19.5	89	4.61	18	0.319	0.276
30	19.6	89	5.07	16.8	0.298	0.258
30	19.7	88	5.53	16	0.284	0.246
30	19.9	87	6.46	15.2	0.270	0.234
30	20	87	7.38	15.2	0.270	0.234

Table 2.8.4: Liquid. 2, viscosity 89 mPa.s (Mix 1).

Curtain height: 80 mm Date: 30/10/2006
Substrate: 53818 Room temperature: 23°C

Die angle β	Liquid Temperature, °C	Viscosity μ (mPa.s)	Flow rate l/min	V_{ae} %	Air entrainment V_{ae} (m/s)	V_{ae} Cos β
30	18.2	96	1.62	33.8	0.629	0.517
30	18.6	94	1.85	35.6	0.654	0.545
30	18.7	93	2.08	37	0.636	0.566
30	19	92	2.31	36	0.601	0.551
30	19.1	91	2.54	34	0.543	0.520
30	19.4	90	2.77	30.7	0.407	0.470
30	19.4	90	3.23	23	0.388	0.353
30	19.5	89	3.46	21.9	0.349	0.336
30	19.5	89	3.69	19.7	0.307	0.302
30	19.5	89	4.15	17.3	0.291	0.266
30	19.6	89	4.61	16.4	0.279	0.252
30	19.8	88	5.53	15.7	0.268	0.241
30	20	87	5.99	15.1	0.294	0.232
30	20.4	85	6.92	16.6	0.302	0.255

Table 2.8.5: Liquid. 2, viscosity 89 mPa.s (Mix 1).

Curtain height: 120 mm Date: 31/10/2006
Substrate: 53818 Room temperature: 23°C

Die angle β	Liquid Temperature, °C	Viscosity μ (mPa.s)	Flow rate l/min	V_{ae} %	Air entrainment V_{ae} (m/s)	V_{ae} Cos β
30	18.4	95	1.85	50	0.882	0.764
30	18.3	95	2.08	52.5	0.926	0.802
30	18.3	95	2.31	53	0.935	0.810
30	18.6	94	2.54	45	0.794	0.688
30	18.6	94	2.77	38	0.671	0.581
30	18.6	94	3.00	32	0.566	0.490
30	18.6	94	3.23	24	0.425	0.368
30	18.6	94	3.46	20.8	0.368	0.319
30	18.6	94	3.69	19.1	0.338	0.293
30	18.6	94	4.15	17.1	0.303	0.263
30	18.6	94	4.61	16.9	0.300	0.260
30	18.6	94	5.07	16.8	0.298	0.258
30	18.7	93	5.53	16.1	0.286	0.247
30	18.8	93	5.99	16.1	0.286	0.247

Table 2.9.1: Liquid. 2, viscosity 83 mPa.s (Milgear 1).

Curtain height: 22.6 mm Date: 13/02/2006

Substrate: 53818 Room temperature: 21°C

Die angle β	Liquid Temperature, °C	Viscosity μ (mPa.s)	Flow rate l/min	V_{ae} %	Air entrainment V_{ae} (m/s)	V_{ae} Cos β
0	19.2	0.080	1.61	15.6	0.277	0.277
0	19.2	0.080	2.09	20.1	0.356	0.356
0	19	0.081	2.57	25	0.442	0.442
0	18.9	0.081	3.05	27.3	0.483	0.483
0	18.9	0.081	3.53	27.1	0.479	0.479
0	18.9	0.081	3.77	25.5	0.451	0.451
0	18.9	0.081	4.01	24.6	0.435	0.435
0	18.9	0.081	4.48	20.8	0.368	0.368
0	19	0.081	4.96	18	0.319	0.319
0	19	0.081	5.44	18	0.319	0.319
0	19	0.081	5.92	18.7	0.331	0.331
0	19.1	0.080	6.40	19.6	0.347	0.347
0	19.1	0.080	6.88	19.3	0.342	0.342
0	18.9	0.081	7.36	19.4	0.344	0.344
0	19.2	0.080	8.32	19.8	0.351	0.351
0	19.7	0.078	8.80	17.8	0.316	0.316

Table 2.9.2: Liquid. 2, viscosity 83 mPa.s (Milgear 1).

Curtain height: 22.6 mm Date: 13/02/2006

Substrate: 53818 Room temperature: 21°C

Die angle β	Liquid Temperature, °C	Viscosity μ (mPa.s)	Flow rate l/min	V_{ae} %	Air entrainment V_{ae} (m/s)	V_{ae} Cos β
30	19.1	0.080	6.5	8.7	0.155	0.135
30	18.9	0.081	7.5	17.4	0.309	0.267
30	18.6	0.083	8.5	21	0.372	0.322
30	18.6	0.083	9.5	22.7	0.402	0.348
30	18.5	0.083	10.5	26.9	0.476	0.412
30	18.5	0.083	11.5	27.5	0.486	0.421
30	18.6	0.083	12.5	27.9	0.493	0.427
30	18.6	0.083	13.5	28	0.495	0.429
30	18.7	0.082	14.5	27.8	0.492	0.426
30	18.8	0.082	15.5	27.3	0.483	0.418
30	18.8	0.082	16.5	26.3	0.465	0.403
30	18.8	0.082	17.5	25.5	0.451	0.391
30	18.8	0.082	18.5	23.9	0.423	0.366
30	18.8	0.082	19.5	22.6	0.400	0.346
30	18.8	0.082	20.5	20.8	0.368	0.319
30	18.8	0.082	23	20.2	0.358	0.310
30	18.9	0.081	25	20	0.354	0.307
30	18.9	0.081	27	20.1	0.356	0.308
30	18.9	0.081	29	19.1	0.338	0.293

Table 2.10.1: Liquid. 2, viscosity 83 mPa.s (Milgear 1).

Curtain height: 37.6 mm Date: 21/02/2006

Substrate: 53818 Room temperature: 22°C

Die angle β	Liquid Temperature, °C	Viscosity μ (mPa.s)	Flow rate l/min	V_{ae} %	Air entrainment V_{ae} (m/s)	V_{ae} Cos β
0	19.3	0.079	1.15	6	0.108	0.108
0	18.9	0.081	1.25	14.3	0.254	0.254
0	18.9	0.081	1.37	18.7	0.331	0.331
0	18.8	0.082	1.49	21.3	0.377	0.377
0	18.8	0.082	1.61	24	0.425	0.425
0	18.6	0.083	1.73	24.5	0.434	0.434
0	18.6	0.083	1.85	25.1	0.444	0.444
0	18.6	0.083	1.97	25.6	0.453	0.453
0	18.6	0.083	2.09	26	0.460	0.460
0	18.6	0.083	2.21	27.3	0.483	0.483
0	18.5	0.083	2.33	27.7	0.490	0.490
0	18.6	0.083	2.45	27.8	0.492	0.492
0	18.6	0.083	2.69	27.8	0.492	0.492
0	18.7	0.082	2.81	27.9	0.493	0.493
0	18.7	0.082	2.93	27.6	0.488	0.488
0	18.7	0.082	3.05	26	0.460	0.460
0	18.7	0.082	3.17	25.7	0.455	0.455
0	18.7	0.082	3.29	24.6	0.435	0.435
0	18.7	0.082	3.41	24.7	0.437	0.437
0	18.7	0.082	3.53	24.7	0.437	0.437
0	18.7	0.082	3.65	23.9	0.423	0.423
0	18.7	0.082	3.77	24.1	0.426	0.426
0	18.8	0.082	3.89	23.3	0.412	0.412
0	19	0.081	4.01	22.6	0.400	0.400
0	19	0.081	4.13	22.5	0.398	0.398
0	19.1	0.080	4.24	22.1	0.391	0.391
0	19	0.081	4.36	21.7	0.384	0.384
0	19.1	0.080	4.48	20.7	0.367	0.367
0	19.1	0.080	4.72	20	0.354	0.354
0	19.2	0.080	4.96	19	0.337	0.337
0	19.2	0.080	5.20	19	0.337	0.337
0	19.2	0.080	5.68	20	0.354	0.354
0	19.2	0.080	6.16	21.2	0.375	0.375
0	19.3	0.079	6.64	22	0.390	0.390
0	19.3	0.079	7.12	22	0.390	0.390
0	19.4	0.079	7.36	22	0.390	0.390
0	19.4	0.079	7.60	21.1	0.374	0.374
0	19.5	0.078	7.84	23.3	0.412	0.412
0	19.5	0.078	8.08	23.4	0.414	0.414

Table 2.10.2: Liquid. 2, viscosity 83 mPa.s (Milgear 1).

Curtain height: 52.6 mm Date: 02/03/2006

Substrate: 53818 Room temperature: 22°C

Die angle β	Liquid Temperature, °C	Viscosity μ (mPa.s)	Flow rate l/min	V_{ae} %	Air entrainment V_{ae} (m/s)	V_{ae} Cos β
0	18.6	83	1.25	19	0.337	0.337
0	18.6	83	1.49	24.9	0.441	0.441
0	18.6	83	1.73	25.6	0.453	0.453
0	18.4	83	1.97	25.5	0.451	0.451
0	18.6	83	2.21	26.4	0.467	0.467
0	18.6	83	2.45	28	0.495	0.495
0	18.4	83	2.69	26.4	0.467	0.467
0	18	85	2.93	25.9	0.458	0.458
0	18	85	3.17	24.1	0.426	0.426
0	18	85	3.41	23.8	0.421	0.421
0	18.1	85	3.65	21.9	0.388	0.388
0	18.2	84	3.89	20	0.354	0.354
0	18.2	84	4.13	18	0.319	0.319
0	18.2	84	4.36	17	0.302	0.302
0	18.3	84	4.60	16.6	0.294	0.294
0	18.4	83	4.96	16.6	0.294	0.294
0	18.5	83	5.44	16.8	0.298	0.298
0	18.5	83	5.92	17.6	0.312	0.312
0	18.5	83	6.40	17.7	0.314	0.314
0	18.6	83	6.88	17.9	0.317	0.317
0	18.6	83	7.12	17.6	0.312	0.312
0	18.6	83	7.36	17.9	0.317	0.317
0	18.6	83	7.60	17.8	0.316	0.316
0	18.7	82	7.84	17.9	0.317	0.317
0	18.8	82	8.08	18.1	0.321	0.321
0	19	81	8.32	18.9	0.335	0.335
0	19.1	80	8.56	18.8	0.333	0.333

Table 2.11.1: Liquid. 2, viscosity 83 mPa.s (Milgear 1).

Curtain height: 67.6 mm Date: 23/02/2006

Substrate: 53818 Room temperature: 22°C

Die angle β	Liquid Temperature, °C	Viscosity μ (mPa.s)	Flow rate l/min	V_{ae} %	Air entrainment V_{ae} (m/s)	V_{ae} Cos β
0	19	81	1.13	20.2	0.358	0.358
0	18.9	81	1.25	22.4	0.397	0.397
0	18.9	81	1.37	23.9	0.423	0.423
0	18.8	82	1.49	25.5	0.451	0.451
0	18.3	84	1.61	27.4	0.485	0.485
0	18.3	84	1.73	28.1	0.497	0.497
0	18.4	83	1.85	27.8	0.492	0.492
0	18.8	82	1.97	29.2	0.516	0.516
0	19.1	80	2.33	29.1	0.514	0.514
0	19.1	80	2.45	29.3	0.518	0.518
0	19.1	80	2.57	28.8	0.509	0.509
0	19.1	80	2.81	27.1	0.479	0.479
0	19.2	80	3.05	27	0.478	0.478
0	19.2	80	3.29	25	0.442	0.442
0	19.3	79	3.53	22.9	0.405	0.405
0	19.5	78	3.65	21.6	0.382	0.382
0	19.4	79	3.77	20.1	0.356	0.356
0	19.4	79	4.01	19.1	0.338	0.338
0	19.5	78	4.27	18.2	0.323	0.323
0	19.5	78	4.48	18	0.319	0.319
0	19.6	78	4.72	18.3	0.324	0.324
0	19.6	78	4.96	19	0.337	0.337
0	19.6	78	5.20	19.2	0.340	0.340
0	19.6	78	5.44	19.5	0.346	0.346
0	19.8	77	5.68	20	0.354	0.354
0	19.8	77	5.92	20	0.354	0.354
0	19.7	78	6.16	20	0.354	0.354
0	19.8	77	6.40	20	0.354	0.354
0	19.7	78	6.64	19.9	0.353	0.353
0	19.7	78	6.88	20	0.354	0.354
0	19.9	77	7.12	20	0.354	0.354
0	20	76	7.36	20.1	0.356	0.356
0	20.1	76	7.60	20	0.354	0.354
0	20.1	76	7.84	20.2	0.358	0.358
0	20.2	75	8.08	20.4	0.361	0.361
0	20.2	75	8.32	20.6	0.365	0.365
0	20.4	74	8.56	21.2	0.375	0.375
0	20.6	74	8.80	21	0.372	0.372

Table 2.11.2: Liquid. 2, viscosity 83 mPa.s (Milgear 1).

Curtain height: 40 mm Date: 13/02/2006
Substrate: 53818 Room temperature: 22°C

Die angle β	Liquid Temperature, °C	Viscosity μ (mPa.s)	Flow rate l/min	V_{ae} %	Air entrainment V_{ae} (m/s)	V_{ae} Cos β
0	19.2	80	1.61	15.6	0.277	0.277
0	19.2	80	2.09	20.1	0.356	0.356
0	19	81	2.57	25	0.442	0.442
0	18.9	81	3.05	27.3	0.483	0.483
0	18.9	81	3.53	27.1	0.479	0.479
0	18.9	81	3.77	25.5	0.451	0.451
0	18.9	81	4.01	24.6	0.435	0.435
0	18.9	81	4.48	20.8	0.368	0.368
0	19	81	4.96	18	0.319	0.319
0	19	81	5.44	18	0.319	0.319
0	19	81	5.92	18.7	0.331	0.331
0	19.1	80	6.40	19.6	0.347	0.347
0	19.1	80	6.88	19.3	0.342	0.342
0	18.9	81	7.36	19.4	0.344	0.344
0	19.2	80	8.32	19.8	0.351	0.351
0	19.7	78	8.80	17.8	0.316	0.316

Table 2.12.1: Liquid. 2, viscosity 83 mPa.s (Milgear 1).

Curtain height: 52.6 mm Date: 15/02/2006
Substrate: 53818 Room temperature: 23°C

Die angle β	Liquid Temperature, °C	Viscosity μ (mPa.s)	Flow rate l/min	V_{ae} %	Air entrainment V_{ae} (m/s)	V_{ae} Cos β
30	19.1	80	1.49	20	0.354	0.337
30	18.9	81	1.73	24	0.425	0.441
30	18.6	83	1.97	25	0.442	0.453
30	18.6	83	2.21	26.5	0.469	0.451
30	18.5	83	2.45	28	0.495	0.467
30	18.5	83	2.69	29	0.513	0.495
30	18.6	83	2.93	30	0.530	0.467
30	18.6	83	3.17	31.2	0.551	0.458
30	18.7	82	3.41	31.6	0.558	0.426
30	18.8	82	3.65	30	0.530	0.421
30	18.8	82	3.89	29	0.513	0.388
30	18.8	82	4.13	25.5	0.451	0.354
30	18.8	82	4.36	23.9	0.423	0.319
30	18.8	82	4.60	22.6	0.400	0.302
30	18.8	82	4.84	20.8	0.368	0.294
30	18.8	82	5.44	20.2	0.358	0.294
30	18.9	81	5.92	20	0.354	0.298
30	18.9	81	6.40	20	0.354	0.312
30	18.9	81	6.88	19.1	0.338	0.314

Coating with polyester substrate:

Table 2.13.1: Liquid. 2, viscosity 83 mPa.s (Milgear 1).

Curtain height: 22.6 mm Date: 27/03/2006

Substrate: Polyester 1 Room temperature: 22°C

Die angle β	Liquid Temperature, °C	Viscosity μ (mPa.s)	Flow rate l/min	V_{ae} %	Air entrainment V_{ae} (m/s)	V_{ae} Cos β
0	19	81	1.13	10	0.178	0.178
0	19	81	1.37	15	0.266	0.266
0	19	81	1.61	18.5	0.328	0.328
0	18.8	82	1.85	22.7	0.402	0.402
0	18.6	83	2.09	24.7	0.437	0.437
0	18.6	83	2.33	27.8	0.492	0.492
0	18.6	83	2.57	30	0.530	0.530
0	18.5	83	2.81	30.7	0.543	0.543
0	18.4	83	3.05	30.7	0.543	0.543
0	18.4	83	3.29	30.1	0.532	0.532
0	18.4	83	3.53	29.7	0.525	0.525
0	18.5	83	3.77	28.6	0.506	0.506
0	18.6	83	4.01	27.3	0.483	0.483
0	18.2	84	4.24	26.4	0.467	0.467
0	18.6	83	4.48	22.9	0.405	0.405
0	18.7	82	4.72	22.1	0.391	0.391
0	18.7	82	5.20	20.5	0.363	0.363
0	18.8	82	5.68	21	0.372	0.372
0	19	81	6.16	22	0.390	0.390
0	19	81	6.64	23.5	0.416	0.416
0	19.2	80	7.12	19.2	0.340	0.340

Table 2.13.2: Liquid. 2, viscosity 83 mPa.s (Milgear 1).

Curtain height: 22.6 mm Date: 24/04/2006

Substrate: Polyester 1 Room temperature: 22°C

Die angle β	Liquid Temperature, °C	Viscosity μ (mPa.s)	Flow rate l/min	V_{ae} %	Air entrainment V_{ae} (m/s)	V_{ae} Cos β
30	19.2	80	1.49	10.1	0.180	0.208
30	19	81	1.73	20.9	0.370	0.427
30	18.7	82	1.97	25.1	0.444	0.513
30	18.7	82	2.21	27	0.478	0.551
30	18.6	83	2.45	30.8	0.544	0.629
30	18.7	82	2.69	33.1	0.585	0.675
30	18.6	83	2.93	33.9	0.599	0.692
30	18.6	83	3.17	33.8	0.597	0.690
30	18.9	81	3.41	33.5	0.592	0.683
30	19	81	3.65	32.9	0.581	0.671
30	19	81	3.89	31.5	0.557	0.643
30	19	81	4.13	29.8	0.527	0.608
30	18.9	81	4.36	28	0.495	0.572
30	18.9	81	4.60	26.3	0.465	0.537
30	19	81	4.96	24.1	0.426	0.492
30	19	81	5.44	22.5	0.398	0.460
30	18.9	81	5.92	22	0.390	0.450
30	18.9	81	6.40	22	0.390	0.450
30	19.3	79	6.88	21.5	0.381	0.440

Table 2.14.1: Liquid. 2, viscosity 83 mPa.s (Milgear 1).

Curtain height: 37.6 mm Date: 22/03/2006

Substrate: Polyester 1 Room temperature: 22°C

Die angle β	Liquid Temperature, °C	Viscosity μ (mPa.s)	Flow rate l/min	V_{ae} %	Air entrainment V_{ae} (m/s)	V_{ae} Cos β
0	19.2	80	1.25	17.1	0.303	0.303
0	19.8	77	1.13	10.5	0.187	0.187
0	19.2	80	1.37	20.8	0.368	0.368
0	18.7	82	1.61	23.3	0.412	0.412
0	18.6	83	1.85	25.3	0.448	0.448
0	18.4	83	2.09	26.7	0.472	0.472
0	18.3	84	2.33	27.5	0.486	0.486
0	18.3	84	2.57	27.7	0.490	0.490
0	18.3	84	2.81	28	0.495	0.495
0	18.3	84	3.05	28	0.495	0.495
0	18.4	83	3.29	28	0.495	0.495
0	18.4	83	3.53	27.6	0.488	0.488
0	18.3	84	3.77	26.7	0.472	0.472
0	18.3	84	4.01	23	0.407	0.407
0	18.4	83	4.24	20.3	0.360	0.360
0	18.4	83	4.48	18.3	0.324	0.324
0	18.4	83	4.72	18.8	0.333	0.333
0	18.4	83	4.96	19.1	0.338	0.338
0	18.4	83	5.20	19.7	0.349	0.349
0	18.5	83	5.68	20.4	0.361	0.361
0	18.6	83	6.16	21.2	0.375	0.375
0	18.2	84	6.64	21.2	0.375	0.375
0	18.4	83	7.12	22.2	0.393	0.393
0	18.5	83	7.36	20.3	0.360	0.360
0	18.6	83	7.60	27	0.478	0.478
0	18.8	82	7.84	28.2	0.499	0.499
0	19.1	80	8.08	31.7	0.560	0.560

Table 2.14.2: Liquid. 2, viscosity 83 mPa.s (Milgear 1).

Curtain height: 37.6 mm Date: 22/03/2006

Substrate: Polyester 1 Room temperature: 22°C

Die angle β	Liquid Temperature, °C	Viscosity μ (mPa.s)	Flow rate l/min	V_{ae} %	Air entrainment V_{ae} (m/s)	V_{ae} Cos β
30	18.7	82	1.25	18.1	0.321	0.208
30	18.6	83	1.49	25.6	0.453	0.427
30	18.6	83	1.73	27	0.478	0.513
30	18.4	83	1.97	31.7	0.560	0.551
30	18.3	84	2.21	33	0.583	0.629
30	18.3	84	2.45	34.1	0.602	0.675
30	18.3	84	2.69	35	0.618	0.692
30	18.3	84	2.93	34.8	0.615	0.690
30	18.3	84	3.17	34.2	0.604	0.683
30	18.3	84	3.41	32	0.566	0.671
30	18.3	84	3.65	28.5	0.504	0.643
30	18.3	84	3.89	27	0.478	0.608
30	18.6	83	4.13	25.4	0.449	0.572
30	18.6	83	4.36	23.4	0.414	0.537
30	18.6	83	4.96	20.4	0.361	0.492
30	18.6	83	5.44	20.2	0.358	0.460
30	19.2	80	5.92	15.2	0.270	0.450
30	19.3	79	6.40	13.9	0.247	0.450
30	19.3	79	6.88	13.2	0.235	0.440
30	19.5	78	7.12	13.3	0.236	0.208
30	19.7	78	7.36	13.3	0.236	0.427

Table 2.15.1: Liquid. 2, viscosity 83 mPa.s (Milgear 1).

Curtain height: 52.6 mm Date: 15/03/2006

Substrate: Polyester 1 Room temperature: 23°C

Die angle β	Liquid Temperature, °C	Viscosity μ (mPa.s)	Flow rate l/min	V_{ae} %	Air entrainment V_{ae} (m/s)	V_{ae} Cos β Psi)
0	18	85	1.58	23.9	0.423	0.423
0	18	85	1.85	25.3	0.448	0.448
0	17.7	87	2.33	27.3	0.483	0.483
0	17.7	87	2.57	31.4	0.555	0.555
0	17.7	87	3.05	31.3	0.553	0.553
0	17.7	87	3.29	31.1	0.550	0.550
0	17.7	87	3.53	28.1	0.497	0.497
0	17.7	87	3.77	25.5	0.451	0.451
0	17.7	87	4.01	23.2	0.411	0.411
0	17.7	87	4.24	21.8	0.386	0.386
0	17.8	86	4.72	19.1	0.338	0.338
0	17.9	86	5.20	19.5	0.346	0.346
0	17.7	87	5.92	20.7	0.367	0.367
0	17.7	87	6.40	20.7	0.367	0.367
0	17.7	87	6.64	20.7	0.367	0.367
0	17.9	86	7.12	20.4	0.361	0.361
0	18.1	85	7.36	20.6	0.365	0.365

Table 2.15.2: Liquid. 2, viscosity 83 mPa.s (Milgear 1).

Curtain height: 52.6 mm Date: 26/04/2006

Substrate: Polyester 1 Room temperature: 23C

Die angle β	Liquid Temperature, °C	Viscosity μ (mPa.s)	Flow rate l/min	V_{ae} %	Air entrainment V_{ae} (m/s)	V_{ae} Cos β
30	19.2	80	1.37	30	0.530	0.612
30	19.3	79	1.61	33.9	0.599	0.692
30	19	81	1.85	34.3	0.606	0.700
30	18.9	81	2.09	35	0.618	0.704
30	18.8	82	2.33	34.8	0.615	0.710
30	18.8	82	2.57	34.7	0.613	0.714
30	18.8	82	2.81	35	0.618	0.722
30	18.7	82	3.05	33.9	0.599	0.692
30	18.7	82	3.29	31	0.548	0.633
30	18.9	81	3.53	27.5	0.486	0.562
30	18.8	82	3.77	25.4	0.449	0.519
30	18.8	82	4.01	24.1	0.426	0.492
30	18.8	82	4.24	22.4	0.397	0.458
30	18.8	82	4.48	20.2	0.358	0.413
30	18.8	82	4.72	19.8	0.351	0.405
30	18.8	82	4.96	19.9	0.353	0.407
30	18.8	82	5.20	19.7	0.349	0.403
30	18.8	82	5.44	19	0.337	0.389
30	18.9	81	5.92	19	0.337	0.389
30	18.9	81	6.40	19.5	0.346	0.399

Table 2.16.1: Liquid. 2, viscosity 83 mPa.s (Milgear 1).

Curtain height: 67.6 mm Date: 20/03/2006
Substrate: Polyester 1 Room temperature: 23°C

Die angle β	Liquid Temperature, °C	Viscosity μ (mPa.s)	Flow rate l/min	Vae%	Air entrainment V_{ae} (m/s)	V_{ae} Cos β
0	18.6	83	1.25	24.9	0.441	30
0	18.3	84	1.49	27.4	0.485	35
0	18.1	85	1.73	31	0.548	40
0	18.1	85	1.97	32.2	0.569	45
0	18.1	85	2.21	30.6	0.541	50
0	18.5	83	2.57	29.7	0.525	55
0	18.3	84	2.81	28.5	0.504	60
0	18.4	83	3.05	27.9	0.493	65
0	18.4	83	3.29	26.4	0.467	70
0	18.2	84	3.53	24.6	0.435	75
0	18.2	84	3.77	23.1	0.409	80
0	18.2	84	4.01	22	0.390	85
0	18.3	84	4.24	21.3	0.377	90
0	18.4	83	4.48	20	0.354	95
0	18.3	84	4.72	19.2	0.340	100
0	18.4	83	4.96	18.6	0.330	105
0	18.3	84	5.20	17.3	0.307	110
0	18.3	84	5.44	17.2	0.305	115
0	18.2	84	5.68	17	0.302	120
0	18.2	84	5.92	21.6	0.382	125
0	18.3	84	6.16	20	0.354	135
0	18.4	83	6.64	20.2	0.358	140
0	18.4	83	7.12	20	0.354	155
0	18.5	83	7.36	20.2	0.358	160
0	18.6	83	7.60	20	0.354	175

Table: 2 .16.2: Liquid. 2, viscosity 83 mPa.s (Milgear 1).

Curtain height: 67.6 mm Date: 28/04/2006
Substrate: Polyester 1 Room temperature: 25°C

Die angle β	Liquid Temperature, °C	Viscosity μ (mPa.s)	Flow rate l/min	Vae%	Air entrainment V_{ae} (m/s)	V_{ae} Cos β
30	20	76	1.25	34.2	0.604	0.698
30	19.5	78	1.49	35	0.618	0.714
30	19.1	80	1.61	41.5	0.733	0.846
30	19.1	80	1.85	42.1	0.743	0.858
30	19.1	80	2.09	42.2	0.745	0.860
30	19.1	80	2.33	43.5	0.768	0.887
30	19.1	80	2.57	44.1	0.778	0.899
30	19.2	80	2.81	45.2	0.798	0.921
30	19.1	80	3.05	43.8	0.773	0.893
30	19.1	80	3.29	39.4	0.696	0.803
30	19.1	80	3.53	36.8	0.650	0.751
30	19.1	80	3.77	31.8	0.562	0.649
30	19.1	80	4.01	29.5	0.522	0.602
30	19.1	80	4.24	26.7	0.472	0.545
30	19.2	80	4.72	22.6	0.400	0.462
30	19.3	79	5.20	21.7	0.384	0.444
30	19.1	80	5.68	21.2	0.375	0.433
30	19.1	80	20.6	20.6	0.365	0.421
30	19.2	80	21.2	21.2	0.375	0.433

Coating with 53847 polyester substrate at different height, angles and liquids viscosity.

Table 2.17.1: Liquid. 2, viscosity 83 mPa.s (Milgear 1).

Curtain height: 22.6 mm Date: 06/06/2006
Substrate: 53847 Room temperature: 23°C

Die angle β	Liquid Temperature, °C	Viscosity μ (mPa.s)	Flow rate l/min	V_{ae} %	Air entrainment V_{ae} (m/s)	Pressure (Psi)
0	18.8	82	1.80	16.3	0.289	0.289
0	18.5	83	2.09	19.6	0.347	0.347
0	18.5	83	2.33	21.9	0.388	0.388
0	18.7	82	2.57	22.3	0.395	0.395
0	18.6	83	2.81	22.6	0.400	0.400
0	18.6	83	3.05	22.6	0.400	0.400
0	18.6	83	3.29	22.2	0.393	0.393
0	18.6	83	3.53	22	0.390	0.390
0	18.6	83	3.77	20.6	0.365	0.365
0	18.6	83	4.01	19.6	0.347	0.347
0	18.6	83	4.24	18.5	0.328	0.328
0	18.6	83	4.48	17.2	0.305	0.305
0	18.7	82	4.72	17.2	0.305	0.305
0	19.1	80	5.20	16.2	0.287	0.287
0	19.1	80	5.68	15.9	0.284	0.284
0	19.1	80	6.16	17.7	0.272	0.272
0	18.9	81	6.64	19.8	0.250	0.250
0	19.5	78	7.12	19.8	0.240	0.240
0	19.4	79	7.36	19.8	0.235	0.235

Table 2.17.2: Liquid. 2, viscosity 83 mPa.s (Milgear 1).

Curtain height: 22.6 mm Date: 06/06/2006

Substrate: 53847 Room temperature: 23°C

Die angle β	Liquid Temperature, °C	Viscosity μ (mPa.s)	Flow rate l/min	V_{ae} %	Air entrainment V_{ae} (m/s)	Pressure (Psi)
30	18.7	82	1.80	16.3	0.289	0.353
30	18.5	83	2.09	19.6	0.347	0.372
30	18.3	84	2.33	21.9	0.388	0.386
30	18.5	83	2.57	22.3	0.395	0.392
30	18.4	83	2.81	22.6	0.400	0.406
30	18.2	84	3.05	22.6	0.400	0.406
30	18.3	84	3.29	22.2	0.393	0.398
30	18.3	84	3.53	22	0.390	0.383
30	18.1	85	3.77	20.6	0.365	0.369
30	18.2	84	4.01	19.6	0.347	0.366
30	18.3	84	4.24	18.5	0.328	0.337
30	18.2	84	4.48	17.2	0.305	0.330
30	18.4	83	4.72	17.2	0.305	0.307
30	18.5	83	5.20	16.2	0.287	0.296
30	18.5	83	5.68	15.9	0.282	0.279
30	18.6	83	6.16	17.7	0.314	0.269
30	18.7	82	6.64	19.8	0.351	0.258
30	18.8	82	7.12	19.8	0.351	0.255
30	18.9	81	7.36	19.8	0.351	0.241
30	18.9	81	7.60	12.5	0.222	0.206

Table 2.18.1: Liquid. 2, viscosity 83 mPa.s (Milgear 1).

Curtain height: 37.6 mm Date: 02/06/2006
Substrate: 53847 Room temperature: 23°C

Die angle β	Liquid Temperature, °C	Viscosity μ (mPa.s)	Flow rate l/min	V_{ae} %	Air entrainment V_{ae} (m/s)	Pressure (Psi)
0	19.1	80	1.80	19.2	0.340	0.340
0	18.8	82	2.09	21.6	0.382	0.382
0	18.5	83	2.33	23.4	0.414	0.414
0	18.3	84	2.57	25.7	0.455	0.455
0	18.3	84	2.81	25.6	0.453	0.453
0	18.3	84	3.05	25.9	0.458	0.458
0	18.3	84	3.29	25.7	0.455	0.455
0	18.3	84	3.53	25.2	0.446	0.446
0	18.3	84	3.77	23.2	0.411	0.411
0	18.5	83	4.01	20.5	0.363	0.363
0	18.8	82	4.24	18.8	0.333	0.333
0	18.9	81	4.48	16.5	0.293	0.293
0	18.8	82	4.72	15.5	0.275	0.275
0	19	81	4.96	14.5	0.258	0.258
0	19	81	5.44	15.7	0.279	0.279
0	19.1	80	5.92	18.1	0.321	0.321
0	19	81	6.40	18.1	0.321	0.321
0	19.5	78	6.88	18.2	0.323	0.323
0	19.1	80	7.12	18.3	0.324	0.324

Table 2.18.2: Liquid. 2, viscosity 83 mPa.s (Milgear 1).

Curtain height: 37.6 mm Date: 09/06/2006
Substrate: 53847 Room temperature: 23°C

Die angle β	Liquid Temperature, °C	Viscosity μ (mPa.s)	Flow rate l/min	V_{ae} %	Air entrainment V_{ae} (m/s)	Pressure (Psi)
30	18.8	82	1.80	22.8	0.404	0.350
30	18.8	82	2.09	24.5	0.434	0.375
30	18.7	82	2.33	27.3	0.483	0.418
30	18.5	83	2.57	28.8	0.509	0.441
30	18.5	83	2.81	28.9	0.511	0.442
30	18.5	83	3.05	28.3	0.500	0.433
30	18.5	83	3.29	25.8	0.456	0.395
30	18.3	84	3.53	24.5	0.434	0.375
30	18.4	83	3.77	21.5	0.381	0.330
30	18.4	83	4.01	20.1	0.356	0.308
30	18.5	83	4.24	19.3	0.342	0.296
30	18.4	83	4.72	18.3	0.324	0.281
30	18.8	82	5.20	17.9	0.317	0.275
30	18.8	82	5.68	17.6	0.312	0.270
30	18.7	82	6.16	14.6	0.259	0.225
30	18.9	81	6.64	16.7	0.296	0.257

Table 2.19.1: Liquid. 2, viscosity 83 mPa.s (Milgear 1).

Curtain height: 52.6 mm Date: 13/06/2006
Substrate: 53847 Room temperature: 23°C

Die angle β	Liquid Temperature, °C	Viscosity μ (mPa.s)	Flow rate l/min	V_{ae} %	Air entrainment V_{ae} (m/s)	Pressure (Psi)
0	19.2	80	1.73	21.8	0.386	40
0	19.1	80	2.09	24	0.425	45
0	18.8	82	2.33	25.1	0.444	50
0	18.7	82	2.57	26.8	0.474	55
0	18.6	83	2.81	28.2	0.499	60
0	18.6	83	3.05	27.9	0.493	65
0	18.6	83	3.29	26.8	0.474	70
0	18.6	83	3.53	24.8	0.439	75
0	18.6	83	3.77	22	0.390	80
0	18.7	82	4.01	20.1	0.356	85
0	18.7	82	4.24	16.7	0.296	90
0	18.9	81	4.72	16.5	0.293	95
0	18.7	82	5.20	16.5	0.293	100
0	19	81	5.68	18.6	0.330	100
0	19.2	80	6.16	18.9	0.335	105
0	19.2	80	6.64	18.6	0.330	110
0	19.2	80	7.12	18.4	0.326	120

Table 2.19.2: Liquid. 2, viscosity 83 mPa.s (Milgear 1).

Curtain height: 52.6 mm Date: 14/06/2006
Substrate: 53847 Room temperature: 23°C

Die angle β	Liquid Temperature, °C	Viscosity μ (mPa.s)	Flow rate l/min	V_{ae} %	Air entrainment V_{ae} (m/s)	Pressure (Psi)
30	18.8	82	1.80	29.2	0.516	40
30	19	81	2.09	30.2	0.534	45
30	18.9	81	2.33	31	0.548	50
30	18.9	81	2.57	31.8	0.562	55
30	18.9	81	2.81	32.8	0.580	60
30	18.9	81	3.05	33	0.583	65
30	19	81	3.29	32	0.566	70
30	18.7	82	3.53	31	0.548	75
30	18.6	83	3.77	30.5	0.539	80
30	18.5	83	4.01	29.5	0.522	85
30	18.6	83	4.24	27.2	0.481	90
30	18.7	82	4.72	25.8	0.456	95
30	18.8	82	5.20	22	0.390	100
30	18.8	82	5.68	17	0.302	100
30	18.9	81	6.16	14.8	0.263	105
30	19	81	6.64	14	0.249	110
30	19	81	7.12	13.2	0.235	120
30	19.5	78	7.36	12.9	0.229	130
30	19.1	80	7.60	12.4	0.221	140
30	19.2	80	7.84	12.5	0.222	150
30	19.3	79	8.08	12.3	0.221	160

Table 2.20.1: Liquid. 2, viscosity 83 mPa.s (Milgear 1).

Curtain height: 67.6 mm Date: 14/06/2006
Substrate: 53847 Room temperature: 23°C

Die angle β	Liquid Temperature, °C	Viscosity μ (mPa.s)	Flow rate l/min	V_{ae} %	Air entrainment V_{ae} (m/s)	Pressure (Psi)
0	18.8	82	1.85	22.6	0.400	40
0	18.8	82	2.09	26.5	0.469	45
0	18.4	83	2.33	28.2	0.499	50
0	18.4	83	2.57	29	0.513	55
0	18.4	83	2.81	28	0.495	60
0	18.4	83	3.05	26.5	0.469	65
0	18.4	83	3.29	23.7	0.419	70
0	18.5	83	3.53	21.9	0.388	75
0	18.8	82	3.77	19.8	0.351	80
0	18.5	83	4.01	17.1	0.303	85
0	18.5	83	4.24	15.9	0.282	90
0	18.6	83	4.72	15.5	0.275	95
0	18.6	83	5.20	16.1	0.286	100
0	18.6	83	5.68	18.2	0.323	100
0	18.4	83	6.16	18.3	0.324	105
0	18.5	83	6.64	18.5	0.328	110
0	18.6	83	7.12	18.1	0.321	120

Table 2.20.2 Liquid. 2, viscosity 83 mPa.s (Milgear 1).

Curtain height: 67.6 mm Date: 07/06/2006
Substrate: 53847 Room temperature: 23°C

Die angle β	Liquid Temperature, °C	Viscosity μ (mPa.s)	Flow rate l/min	V_{ae} %	Air entrainment V_{ae} (m/s)	Pressure (Psi)
30	18.4	83	1.80	32	0.566	40
30	18.4	83	2.09	33	0.583	45
30	18.4	83	2.33	34	0.601	50
30	18.4	83	2.57	35.2	0.622	55
30	18.4	83	2.81	36.4	0.643	60
30	18.5	83	3.05	35.4	0.625	65
30	18.6	83	3.29	33.4	0.590	70
30	18.6	83	3.53	30	0.530	75
30	18.5	83	3.77	28.3	0.500	80
30	18.5	83	4.24	25.4	0.449	85
30	18.5	83	4.72	22.8	0.404	90
30	18.5	83	5.20	19.1	0.338	95
30	18.6	83	5.68	18.5	0.328	100
30	18.7	82	6.16	14.8	0.263	100
30	18.6	83	6.64	12.7	0.226	105
30	18.9	81	7.12	12.4	0.221	110

Table 2.21.1: Liquid. 2, viscosity 83 mPa.s (Milgear 1).

Curtain height: 85 mm Date: 02/08/2006
Substrate: 53847 Room temperature: 24°C

Die angle β	Liquid Temperature, °C	Viscosity μ (mPa.s)	Flow rate l/min	V_{ae} %	Air entrainment V_{ae} (m/s)	Pressure (Psi)
0	18.8	82	1.85	36.5	0.645	40
0	18.8	82	2.09	37	0.654	45
0	18.8	82	2.33	36	0.636	50
0	18.9	81	2.57	29	0.513	55
0	18.8	82	2.81	25	0.442	60
0	18.8	82	3.05	24.6	0.435	65
0	19	81	3.29	23.8	0.421	70
0	19	81	3.53	20	0.354	75
0	19.1	80	3.77	19	0.337	80
0	19.1	80	4.24	18.1	0.321	85
0	19.1	80	4.72	18	0.319	90
0	19.2	80	5.20	20	0.354	95
0	19.2	80	5.68	21	0.372	100
0	19.2	80	6.16	21	0.372	110
0	19.3	79	6.64	21	0.372	115
0	19.3	79	7.12	20	0.354	120
0	19.4	79	7.36	20	0.354	130
0	19.6	78	7.60	20	0.354	135

Table 2.21.2: Liquid. 2, viscosity 83 mPa.s (Milgear 1).

Curtain height: 150 mm Date: 03/08/2006
Substrate: 53847 Room temperature: 23°C

Die angle β	Liquid Temperature, °C	Viscosity μ (mPa.s)	Flow rate l/min	V_{ae} %	Air entrainment V_{ae} (m/s)	Pressure (Psi)
0	18.9	81	2.69	33.7	0.595	40
0	18.7	82	2.81	26.5	0.469	45
0	18.4	83	3.05	21.1	0.374	50
0	18.4	83	3.29	18.7	0.331	55
0	18.4	83	3.53	17.7	0.314	60
0	18.4	83	3.77	18	0.319	65
0	18.7	82	4.01	17.4	0.309	70
0	18.9	81	4.24	18.5	0.328	75
0	18.9	81	4.48	19	0.337	80
0	18.9	81	4.72	19	0.337	85
0	19	81	5.20	18.2	0.323	90
0	19.1	80	5.92	18.5	0.328	95
0	19.2	80	6.64	18.7	0.331	100
0	19.2	80	7.12	18.9	0.335	110
0	19.4	79	7.60	18.5	0.328	115

Table 2.22.1: Liquid. 4, viscosity 116 mPa.s (Millmax 46).

Curtain height: 80 mm Date: 11/08/2006

Substrate: 53847 Room temperature: 23°C

Die angle β	Liquid Temperature, °C	Viscosity μ (mPa.s)	Flow rate l/min	V_{ae} %	Air entrainment V_{ae} (m/s)	Pressure (Psi)
0	18.9	116	1.86	20	0.354	65
0	18.9	116	2.10	20.5	0.363	70
0	18.9	116	2.33	20.8	0.368	75
0	18.9	116	2.56	22.3	0.395	80
0	18.8	117	2.79	22	0.390	85
0	18.9	116	3.03	21.8	0.386	100
0	19	116	3.26	20.6	0.365	105
0	19	116	3.49	20	0.354	110
0	19	116	3.72	19	0.337	115
0	19.1	115	3.96	17.9	0.317	120
0	19.1	115	4.42	12.4	0.221	125
0	19.1	115	4.89	13	0.231	65
0	19.1	115	5.35	13	0.231	70
0	19.3	114	5.81	15.2	0.270	75
0	19.7	111	6.28	16.4	0.291	80
0	19.7	111	6.74	14.9	0.265	85
0	19.8	110	6.98	15.5	0.275	100
0	19.9	110	7.21	15.9	0.282	105
0	20.1	108	7.44	15.3	0.272	110
0	20.1	108	7.67	15.8	0.280	115
0	20.4	106	7.91	15.8	0.280	125

Table 2.22.2: Liquid. 4, viscosity 122 mPa.s (Millmax 46).

Curtain height: 80 mm Date: 08/09/2006
Substrate: 53847 Room temperature: 23°C

Die angle β	Liquid Temperature, °C	Viscosity μ (mPa.s)	Flow rate l/min	V_{ae} %	Air entrainment V_{ae} (m/s)	Pressure (Psi)
30	18.1	122	1.86	23.8	0.421	70
30	18.1	122	2.10	24.8	0.439	75
30	18.3	120	2.33	24.8	0.439	80
30	17.9	123	2.56	26.0	0.460	85
30	18.1	122	2.79	25.5	0.451	100
30	18.2	121	3.03	22.9	0.405	105
30	18.2	121	3.26	22.2	0.393	110
30	18.3	120	3.49	21.1	0.374	120
30	18.3	120	3.96	17.2	0.305	125
30	18.7	118	4.42	14.4	0.256	140
30	18.7	118	4.89	14.0	0.249	150
30	18.7	118	5.35	13.7	0.243	160
30	18.8	117	5.81	12.4	0.221	175
30	18.9	116	6.28	12.2	0.217	190
30	19.1	115	6.74	12.3	0.219	195
30	19.1	115	7.21	12.2	0.217	200
30	19.1	115	7.67	13.0	0.231	220
30	18.1	122	8.14	12.1	0.215	225
30	18.3	120	8.37	12.2	0.217	2230
30	18.5	119	8.84	12.2	0.217	240
30	18.6	118	9.30	12.5	0.222	250

Table 2.22.3: Liquid. 4, viscosity 116 mPa.s (Millmax 46).

Curtain height: 100 mm Date: 31/08/2006
Substrate: 53847 Room temperature: 23°C

Die angle β	Liquid Temperature, °C	Viscosity μ (mPa.s)	Flow rate l/min	V_{ae} %	Air entrainment V_{ae} (m/s)	Pressure (Psi)
0	18.4	120	7	22.8	0.404	65
0	18.2	121	8	23.8	0.421	70
0	18.2	121	9	24.6	0.435	75
0	18.3	120	10	25.3	0.448	80
0	18.2	121	11	26.4	0.467	85
0	18.2	121	12	24.6	0.435	100
0	18.2	121	14	21.0	0.372	105
0	18.3	120	16	15.5	0.275	110
0	18.5	119	18	14.2	0.252	115
0	18.5	119	20	13.8	0.245	120
0	18.5	119	22	13.5	0.240	125
0	18.5	119	24	13.9	0.247	130
0	18.6	118	26	13.9	0.247	140
0	18.7	118	28	13.9	0.247	150
0	18.9	116	30	14.1	0.250	165
0	19	116	32	14.5	0.258	170
0	19.5	112	33	14.5	0.258	180
0	18.8	117	34	13.5	0.240	190
0	18.9	116	36	15.6	0.277	195

Table 2.22.4: Liquid. 4, viscosity 116 mPa.s (Millmax 46).

Curtain height: 150 mm Date: 08/09/2006
Substrate: 53847 Room temperature: 23°C

Die angle β	Liquid Temperature, °C	Viscosity μ (mPa.s)	Flow rate l/min	V_{ae} %	Air entrainment V_{ae} (m/s)	Pressure (Psi)
0	18.1	122	8	24.1	0.426	65
0	18.1	122	9	24.3	0.430	70
0	18	122	10	25.0	0.442	75
0	18	122	11	22.3	0.395	80
0	18.3	120	12	19.3	0.342	85
0	18.3	120	13	18.4	0.326	100
0	18.4	120	14	15.1	0.268	105
0	18.5	119	15	12.1	0.215	110
0	18.5	119	16	11.7	0.208	115
0	18.5	119	17	12.0	0.214	120
0	18.5	119	18	12.5	0.222	125
0	18.6	118	25	15.0	0.266	130
0	18.7	118	27	14.8	0.263	140
0	19	116	29	15.6	0.277	150
0	19	116	31	15.7	0.279	165
0	19.2	114	33	15.5	0.275	175

Table 2.23.1: Liquid. 5, viscosity 218 mPa.s (Millmax 68).

Curtain height: 90 mm Date: 20/03/2007
Substrate: 53847 Room temperature: 23°C

Die angle β	Liquid Temperature, °C	Viscosity μ (mPa.s)	Flow rate l/min	V_{ae} %	Air entrainment V_{ae} (m/s)	Pressure (Psi)
0	17.5	218	1.42	137	137	80
0	17.8	214	1.95	185	185	100
0	18.3	207	2.49	230	230	120
0	18.8	201	3.03	255	255	140
0	18.8	201	3.56	235	235	150
0	19.5	191	4.10	200	200	170
0	20	185	4.63	125	125	180
0	20	185	5.17	87	87	190
0	20.2	182	5.71	89	89	200
0	20.4	180	6.24	100	100	220
0	20.5	178	6.78	106	106	225
0	20.7	176	7.32	124.0	124.0	230
0	21	172	7.85	141.0	141.0	240
0	21.1	170	8.39	146	146	250

Table 2.23.2: Liquid. 5, viscosity 201 mPa.s (Millmax 68).

Curtain height: 105 mm Date: 23/03/2007
Substrate: 53847 Room temperature: 23°C

Die angle β	Liquid Temperature, °C	Viscosity μ (mPa.s)	Flow rate l/min	V_{ae} %	Air entrainment V_{ae} (m/s)	Pressure (Psi)
0	18.8	201	1.74	190	0.432	80
0	18.8	201	2.22	230	0.524	100
0	19	198	2.76	295	0.673	120
0	19	198	3.29	340	0.777	140
0	19.4	193	3.83	360	0.823	150
0	19	198	4.37	355	0.811	170
0	20	185	4.90	105	0.236	180
0	20	185	5.44	91	0.204	190
0	20	185	5.98	96	0.216	200
0	20.1	183	6.51	101	0.227	220
0	20.5	178	7.05	108	0.243	225
0	20.6	177	7.59	102.0	0.229	230
0	20.8	174	8.12	105.0	0.236	240
0	20.8	174	8.39	101	0.227	250
0	20.8	174	8.66	104	0.234	260

Table 2.23.3: Liquid. 5, viscosity 183 mPa.s (Millmax 68).

Curtain height: 150 mm Date: 21/05/2007
Substrate: 53847 Room temperature: 23°C

Die angle β	Liquid Temperature, °C	Viscosity μ (mPa.s)	Flow rate l/min	V_{ae} %	Air entrainment V_{ae} (m/s)	Pressure (Psi)
0	20.1	183	1.68	180	0.835	80
0	19.9	186	1.95	215	1.000	100
0	19.6	190	2.49	260	1.211	120
0	19.6	190	3.03	340	1.587	140
0	19.8	187	3.56	570	2.668	150
0	19.8	187	4.10	550	2.574	170
0	20	185	4.63	506	2.368	180
0	20.4	180	5.17	490	2.292	190
0	20.8	174	5.71	480	2.245	200
0	21	172	6.24	355	1.658	210

Table 2.23.3: Liquid. 5, viscosity 198 mPa.s (Millmax 68).

Curtain height: 200 mm Date: 21/05/2007
Substrate: 53847 Room temperature: 23°C

Die angle β	Liquid Temperature, °C	Viscosity μ (mPa.s)	Flow rate l/min	V_{ae} %	Air entrainment V_{ae} (m/s)	Pressure (Psi)
0	19	198	1.68	215	1.000	80
0	19	198	1.95	290	1.352	100
0	19	198	2.49	380	1.775	120
0	19.3	194	3.03	495	2.316	140
0	19.5	191	3.56	540	2.527	150
0	20	185	4.10	580	2.715	170
0	20.5	178	4.63	610	2.856	180
0	20.9	173	5.17	660	3.091	190
0	21.2	169	5.71	730	3.420	200
0	22	159	6.24	650	3.044	210

Table 2.24.1: Liquid. 8, viscosity 441 mPa.s (Millmax 150).

Curtain height: 100 mm Date: 11/06/2007
Substrate: 53847 Room temperature: 22°C

Die angle β	Liquid Temperature, °C	Viscosity μ (mPa.s)	Flow rate l/min	V_{ae} %	Air entrainment V_{ae} (m/s)	Pressure (Psi)
0	20.6	441	1.18	39	0.173	80
0	20.4	448	1.73	56	0.253	90
0	20.4	448	2.27	74	0.337	110
0	20.4	448	3.09	97	0.445	140
0	20.8	434	3.63	113	0.521	160
0	21	427	4.17	140	0.647	180
0	21.5	409	4.72	154	0.713	190
0	21.8	398	5.26	170	0.788	210
0	22.2	384	5.80	190	0.882	215
0	23.2	348	6.35	220	1.023	240
0	23.4	341	6.89	239	1.113	250
0	23.8	327	7.43	223	1.038	255
0	23.9	324	7.98	200	0.929	265
0	24	320	8.52	173	0.803	270
0	24.3	309	9.06	150	0.694	275

Table 2.24.2: Liquid. 8, viscosity 441 mPa.s (Millmax 150).

Curtain height: 100 mm Date: 11/06/2007
Substrate: 53847 Room temperature: 22°C

Die angle β	Liquid Temperature, °C	Viscosity μ (mPa.s)	Flow rate l/min	V_{ae} %	Air entrainment V_{ae} (m/s)	Pressure (Psi)
30	20.3	451	1.18	38	0.168	60
30	20.1	458	1.73	58	0.262	90
30	20.1	458	2.27	70	0.318	110
30	20.1	458	3.09	85	0.389	140
30	20.5	444	3.63	130	0.600	160
30	21	427	4.17	200	0.929	180
30	21.2	419	4.72	220	1.023	190
30	21.6	405	5.26	261	1.216	200
30	21.8	398	5.80	270	1.258	220
30	22.1	387	6.35	283	1.320	230
30	22.3	380	6.89	269	1.254	240
30	22.7	366	7.43	255	1.188	250
30	23.2	348	7.98	191	0.887	260
30	23.5	338	8.52	173	0.803	270

Table 2.24.3: Liquid. 8, viscosity 441 mPa.s (Millmax 150).

Curtain height: 150 mm Date: 08/06/2007
Substrate: 53847 Room temperature: 23°C

Die angle β	Liquid Temperature, °C	Viscosity μ (mPa.s)	Flow rate l/min	V_{ae} %	Air entrainment V_{ae} (m/s)	Pressure (Psi)
0	21.4	412	21.4	43	0.192	80
0	21.4	412	21.4	64	0.290	90
0	21.5	409	21.5	110	0.506	110
0	21.7	402	21.7	159	0.737	140
0	22	391	22	195	0.906	160
0	22	391	22	223	1.038	180
0	22	391	22	240	1.117	190
0	22.2	384	22.2	260	1.211	210
0	22.2	384	22.2	290	1.352	215
0	22.3	380	22.3	324	1.512	240
0	22.3	380	22.3	330	1.540	250
0	22.3	380	22.3	333	1.555	255
0	22.4	377	22.4	315	1.470	265
0	22.5	373	22.5	286	1.334	270
0	22.6	370	22.6	230	1.070	275
0	22.7	366	22.7	190	0.882	280

Table 2.24.4: Liquid. 8, viscosity 458 mPa.s (Millmax 150).

Curtain height: 150 mm Date: 18/06/2007
Substrate: 53847 Room temperature: 22°C

Die angle β	Liquid Temperature, °C	Viscosity μ (mPa.s)	Flow rate l/min	V_{ae} %	Air entrainment V_{ae} (m/s)	Pressure (Psi)
30	20.1	458	1.18	50	0.224	60
30	20.2	455	1.73	80	0.365	90
30	20.3	451	2.27	142	0.657	110
30	20.5	444	3.09	200	0.929	140
30	20.7	437	3.63	218	1.014	160
30	21	427	4.17	257	1.197	180
30	21	427	4.72	277	1.291	190
30	21.7	402	5.26	340	1.587	200
30	22	391	5.80	384	1.794	220
30	22.4	377	6.35	400	1.869	230
30	22.6	370	6.89	420	1.963	240
30	23	356	7.43	415	1.940	250
30	23.2	348	7.98	390	1.822	260
30	23.4	341	8.52	375	1.752	280
30	23.6	334	9.06	345	1.611	290
30	24.2	313	9.61	308	1.437	300
30	24.3	309	10.15	272	1.268	310
30	24.8	292	10.69	228	1.061	320

Table 2.24.5: Liquid. 8, viscosity 409 mPa.s (Millmax 150).

Curtain height: 200 mm Date: 08/06/2007
Substrate: 53847 Room temperature: 22°C

Die angle β	Liquid Temperature, °C	Viscosity μ (mPa.s)	Flow rate l/min	V_{ae} %	Air entrainment V_{ae} (m/s)	Pressure (Psi)
0	21.5	409	1.18	48	0.215	80
0	20.8	434	1.73	51	0.229	90
0	20.6	441	2.27	95	0.436	110
0	20.8	434	3.09	258	1.202	140
0	21.4	412	3.63	300	1.399	160
0	21.6	405	4.17	327	1.526	180
0	21.9	395	4.72	341	1.592	190
0	22	391	5.26	365	1.705	210
0	22.1	387	5.80	375	1.752	215
0	22.6	370	6.35	410	1.916	240
0	22.8	363	6.89	423	1.978	250
0	23.3	345	7.43	435	2.034	255
0	23.5	338	7.98	381	1.780	265
0	24.2	313	8.52	247	1.150	270
0	24.7	295	9.06	210	0.976	275

Table 2.24.6: Liquid. 8, viscosity 437 mPa.s (Millmax 150).

Curtain height: 200 mm Date: 19/06/2007
Substrate: 53847 Room temperature: 23°C

Die angle β	Liquid Temperature, °C	Viscosity μ (mPa.s)	Flow rate l/min	V_{ae} %	Air entrainment V_{ae} (m/s)	Pressure (Psi)
30	20.7	437	1.73	98	0.450	60
30	20.7	437	2.27	114	0.525	90
30	20.5	444	3.09	230	1.070	110
30	21	427	3.63	280	1.305	140
30	21.5	409	4.17	320	1.493	160
30	22.7	366	4.72	360	1.681	180
30	23.2	348	5.26	400	1.869	190
30	24.1	316	5.80	420	1.963	200
30	24.5	302	6.35	460	2.151	220
30	25.5	267	6.89	490	2.292	230
30	25.8	256	7.43	460	2.151	240
30	25.9	253	7.98	440	2.057	250
30	26.3	238	8.52	390	1.822	260
30	26.6	228	9.06	295	1.376	280
30	26.7	224	9.61	270	1.258	290

Table 2.25.1: Liquid. 9, viscosity 779 mPa.s (Millmax 220).

Curtain height: 100 mm Date: 25/07/2007
Substrate: 53847 Room temperature: 22°C

Die angle β	Liquid Temperature, °C	Viscosity μ (mPa.s)	Flow rate l/min	V_{ae} %	Air entrainment V_{ae} (m/s)	Pressure (Psi)
0	20	779	1.17	15	0.060	130
0	20	779	1.86	18	0.074	170
0	19.9	784	2.56	21	0.088	210
0	20	779	3.59	28	0.121	280
0	20	779	4.29	31	0.135	310
0	20.1	775	4.98	37	0.163	330
0	20.7	749	5.67	44	0.196	350
0	21.4	718	6.36	54	0.243	370
0	21.9	696	7.05	59	0.267	390
0	22.5	669	7.75	68	0.309	400
0	23.2	638	8.44	75	0.342	405
0	23.7	616	9.13	86	0.394	400
0	24.6	577	9.82	94	0.431	410
0	25.5	537	10.51	112	0.516	415
0	26	515	11.21	102	0.469	415
0	26	515	11.90	92	0.422	420

Table 2.25.2: Liquid. 9, viscosity 766 mPa.s (Millmax 220).

Curtain height: 100 mm Date: 26/07/2007
Substrate: 53847 Room temperature: 22°C

Die angle β	Liquid Temperature, °C	Viscosity μ (mPa.s)	Flow rate l/min	V_{ae} %	Air entrainment V_{ae} (m/s)	Pressure (Psi)
30	20.3	766	0.48	11	0.041	80
30	20.2	771	1.17	17	0.069	100
30	20.2	771	1.86	21	0.088	140
30	20.1	775	2.56	25	0.107	180
30	20	779	3.59	32	0.140	220
30	20	779	4.29	37	0.163	270
30	20	779	4.98	43	0.192	280
30	20.4	762	5.67	50	0.224	310
30	21.2	727	6.36	63	0.286	320
30	21.6	709	7.05	75	0.342	340
30	22.3	678	7.75	85	0.389	360
30	22.8	656	8.44	91	0.417	370
30	23.2	638	9.13	105	0.483	380
30	24	603	9.82	115	0.530	390
30	24.6	577	10.51	125	0.577	380
30	25.6	533	11.21	138	0.638	380
30	25.9	519	11.90	121	0.558	380
30	26.5	493	12.59	105	0.483	380

Table 2.25.3: Liquid. 9, viscosity 766 mPa.s (Millmax 220).

Curtain height: 100 mm Date: 26/07/2007
Substrate: 53847 Room temperature: 22°C

Die angle β	Liquid Temperature, °C	Viscosity μ (mPa.s)	Flow rate l/min	V_{ae} %	Air entrainment V_{ae} (m/s)	Pressure (Psi)
45	20.3	766	1.17	22	0.093	80
45	20	779	1.86	24	0.102	100
45	20.2	771	2.56	28	0.121	140
45	20.2	771	3.59	36	0.159	180
45	20.7	749	4.29	44	0.196	220
45	21.1	731	4.98	54	0.243	270
45	21.5	713	5.67	175	0.812	280
45	23.5	625	6.36	228	1.061	310
45	24	603	7.05	284	1.324	320
45	24.5	581	7.75	320	1.493	340
45	24.8	568	8.44	362	1.691	360
45	25	559	9.13	400	1.869	370
45	25.6	533	9.82	406	1.898	380
45	25.8	524	10.51	385	1.799	390
45	26	515	11.21	370	1.728	380
45	26.3	502	11.90	351	1.639	380
45	26.7	484	12.59	330	1.540	380
45	27.8	436	13.28	300	1.399	380

Table 2.25.4: Liquid. 9, viscosity 766 mPa.s (Millmax 220).

Curtain height: 100 mm Date: 26/07/2007
Substrate: 53847 Room temperature: 22°C

Die angle β	Liquid Temperature, °C	Viscosity μ (mPa.s)	Flow rate l/min	V_{ae} %	Air entrainment V_{ae} (m/s)	Pressure (Psi)
55	20.3	766	1.17	24	0.102	80
55	20.5	757	1.86	28	0.121	100
55	21.2	727	2.56	36	0.159	140
55	22	691	3.59	51	0.229	180
55	22.7	660	4.29	65	0.295	220
55	23.4	630	4.98	84	0.384	270
55	23.5	625	5.67	100	0.459	280
55	23.7	616	6.36	112	0.516	310
55	24.3	590	7.05	120	0.553	320
55	24.7	572	7.75	128	0.591	340
55	25.2	550	8.44	140	0.647	360
55	25.6	533	9.13	155	0.718	370
55	26	515	9.82	160	0.741	380
55	26.8	480	10.51	150	0.694	390

Table 2.26.1: Liquid. 10, viscosity 1131 mPa.s (Millmax 320).

Curtain height: 100 mm Date: 11/07/2007
Substrate: 53847 Room temperature: 22°C

Die angle β	Liquid Temperature, °C	Viscosity μ (mPa.s)	Flow rate l/min	V_{ae} %	Air entrainment V_{ae} (m/s)	Pressure (Psi)
0	20.5	1131	1.85	14	0.055	180
0	20.5	1131	2.45	18	0.074	290
0	20.6	1124	3.35	22	0.093	300
0	20.7	1116	3.95	26	0.112	320
0	21	1095	4.55	30	0.130	350
0	21.2	1080	5.15	35	0.154	370
0	21.3	1073	5.75	39	0.173	390
0	21.7	1044	6.34	47	0.210	400
0	23.1	942	6.94	57	0.257	410
0	24.2	862	7.54	70	0.318	420
0	24.5	841	8.14	81	0.370	430
0	24.7	826	8.74	92	0.422	440
0	26	732	9.34	104	0.478	450
0	26.6	688	9.94	80	0.365	455
0	26.7	681	10.54	70	0.318	460

Table 2.26.2: Liquid. 10, viscosity 1146 mPa.s (Millmax 320).

Curtain height: 100 mm Date: 06/07/2007
Substrate: 53847 Room temperature: 22°C

Die angle β	Liquid Temperature, °C	Viscosity μ (mPa.s)	Flow rate l/min	V_{ae} %	Air entrainment V_{ae} (m/s)	Pressure (Psi)
30	20.3	1146	1.25	12	0.046	180
30	20.3	1146	1.85	16	0.065	290
30	20.3	1146	2.45	21	0.088	300
30	20.5	1131	3.35	26	0.112	320
30	20.4	1138	3.95	30	0.130	350
30	20.8	1109	4.55	34	0.149	370
30	21	1095	5.15	39	0.173	390
30	21.7	1044	5.75	46	0.206	400
30	22.3	1000	6.34	50	0.224	410
30	23.8	891	6.94	60	0.271	420
30	25	804	7.54	95	0.436	430
30	25.6	761	8.14	110	0.506	440
30	25.8	746	8.74	125	0.577	450
30	25.8	746	9.34	120	0.553	455
30	25.8	746	9.94	110	0.506	460
30	26.2	717	10.54	90	0.412	470

Table 2.26.3: Liquid. 10, viscosity 1146 mPa.s (Millmax 320).

Curtain height: 100 mm Date: 11/07/2007
Substrate: 53847 Room temperature: 22°C

Die angle β	Liquid Temperature, °C	Viscosity μ (mPa.s)	Flow rate l/min	V_{ae} %	Air entrainment V_{ae} (m/s)	Pressure (Psi)
45	21.4	1066	1.25	16	0.065	180
45	21.6	1051	1.85	21	0.088	290
45	21.5	1058	2.45	25	0.107	300
45	21.4	1066	3.35	32	0.140	320
45	21.5	1058	3.95	37	0.163	350
45	21.8	1037	4.55	44	0.196	370
45	22.2	1008	5.15	50	0.224	390
45	22.8	964	5.75	58	0.262	400
45	23.2	935	6.34	70	0.318	410
45	24.9	812	6.94	108	0.497	420
45	25	804	7.54	126	0.582	430
45	25.5	768	8.14	135	0.624	440
45	26	732	8.74	140	0.647	450
45	26	732	9.34	120	0.553	455
45	26.8	674	9.94	100	0.459	460

Table 2.26.4: Liquid. 10, viscosity 1095 mPa.s (Millmax 320).

Curtain height: 100 mm Date: 06/07/2007
Substrate: 53847 Room temperature: 22°C

Die angle β	Liquid Temperature, °C	Viscosity μ (mPa.s)	Flow rate l/min	V_{ae} %	Air entrainment V_{ae} (m/s)	Pressure (Psi)
55	21	1095	1.25	17	0.069	180
55	21.2	1080	1.85	23	0.098	290
55	21.2	1080	2.45	28	0.121	300
55	21.5	1058	3.35	37	0.163	320
55	21.5	1058	3.95	43	0.192	350
55	22	1022	4.55	50	0.224	370
55	22.5	986	5.15	60	0.271	390
55	24	877	5.75	70	0.318	400
55	24.3	855	6.34	86	0.394	410
55	24.5	841	6.94	101	0.464	420
55	24.3	855	7.54	119	0.549	430
55	24.6	833	8.14	130	0.600	440
55	25	804	8.74	155	0.718	450
55	25.2	790	9.34	131	0.605	455
55	25.3	783	9.94	100	0.459	460
55	25.5	768	10.54	90	0.412	470

Table 2.26.5: Liquid. 10, viscosity 1066 mPa.s (Millmax 320).

Curtain height: 150 mm Date: 16/07/2007
Substrate: 53847 Room temperature: 22°C

Die angle β	Liquid Temperature, °C	Viscosity μ (mPa.s)	Flow rate l/min	V_{ae} %	Air entrainment V_{ae} (m/s)	Pressure (Psi)
0	21.4	1066	1.25	14	0.055	130
0	21.2	1080	1.85	18	0.074	170
0	21.1	1087	2.45	21	0.088	210
0	21.2	1080	3.35	27	0.116	280
0	21.3	1073	3.95	31	0.135	310
0	21.6	1051	4.55	35	0.154	330
0	22	1022	5.15	41	0.182	350
0	22.5	986	5.75	48	0.215	370
0	23	950	6.34	56	0.253	390
0	24	877	6.94	71	0.323	400
0	25	804	7.54	83	0.380	405
0	25.4	775	8.14	96	0.441	400
0	26.1	724	8.74	107	0.492	410
0	26.6	688	9.34	92	0.422	415
0	26.8	674	9.94	79	0.361	420

Table 2.26.6: Liquid. 10, viscosity 1124 mPa.s (Millmax 320).

Curtain height: 150 mm Date: 13/07/2007
Substrate: 53847 Room temperature: 22°C

Die angle β	Liquid Temperature, °C	Viscosity μ (mPa.s)	Flow rate l/min	V_{ae} %	Air entrainment V_{ae} (m/s)	Pressure (Psi)
30	20.6	1124	1.25	16	0.065	130
30	20.6	1124	1.85	19	0.079	170
30	20.6	1124	2.45	23	0.098	210
30	20.7	1116	3.35	30	0.130	280
30	21	1095	3.95	35	0.154	310
30	21.4	1066	4.55	40	0.177	330
30	21.7	1044	5.15	47	0.210	350
30	22.2	1008	5.75	54	0.243	370
30	23.1	942	6.34	66	0.300	390
30	24.1	870	6.94	78	0.356	400
30	24.6	833	7.54	95	0.436	405
30	24.9	812	8.14	110	0.506	400
30	25.2	790	8.74	90	0.412	410
30	26	732	9.34	80	0.365	415
30	26.5	695	9.94	70	0.318	420

Table 2.26.7: Liquid. 10, viscosity 1066 mPa.s (Millmax 320).

Curtain height: 150 mm Date: 13/07/2007
Substrate: 53847 Room temperature: 22°C

Die angle β	Liquid Temperature, °C	Viscosity μ (mPa.s)	Flow rate l/min	V_{ae} %	Air entrainment V_{ae} (m/s)	Pressure (Psi)
45	21.4	1066	1.25	18	0.074	180
45	21.3	1073	1.85	22	0.093	290
45	21.2	1080	2.45	27	0.116	300
45	20.9	1102	3.35	35	0.154	320
45	21.1	1087	3.95	40	0.175	350
45	21.2	1080	4.55	45	0.201	370
45	21.4	1066	5.15	52	0.234	390
45	21.9	1029	5.75	58	0.262	400
45	23	950	6.34	70	0.318	410
45	23.8	891	6.94	81	0.370	420
45	24	877	7.54	102	0.469	430
45	24.5	841	8.14	125	0.577	440
45	25.5	768	8.74	110	0.506	450
45	26	732	9.34	90	0.412	455

Table 2.26.8: Liquid. 10, viscosity 964 mPa.s (Millmax 320).

Curtain height: 150 mm Date: 13/07/2007
Substrate: 53847 Room temperature: 22°C

Die angle β	Liquid Temperature, °C	Viscosity μ (mPa.s)	Flow rate l/min	V_{ae} %	Air entrainment V_{ae} (m/s)	Pressure (Psi)
55	22.8	964	1.25	25	0.107	180
55	22.5	986	1.85	30	0.130	290
55	22.4	993	2.45	36	0.159	300
55	22	1022	3.35	45	0.201	320
55	21.9	1029	3.95	51	0.229	350
55	22	1022	4.55	60	0.271	370
55	22.5	986	5.15	69	0.314	390
55	22.8	964	5.75	78	0.356	400
55	23.5	913	6.34	99	0.455	410
55	24.8	819	6.94	113	0.521	420
55	25.5	768	7.54	131	0.605	430
55	26	732	8.14	149	0.690	440
55	26.2	717	8.74	155	0.718	450
55	27.5	623	9.34	142	0.657	455
55	28.5	550	9.94	120	0.553	460

Table 2.26.9: Liquid. 10, viscosity 1095 mPa.s (Millmax 320).

Curtain height: 200 mm Date: 17/07/2007
Substrate: 53847 Room temperature: 22°C

Die angle β	Liquid Temperature, °C	Viscosity μ (mPa.s)	Flow rate l/min	V_{ae} %	Air entrainment V_{ae} (m/s)	Pressure (Psi)
0	21	1095	1.25	16	0.065	130
0	20.7	1116	1.85	19	0.079	170
0	20.6	1124	2.45	23	0.098	210
0	20.6	1124	3.35	28	0.121	280
0	20.6	1124	3.95	33	0.145	310
0	20.8	1109	4.55	37	0.163	330
0	21.2	1080	5.15	43	0.192	350
0	21.7	1044	5.75	50	0.224	370
0	22.3	1000	6.34	55	0.248	390
0	23.2	935	6.94	65	0.295	400
0	24.3	855	7.54	79	0.361	405
0	25.1	797	8.14	90	0.412	400
0	25.3	783	8.74	105	0.483	410
0	26.5	695	9.34	124	0.572	415
0	26.8	674	9.94	117	0.539	415
0	26.9	666	10.54	113	0.521	420
0	27	659	11.14	91	0.417	420

Table 2.26.10: Liquid. 10, viscosity 1124 mPa.s (Millmax 320).

Curtain height: 200 mm Date: 17/07/2007
Substrate: 53847 Room temperature: 22°C

Die angle β	Liquid Temperature, °C	Viscosity μ (mPa.s)	Flow rate l/min	V_{ae} %	Air entrainment V_{ae} (m/s)	Pressure (Psi)
30	22.6	979	1.25	20	0.083	130
30	22.4	993	1.85	24	0.102	170
30	22.4	993	2.45	28	0.121	210
30	22.4	993	3.35	33	0.145	280
30	22.5	986	3.95	41	0.182	310
30	22.9	957	4.55	46	0.206	330
30	23.2	935	5.15	52	0.234	350
30	23.7	899	5.75	62	0.281	370
30	24.2	862	6.34	76	0.347	390
30	24.3	855	6.94	92	0.422	400
30	25.2	790	7.54	107	0.492	405
30	25.7	753	8.14	120	0.553	400
30	26.3	710	8.74	130	0.600	410
30	26.3	710	9.34	135	0.624	415
30	26.5	695	9.94	115	0.530	415
30	26.9	666	10.54	105	0.483	420
30	27	659	11.14	80	0.365	420

Table 2.26.11: Liquid. 10, viscosity 1124 mPa.s (Millmax 320).

Curtain height: 200 mm Date: 17/07/2007
Substrate: 53847 Room temperature: 22°C

Die angle β	Liquid Temperature, °C	Viscosity μ (mPa.s)	Flow rate l/min	V_{ae} %	Air entrainment V_{ae} (m/s)	Pressure (Psi)
45	21	1095	1.25	20	0.083	130
45	20.8	1109	1.85	24	0.102	170
45	20.9	1102	2.45	27	0.116	210
45	20.8	1109	3.35	36	0.159	280
45	20.9	1102	3.95	43	0.192	310
45	21.1	1087	4.55	50	0.224	330
45	21	1095	5.15	56	0.253	350
45	22.1	1015	5.75	62	0.281	370
45	23	950	6.34	78	0.356	390
45	23.6	906	6.94	94	0.431	400
45	24.2	862	7.54	117	0.539	405
45	24.6	833	8.14	134	0.619	400
45	25.6	761	8.74	139	0.643	410
45	26	732	9.34	142	0.657	415
45	26.2	717	9.94	120	0.553	415
45	26.9	666	10.54	100	0.459	420

Table 2.26.12: Liquid. 10, viscosity 1015 mPa.s (Millmax 320).

Curtain height: 200 mm Date: 17/07/2007
Substrate: 53847 Room temperature: 22°C

Die angle β	Liquid Temperature, °C	Viscosity μ (mPa.s)	Flow rate l/min	V_{ae} %	Air entrainment V_{ae} (m/s)	Pressure (Psi)
55	22.1	1015	1.25	26	0.112	130
55	22	1022	1.85	28	0.121	170
55	21.7	1044	2.45	30	0.130	210
55	21.6	1051	3.35	43	0.192	280
55	20.8	1109	3.95	50	0.224	310
55	21.8	1037	4.55	62	0.281	330
55	22	1022	5.15	72	0.328	350
55	23.2	935	5.75	81	0.370	370
55	24.3	855	6.34	105	0.483	390
55	24.5	841	6.94	126	0.582	400
55	25	804	7.54	148	0.685	405
55	25.1	797	8.14	154	0.713	400
55	26.1	724	8.74	163	0.756	410
55	26.1	724	9.34	151	0.699	415
55	26.3	710	9.94	125	0.577	415

Coating with PVP

Table 2.27.1: Liquid. 11, viscosity 63 mPa.s (PVP).

Curtain height: 100 mm Date: 26/02/2008
Substrate: 53847 Room temperature: 22°C

Die angle β	Liquid Temperature, °C	Viscosity μ (mPa.s)	Flow rate l/min	V_{ae} %	Air entrainment V_{ae} (m/s)	Pressure (Psi)
0	25	63	4.97	538	2.518	80
0	25.1	62	6.89	528	2.471	100
0	25.1	62	8.81	512	2.396	140
0	25.6	60	10.72	492	2.302	180
0	25.7	59	12.64	482	2.255	220
0	25.8	58	14.56	463	2.166	270
0	26	57	16.47	450	2.104	280
0	26.2	56	18.39	438	2.048	310

Table 2.27.2: Liquid. 11, viscosity 66 mPa.s (PVP).

Curtain height: 100 mm Date: 20/02/2008
Substrate: 53847 Room temperature: 22°C

Die angle β	Liquid Temperature, °C	Viscosity μ (mPa.s)	Flow rate l/min	V_{ae} %	Air entrainment V_{ae} (m/s)	Pressure (Psi)
30	24.5	66	6.89	570	2.668	80
30	24.6	65	8.81	555	2.598	100
30	24.7	64	10.72	530	2.480	140
30	24.8	64	12.64	520	2.433	180
30	24.9	63	14.56	500	2.339	220
30	24.9	63	16.47	489	2.288	270
30	25	63	20.31	470	2.198	280

Table 2.27.3: Liquid. 11, viscosity 1015 mPa.s (PVP).

Curtain height: 150 mm Date: 26/02/2008
Substrate: 53847 Room temperature: 22°C

Die angle β	Liquid Temperature, °C	Viscosity μ (mPa.s)	Flow rate l/min	V_{ae} %	Air entrainment V_{ae} (m/s)	Pressure (Psi)
0	24.9	6355	5.74	570	2.668	80
0	25.2	6190	6.89	560	2.621	100
0	25.3	6135	8.81	540	2.527	140
0	25.4	6080	10.72	520	2.433	180
0	25.5	6025	12.64	510	2.386	220
0	25.6	5970	14.56	508	2.377	270
0	25.6	5970	16.47	488	2.283	280
0	25.7	5915	18.39	446	2.086	310

Table 2.27.4: Liquid. 11, viscosity 1015 mPa.s (PVP).

Curtain height: 150 mm Date: 27/02/2008
Substrate: 53847 Room temperature: 22°C

Die angle β	Liquid Temperature, °C	Viscosity μ (mPa.s)	Flow rate l/min	V_{ae} %	Air entrainment V_{ae} (m/s)	Pressure (Psi)
30	24	68	5.93	610	2.856	80
30	24.3	67	7.85	600	2.809	100
30	24.5	65	8.81	590	2.762	130
30	24.6	65	10.72	570	2.668	170
30	24.8	64	12.64	540	2.527	210
30	25	63	14.56	520	2.433	260
30	25.3	61	16.47	515	2.410	280
30	25.6	59	18.39	500	2.339	300

Table 2.27.5: Liquid. 11, viscosity 63 mPa.s (PVP).

Curtain height: 200 mm Date: 27/02/2008
Substrate: 53847 Room temperature: 22°C

Die angle β	Liquid Temperature, °C	Viscosity μ (mPa.s)	Flow rate l/min	V_{ae} %	Air entrainment V_{ae} (m/s)	Pressure (Psi)
0	25	63	6.89	585	2.739	80
0	25	63	7.85	580	2.715	100
0	25.3	61	9.77	560	2.621	140
0	25.4	60	11.68	554	2.593	180
0	25.5	60	12.64	546	2.556	220
0	25.7	59	14.56	540	2.527	270
0	25.8	58	16.47	520	2.433	280
0	26	575	18.39	500	2.339	310

Table 2.27.6: Liquid. 11, viscosity 65.7 mPa.s (PVP).

Curtain height: 200 mm Date: 29/02/2008

Substrate: 53847 Room temperature: 22°C

Die angle β	Liquid Temperature, °C	Viscosity μ (mPa.s)	Flow rate l/min	V_{ae} %	Air entrainment V_{ae} (m/s)	Pressure (Psi)
30	24.5	65	6.89	640	2.997	80
30	24.6	65	7.85	633	2.965	100
30	25	63	8.81	626	2.932	140
30	25.1	62	10.72	605	2.833	180
30	25.2	62	12.74	590	2.762	220
30	25.4	61	14.56	579	2.711	270
30	25.6	60	16.47	560	2.621	280
30	25.8	58	18.39	540	2.527	310